Applications des nanoparticules à base de Squalène dans les maladies cardiovasculaires et inflammatoires : Exemples pour l'ischémie/reperfusion cardiaque, l'athérosclérose et le sepsis

Romain Brusini

université
PARIS-SACLAY

Applications des nanoparticules à base de Squalène dans les maladies cardiovasculaires et inflammatoires : Exemples pour l'ischémie/reperfusion cardiaque, l'athérosclérose et le sepsis

Thèse de doctorat de l'Université Paris-Saclay

École doctorale n°569 - Innovation thérapeutique : du fondamental à l'appliqué (ITFA)
Spécialité de doctorat : Pharmacotechnie et biopharmacie
Unité de recherche : Université Paris-Saclay, CNRS, Institut Galien Paris-Saclay, 92296, Châtenay-Malabry, France.
Référent : Faculté de Pharmacie

Thèse présentée et soutenue à Châtenay-Malabry, le 27/01/2021, par

Romain BRUSINI

Composition du Jury

Karine ANDRIEUX Professeure, Université Paris Descartes (UMR 8258)	Présidente
Jean-Michel DOGNE Professeur, Université de Namur	Rapporteur & Examinateur
Florence GAZEAU Chercheuse, HDR, Université Paris Diderot (UMR 7057)	Rapporteur & Examinatrice
Hervé HILLAIREAU Professeur, Université Paris-Saclay (UMR 8612)	Examinateur
Patrick COUVREUR Professeur, Université Paris-Saclay (UMR 8612)	Directeur de thèse
Mariana VARNA-PANNEREC Maîtresse de Conférences, Univ. Paris-Saclay (UMR 8612)	Co-encadrante de thèse

Thèse de doctorat

NNT : 2021UPASQ006

« Vous ne trouverez jamais ce que vous ne cherchez pas », Confucius

Remerciements

L'ensemble de ces travaux de Thèse furent le fruit d'un travail de longue haleine semé d'embuches et dont une partie s'est déroulée dans un contexte sanitaire très particulier. De nombreuses personnes se retrouvèrent mêlées, pour le pire ou le meilleur, à ces 3 ans de doctorat. Et je peux affirmer avec certitude que je n'aurais jamais pu mener à terme tout cela sans la collaboration et l'aide irremplaçable de tous mes pairs et mentors qui m'ont tant appris, ainsi que le soutien si précieux de mes proches.

J'aimerai tout d'abord remercier l'ensemble des membres de mon jury de thèse, en commençant par Pr **Jean-Michel Dogné**, et **Dr. Florence Gazeau** qui m'ont fait l'honneur d'accepter d'évaluer ce manuscrit en tant que rapporteurs/rapportrices ; ainsi que **Pr. Karine Andrieux** et **Dr. Hervé Hillaireau** pour avoir accepté de porter un regard critique sur mon travail en tant qu'examinateurs.

Je tiens ensuite à remercier chaleureusement mon directeur de Thèse, **Pr. Patrick Couvreur**. Patrick, je vous remercie vraiment pour m'avoir donné la chance incroyable de travailler au sein de cette équipe formidable, pleine de personnalités différentes mais unies dans la générosité. Vous m'avez fait confiance sur tous mes projets durant ces 3 ans, m'avez accompagné, guidé, et avez même su me rebooster dans les moments où, stressé, je pensais que je n'aboutirai à rien. Vous avez aussi su tempérer mon optimisme débordant dans certaines situations pour me permettre de développer mon sens critique. Malgré votre emploi du temps chargé digne d'un ministre, vous avez toujours été disponible et extrêmement réactif dès que j'en avais besoin. Et j'ai la petite satisfaction personnelle d'être un de vos derniers doctorants en tant que directeur de l'équipe 7, ce qui me réjouis d'autant plus. J'espère avoir été à la hauteur.
De la même façon, je tiens à infiniment remercier **Dr. Mariana Varna-Pannerec,** ma co-directrice de Thèse. Mariana, un immense merci pour tout le temps que tu m'as accordé. Malgré tous les enseignements que tu devais donner, tu as toujours été à mes côtés, toujours disponible, et toujours présente même les mauvais jours. Tu m'as suivi, encadré, parfois poussé et encouragé, fait grandir et évoluer, depuis le premier jusqu'au dernier jour de ma Thèse. Tu m'as été d'une grande aide tant par tes conseils scientifiques que par ton management au quotidien, toujours prête à résoudre mes problèmes et toujours à l'écoute. Je me souviendrai de tout ton enseignement et m'en inspirerai dans ma vie professionnelle future. Et pour tout cela, je t'exprime ma gratitude.

Après avoir passé plus de trois années au sein de l'Institut Galien, je ne sais comment exprimer ma gratitude à tous les gens que j'ai côtoyé. Je tiens à sincèrement remercier **l'ensemble des membres, passé et présent, de l'Institut Galien.** Je suis en premier lieu reconnaissant envers **Pr. Elias Fattal**, ancien directeur de l'UMR 8612, pour m'avoir accueilli au sein de cette incroyable unité multiculturelle et pluridisciplinaire, et pour m'avoir permis de mener au mieux ce projet de Thèse, dans un environnement chaleureux,

enrichissant et dynamique. Je suis tout autant reconnaissant envers **Pr. Myriam Taverna**, actuelle directrice de l'Institut Galien, qui m'a aussi été d'une très grande aide en cette fin de thèse, pour m'avoir soutenu et épaulé pour l'obtention d'un financement supplémentaire de quelques mois pour pallier aux problèmes de la Covid-19.

Au sein de l'Institut, j'ai été entouré de scientifiques exceptionnelles qui ont toutes et tous contribué, de près ou de loin, à la réussite de cette Thèse et que j'aimerai remercier : **Didier**, pour son aide pour toute la partie « chimie », une personne d'une culture rare et d'un humour léché. Merci aussi de m'avoir accueilli au sein de votre tour pendant quelques mois, cela m'a permis de finir au mieux ma thèse. **Juliette**, qui m'a guidé tout en gentillesse et patience sur la culture cellulaire et la cytométrie en flux. Et **Stéphanie**, toujours souriante et dynamique pour nos échanges sur la culture cellulaire. **Sinda**, toujours de bonne humeur et toujours prête à aider pour n'importe quel problème, notamment en ce qui concernait la formulation des nanoparticules. **Catherine**, la pro des animaux, qui m'a permis de tant apprendre et progresser sur les expériences *in vivo*, toujours disponible et toujours prête à résoudre mes problèmes. Merci pour tout ton soutien et ton aide sur les modèles rats et souris, ainsi que sur l'utilisation du Lumina. **Nicolas**, avec qui je pouvais discuter autour d'un repas de tout et de rien, à la fois d'une grande aide pour des questions techniques, ou pour suggérer quelqu'un à qui s'adresser, et d'une grande humilité. Ce fut également un véritable plaisir de partager un petit moment sport, diététique ou famille avec toi. **Simona**, qui m'a gratifié de son expertise scientifique dans bien des domaines et notamment sur le squalène. Mentions spéciales aussi pour tes incroyables gâteaux qui venaient égayer nos lundis. Et enfin **Julien**, que je félicite d'être devenu au cours de ces trois ans le nouveau directeur d'équipe, et que je remercie pour son encadrement, sa réactivité et son aide lorsque nécessaire. Je me souviendrai aussi de ton goût prononcé pour le chocolat. Également, je souhaite chaudement remercier **Sylvie, Marie-Claude, Patricia, Dominique** et toute l'équipe administrative pour leur aide précieuse, sans perdre patience, tout en gardant leur bonne humeur.

Par ailleurs, ce travail n'aurait jamais pu aboutir sans toute l'aide reçue par l'ensemble des collaborateurs externes à l'Institut Galien. Je tiens donc à remercier grandement **Denis Calise**, responsable du service de microchirurgie du CREFRE à Toulouse, avec qui j'ai réalisé toutes les expériences d'ischémie/reperfusion cardiaque sur modèle murin. Denis, tu as rendu possible une grande partie de mes travaux. Tu m'as gentiment accueilli au sein de ton laboratoire, m'a appris les bons gestes chirurgicaux, m'a fait grandir humainement. Ce fut un réel plaisir de travailler à tes côtés ces quelques semaines. Je remercie aussi les responsables des plateformes de la faculté de pharmacie, notamment les deux Valérie. **Valérie Nicolas** ainsi que **Séverine** pour leurs explications limpides et avisées sur la microscopie confocale. Et **Valérie Domergue** et toutes les personnes travaillant au sein de l'animalerie avec elle, pour m'avoir appris le modèle d'ischémie/reperfusion sur rats, avoir toujours répondu présents pour toutes mes demandes, et avoir toujours réussi à m'apporter un soutien, tant au niveau des souris que vous me confiiez, que moralement.

Je tiens également à remercier **Sophie Leboucher** pour nous avoir gentiment permis de venir faire des coupes histologiques et des images microscopiques au sein de son laboratoire, tout en nous guidant et nous aidant au cours du processus.

Je remercie par ailleurs **L'Agence National de la Recherche** et toutes les autres institutions ayant collaboré à créer et financer le **projet Euronanomed III**, projet de recherche dans lequel s'inscrit ma Thèse et sans quoi rien n'aurait été possible. Je tiens ainsi à remercier toutes les personnes ayant participé au **projet européen NanoHeart**, et ayant contribué au bon fonctionnement de cet enrichissante collaboration.

Tout ce temps passé à Chatenay-Malabry m'a aussi et surtout permis de rencontrer et côtoyer une foule de doctorants/post-doctorants incroyables avec qui j'ai vécu de merveilleux moments. En tout premier lieu, il y a eu bien évidemment eu **Flavio**, mon compagnon de bureau, compagnon de galère, celui qui m'a soutenu, porté, encouragé, motivé pendant plus de 2 ans. Ta bonne humeur, ton enthousiasme et ta vigueur étaient pour moi un rayon de soleil quand mes expériences ne fonctionnaient pas. J'ai adoré toutes nos discussions, ton érudition et tes hypothèses et théories toujours plus incroyables les unes que les autres. Sans oublier bien sûr nos conversations foot et nutrition ! La dernière année de ma Thèse sans toi n'avait pas la même saveur. Et tu auras aussi été celui avec qui j'ai travaillé au quotidien, celui qui a le plus contribué à mes travaux et je te suis vraiment reconnaissant de m'avoir en quelques sortes pris sous ton aile. Un immense merci pour tous ces moments de partage, de rire et d'entraide. **Arnaud**, mon « pitcher » préféré, compagnon de sport, pas géographiquement dans la même tour mais toujours prêt à m'aider sur une question de science et de chimie, ou tout autre sujet. Ce fut un réel plaisir de travailler avec toi sur l'article de l'athérosclérose, et de faire nos pauses du midi au parc de Sceaux ou nos petits moments de détente avec ton fameux 7 layers dip. **Serra,** la joie de vivre incarnée, tu illuminais le laboratoire, et j'ai eu la chance de côtoyer quelques mois le même bureau, devenu le bureau des « Galien's Angels ». Je t'ai vu progresser à une vitesse folle en français, et toi tu m'as fait pratiquer mon anglais avec nos agréables conversations sur les trajets de retour du laboratoire à Paris. **Eléonore**, ex-Biotech, Belge assumé, on se connait depuis bien longtemps maintenant. On a commencé la Thèse en même temps et on a suivi mutuellement nos avancées et nos tracas. Ta gentillesse extrême et ton sourire étaient un vrai plaisir au quotidien, je te suis reconnaissant d'avoir toujours été présente, même en dehors du laboratoire au détour d'un footing ou d'une soirée. **Julie**, encore une acolyte de footing, de pause repas et de pause thé, tu m'as souvent permis de souffler et oublier mes problèmes. Et tu étais aussi la première lorsqu'il fallait aider avec les nanoparticules. **Marie**, tout en peps, dynamisme et gentillesse. Tu auras aussi été une de mes mentors du squalène avec Flavio, je te remercie pour tout ce que tu m'as appris, tu m'auras inspiré par ton exigence scientifique, ta générosité et ton franc-parler. **Raul**, mon coloc' de Finlande, le plus marrant des hispano-français, toujours le premier pour une bonne bière. Tu auras su me rafraîchir par ton humour, mais aussi par tes idées et tes conseils scientifiques avisés. **Quentin**, compagnon des foots d'été, j'ai adoré parler avec toi de nos projets présents et de nos

aspirations futures. Ton calme et ta bonté étaient très rafraichissants. **Céline**, avec qui j'ai aussi commencé la Thèse, ma (presque) voisine d'Antony. D'une grande intelligence et perspicacité, tu savais toujours me contredire et me faire savoir quand je disais n'importe quoi, mais toujours avec sollicitude. **Baptiste**, pour tous les bons moments passés en Finlande, pour nos échanges sur nos projets. Merci à **Gianpiero, Federica, Alex, Marion** et toute l'ancienne génération de l'Institut avec qui j'ai eu la chance de partager ne serait-ce qu'un court moment, pour leur ouverture d'esprit, leur gentillesse à mon égard, et pour toutes nos discussions diverses et variées. Merci à **Clélia, Maud, Marianne** et toute la nouvelle génération, pour avoir perpétué la superbe ambiance du laboratoire, pour avoir pris la relève et m'avoir supporté durant ma fin de Thèse. Et un merci spécial à **Natalie** et **Amandine**, les deux nouvelles doctorantes de mon groupe avec qui je partageais mon bureau. En si peu de temps, j'ai eu la chance de pouvoir partager mon expérience avec vous, qui probablement allez continuer à développer les nanoparticules de squalène. Bon courage pour la suite et merci pour vos petites attentions culinaires. Je ne peux malheureusement pas citer **tous les doctorants, post-doctorants et stagiaires** dont j'ai croisé la route et qui m'ont influencé. Vous avez chacun contribué à créer cette ambiance si enjoué, amicale et dynamique au sein du laboratoire. Merci beaucoup d'avoir égayer mes journées et d'avoir rendu plus plaisant le fait de venir tous les matins.

Enfin, mais non des moindres, je n'aurai pas pu aller au bout de ce parcours sans la présence et le soutien de ma famille et de mes amis. Je suis passé par tous les états : excitation, joie, passion, mais aussi frustration, déception, anxiété. Mais je n'ai jamais baissé les bras et toujours fait preuve de force grâce à tous mes proches. En particulier mes parents, **Mario et Marlène**, ma petite sœur **Lisa**, et mes grands-parents **Daniel et Brigitte**. Malgré les 947 km qui nous ont séparés pendant toute cette Thèse, vous avez toujours été présents, par la pensée mais surtout par téléphone. Je ne manquais jamais une occasion de vous appeler pendant mes longs trajets entre l'Institut et mon domicile et vous avez toujours su répondre présents. Vous avez fait preuve de beaucoup de patience et de réconfort. Grâce à vous, j'arrivai quotidiennement à m'évader dans mon « Sud » qui m'a beaucoup manqué. J'avais des nouvelles du toutou Maverick, et des conversations endiablées autour du club de foot. Vous avez toujours cru en moi, déjà bien avant cela. Je vous en serai toujours infiniment reconnaissant. Un merci spécial aussi à ma marraine **Gisèle**, qui est la gentillesse et le calme incarné, et qui ne cesse de nous étonner par ses talents de cuisinières. Sache que tonton **Phillipe** tient toujours une grande place dans mon cœur et qu'il fait partie de mes motivations de scientifique au quotidien. Un grand merci à tous mes amis pour les moments de bonheur et les bouffées d'air frais, les **ex-Biotech, les ex-SupAgro, Stephen** mon véto marseillais préféré **et les niçois Loïck et Michael**, mes compagnons niçois dans la vie parisienne, mes partenaires de squash, mes amis de toujours. Et pour finir, je remercie énormément **Solenn**, pour son soutien de tous les instants, pour m'avoir apporté tout ce bonheur et ce réconfort, mais aussi m'avoir supporté ces 2 dernières années dans la vie de tous les jours. Comme tu aimes si bien le dire, tu auras souvent été « mon phare dans la nuit », merci pour tout.

Table des matières

Abréviations

5-ASA: 5-AminoSalicylic Acid (also called Mesalazine)
AAR: Area At Risk
Ad: Adenosine
APCs: antigen-presenting cells
AMPS: 2-Acrylamido-2-MethylPropane-Sulfonic acid
ATP: Adenosine Triphosphate
bFGF: basic fibroblast growth factor
BSA: Bovine Serum Albumine
COVID-19: coronavirus disease 2019
DC: dendritic cells
Dex: Dexamethasone
DLS: Dynamic Light Scattering
DMEM: Dulbecco's Modified Eagle Medium
DMSO: Dimethylsulfoxyde
DNA: DeoxyriboNucleic Acid
DXT: Dextrose
EAE: experimental autoimmune encephalomyelitis
ELVIS: Extravasation through Leaky Vasculature and subsequent Inflammatory cell-mediated Sequestration
EPR: Enhanced Permeability and Retention
FBS: Foetal Bovine Serum
FDA: Food and Drug Administration
HA: Hyaluronic Acid
HDL: High-density Lipoprotein
HIF: Hypoxia-Inducible transcription Factor
HPLC: high-performance liquid chromatography
IA: Infarct Area
IBD: Inflammatory Bowel Diseases
ICAM: Inter-Cellular Adhesion Molecule
IFN-γ: Interferon gamma
IL-10: Interleukin 10
I/R: Ischemia/reperfusion
LAD: Left Anterior Descending (artery)
LDL: Low-Density Lipoprotein
LMWH: Low Molecular Weight Heparin
LOX-R: Lectin-like Receptors
LPS: LipoPolySaccharide
LV: Left Ventricle
LXR: Liver X Receptor
MAPK: Mitogen Activated Protein Kinase
MFI: Mean Fluorescence Intensity
MPO: Myeloperoxidase
MPSS: MethylPrednisolone Sodium Succinate
NF-κB: Nuclear Factor-kappa B
NIPAM: N-Isopropyl acrylamide
NPs: Nanoparticles
NSAID: Non-Steroidal Anti-inflammatory Drug
PAMP: Pathogen-associated Molecular Pattern
PBS/ Phosphate-Buffered Saline
pDNA: plasmid DeoxyriboNucleic Acid
PEG: Polyethylene Glycol
PEI: Polyethyleneimine
PFA: ParaFormAldehyde
PLGA: Poly(Lactic-co-Glycolic Acid)
PRR: Pattern-Recognition Receptor
PSL: PhosphatidylSerine-containing Liposome
RA: Rheumatoid arthritis
ROS: Radical Oxygen Species
RT: Room Temperature
siRNA: small interfering RiboNucleic Acid
SQAd(-BP): Squalene-adenosine(-BODIPY)
SQCOOH: Squalenic acid
SRA: Scavenger Receptor A
SQRho: Squalene-Rhodamine B
TCR: T cell receptors
TEM: Transmission Electron Microscopy
TLR: Toll-Like Receptor
TNF-α: Tumor Necrosis Factor alpha
TTC: Tetrazolium Chloride
TUNEL: Terminal deoxynucleotidyl transferase dUTP nick-end labelling
VCAM: Vascular Cell Adhesion Molecule
VEGF: Vascular Endothelial Growth Factor
VitE: Vitamin E

Introduction générale

L'Organisation mondiale de la Santé (OMS) définit les maladies cardiovasculaires comme recouvrant l'ensemble des troubles graves et fréquents affectant le cœur et les vaisseaux sanguins. A l'échelle mondiale, les maladies cardiovasculaires représentent un des plus gros problèmes de santé publique, constituant la principale cause de mortalité et de morbidité avec plus de 17 millions de décès chaque année, soit environ 31% de la mortalité mondiale totale[1]. A l'échelle nationale, cela représente plus d'1 million d'hospitalisations par an qui sont à l'origine en 2018 d'environ 140 000 décès, soit près de 400 décès par jour[2]. Il existe un large éventail de maladies émergeant du système cardiovasculaire, parmi lesquelles les lésions d'ischémie/reperfusion cardiaque et l'athérosclérose, dont le développement est étroitement associé à une forte réponse inflammatoire incontrôlée qui échoue à être résolue. De tels troubles inflammatoires incontrôlés se retrouvent aussi dans le sepsis, une autre maladie grave où l'inflammation est souvent exacerbée par des boucles de rétroaction positives entre des signaux pro-inflammatoires et du stress oxydant[3].

L'inflammation est un processus de défense immunitaire essentiel de l'organisme capable de reconnaître, détruire et éliminer toute substance étrangère nocive. Cela permet le maintien de l'homéostasie et la réparation des tissus et est ainsi indispensable à la survie face à une agression telle qu'un agent infectieux ou un stress métabolique par exemple. Toutefois, dans certaines situations, cette réaction inflammatoire peut aussi devenir néfaste et peut aggraver le développement d'une maladie. L'inflammation est en effet une caractéristique commune de nombreuses maladies telles que certaines maladies cardiovasculaires (*e.g.* l'ischémie/reperfusion cardiaque, l'athérosclérose, …) ou le sepsis comme évoquées précédemment.

Dans le cadre des lésions d'ischémie/reperfusion cardiaque, bien qu'en l'absence de micro-organisme, la réponse inflammatoire est similaire à celle provoquée par l'infection par des pathogènes[4]. Cela se produit essentiellement dès la reperfusion qui restore le flux sanguin et permet notamment le recrutement de globules blancs (leucocytes et neutrophiles principalement) au niveau du tissu cible, associé à une forte production de cytokines, chimiokines et autres modulateurs pro-inflammatoires ainsi qu'à l'activation en cascade du système du complément[4, 5]. Tout cela est fortement associé à un stress oxydant conséquent et participe à l'aggravation des dommages tissulaires induits au cours de l'ischémie.
Dans le cadre de l'athérosclérose, le processus inflammatoire est présent à toutes les étapes de manière chronique. Il apparaît très tôt, pendant l'athérogenèse avec un recrutement précoce de monocytes dans l'intima des vaisseaux induit par de multiples médiateurs pro-inflammatoires (cytokines, chimiokines) libérés à la suite de l'accumulation de LDL sous forme oxydée dans l'espace sous-endothélial. S'ensuit une maturation des monocytes en macrophages, leur multiplication et la conséquente augmentation de

production de nombreux médiateurs pro-inflammatoires[6, 7].
Dans le cadre du sepsis, il s'agit d'un syndrome inflammatoire généralisé et incontrôlé associé à une infection grave. Brièvement, certains motifs moléculaires associés aux pathogènes (« PAMPs » en anglais, acronyme pour Pathogen-Associated Molecular Pattern) sont reconnus par des récepteurs endogènes (ex : les récepteurs de type TOLL) entraînant l'activation des cellules du système immunitaire. Par suite, cela conduit à la sécrétion d'une variété de médiateurs de l'inflammation (cytokines, chimiokines, espèces réactives de l'oxygène, etc)[8, 9].

Malgré l'amélioration de la prévention des facteurs de risque et de la prise en charge thérapeutique, le diagnostic et le traitement de ces maladies cardiovasculaires et inflammatoires demeure aujourd'hui très limité, inadapté et peu efficace. Le développement de nouvelles stratégies thérapeutiques pour atténuer l'inflammation aigüe, prévenir et limiter le développement des plaques d'athérosclérose, ou réduire voire traiter les lésions d'ischémie-reperfusion constitue ainsi un des défis contemporains majeurs.

Ces dernières années, le rapide essor des nanosciences et de leurs applications dans le domaine de la médecine, alors désignées comme « nanomédicaments », ainsi que les remarquables performances des nanomatériaux développés d'année en année, ont fait de cette alternative thérapeutique une solution innovante pour surpasser les obstacles des traitements conventionnels. L'application de ces nano-systèmes aux stratégies de diagnostic et thérapeutique des maladies cardiovasculaires permet notamment le développement d'outils plus efficaces qui améliorent la stratégie d'administration d'un principe actif tout en prenant en compte sa cible thérapeutique. En effet, les nanomédicaments peuvent d'une part fournir un dispositif d'imagerie moléculaire performant et spécifique pour la détection précoce des troubles tels que l'athérosclérose, et ceci de manière non-invasive. D'autre part, les systèmes nanoparticulaires, par leur grande modularité en termes de matériaux, taille, forme, et caractéristiques de surface, ont l'avantage d'accroître la stabilité et la solubilité des médicaments, de prolonger le temps de circulation dans l'organisme, d'améliorer le ciblage thérapeutique, la biodisponibilité, ainsi que leur capture par les cellules et les tissus, tout en protégeant les molécules actives d'une rapide dégradation métabolique. Tout ceci réduit les doses nécessaires pour obtenir un effet thérapeutique, et donc limite la toxicité et les effets secondaires sur l'organisme[10].

Toutefois, l'utilisation des nanomédicaments s'accompagne aussi de divers inconvénients limitant à terme leur mise sur le marché. En effet, les nanoparticules présentent parfois de faibles taux de charge en substance active. Elles sont aussi associées à des difficultés de contrôle du relargage du principe actif tel que des phénomènes de relargage anticipé et excessif appelé « burst release », affichent des problèmes d'élimination ou de métabolisation, accompagné de la toxicité de certains nanomatériaux[11, 12].

Tout cela, amplifié par des complications de transposition à l'échelle industrielle[13], engendre une augmentation de risques sanitaires et toxicologiques, freinant leur utilisation en clinique et leur mise sur le marché.

Au sein de notre laboratoire, l'équipe du Pr. Patrick Couvreur tente de surmonter certains de ces obstacles en s'appuyant sur le processus d'encapsulation chimique appelé « squalénisation ». Cela consiste en un couplage chimique entre un dérivé du squalène, un lipide naturel biocompatible et biodégradable précurseur du cholestérol, et une substance thérapeutique active, dans le but de concevoir un bio-conjugué capable de former de manière spontanée en milieu aqueux des nanoparticules stables de l'ordre d'une centaine de nanomètres. Contrairement à d'autres nano-formulations, ces nanoparticules biocompatibles ont l'avantage d'être très peu cytotoxiques et d'offrir un taux de charge élevé, une meilleure pharmacocinétique par rapport à la molécule active seule ainsi qu'un ciblage plus efficace de la zone d'intérêt thérapeutique[14-16]. De tels bio-conjugués à base de squalène ont déjà fournis de résultats très prometteurs dans des modèles pré-cliniques d'inflammation aigüe[8, 17] ainsi que d'ischémie cérébrale et de trauma de la moëlle épinière[14].

Ce travail de Thèse, qui s'inscrit dans le cadre du projet Euronanomed II – NanoHeart (n°ANR-16ENM2–0005-01), a pour but principal d'évaluer des nanoparticules de squalène chargées avec de l'adénosine, dans un modèle pré-clinique de lésions d'ischémie/reperfusion cardiaque. Plus précisément, cette recherche a été axée sur la bio-conjugaison entre le squalène et l'adénosine (SQAd), modulateur endogène de l'inflammation qui possède un très fort potentiel thérapeutique avec des effets anti-apoptotiques et anti-inflammatoires, mais qui est limitée par un temps de demi-vie plasmatique extrêmement court (de l'ordre de 10s). L'objectif était de protéger la molécule active d'une rapide dégradation tout en ciblant spécifiquement le tissu cardiaque endommagé et ce pour le traitement des lésions d'ischémie/reperfusion cardiaque. Ce projet de thèse se focalise ainsi sur l'évaluation de l'effet cardioprotecteur des nanoparticules d'adénosine-squalène et des mécanismes impliqués à travers de modèles cellulaires et murins se rapprochant des conditions cliniques.
Les nanoparticules à base de squalène ont été également évaluées pour leur capacité à interagir avec les lipoprotéines plasmatiques, afin de détecter des plaques d'athérosclérose, dont la rupture conduit notamment la formation d'un thrombus dont les complications induisent généralement ischémie myocardique[18, 19]. Par ailleurs, dans un dernier temps, les nanoparticules à base de squalène furent évaluées dans un autre modèle de maladie inflammatoire, le sepsis.

La première partie de ce manuscrit se focalisera sur une **étude bibliographique** portant sur les avancées dans le domaine des nanomédicaments pour le traitement des troubles inflammatoires. Un bref aperçu de la physiopathologie de l'inflammation et des stratégies thérapeutiques actuelles seront présentés, avant de

discuter des principales approches nano-médicinales innovantes à un stade pré-clinique développées ces 5 dernières années pour la résolution des troubles inflammatoires. Une attention particulière sera aussi donnée au petit nombre de nanomédicaments actuellement en essai clinique ou déjà mis sur le marché.

La **section expérimentale** du manuscrit sera divisée en **trois chapitres**.

Le premier chapitre présentera le développement de nanoparticules à base de squalène pour le ciblage des lésions d'athérosclérose *via* l'utilisation des lipoprotéines endogènes. Plus précisément, dans cette preuve de concept, après avoir déterminé *in vitro* la capacité de nanoparticules fluorescentes de rhodamine-squalène à être captées par des macrophages, nous évaluerons *in vivo* la biodistribution de ces nanoparticules dans un modèle murin *ApoE*$^{-/-}$ d'athérosclérose. Et nous démontrerons par immunohistochimie qu'elles s'accumulent spécifiquement dans les plaques d'athérosclérose dans les aortes des animaux, où elles interagissent avec les macrophages résidents.

Le second chapitre est axé sur l'évaluation des nanoparticules de squalène-adénosine comme traitement cardioprotecteur et potentiellement anti-inflammatoire dans un modèle murin d'ischémie/reperfusion cardiaque. Nous détaillerons tout d'abord la caractérisation des nanoparticules d'adénosine-squalène utilisées pour cette étude. Puis nous analyserons l'efficacité pharmacologique et la cytotoxicité de ces nanoparticules sur des cellules cardiaques. Enfin, nous dépeindrons la pharmacocinétique et les effets pharmacologiques des nanoparticules sur des modèles d'ischémie-reperfusion *in vivo*.

Le dernier chapitre étudiera si les nanoparticules à base de squalène adénosine encapsulant en plus un antioxydant peuvent prouver leur efficacité dans le cadre d'une autre maladie inflammatoire, le sepsis. Plus précisément, cette étude, qui a aussi fait l'objet de la thèse du Dr. Flavio Dormont, se consacrera au développement d'une nouvelle formulation novatrice encapsulant à la fois de l'adénosine et du tocophérol au sein d'une même nanoparticule. Ces nanoparticules possèdent des effets anti-inflammatoire et antioxydant, et furent testés dans des modèles *in vivo* d'endotoxémie. Dans ce chapitre seront mis en valeur les résultats pour lesquelles j'ai participé activement.

L'ensemble de ces travaux illustre ainsi le potentiel des nanoparticules à base de squalène en tant que dispositifs de diagnostic et de thérapie ingénieux pour le traitement des maladies cardiovasculaires et inflammatoires.

Références

[1] : https://www.who.int/fr/news-room/fact-sheets/detail/cardiovascular-diseases-(cvds)
[2] : https://destinationsante.com/maladies-cardiovasculaires-400-morts-par-jour-enfrance.html#:~:text=En%20France%2C%20les%20maladies%20cardiovasculaires,environ%209%20morts%20par%20jour.
[3] : T. Van Der Poll, F. L. Van De Veerdonk, B. P. Scicluna,M. G. Netea, The immunopathology of sepsis and potential therapeutic targets. Nature Reviews Immunology. 17, 407 (2017)
[4] : Kalogeris, T., Baines, C. P., Krenz, M., & Korthuis, R. J. Ischemia/Reperfusion. Comprehensive Physiology, 7(1), 113–170. (2016).
[5] : Ioannou, A., Dalle Lucca, J., & Tsokos, G. C. Immunopathogenesis of ischemia/reperfusion-associated tissue damage. Clinical immunology (Orlando, Fla.), 141(1), 3–14. (2011).
[6] : Libby, P., Ridker, P. M., Hansson, G. K., & Leducq Transatlantic Network on Atherothrombosis. Inflammation in atherosclerosis: from pathophysiology to practice. Journal of the American College of Cardiology, 54(23), 2129–2138. (2009).
[7] : Tedgui A., Mallat Z. Athérosclérose et inflammation. Ipubli inserm Médecine/sciences synthèse. 2001:17:162-9
[8] : Dormont, F., Brusini, R., Cailleau, C., Reynaud, F., Peramo, A., Gendron, A., Mougin, J., Gaudin, F., Varna, M., & Couvreur, P. Squalene-based multidrug nanoparticles for improved mitigation of uncontrolled inflammation in rodents. Science advances, 6(23), eaaz5466. (2020).
[9] : T. Van Der Poll, F. L. Van De Veerdonk, B. P. Scicluna,M. G. Netea, The immunopathology of sepsis and potential therapeutic targets. Nature Reviews Immunology. 17, 407 (2017)
[10] : Gupta, P., Garcia, E., Sarkar, A., Kapoor, S., Rafiq, K., Chand, H. S., & Jayant, R. D. Nanoparticle Based Treatment for Cardiovascular Diseases. Cardiovascular & hematological disorders drug targets, 19(1), 33–44. (2019).
[11] : Desai N. Challenges in development of nanoparticle-based therapeutics. The AAPS journal, 14(2), 282–295. (2012).
[12] : Seaton, A., Tran, L., Aitken, R., & Donaldson, K. Nanoparticles, human health hazard and regulation. Journal of the Royal Society, Interface, 7 Suppl 1(Suppl 1), S119–S129. (2010).
[13] : Hua S , de Matos MBC , Metselaar JM , Storm G . Current trends and challenges in the clinical translation of nanoparticulate nanomedicines: pathways for translational development and commercialization. Front. Pharmacol. 9, 790 (2018).
[14] : Gaudin, A., Yemisci, M., Eroglu, H., Lepetre-Mouelhi, S., Turkoglu, O. F., Dönmez-Demir, B., Caban, S., Sargon, M. F., Garcia-Argote, S., Pieters, G., Loreau, O., Rousseau, B., Tagit, O., Hildebrandt, N., Le Dantec, Y., Mougin, J., Valetti, S., Chacun, H., Nicolas, V., Desmaële, D., … Couvreur, P. Squalenoyl adenosine nanoparticles provide neuroprotection after stroke and spinal cord injury. Nature nanotechnology, 9(12), 1054–1062. (2014).
[15] : Desmaële, D., Gref, R., & Couvreur, P. Squalenoylation: a generic platform for nanoparticular drug delivery. Journal of controlled release : official journal of the Controlled Release Society, 161(2), 609–618. (2012).
[16] : Couvreur, P., Stella, B., Reddy, L. H., Hillaireau, H., Dubernet, C., Desmaële, D., Lepêtre-Mouelhi, S., Rocco, F., Dereuddre-Bosquet, N., Clayette, P., Rosilio, V., Marsaud, V., Renoir, J. M., & Cattel, L. Squalenoyl nanomedicines as potential therapeutics. Nano letters, 6(11), 2544–2548. (2006).
[17] : Feng, J., Lepetre-Mouelhi, S., Gautier, A., Mura, S., Cailleau, C., Coudore, F., Hamon, M., &

Couvreur, P. A new painkiller nanomedicine to bypass the blood-brain barrier and the use of morphine. Science advances, 5(2), eaau5148. (2019).
[18] : B. Furie,B. C. Furie, Mechanisms of thrombus formation. N Engl J Med. 359, 938-949 (2008)
[19] : Varna, M., Juenet, M., Bayles, R., Mazighi, M., Chauvierre, C., & Letourneur, D. Nanomedicine as a strategy to fight thrombotic diseases. Future science OA, 1(4), FSO46. (2015).

Introduction bibliographique

Advanced nanomedicines for the treatment of inflammatory diseases

Romain Brusini[1], Mariana Varna[1], Patrick Couvreur[1#]

[1]Institut Galien Paris-Sud, UMR 8612, CNRS, Université Paris-Sud, Université Paris-Saclay, Faculté de Pharmacie, F-92296 Châtenay-Malabry Cedex, France

[#]**Corresponding author:** Prof. Patrick COUVREUR

Email: patrick.couvreur@universite-paris-saclay.fr

Tél: +33 146 835 582
+33 146 835 396
Fax: +33 146 619 334

Abstract

Inflammation, a common feature of many diseases, is an essential immune response that enables survival and maintains tissue homeostasis. However, in some conditions, the inflammatory process becomes detrimental, contributing to the pathogenesis of a disease. Targeting inflammation by using nanomedicines (*i.e.* nanoparticles loaded with a therapeutic active principle), either through the recognition of molecules overexpressed onto the surface of activated macrophages or endothelial cells, or through enhanced vasculature permeability, or even through biomimicry, offers a promising solution for the treatment of inflammatory diseases. After providing a brief insight on the pathophysiology of inflammation and current therapeutic strategies, the review will discuss, at a pre-clinical stage, the main innovative nanomedicine approaches that have been proposed in the past five years for the resolution of inflammatory disorders, finally focusing on those currently in clinical trials.

Keywords: nanoparticles, drug delivery systems, inflammation, biomimetic nanoparticles, pre-clinical assessment, clinical application

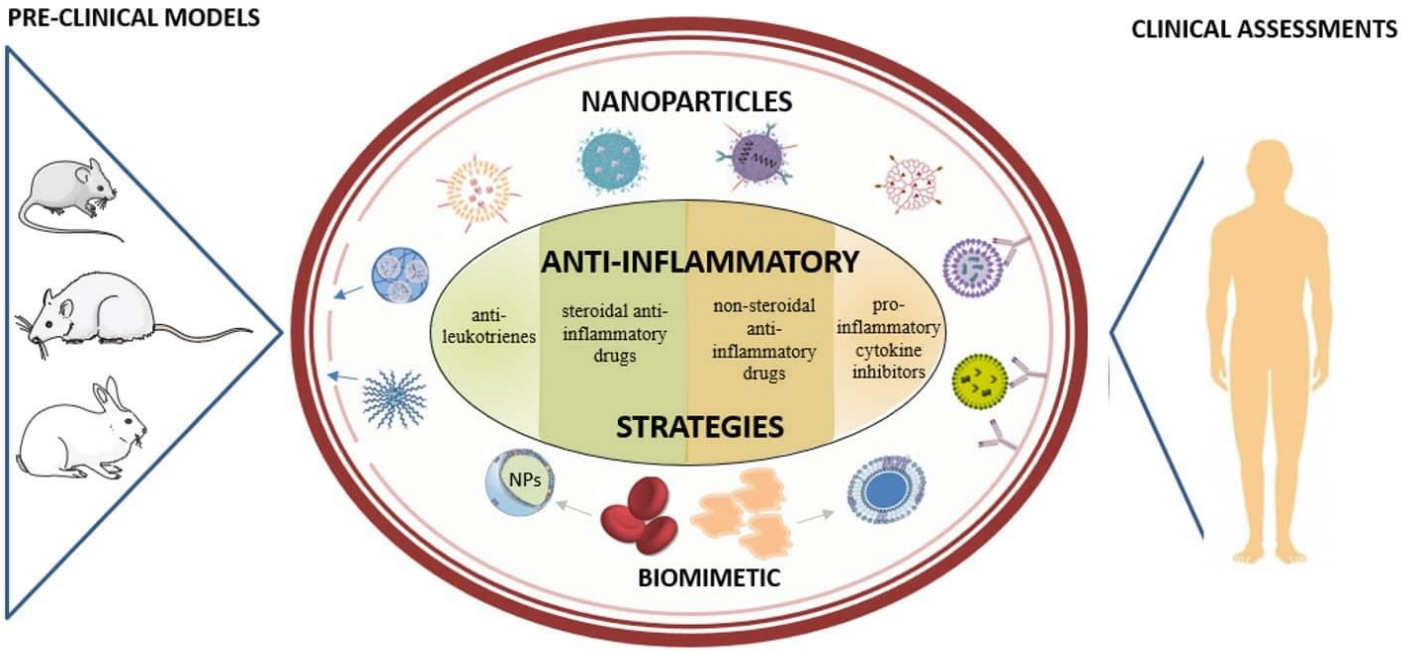

List of abbreviations

5-ASA: 5-AminoSalicylic Acid (also called Mesalazine)
APCs: antigen-presenting cells
AMPS: 2-Acrylamido-2-MethylPropane-Sulfonic acid
ATP: Adenosine Triphosphate
bFGF: basic fibroblast growth factor
COVID-19: coronavirus disease 2019
DC: dendritic cells
Dex: Dexamethasone
EAE: experimental autoimmune encephalomyelitis
ELVIS: Extravasation through Leaky Vasculature and subsequent Inflammatory cell-mediated Sequestration
EPR: Enhanced Permeability and Retention
FDA: Food and Drug Administration
HA: Hyaluronic Acid
HIF: Hypoxia-Inducible transcription Factor
IBD: Inflammatory Bowel Diseases
ICAM: Inter-Cellular Adhesion Molecule
IFN-γ: Interferon gamma
IL-10: Interleukin 10
LMWH: Low Molecular Weight Heparin
LPS: LipoPolySaccharide
LXR: Liver X Receptor
MAPK: Mitogen Activated Protein Kinase
MPO: Myeloperoxidase
MPSS: MethylPrednisolone Sodium Succinate
MTT:3-(4,5-dimethylthiazol-2-yl)-2,5-diphenyltetrazolium bromide
NF-κB: Nuclear Factor-kappa B
NIPAM: N-Isopropyl acrylamide
NPs: NanoParticles
NSAID: Non-Steroidal Anti-inflammatory Drug
pDNA: plasmid DeoxyriboNucleic Acid
PEG: Polyethylene Glycol
PEI: Polyethyleneimine
PLGA: Poly(Lactic-co-Glycolic Acid)
PRR: Pattern-Recognition Receptor
PSL: PhosphatidylSerine-containing Liposome
ROS: Radical Oxygen Species
RA: Rheumatoid arthritis
TCR: T cell receptors
TLR: Toll-Like Receptor
TNF-α: Tumor Necrosis Factor alpha
VCAM: Vascular Cell Adhesion Molecule
VEGF: Vascular Endothelial Growth Factor

1. Introduction

Inflammation represents a mechanism of the body's defence, originating from multiple causes such as infectious agents (viruses, bacteria), physical agents, radical oxygen species (ROS), metabolic stress (hypoxia), to cite only few examples[1]. In some situations, the inflammatory process may, however, become detrimental. The COVID-19 infection, associated in certain cases with a strong cytokine storm, a viral sepsis and an uncontrolled systemic inflammation, leading to acute respiratory distress represents an example of such adverse reaction[2, 3].

Historically, the first to define the clinical symptoms of inflammation was Celsus in the first century AD, who described four cardinal signs of inflammation as follows: "*rubor et tumor cum calore et dolore"* (redness and swelling with heat and pain). In 1858, Virchow added a fifth cardinal sign: *"functio laesa"* (disturbance of function)[1].

Depending on the origin of the agent, inflammation can be classified by whether it is caused by an external agent or an endogenous abnormal response. Based on its duration, inflammation can either be acute or chronic. Acute inflammation has been considered a defence of innate immune response induced by infection or injury[4], while chronic inflammation can accompany some pathological states without any infection or injury, like in obesity[5].

Recently, Antonelli and Kushner redefined inflammation as the innate immune response to potentially harmful stimuli such as pathogens, injury, and metabolic stress[6]. Indeed, proper inflammatory responses initiate a broad spectrum of innate immune protection and orchestrate long-term adaptive immunity toward specific pathogens. As such, the host immune system brings out layers of regulatory mechanisms that in return modulate the initiation, progression and resolution of inflammation[6, 7]**.** Generally, the inflammatory response (Figure 1) is perceived as a reaction of recognition of the infectious agent (inducers), a step which involves specialized (sensors) body cells as well as circulating proteins. After recognition, there is a production of mediators of inflammation which target the diseased tissue[6, 8]. But both, innate and adaptive immune system, trigger the inflammatory process. Indeed, the components of the innate immunity include phagocytes (*i.e.*, neutrophils, monocytes, macrophages), inflammation-related serum proteins (*e.g.*, complement, C-reactive protein), cell receptors that signal a defensive response (*e.g.*, Toll-like receptors) and cells that release cytokines and inflammatory mediators (*i.e.*, macrophages, mast cells, natural-killer cells)[7]. The complement system not only acts as the first line of defense for the body, but also links innate and adaptive immunity and plays an important role in peripheral lymph nodes to enhance B and T cell responses. Activation of adaptative immunity occurs after innate immunity signaling and/or antigen presentation by specialized cells known as antigen-presenting cells (APCs), which include dendritic cells (DC) and macrophages. In contrast to the innate immune system, the adaptive immune system is highly specific against one or more antigens after their recognition by specialized receptors at the surface

of B and T lymphocytes[9]. B cells are the main producers of antibodies which recognize and bind antigens. T cells are lymphocytes that express T cell receptors (TCR) on their surface and serve essential roles in cell-mediated immunity. However, more and more data show that this distinction between innate immunity and adaptive immunity, does not correspond to reality since enormous interdependence between the two immune responses exists. For example, nitric oxide and reactive oxygen species (ROS) produced by macrophages, dendritic cells or other components of the innate immunity can modulate T cell function and survival[10].

In most cases, the acute inflammatory response is controlled over time, and is normally finished once the insult is eliminated and the damaged tissue repaired. However, in some situations, when the inflammatory inducer persists, a chronic inflammatory response may establish. And when the inflammatory processes last for a long period of time, inflammation may become harmful and damaging for the tissues, which can in turn, contribute to the development and pathogenesis of chronic diseases of altered homeostasis. For example, lymphocyte T cells are thought to be the main triggers of autoimmune disease processes. In addition to innate immunity, adaptive mechanisms, through antigen recognition by the lymphocytes, production of antibodies, and their interaction with complement and phagocytic cells of the innate immunity such as macrophages, control both the nature and shape of the inflammatory responses. Thus, through this retro-activation of innate mechanisms, adaptive responses frequently provoke a persistent inflammation, which contributes to the process of chronic inflammation[7].

Inflammation is a very complex mechanism with, however, new advances in the understanding of its molecular mechanisms each year. Excellent reviews exist in this area describing the pathophysiological mechanisms[1, 6, 8]. It is now known that a large spectrum of diseases are accompanied by an uncontrolled inflammatory response, among these being sepsis, asthma, obesity and type 2 diabetes, neurodegenerative diseases, cardiovascular diseases (*e.g.* atherosclerosis, cardiac ischemia/ reperfusion), cancer, bowel disease, Crohn disease, rheumatoid polyarthritis, to cite only a few[11]. The understanding of the pathophysiology of the inflammation has allowed to identify proteins expressed by certain cells during inflammation (*e.g*. ICAM, VCAM, Selectins, ...). Additional phenomena such as the EPR (enhanced permeability and retention) effect have been identified. This effect, which is an interesting feature of inflamed tissues, leads to an increased vascular permeability coupled to a deregulated neovascularization[12]. EPR effect was first described in tumors were discontinuous endothelium in newly formed and immature vessels are formed. In inflammatory diseases, a similar effect was described with, however, some specificity. Thus, loss of endothelium integrity can result in abnormal neoangiogenesis observed in diseased tissues. The neovascularization mechanisms are described to be induced by hypoxia and inflammation which are critical factors. Hypoxia promotes activation of hypoxia-inducible transcription factors (*e.g.* HIF-1, HIF-2) and subsequently expression of growth factor (*e.g*. endothelial growth factor (VEGF), basic fibroblast growth factor (bFGF)), finally leading to a loss of intercellular

junctions between endothelial cells[12, 13]. On the other hand, neutrophils, which are predominate in acute inflammation, promote vascular permeability by releasing neutrophil elastase, myeloperoxidase and MMP-9, which contribute to enhanced vascular permeability. Wang *et al*, referred this phenomenon as ELVIS effect (Extravasation through Leaky Vasculature and subsequent Inflammatory cell-mediated Sequestration) and use it to deliver polymer prodrugs[14, 15]. Other studies have exploited the leaky vasculature during inflammation to deliver nanomedicines like PEGylated polycyanoacrylate [16] or liposomes [17] to the spinal cord of rats with experimental autoimmune encephalomyelitis (EAE).

Today, the therapeutic strategies include the use of steroidal or non-steroidal anti-inflammatory drugs. But two additional therapeutic approaches have recently emerged: the use of anti-leukotrienes that inhibit the recruitment of inflammatory cells and of pro-inflammatory cytokine inhibitors, like anti-TNF alpha or anti-IL-1 monoclonal antibodies. However, these treatments are sometimes not enough to obtain an optimal pharmacological activity. Drug limitations include non-specific biodistribution, low bioavailability and/or short half-life into the body. Moreover, high dosages are needed to be administered to patients, which cause off-target side effects with only modest success in controlling inflammatory disease symptoms[18].

To avoid some of these limitations, the use of nanoparticles (NPs), with a size from a few tenths to a few hundred of nanometers, has gained increasing interest. It is nowadays possible to obtain biocompatible nanomedicines (*i.e.* NPs loaded with active principle) with a highly controlled shape, size and surface charge[19-22]. Moreover, a passive exploitation of this characteristic leaky vasculature has allowed an increased delivery and accumulation of nanomedicines through sub-endothelial space. Additionally, targeting moieties on nanoparticles' surface may allow an active accumulation and a controlled drug release into the diseased cells and tissues, reducing toxicity and side-effects[23-25]. Therefore, many nanomedicines were developed with the aim to treat diseases with an inflammatory background, including cancer[26, 27], cardiovascular pathologies[28-30], autoimmune diseases[31], metabolic syndrome[32], neurodegenerative diseases[22, 33, 34].

We have excluded in this review nanomedicines dedicated to cancer therapy where inflammatory processes occurs, because there are already excellent reviews on this subject[35-37]. Nevertheless, to the best of our knowledge, there is no recent review making the state of the art on the use of nanomedicines when inflammation in general becomes detrimental.

This review will focus on the new nanomedicine concepts that have emerged during the last five years concerning the management of inflammatory diseases at the pre-clinical stage. The last part deals with the very low number of nanomedicines in clinical trials.

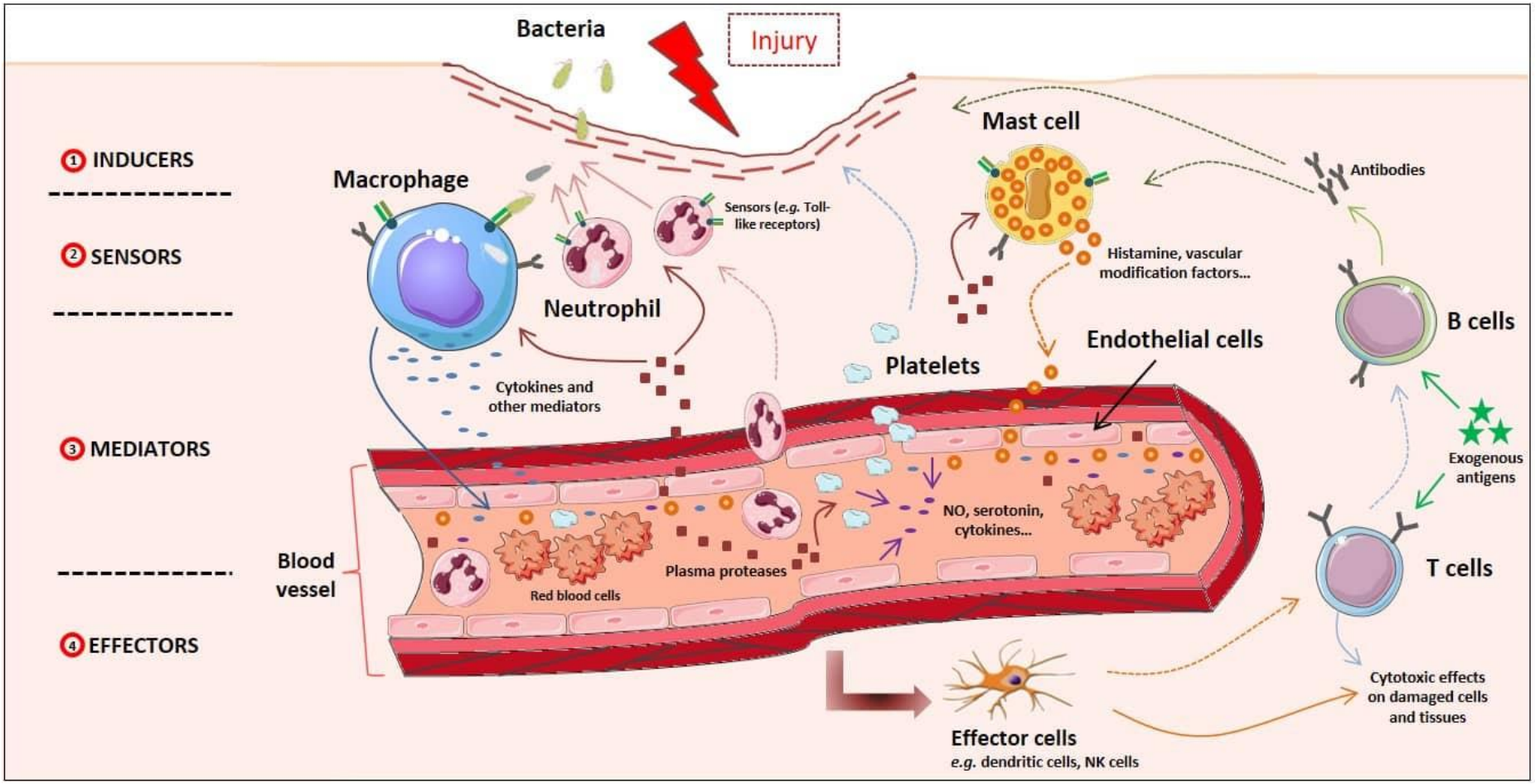

Figure 1: Schematic representation of the inflammatory response.

Briefly, inducer signals (1) (*e.g.* wound, pathogens) trigger sensors (2) on inflammatory cells present in the damaged area, which start to induce the production and release of multiple mediators (3). Mediators, including plasma proteases, chemokines, cytokines, and vascular modification factors lead in turn to vascular modifications, recruitment of blood platelets and other inflammatory cells such as phagocytic leukocytes (*e.g.* neutrophils) and act on effector cells (4) and tissues to resolve inflammation. Adaptive immunity is also implicated in inflammation response, through lymphocytes B and T able to recognize and respond to antigens presented by antigen-presenting cells such as dendritic cells. Adaptive mechanisms may function either by direct cytotoxic effects or by secretion of antibodies interacting with elements of the innate inflammatory response (complement proteins, phagocytic cells...).

2. Recent nanomedicines for the treatment of inflammation

A better understanding of the molecular and cellular events underlying the inflammatory response has opened some new perspectives in the treatment of inflammation, particularly through the development of well-designed nanomedicines. Indeed, nanoparticles (NPs) can be specifically engineered to go preferentially to the target tissue from the site of administration, thus addressing issues of conventional therapies such as off-target organ side effects and systemic toxicity, exacerbated by frequent and long-term dosing. The formulation of nanoparticles regulating the expression of pro- and anti-inflammatory molecules and targeting inflammatory sensors or macrophages through phagocytosis, holds great promise for the treatment of inflammatory diseases (Figure 2, Table 1). In addition, using nanocarriers to specifically target effector cells, particularly antigen-presenting cells, could be of great value to promote cellular response or immune tolerance thanks to their modulability which allows them to passively (optimizing the size and/or surface charge of nanoparticles) or actively (decorating nanoparticles with specific antibodies) target these cells[38]. Considerable attention to develop more effective anti-inflammatory nanomedicines, in order to overcome the side effects observed with conventional therapy, has resulted in the development on anti-inflammatory nanomedicines.

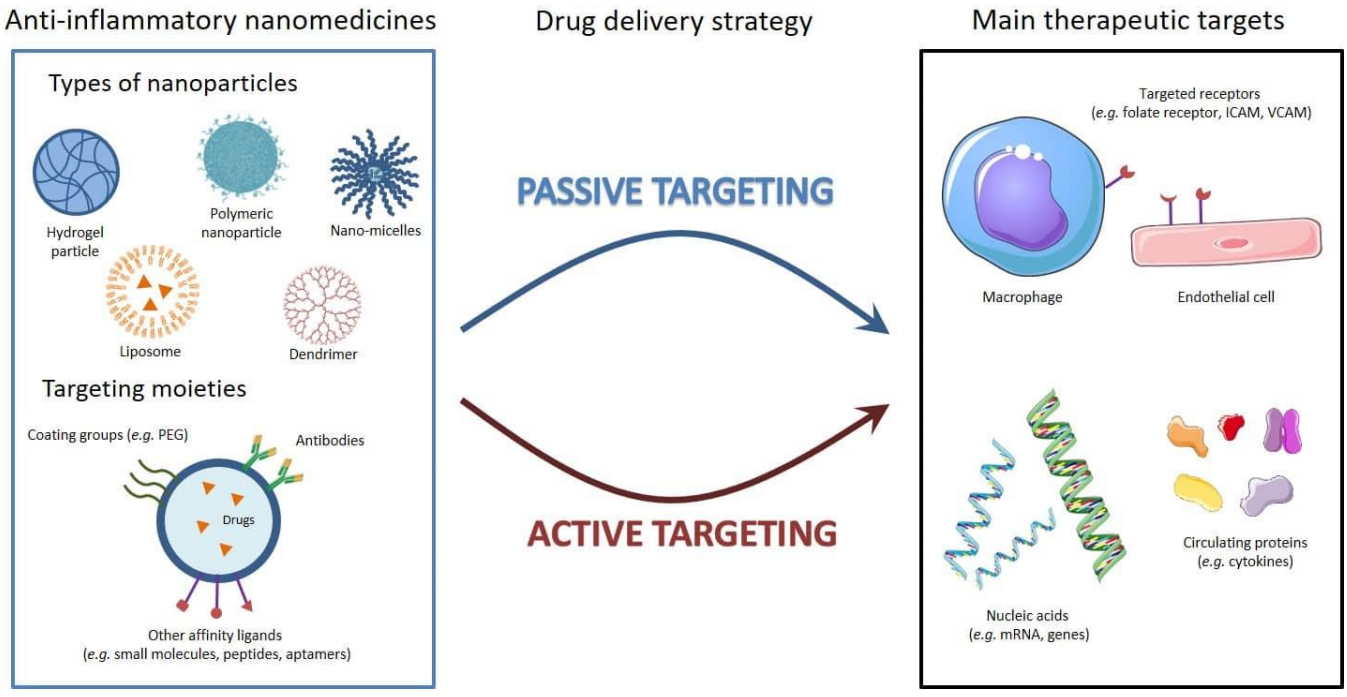

Figure 2: Anti-inflammatory nanomedicines: strategies and targets

Different types of nanoparticles were developed or are still in pre-clinical development for the management of inflammation. Among them liposomes, polymer nanoparticles, micelles, dendrimers, or hydrogel-based formulations. These nanoparticles could be naked or functionalized with targeting moieties, such as coating groups and antibodies or other affinity ligands. This allows them to target passively, through the leaky vasculature or actively the main actors of inflammation, including macrophages, endothelial cells, membrane receptors on inflammatory cells, anti-inflammatory genes and cytokines.

2.1. Steroid-based nanomedicines

Corticosteroids are a class of steroid hormones involved in a wide range of physiological processes, including stress response, immune response and regulation of inflammation. Particularly, glucocorticoids are potent anti-inflammatory corticosteroids, regardless of the inflammation's cause, whose effect is mainly through a lipocortin-1 synthesis mechanism[39, 40]. Some examples of the mostly used glucocorticoids for the treatment of inflammation are hydrocortisone and derivatives, prednisolone, dexamethasone or budesonide. Their therapeutic strength is extensively recognized, but they inexorably exhibit severe side effects after few weeks of treatment (such as weight gain, high blood pressure, high blood sugar, or even cataracts, bone loss, and muscle weakness)[41, 42] limiting their clinical use. Thus, various nano-formulations of corticosteroids[43] were proposed to overcome those limitations (Figure 3, Table 1).

Prednisolone is one of the most popular corticosteroids used for encapsulation into nanocarriers. For example, prednisolone nanocapsules, composed of a polymer wall surrounding an oily core, and coated with a pH-responsive enteric polymer (Eudragit S100), were designed and tested in healthy rats. This oral system allowed a high encapsulation efficiency of ca. 90% and a drug release triggered into the colon, as a consequence of neutral pH. This should increase the selectivity and efficacy of prednisolone for the treatment of inflammatory bowel diseases (IBD) or other colonic diseases[44].

Similarly, for oral administration, spherical polymer microsponges with a size of around 30µm, but with nano-porous microstructures, were also loaded with prednisolone and coated with Eudragit S100. The microsponges structure facilitated plastic deformation which was needed for the formation of mechanically strong tablets applicable for clinics. In addition, these microsponges displayed a high drug loading (around 86%), allowing dose and dose frequency reduction which should decrease prednisolone side effects and have some interest for the treatment of IBD[45]. However, the proof of concept was only validated *in vitro*, while *in vivo* studies are still lacking to validate this approach.

Another interesting strategy, based on orally or/and rectally administered lectin-decorated glucocorticoid loaded nanoparticles, was developed for an active targeting and selective adhesion to the inflamed tissue *in vitro* in experimental colitis. This strategy seems to be a promising tool for treatment of inflammatory bowel diseases[46]. Other recent pre-clinical studies have further demonstrated the therapeutic added value of prednisolone nano-formulations. For example, prednisolone loaded liposomes were assessed in a 8-week-old male LEWIS rat model of renal ischaemia-reperfusion injury, and liposomes were found to accumulate in the inflamed kidney after systemic delivery. The treatment increased the presence of anti-inflammatory macrophages and reduced monocyte chemoattractant protein-1 mRNA production, concomitant to a reduced pro-inflammatory profile in the kidney[47]. Although leading to very interesting data, it is important to note that the experiments were performed with young age animals and the final point of

analysis remained quite short (*i.e*. 96 h). And young animals respond more efficiently than older ones, whereas, in the daily medical practice elderly people represent the population of patients the more affected by inflammatory diseases.

Rheumatoid arthritis (RA) is a chronic, systemic inflammatory disease treated with high doses of glucocorticoids. To avoid non-specific body biodistribution, solid-lipid nanoparticles were coated with hyaluronic acid in order to target hyaluronic receptor CD44 over-expressed on the surface of synovial lymphocytes, macrophages and fibroblasts in inflamed joints in RA. After intravenous injection into 6-week-old mice with collagen-induced arthritis, a significant improvement of the disease has been obtained, likely due to the specific accumulation of NPs into the inflamed tissue[48]. Folate-targeted double liposomes (*i.e*. small unilamellar vesicles encapsulated into a big liposome) containing two therapeutic agents (Prednisolone and Methotrexate) were also developed and assessed by systemic administration in collagen-induced arthritis in rats. These liposomes displayed high stability, enhanced loading capability and further enhanced the site-specific drug delivery to activated macrophages at inflamed joints in RA[49]. Gaafar *et al.* designed elastic niosome ("ethoniosomes") nanoparticles loaded also with prednisolone for ocular delivery. The ethoniosomes composed of Span60 and cholesterol and using ethanol 20% v/v as a hydrating solution to the surfactant/lipid materials were tested in rabbits subjected to a clove oil-induced severe ocular inflammation. A reduction to half of the time for complete healing was observed, in addition to a reduced intraocular pressure, one of the main side effects observed with conventional anti-inflammatory treatments. Besides, this system demonstrated good physical stability for at least 2 months at the fridge temperature with good ocular tolerability and minimal ocular irritation, suggesting good potential for translation into the clinic[50].

Methylprednisolone, already used in clinics for spinal cord injury treatment, is unfortunately accompanied by dose-related side effects due to systemic injection. The loading of methylprednisolone sodium succinate (MPSS) into polycaprolactone NPs dispersed in a fibrin glue-based gel system was tested in a rat model of induced spinal cord injury either by topical or intraperitoneal administration. The localized delivery of MPSS onto the lesion site enabled a reduced damage on spinal cord[51]. This therapeutic effect was explained by a dramatic decrease of caspase-3 and a moderate decrease in pro-inflammatory cytokines.

Dexamethasone (Dex) is another glucocorticoid drug with anti-inflammatory activity. A recent study demonstrates that dendrimer-Dex gel attenuated corneal inflammation more efficiently than free-Dex, by decreasing macrophage infiltration and pro-inflammatory cytokines expression, in a rat corneal inflammation model. The designed system is a biocompatible hydrogel conjugated to Dex and based on hydroxyl-terminated polyamidoamine dendrimers and hyaluronic acid, cross-linked *via* thiolene click

chemistry for subconjunctival injection[52]. Noteworthy, a single subconjunctival injection of this nano-formulation led to a prolonged efficacy for a period of 2 weeks with a reduced central corneal thickness and an improved corneal clarity, without elevation of the intraocular pressure. Moreover, the subconjunctival route is clinically accessible and can allow the administration of a relatively large volume of nanomedicine. Dexamethasone nanomedicines could also be very efficient for the treatment of rheumatoid arthritis or ulcerative colitis, bypassing the serious adverse effects associated with important doses of drug free. Thus, Wang *et al.* developed self -assembled poly(ethylene glycol) / poly(ε-caprolactone) polymer micelles loaded with Dex for intravenous injection at low dose of Dex (0.8 mg/kg body weight) in a rat model of arthritis. Although displaying moderate adverse effects, these polymeric micelles demonstrated substantial anti-inflammatory potential, including suppression of paw swelling and erythema, down-regulation of pro-inflammatory cytokines expression and protection of articular cartilage and bone from degradation and erosion[53].

Spherical polymer nanoconstructs loaded with Dex were also intravenously injected to a mouse model of colitis. A strong systemic anti-inflammatory effect was observed through a reduced macrophage infiltration and the expression of pro-inflammatory cytokines. These cellular effects were accompanied by a better animal recovery manifested by a reduced weight loss and a decreased rectal bleeding. These benefits were less evident in animals treated with the drug free[54]. Furthermore, using the same model, Dianzani *et al.* assessed the efficacy of orally administered multi-drug nanoparticles co-loaded with Dexamethasone and Butyrate. Both *in vitro* and *in vivo*, the treatment induced a significant decrease of pro-inflammatory cytokine release, which was more effective at doses 10-fold lower than the dose required to achieve the similar pharmacological efficacy with the single free drugs treatments[55]. If delivering simultaneously multiple drugs may be interesting, further research is, however, necessary to better understand the exact mechanism underlying the enhanced anti-inflammatory effect of this multidrug nano-formulation. Very recently, by using an interesting approach, Wang's team optimized a prodrug composed of N-(2-hydroxypropyl) methacrylamide (HPMA) copolymer linked to dexamethasone for the treatment of inflammatory arthritis. By intravenous injection in a rat model of arthritis, they observed very effective and safe therapeutic anti-inflammatory effects compared to other prodrug formulations. This attractive study promoted the importance of identifying the most potent therapeutic nanomedicines by evaluating the design and screening of activation mechanism[56].

Budesonide is a topical anti-inflammatory synthetic steroid, which was formulated for oral administration as first-line therapy in mild to moderate ileocecal Crohn's disease patients[57]. In order to minimize early drug release and activity in the stomach and small intestine, Naeem *et al.* encapsulated Budesonide into dual pH- and time-dependent polymer nanoparticles composed of Eudragit FS30D, as a pH-sensitive

polymer, and Eudragit RS100, as a controlled-release polymer. It was shown that in a mouse model of colitis, dual pH/time-dependent systems had greater therapeutic potential than single Eudragit FS30D or single Eudragit RS100 system. This beneficial effect was explained by the release of Budesonide at the right place (*i.e.* colon) during the right time (*i.e.* 24h)[58]. The use of Eudragit with various functionalities, either pH-sensitive or for controlled release, opens interesting perspective for clinical applications, particularly for colon-targeting treatments such as in IBD. Thus, nanotechnology has been used in oral dosage formulation design as strategies to further enhance uptake into diseased tissue within the colon [59] Other nano-formulations to target and decrease inflammation are in development. For example, Budesonide loaded into Hyaluronic Acid (HA) or poly(lactic-co-glycolic acid) (PLGA) nanoparticles exhibited higher anti-inflammatory effects than the free drug *in vitro* on human colon carcinoma Caco-2 cell line and on inflamed intestinal mucosa in mice respectively[60, 61].

Together these preclinical results underline the feasibility to improve the delivery of anti-inflammatory drugs *in vivo*. However, to be closer to the human diseases, the choice of the animal model, the duration of the treatment and the end points deserve to be better thoughtful, as will be discussed below (see part 4).

2.2. Non-Steroidal Anti-Inflammatory Drugs (NSAIDs) nanomedicines

Non-Steroidal Anti-Inflammatory Drugs (NSAIDs) act through the inhibition of cyclooxygenase proteins that metabolize arachidonic acid into prostaglandins[62]. Due to short half-life and high percentage of protein binding, high doses of NSAIDs are needed to be efficient, which in turn causes undesirable side effects, such as an increased risk of gastrointestinal and cardiovascular complications[62, 63]. Some NSAIDs NPs have recently been in development in order to counteract these side effects but, for the moment, they are only investigated at an *in vitro* pre-clinical stage.

Gonçalves *et al.* have loaded Diclofenac, a NSAID that inhibits prostaglandin synthesis by reducing cyclooxygenase-1 and cyclooxygenase-2 with relative equivalence, into chitosan-poly(γ-glutamic acid) NPs. This approach did not show any cytotoxicity for human macrophages. NPs were rapidly phagocyted and activated these cells, also inhibiting prostaglandin E2 and IL-6 production[64]. More recently, Shang *et al.* designed a novel intestinal targeted drug delivery system for oral administration; this system that combines PEG_{950} and methacrylic acid (MAA)) hydrogel and Ibuprofen-loaded PLGA NPs, could site-specifically deliver the drug into alkaline environment at a sustained-release manner. Such process improved the bioavailability and decreased the side effects of Ibuprofen[65].

Celecoxib is a COX-2 inhibitor indicated for long-term treatment of rheumatoid arthritis. It is administered orally, but unfortunately, this molecule shows adverse systemic complications in patients. In rats with experimental arthritis, the topical application of a gel containing this anti-inflammatory drug into solid lipid nanoparticles was found more efficient in inhibiting the inflammatory process, compared to untreated or conventional gel treated animals[66].

2.3. Nano-encapsulated anti-inflammatory mediators

Anti-inflammatory mediators represent another approach for the treatment of inflammatory diseases. For instance, cytokine IL-10, one of the main anti-inflammatory cytokines possesses multiple effects in immuno-regulation and inflammation[67]. It mainly downregulates the expression of other pro- or anti-inflammatory cytokines, enhances immune B cell survival, proliferation, as well as antibody production. Besides, IL-10 is implied in blocking NF-κB activity and is involved in the regulation of the JAK-STAT signalling pathway. But its clinical use is complicated by important cytokine-related side effects [68]. To overcome these limitations, new IL-10 anti-inflammatory nano-formulations were developed (Table 1).

A typical example is the development of nano-sized phosphatidylserine-containing liposomes (PSL) conjugated to IL-10. Toita *et al.* showed in a mouse model of obesity that intraperitoneal injection of IL-10-conjugated PSL had a better macrophage targeting ability and an enhanced anti-inflammatory effect than PSL alone, due to the synergistic anti-inflammatory effects of IL-10 and PSL. It was suggested that this association could be used as a macrophage-targeted therapy for inflammation-related diseases[69].

Another example is the development of biodegradable polyester NPs incorporating IL-10 for the targeted delivery of atherosclerotic plaques. Intravenous injection of these NPs significantly reduced acute inflammation in an atherosclerotic murine model and were shown to be more potent than IL-10 free. In addition, it was observed that plaque rupture was prevented by increasing the fibrous cap thickness, simultaneously to the decrease of the necrotic cores[70]. More recently, Baganizi *et al.* have bioconjugated recombinant IL-10 to poly(vinylpyrolidone)-coated silver NPs. These nanoparticles showed an improvement of the cytokine stability and a better anti-inflammatory effectiveness in mouse macrophages as manifested by a decrease in IL-6 and TNFα production[71]. However, this study was limited by the fact that silver NPs could not be delivered *in vivo* for inflammation treatment. Indeed, at the cellular level, toxicities have been reported, including reactive oxygen species generation, DNA damages and cytokine induction during *in vitro* studies[72, 73]. *In vivo,* studies also indicated adverse effects on many organs of the circulatory, respiratory, central nervous, hepatic and dermal systems[74, 75].

Other studies focused on the nano-formulation of antagonists of the pro-inflammatory cytokine IL-1 receptor. Particularly, self-assembled IL-1 receptor antagonist (IL-1Ra)-presenting nanoparticles were developed. Two examples of this kind of NPs are: IL-1Ra-poly(2-hydroxyethyl methacrylate)-pyridine NPs and IL-1Ra core/satellite NPs, based on methyl viologen-functionalized polymeric NPs as the core, and a trans-isomer of azobenzene modified IL-1Ra as the corona. The pharmacological efficacy of these nanodevices were investigated after local injection in a rat model of inflamed joints[76,77] and both IL-1Ra-presenting nanoparticles demonstrated interesting anti-inflammatory effects, mainly inhibiting the IL-1β-stimulated pro-inflammatory production.

2.4. Anti-inflammatory peptides nanomedicines

Anti-inflammatory peptides, which are small bioactive molecules containing up to 50 amino acids, are raising increasing interest[78]. For example, the anti-inflammatory peptide KAFAK, an inhibitor of mitogen-activated protein kinase-2, was assessed in a cartilage explant inflammation model. To increase the peptide's therapeutic lifetime, KAFAK was first loaded into co-polymerized 2-acrylamido-2-methylpropane sulfonic acid (AMPS) and N-isopropylacrylamide (NIPAM) monomers, to form pH-dependant poly(NIPAM-co-AMPS) nanoparticles[79, 80]. These NPs demonstrated the ability to selectively diffuse through the degraded cartilage explants before to release the peptide, allowing a significant reduction of pro-inflammatory cytokine production. However, the authors noted that the high affinity of KAFAK towards the nanoparticles core and the lack of core degradation resulted in the release of less than half of the loaded peptides, thus limiting the therapeutic applications of this approach[80]. Then, the same authors developed a more complex delivery system, based on poly(NIPAM) nanoparticles with degradable disulfide crosslinks (abbreviated as NGPEGSS), loaded with KAFAK peptides. The system relies on the co-polymerization of NIPAM and AMPS monomers, coated with polyethylene glycol (PEG) and using the degradable crosslinker bis(acryloyl)cystamine (BAC) for more effective release into the intracellular compartment[80, 81]. *Ex vivo*, a preferential accumulation of the NPs was observed throughout the inflamed aggrecan-depleted cartilage explants compared to their healthy counterparts and, simultaneously, a significant reduction of IL-6 pro-inflammatory cytokine was measured. Moreover, these NPs were stable and released less than 10% of the loaded KAFAK over 96h at pH=7.4 in a non-reducing environment. Thus, their ability to diffuse into the damaged cartilage, maintaining the majority of their payload prior to cell uptake by chondrocytes and macrophages, combined with a release of the peptide into these cells, represented an improvement comparatively to the treatment with the free peptide or with the previously described poly(NIPAM-co-AMPS) NPs[81].

2.5. Nanomedicines for gene therapy

Another strategy to control the inflammation is based on the manipulation of genetic material. In recent years, significant progresses have been made to design gene delivery systems for obtaining enhanced therapeutic efficacy with less off-target side effects. It is expected that targeted gene therapy could reduce the above-mentioned limitation by localizing the targeted gene at the site of the inflammation. Small interfering RNAs (siRNAs) were found to be a promising approach for silencing specific genes involved in inflammation. However, siRNA delivery into the cytosol of immune cells remains a challenge.

Many different mediators were considered for the development of gene nano-therapies (Table 1). For example, siRNA silencing proinflammatory cytokine tumor necrosis factor (TNFα) expression was entrapped into mannose-modified trimethyl chitosan-cysteine nanoparticles. *In vitro*, the NPs were internalized by rat peritoneal exudate cells, through endocytosis and micropinocytosis pathways. But more interestingly, in a rat model of acute hepatic injury, TNFα siRNA-loaded NPs orally administered induced an effective TNFα knockdown at a very low dose (*i.e.* 50μg/kg)[82]. Along the same line, cationic lipid nanoemulsions were also proposed for the delivery of anti-TNFα siRNA to the brain. It was shown that after intranasal administration in a rat model of LPS-induced neuroinflammation, the nanoemulsion concentrated preferentially into the brain, inducing a local down-regulation of TNFα[83]. Similarly, poly(ethylene glycol)-poly(caprolactone) polymeric micelles conjugated with anti- TNFα siRNA were administered intranasally in a rat model of cerebral ischemia-reperfusion injury associated with neuroinflammation. The rats subjected to the micelles treatment exerted a decrease of TNFα production and a significant improvement of their neurological score, as compared with the treatment using naked anti-TNFα siRNA[84].

Very recently, intranasal administration of cationic phosphorus dendriplexes loaded with anti-TNFα siRNA were shown very effective in a murine acute lung inflammatory model. Indeed, the authors observed a specific targeting toward macrophages, resulting in a major inhibition of TNFα, as well as, a better anti-inflammatory regulation of other cytokines[85].

Since in inflammation sites there is an overexpression of folic acid receptors by macrophages, a modified chitosan nanocarrier has been constructed, deploying folic acid, diethylethylamine and PEG groups to deliver TNFα siRNA. A significant decrease of inflammation in a murine arthritis model, close to human disease, was observed in animal receiving intraperitoneal injections of these NPs[86]. Nevertheless, the observed results should be discussed since the effects were observed only after multiple days of treatment, whereas TNFα levels usually tend to decrease rapidly (within a day) after siRNA treatment.

In order to downregulate TNFα and reduce RA progression, Aldayel *et al* designed PEGylated solid-lipid nanoparticles composed of lecithin and cholesterol and loaded with lyophilized TNF-α-siRNA. When this formulation was intravenously injected in a mouse model of collagen antibody-induced arthritis refractory to methotrexate therapy, the results obtained showed a good treatment efficacy, opening the hope for patients refractory to methotrexate[87]. Similar results have been obtained with lipid-polymer hybrid nanoparticles loaded with siRNA directed against TNFα. Intra-articular injection, in an experimental arthritis mouse model, showed that this nanotherapy could efficiently suppress the inflammatory process, this effect being obtained with a low TNFα-siRNA dose (*i.e* 1µg)[88].

Gene therapy was also evaluated on a different aspect of inflammation, relying on the control of macrophage polarization. Indeed, M1 macrophages are pro-inflammatory and have a central role in host defence against infection, while M2 macrophages are associated with responses to anti-inflammatory reactions and tissue remodelling[89]. Therefore, re-polarization of macrophages from the M1 phenotypes to M2 phenotypes by plasmid DNA (pDNA), siRNA or miRNA, represents an exciting prospect for the treatment of inflammatory diseases. In this context, IL-10 pDNA was encapsulated into alginate-based nanoparticles decorated with tuftsin, a tetrapeptide located in the heavy chain of immunoglobulin G which actively targets macrophages[90]. After intraperitoneal administration, these NPs were found to concentrate in inflamed paws of arthritic rats, due to a continuous recruitment of macrophages in the inflamed tissues, and a sustained local and systemic IL-10 expression was observed. Another nano-formulation of IL-10 pDNA was designed, using hyaluronic acid-poly(ethyleneimine) (HA-PEI) NPs. In this study, IL-10 pDNA and IL-4 pDNA, who are both supposed to play a key role in the polarization of macrophages, were encapsulated into these NPs. It was found that the *in vitro* transfection occurred in peritoneal macrophages over-expressing CD44 receptor and increased M2 phenotype surface markers due to the expression of IL-4 and IL-10. Besides, the intraperitoneal administration of these NPs to LPS-induced inflamed mice also significantly increased the M2 markers expression, showed elevated levels of serum IL-10 and reduced inflammation[91]. When microRNA-223, which is a miRNA that has been proved to alter macrophage polarization and activation, was encapsulated in the same nanocarrier[92], similar re-polarization of macrophages and anti-inflammatory effects were observed *in vitro*[93].

Other similar approaches are described in Table 1. But the crucial message here is that if gene nanotherapy could be effective in pre-clinical rodent models, it remains urgent to validate the proof-of-concept in bigger animal models, closer to human diseases.

2.6. Biomimetic nanoparticles

When injected intravenously, most of the nanomedicines are rapidly captured and eliminated by the immune system if they are not PEGylated. Biomimetic nanoparticles are hybrid nanostructures in which the uppermost layer is similar to a cell membrane (*e.g*. erythrocytes, immune cells, cancer cells and platelets)[94, 95]. In this category are included cell membrane-coated nanoparticles and liposomes engineered with cell membrane proteins. This strategy brings the biological characteristics of the source cells and leads to an exhibited prolonged circulation of the nanoparticles and an active targeting capability; moreover, these biomimetic nanoparticles are less likely to be recognized by the immune system since the membrane coating has the inherent characteristics of the mother cells. Excellent reviews have been published in this field [96-99] and we cover here only the very recent publications.

Current clinical treatment of rheumatoid arthritis primarily targets the inflammatory response by using anti-cytokine biologics such as those inhibiting tumour necrosis factor alpha (TNF-α) and interleukin (IL-1). However, the response rate still remains unsatisfactory[100]. Since neutrophils play an important role in resolving inflammation and repairing tissues damage[101], in a very interesting approach Zhang *et al*., fused neutrophil membrane onto polymeric cores and injected these hybrid biomimetic nanoparticles into the knee joint in a mouse model of collagen-induced arthritis and in a human transgenic mouse model of arthritis. The results showed a significant therapeutic efficacy by reducing joint damage and suppressing overall arthritis severity[102]. Of note, the authors used a biodegradable polymer which is FDA approved (*i.e* PLGA), to prepare the nanoparticles core. In another strategy, macrophage membrane-coated polymeric nanoparticles have shown to bind and neutralize endotoxins and to inhibit systemic inflammatory response in a mice lipopolysaccharide (LPS) model of inflammation after intravenous injection[103].

In another study, biomimetic nanoparticles were synthesized using membrane proteins purified from activated J774 macrophages and loaded with rapamycine. In a model of *ApoE*$^{-/-}$ mice with atherosclerotic plaques, it was observed that systemic injection of these hybrid NPs was able to suppress cell proliferation within the aorta[104].

Other strategies have been developed such as leukocyte-mimetic liposomes with the ability to translocate through inflamed endothelial cell layers[105]. Macrophage-derived microvesicles-coated PLGA nanoparticles were able to target rheumatoid arthritis (RA) after intravenous injection, displaying significant enhancement of the therapeutic efficacy in a collagen-induced arthritis mouse model. Similarly, macrophage-coated nanoparticles encapsulating tacrolimus significantly suppressed the progression of RA in mice[106].

Together these studies suggest that hybrid biomimetic nanomedicines represent a new and promising approach, since they possess unique biodistribution characteristics exhibited by different cell types used and, flexible designs derived from adaptable nanoparticle cores. However, some important concerns remain including possible immune reactions and complement activation after their administration. Besides, the scaling-up and the sterilisation of these biomimetic nanodevices also require specific developments.

2.7. Other applications of nanoparticles for immune system modulation

Strategies to activate or inhibit receptors implied in the inflammatory response are also potential ways to reduce inflammation (Table 1, Figure 3). One example is the liver X receptors (LXRs), whose activation in macrophages is atheroprotective and suppresses inflammation[107]. Thus, some recent studies focused on the formulation of LXR agonists in macrophage-targeted nanoparticles, such as mannose functionalized dendrimeric NPs[108], biodegradable diblock PLGA-b-PEG copolymer NPs[109], or synthetic high density lipoprotein NPs[110]. Intravenous injection of all these different nano-formulations were found to increase the expression of LXR target genes, to exert anti-inflammatory effects and to inhibit the development and necrosis of plaques in LDLr-deficient and *ApoE*-deficient mouse models of atherosclerosis. Particularly, these nano-formulations allowed an enhanced cholesterol efflux[108-110], a reduction of CD68-positive macrophage content of plaques by 50%[109] and an up-regulation of expression of ATP-binding cassette transporters[110].

Nanomedicines with immunosuppressants are also in development for improving the pharmacological efficacy and reducing the adverse events of these molecules. Topical administration of tacrolimus (FK506) loaded onto monolein nanoparticles were tested in a psoriasis-like skin inflammation in mice, and appeared to be more efficient than tacrolimus free dissolved in propylene glycol[111]. Positively charged Tacrolimus-loaded nanomicelles were found to prolong eye surface retention, to enhance corneal permeability, to exert anti-apoptotic effects on the corneal epithelium and overall to suppress expression of inflammatory related factors in a dry eye disease rabbit model.[112]. Besides, PEGylated liposomes loaded with the immunosuppressive drug FK506, were found to inhibit the expression of cytokines, such as interferon-γ and tumor necrosis factor-α, and reduced inflammation and fibrosis of the myocardium in a rat experimental autoimmune myocarditis after systemic administration[113]. Liposomal nano-formulations were also used to encapsulate cyclosporine A, another immunosuppressive drug. For example, intravenous administration of liposomal-cyclosporine A could improve cerebral ischemia and reperfusion injuries like neuroinflammation in a rat model, by inhibiting the inflammatory responses including MPO activity and TNFα level[114]. A further study on neuroinflammation in rats also proved the anti-inflammatory efficacy of cyclosporine-A using a cationic oil-in-water nanoemulsion upon intranasal administration[115].

Studies on mesalazine (5-ASA), an aminosalicylate anti-inflammatory drug mainly used in inflammatory bowel disease, focused in ameliorating the contact between the drug and the inflamed tissues by increasing adhesion and retention time. Practically, 5-ASA loaded onto silicon dioxide nanoparticles were tested in a dextran sodium sulfate-induced mouse model of ulcerative colitis. A significant decrease of IL-6, TNF-α and MPO was noted after oral administration of these NPs[116]. Along the same line, a very recent study designed an inclusion complex of 5-ASA in hydroxypropyl-β-cyclodextrin loaded onto chitosan NPs. This delivery system exhibited a sustained-release profile, and the NPs were more effective than the free drug in inhibiting the secretion of pro-inflammatory cytokine-stimulated colon cancer cells[117]. In another study, polymeric nanoparticles were rectally administered to protect low molecular weight heparin (LMWH) from intestinal degradation and to provide targeted delivery to inflamed tissue in experimental colitis mice. Such a combination shows a highly specific therapy by its protection against degradation in luminal environment and selective drug delivery inflamed intestinal tissue[118].

An unusual approach consisted in the design of prodrugs that will spontaneously self-assemble as nanoparticles in solution. This is what our group has developed through the construction of nanoparticles made of squalene, a natural and biocompatible lipid precursor of the cholesterol's biosynthesis. Of note, this lipid is already used in clinic as vaccine adjuvant. Squalene has been employed as a building block for the bio-conjugation with different hydrophilic drug molecules, and demonstrated the ability to self-assemble in aqueous medium in the form of nanoparticles[119, 120]. In general, these squalene-based nanoparticles were found to be non-cytotoxic, exhibited a high drug payload, an enhanced therapeutic response, and they were quite simple to prepare. Based on this concept, very recently, we discovered a new painkiller nanomedicine consisting in leu-enkephalin conjugated to squalene. And, the nanoparticles showed prolonged anti-pain effects on inflammatory pain in rats. Since they were found to target the inflamed area after intravenous administration and to act only on the peripheral opioid receptors, this nanomedicine opens the door to the treatment of intense pain without inducing tolerance and addiction, as observed with morphine and related synthetic opioids. The targeting of the inflamed area was found to occur by the EPR-like effect[121].

Squalene has also been conjugated to adenosine, a crucial regulatory autocrine and paracrine factor with anti-inflammatory properties[122, 123]. Adenosine is physiologically presents at low levels in unstressed tissues, and is rapidly released from the intracellular space to the extracellular space in response to pathophysiological conditions, such as hypoxia, ischemia, inflammation or trauma, to generate various cellular responses that aim to restore tissue homeostasis[122, 123]. Nevertheless, the use of adenosine in clinic is limited because of a very short plasma half-life and the need to administer high dosages which induce important side effects. Squalenoyl-adenosine nanoparticles may therefore represent a promising

approach in the treatment of inflammatory disorders surpassing adenosine limitations. Intravenous administration of these nanoparticles already demonstrated a significant neuroprotective effect in experimental models of stoke in mice and spinal cord injury in a rats, where inflammation is part of the diseases[124].

Since inflammation is accompanied by the overproduction of radical oxygen species[125], molecules with antioxidant capacities have been formulated as nanoparticles in order to increase the targeting of inflamed tissues and improve drug bioavailability. For example lycopene, a carotenoid drug with antioxidant and anti-inflammatory activity[126] and glutathione[127] were both tested in animals with experimental rheumatoid arthritis. Wu *et al.* also developed andrographolide-loaded poly(ethylene glycol) and poly(propylene sulphide) micelles which showed to synchronically alleviate inflammation and oxidative stress in an *ApoE*$^{-/-}$ atherosclerotic mice model[128]. In addition, our group recently developed a novel antioxidant/anti-inflammatory multidrug squalene-based nanoparticle formulation, allowing simultaneous delivery of adenosine and tocopherol in tandem to targeted sites by exploiting dysfunctions of the endothelial barrier at the sites of acute inflammation. These nanoparticles demonstrated promising anti-inflammatory and protective effects in mice models of endotoxemia and lethal systemic shock, with potential to treat uncontrolled inflammation associated with many diseases, including severe COVID-19[129].

Another interesting example is represented by metallic nanoparticles, the archetype being gold nanoparticles. The use of gold for therapeutic purposes dates back to Antiquity in China and Egypt, but only recently the scientific community developed a strong interest in gold nanoparticles for biomedical applications, especially because they can be easily functionalised and possess imaging and therapeutic capabilities[130]. The anti-inflammatory property of nanogold was recently explained by the down regulation of inflammatory mediators like TNF-α, IL-1β, COX-2 and transcription factor NF-kB (Nuclear factor-kB)[131]. Although systemic administration of these nanoparticles produced a significant anti-inflammatory activity *in vivo,* on different mouse models[132, 133], it has to be noted that gold, even if well tolerated by the body, is not a biodegradable material and may remain for a long time into the body, as previously demonstrated in a mouse model[134].

Apart from being used as drug delivery platforms, NPs have also been engineered to modulate the immune system. The induction of antigen-specific adaptive immunity exclusively occurs in lymphoid tissues, where T and B cells meet antigen or antigen-loaded APC (dendritic cells, macrophages). Since dendritic cells can activate T cells, vaccination protocols targeting DCs are promising approaches to enhance immune responses. When injected into the blood, nanoparticles interact most frequently with antigen-presenting

cells (APCs). Among the APCs, dendritic cells (DCs), which are the most specialized, are capturing and processing antigens before migration to lymphoid tissues, allowing T or B cells activation. By this way, nanoparticles may allow modulating the immune response. For example, De Koker *et al.* engineered hybrid nanoparticles composed of silica- poly(methacrylic acid) polymer. When injected *in vivo*, these NPs target and accumulate in lymph nodes, suggesting a possible application for the lymphatic delivery of antigens and immune-modulation[135]. And Muller *et al.* designed a versatile nanoparticle vaccine platform to promote an antigen-specific humoral response. These NPs were able to sustain a prolonged antigen presentation to APCs and to produce a strong immune response, as compared to the free antigen. Moreover, the size, charge, and surface characteristics of the NPs were found to be key parameters for improving the lymphatic trafficking of the NPs and their subsequent uptake by APCs[136].

To overcome resistance or production of antibodies which may occur after treatment with Rituximab (anti-CD20), another interesting approach was developed by Kopeček *et al*. who developed polymer prodrugs to target B cells. This approach, initially tested for B-cell malignancy treatment[137-140], was recently evaluated in a pre-clinical model of inflammatory rheumatoid arthritis (RA)[141]. The treatment, tested in a collagen-induced rheumatoid arthritis in mice, was composed of two conjugates: (i) a bispecific engager, Fab′-MORF1 (obtained by linking Fab′ fragment of CD20 mAb to the 3′ end of a morpholino oligonucleotide (MORF1) via a thioether bond) and (ii) a receptor crosslinking mediated by HPMA-based P-(MORF2). Compared to untreated mice, a delayed progress of RA was observed. And this new approach could open the way for the treatment of other autoimmune diseases.

However, this research area based on the modulation of the immune system has mainly been developed for cancer immunotherapy (see reviews[142-144]), while the studies reporting the modulation of immune system in other inflammatory diseases are less. In this sense, Gao *et al.*, designed an innovative antibacterial vaccine. The authors used *Escherichia coli* as a model pathogen membrane and coated them onto small gold nanoparticles (AuNPs) with a diameter of 30 nm. When injected subcutaneously, the NPs induced rapid activation and maturation of dendritic cells in the lymph nodes of the vaccinated mice, with in addition, the generation of durable antibody responses. These results demonstrated that using natural bacterial membranes to coat synthetic nanoparticles holds great promise for antibacterial vaccines[145]. Autoimmune diseases are caused by antigenically complex immune responses of the adaptive and innate immune system against specific cells, tissues or organs. Type 1 diabetes is a T cell-dependent autoimmune disease that is characterized by the destruction of insulin-producing β cells in the pancreas. Yeste *et al.*, engineered nanoparticles to deliver a tolerogenic molecule, for inducing a tolerogenic phenotype in DCs. A significant delay of diabetes onset was observed in nonobese diabetic mice receiving this immunomodulatory nanoformulation[146]. For the future, a deeper understanding on the NP-immune cell

crosstalk could guide the development of nano-immunotherapeutic approaches with an increased therapeutic efficacy.

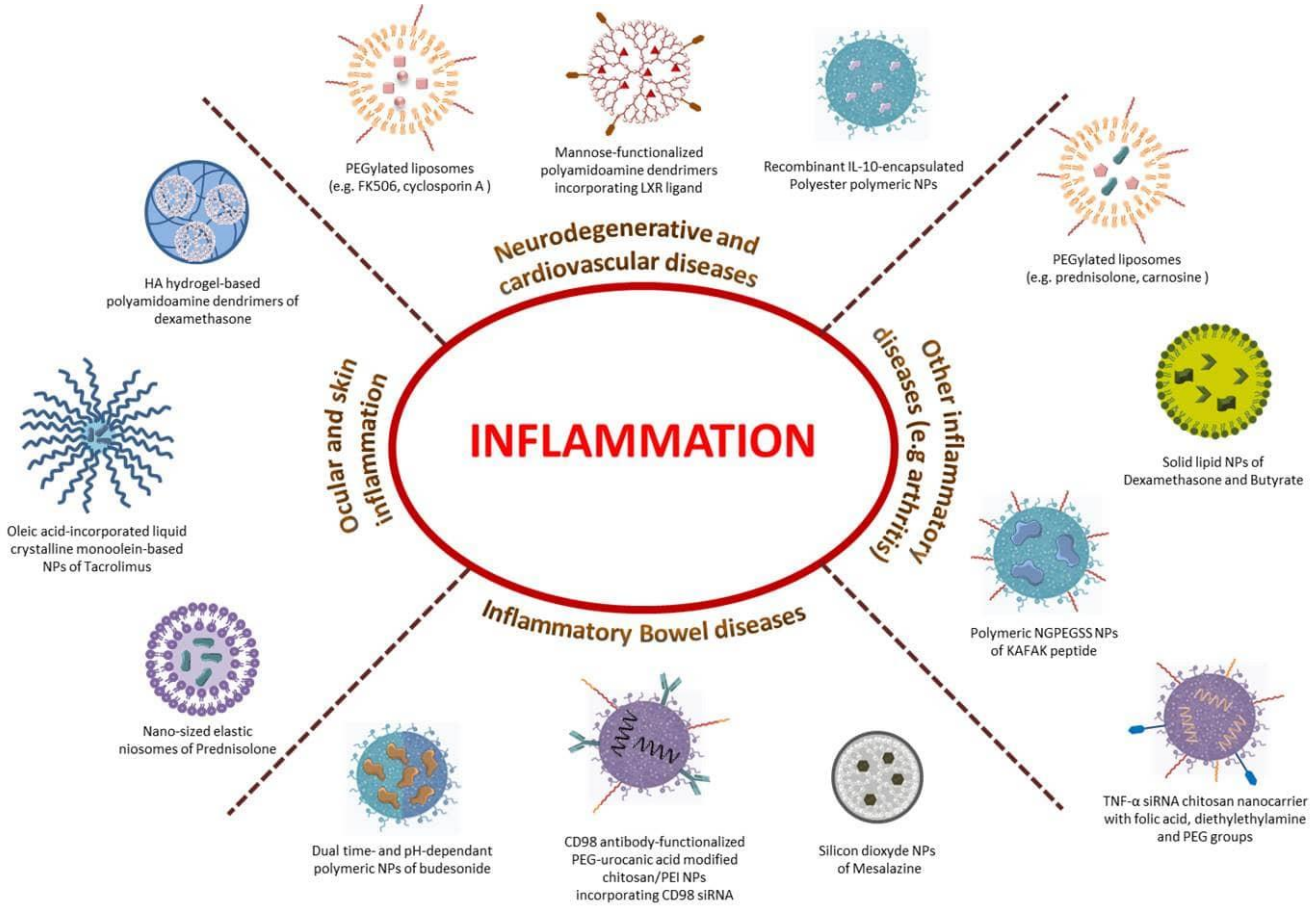

Figure 3: Examples of anti-inflammatory diseases and their innovative nanomedicines.

A large spectrum of materials and different strategies are developed for the treatment of inflammatory diseases.

Table 1: Some examples of new innovative nanomedicine systems for pre-clinical therapies against inflammatory disorders

Nanocarrier	Active principle	Inflammatory lesion	Animal model	Treatment time	Tested doses and route of administration	Main results	Ref
Eudragit S100 polymeric NPs	Prednisolone	Healthy	Wistar Albino rats	Every 30mins, from 1h to 6h	5 mg/kg of NPs, oral administration	• Specific colon targeting with a lag time	[45]
Pegylated liposomes	Prednisolone	Renal ischemia and reperfusion injury	8-week-old male LEW/HanHsd rats	96h	10 mg/kg of NPs, intravenous (i.v.) injection	• Specific accumulation in inflamed kidney • Increase of anti-inflammatory macrophages recruitment • Decrease of MCP-1 mRNA production	[47]
Hyaluronic acid-coated solid lipid NPs	Prednisolone	Collagen-antibody induced model of arthritis in Freud's adjuvant	6-week-old male DBA/1 mice	4 injections, once every three days	15 mg/kg of equivalent prednisolone each time, intra-articular injections	• Selective accumulation in inflamed tissue • Good therapeutic efficacy based on analysis of joints, pannus formation, bone preservation and reduction of pro-inflammatory cytokines	[170]
Nano-sized elastic niosomes	Prednisolone	Clove oil-induced severe ocular inflammation	Albino rabbits	Every 4h, 3 times a day, for 6 days	Equivalent to 500 µg of prednisolone (A or P) each time, ocular delivery	• Time for complete healing reduced to half • Significant decrease of intraocular pressure elevation	[50]
Polycaprolactone NPs dispersed in fibrin glue-based gel system	Methyl-prednisolone sodium succinate	Acute spinal cord injury	Male Wistar Albino rats	24h	Doses = N/A, topical and intraperitoneal administration	• Reduced damage on spinal cord • Decrease in caspase 3 and pro-inflammatory cytokines levels	[51]
Hyaluronic acid hydrogel-based hydroxyl-terminated polyamidoamine dendrimers	Dexamethasone	Corneal alkali burn model	8-week-old Lewis rats	24h, 72h, 7 days or 14 days	Equivalent to 1.76 mg /kg of Dex, subconjunctival injection	• 1.6-fold better anti-inflammatory activity at 10-fold lower concentration than free drug *in vitro* • *In vivo*: corneal features improvements, and decrease in macrophage infiltration and pro-inflammatory cytokines production	[52]

Poly(ethylene glycol)-poly (ε-caprolactone) polymer micelles	Dexamethasone	Adjuvant arthritis model by *mycobacteria* inoculation in Freund's adjuvant	6 to 8-week-old Wistar rats	4 injections of Dex, on days 14, 16, 18, 20 after arthritis induction	0.8 mg/kg of Dex, intravenous injection	• Paw swelling and erythema suppression • Down-regulation of pro-inflammatory cytokines • Protection of articular cartilage and bone from degradation and erosion	[53]
Spherical polymeric nanoconstructs	Dexamethasone	Dextran sodium sulfate-induced model of arthritis	8-week-old female C57Bl/6J mice	At day 2 after lesion: 6 consecutive treatments distributed until 16 days	5 mg/kg each time, i.v. injections	• Reduced weight loss and rectal bleeding • Reduced macrophage infiltration and pro-inflammatory cytokines production	[54]
Solid lipid NPs	Dexamethasone and Butyrate	Dextran sodium sulfate-induced model of arthritis	8-week-old male BALB/c mice	Daily treatment started from day 6 after lesion, for 3 days	0.1 mg/kg of dexamethasone and 4 mg/kg of Butyrate, oral administration	• Significant decrease of pro-inflammatory cytokines, more effectively at doses 10-fold lower than with free drugs	[55]
N-(2-hydroxypropyl)methacrylamide (HPMA) copolymer NPs	Dexamethasone	Adjuvant-induced arthritis	Male Lewis rats	One injection, at day 14, 15, 16 or 17 after arthritis induction	10 mg/kg of dexamethasone, intravenous injection	• Better systemic bone quality and bone protection • Amelioration of joint inflammation	[56]
Dual pH- and time-dependant polymeric NPs composed of Eudragit FS30D and Eudragit RS100	Budesonide	Dextran sodium sulfate-induced model of colitis	7-week-old mice	2h, 6h, or 10h	0.5 mg/kg of drug (0.168 mg/kg of budesonide), oral administration	• Improved colon-specific drug targeting • Body characteristics improvement	[58]
PLGA NPs	Budesonide	Oxazolone-mediated experimental colitis	8 to 12-week-old BALB/c mice	18h	42 µg of NPs, oral administration	• Selective targeting at the site of inflammation	[60]
Phosphatidyl serine:phosphatidyl choline (3:7 mol/mol) liposomes	Recombinant mouse IL-10	12 weeks High Fat Diet-induced obesity and atherosclerosis	C57Bl/6 mice	One treatment after 12 weeks of diet	1 µg/mouse of equivalent rIL-10, intraperitoneal injection	• Significant decrease in visceral fat weight • Reduced size of adipocytes • Reduced IL-6 and TNF-α secretion, and level of alanine amino transferase (decreased liver injury)	[69]

Biodegradable polyester polymeric NPs made with core polymer I, II and PLGA-PEG-ColIV	Recombinant mouse IL-10	Zymosan A (0.2 mg/mouse)-induced peritonitis (1) and 12 weeks of Western Diet-induced atherosclerosis (2)	8 to 10-week-old female C57Bl/6J (1) and 8 to 10-week-old male $Ldlr^{-/-}$ (2)	4h treatment (1) and 1/week for 4 weeks (2)	100 or 500 ng/mouse of equivalent rIL-10 (1) and 5 µg of rIL-10/ i.v. injection (2)	• Improvement of fibrous cap thickness • Reduction of necrotic core area • Tempered inflammation in peritonitis with decrease in polymorphonuclear neutrophils infiltration • Better macrophage targeting ability	[70]
Poly(NIPAm-co-AMPS) NPs	Anti-inflammatory cell penetrating peptide KAFAK	Osteoarthritis model induced by removal of native aggrecan of cartilage explants and IL1β treatment	3-month-old bovine knee joint explants	One treatment after 2 days of culture	50 µg NPs, treatment on cartilage explants	• Specific targeting of inflamed joint tissues • Reduction of pro-inflammatory cytokines	[79]
NGPEGSS NPs system incorporating NIPAm, AMPS, BAC, and PEG polymers	Anti-inflammatory cell penetrating peptide KAFAK	Osteoarthritis model by removal of native aggrecan cartilage explants and IL1β treatment	3-month-old bovine knee joint explants	One treatment after 2 days of culture	50 µg NPs, treatment on cartilage explants	• Specific targeting of inflamed joint tissues • Significant suppression of IL-6 production on days 4,6 and 8	[81]
Chitosan/poly(γ-glutamic acid) NPs	Diclofenac	LPS-induced inflammation	*In vitro* human macrophages	24h, 48h	0.7 mg/mL, *in vitro* treatment	• Rapid internalization (within 3 hours) without toxicity below 0.7 mg/mL • Stimulation of production of prostaglandin E2 Reduction of IL-6 production	[64]
Mannose-modified trimethyl chitosan-cysteine NPs	TNF-α siRNA	Acute hepatic injury induced by LPS and D-GaIN	Male Sprague-Dawley rats	2h	20 µg or 50 µg of equivalent TNF-α siRNA/kg, oral administration	• Effective TNF-α knockdown at low doses • Dramatic alleviation of inflammatory conditions in the liver (congested central vein, swollen, disarranged hepatocytes, and broken cytolemma)	[82]

Nanoemulsion formulation of cationic lipid DOTAP	TNF-α siRNA	LPS intranigral injection-induced Parkinson's disease model	Male Sprague-Dawley rats	6h, 24h	1.5 mg/kg of NPs, intranasal administration	• Preferential concentration into the brain Brain downregulation of TNF-α	[115]
Poly(ethylene glycol)-poly(caprolactone) polymer micelles conjugated with Tat cell-penetrating peptide and siRNA targeting TNF-α	TNF-α siRNA	transient middle cerebral artery occlusion model of cerebral ischemia-reperfusion injury	10-week-old Sprague-Dawley male rats	At 30 min after middle cerebral artery occlusion	Equivalent of 30 µg of siRNA, intranasal administration	• Transport of the drug to the brain directly across the nasal mucosa, without going through the BBB • Reduced infarcted area and better neurological scores • Significant suppression of TNF-α production	[84]
Dendrimers functionalized with cationic pyrrolidinium or morpholinium surface groups	TNF-α siRNA	LPS-induced acute lung inflammation model by intranasal administration of LPS	6 to 8-week-old female CD-1 mice	28h, 96h	Pre-treatment 24h before inflammation, with 2 mg/kg of eq. siRNA concentration, intranasal administration	• Specific targeting in macrophages • Major inhibition of TNF-α • Modulation of all other cytokines (strong anti-inflammatory effect)	[85]
Modified chitosan nano-carrier deploying folic acid, diethylethylamine and PEG groups	TNF-α siRNA	Collagen-antibody induced model of arthritis	8 to 12-week-old female DBA/1 mice	Treatment at day 1, 3, 5, 7 after induction of inflammation and sacrifice at day 10	4 intraperitoneal injections at 50 µg of siRNA each	• Significant decrease of inflammation observed by improved clinical scores and lower TNF-α concentration in inflamed tissues • Decrease in articular cartilage destruction and bone loss	[86]
Tuftsin/alginate NPs	IL-10 pDNA	Adjuvant arthritis model by inoculation with *Mycobacterium butyricum* in Freund's adjuvant	Male Lewis rats	From 1h to 24h	Intraperitoneal injection at day 19 post-lesion of 3 mg of NPs	• Specific targeting of macrophages in inflamed paws • Continuous recruitment of M2 macrophages to inflamed tissues • Sustained local and systemic IL-10 expression	[90]

Hyaluronic acid/ polyetyleneimine NPs	IL-10 and IL-4 pDNAs	Intraperitoneal injection of Brewer-thioglycollate medium to recruit peritoneal macrophages	6 to 8-week-old C57Bl/6 mice	48h	2h post inflammation, intraperitoneal injection of 100 µg of equivalent pDNA	• Effective targeting of peritoneal macrophages over-expressing CD44 receptors • Significant increase of Arg/iNOS ratios and CD163 expression • Reduced level of TNF-α and IL-1β in peritoneal macrophages and fluid • Increased IL-10 and IL-4 expressions	[91]
Hyaluronic acid/chitosan NPs	Cytokine response modifier A pDNA	Anterior cruciate ligament transection model of osteoarthritis	6 to 8-week-old Male Sprague-Dawley rats	3 injections, every 4 weeks starting 4 weeks after lesion	4 µg of NPs/rat each time, i.v. injections	• Significant inhibition of cartilage damage, synovial inflammation, and loss of type II collagen • Down regulation of IL-1β, MMP-3 and MMP-13 in synovial tissues	[48]
Mannose-functionalized dendrimeric NPs using polyamidoamine dendrimer	Liver X receptor (LXR) ligand T0901317	12 weeks of Western Diet to induce atherosclerosis	$Ldlr^{-/-}$ mice	Once per week for 4 weeks after the 12 weeks of diet	200 µg of NPs by i.v. injection	• Specific uptake by macrophages and not hepatocytes in atherosclerotic plaques • Increased expression of LXR target genes (ABCA1/ABCG1) • Enhanced cholesterol efflux • Significant reduction in atherosclerotic plaque progression, plaque necrosis, and plaque inflammation	[108]
Biodegradable diblock PLGA-b-PEG copolymer NPs	Liver X receptor (LXR) ligand GW3965	Zymosan A-induced peritonitis	$Ldlr^{-/-}$ mice	5h treatment (1) or over 2 weeks (2)	10 mg/kg of equivalent agonist 1h prior to Zymosan injection (1) or 6 injections of 10 mg/kg (2), i.v. injections	• Significantly more efficient than free drug for inducing LXR target gene expression and suppressing inflammatory factors • Reduction of CD68-positive macrophage content of plaques (by 50%)	[109]

Phospholipid-reconstituted ApoA-I peptide-derived synthetic HDL	Liver X receptor (LXR) ligand T0901317	Atherogenic diet for 14 weeks	8-week-old male ApoE-deficient mice	3 times a week for 6 weeks	30 mg/kg of NPs, which is equal to 1.5 mg/kg of ligands, i.v. injections	• Specific accumulation in plaque and plaque regression • Up-regulation of expression of ATP-binding cassette transporters and increased cholesterol efflux in macrophages	[110]
Raspberry-like core/satellite NPs with methyl viologen-functionalized polymeric NPs (core) and azobenzene (corona)	IL-1Ra antagonist protein	Healthy	8 to 10-week-old male Sprague-Dawley rats	One treatment	5 µg of cy7-labelled NPs, intra-articular injection	• Improved retention time due to prolong half-life time of IL-1Ra in the joint compared to soluble form	[77]
Oleic acid-incorporated liquid crystalline monoolein-based NPs	Tacrolimus (FK506)	Daily topical dose (1.5 mg) of Imiquimod on shaved back for 5 days to induce a skin inflammation (psoriasis)	8 to 11-week-old BALB/c mice	Once a day, for 7 days after inflammation induction	30 µg of equivalent Tacrolimus each time, topical administration	• Significant increase in the amount of drug permeated and retained • More efficient in the treatment of skin inflammation than Tacrolimus in propylene glycol	[111]
Positively charged PEP−PEG−PBG polymer micelles	FK506	Dry eye disease animal model by subcutaneous injection of scopolamine	6-week-old C57BL/6 mice	4 times a day for 5 days	Topical application of 30 µg of the formulation each time	• Significantly reduce apoptosis of corneal epithelium • Suppression of inflammatory-related factors (TNF-α, IL-6, MMP-9…)	[112]
PEGylated liposomes	FK506	Experimental autoimmune myocarditis model induced by immunization with porcine myosin	7-week-old male Lewis rats	Treatment on day 14 and 17, sacrificed on day 21	0.035 mg/kg, 0.17 mg/kg or 0.35 mg/kg of equivalent drug per treatment, i.v. injection	• Increased level of FK506 in both plasma and hearts • Suppression of pro-inflammatory cytokine expression such as TNF-α and IFNγ • Reduced inflammation and fibrosis in the myocardium	[113]
PEGylated liposomes	Cyclosporin A	Transient middle cerebral artery occlusion by 90 min brain ischemia induction,	Male Wistar rats	5min after ischemia, for 48h	2.5 mg/kg of equivalent cyclosporin A, i.v. injection	• Significant recovery of the infarct size, brain oedema, and neurological activities compared to free drug	[114]

		followed by 48h reperfusion				• Inhibition of inflammatory responses including MPO activity and TNF-α levels	
Omega-3 fatty acid rich flaxseed oil-based nanoemulsion system	Cyclosporin A	LPS model of neuroinflammation	Sprague-Dawley rats	9h	Pre-treatment 3h prior to inflammation, with 5 mg/kg of NPs, intranasal administration	• Higher uptake in major regions of the brain • Inhibition of pro-inflammatory cytokines	[115]
Silicon dioxide NPs	Mesalazine	5% dextran sodium sulphate-induced ulcerative colitis model	8 to 9-week-old male BALB/c mice	Once a day, for 7 days, sacrifice on day 8	100 mg/kg per day of NPs, oral administration	• Significant decrease of IL-6 and TNF-α cytokine production and MPO activity	[116]
Squalene-adenosine NPs	Tocopherol (VitE)	Endotoxemia model of inflammation induced by intraperitoneal injection of LPS	8 to 12-week-old male C57BL/6 and female BALB/c mice	One treatment, 30 min after LPS injection	15 mg/kg SQAd NPs (5.5 mg/kg of equivalent adenosine) and 15 mg/kg VitE, intravenous injection	• Significant decrease in TNF-α and increase in IL-10 production • Significant reduction of MCP-1 and IL-6 in the lung and kidney • Mitigation of MDA levels • Improved survival rate and clinical scores in lethal LPS model	[129]

* Lack of information in a table cell was noted N/A (not available).

3. Clinical trials and commercial markets

Many nanomedicines, mainly liposomes, have entered clinical practice, and even more are being investigated in clinical trials for a wide variety of therapeutic and imaging indications. To date, only few tenths of nanomedicines are FDA approved and few hundreds of clinical trials are investigating new nanomedicines[147], cancer therapy being the main application. Recently, three other nanomedicines have been approved: Patisiran/ONPATTRO, VYXEOS, AND NBTXR3/Hensify[148]. However, to the best of our knowledge, very few anti-inflammatory nanoparticles have succeeded to reach clinical trials (Table 2).

Anti-inflammatory liposomal formulations are one of the most promising nanomedicines for the treatment of acute and chronic inflammation. For example, after intravenous administration, long-circulating prednisolone-containing liposomes were found to accumulate into macrophages of patients with symptomatic iliofemoral atherosclerosis, as a result of prolonged circulation half-life. Nevertheless, in contrast to the pre-clinical efficacy data obtained in rabbits[149], short-term treatment did not reduce arterial wall permeability or arterial wall inflammation in humans[150-152]. This may have resulted from an insufficient dose of prednisolone reaching the plaque; and although increasing the dose will likely resolve this issue, it would also introduce the risk of adverse effects. Another possible explanation may be a timing issue since, based on pre-clinical results, the authors evaluated the clinical results only after 10 days of treatment. But most studies evaluating the impact of anti-inflammatory agents in human cardiovascular diseases showed therapeutic efficacy only after several weeks of treatment [150]. Despite the lack of anti-inflammatory activity, the study proved for the first time that targeted delivery of nanomedicines to atherosclerotic lesions is feasible in humans. This could provide guidance for the development of future nano-formulations for the imaging or the treatment of atherosclerosis.

Interestingly, such prednisolone-encapsulated liposome formulations were also tested in phase II clinical trials for the treatment of arteriovenous fistula[153], graves ophthalmopathy, and ulcerative colitis[154]. Recently, the clinical study for the treatment of ulcerative colitis exhibited strong positive results in 70% of the patients, with 4 patients out of 13 in remission, and 7 out of 13 showing a reduction of the endoscopy sub-score[155]. In addition, a phase III clinical trial for the treatment of rheumatoid arthritis has started but no results are available for the moment.

A liposomal formulation of cyclosporine A in a lipogel was also developed for a topical application to treat mild to moderate stable plaque psoriasis and tested in an early-phase clinical trial[156]. The clinical performance of this liposomal gel was superior to that of cyclosporine incorporated in a conventional dermatological formulation at equal drug concentration. Pharmacokinetic studies and other safety

evaluation protocols indicated the good tolerance of the liposomal formulation which has induced uniform reduction of plaque elevation[156]. Other liposomal formulations are currently in development, such as liposomal corticosteroids or liposomal dexamethasone, whose clinical translation has started very recently in patients with progressive multiple myeloma[157].

Pitavastatin is a statin known to have vasodilating properties and to modulate inflammatory response. To evaluate the safety, tolerability, and pharmacokinetics for intravenous administration of Pitavastatin-loaded PLGA nanoparticles (NK-104-NP), a phase I clinical trial was recently conducted in healthy Japanese male subjects. The study proved that NK-104-NPs exhibited dose-dependent pharmacokinetics and was well tolerated with no significant adverse effects in healthy volunteers[158].

In a very recent pilot clinical study, an oil-in-water nanoemulsion containing all trans- retinoic acid (Tretinoin), showed a good efficiency against acne after topical application[159]. Similarly, when subjected to focal thermolysis of sebaceous gland by near infrared laser, silica-gold nanoshells (150 nm) coated with PEG, were effective to provide a significant reduction in occurrence and appearance of inflammatory lesions[160].

In conclusion, very few nanomedicines specifically designed for the treatment of inflammation are nowadays assessed in clinical trials. In order to operate translation from the bench to the bedside, several experimental challenges need to be addressed. Key issues related to the clinical development of anti-inflammatory nanoparticles include biological challenges such as understanding the biology of specific diseases and the biological interaction of nanoparticles in patients, commercialization hurdles related to large-scale manufacturing, to cost-effectiveness in comparison to current therapies and to regulatory standards, biocompatibility and safety[161]. Reducing complexity in nanoparticle design and synthesis should, therefore, be one of the main goals to generate clinically translatable nano-sized therapeutics.

Table 2: Some examples of nanomedicines under clinical trials

Nanocarrier	Active principle	Disease	Patients and clinical phase	Main Results	Ref.
PEGylated liposomes	Prednisolone	Illio-femoral atherosclerosis	14 patients, mean age 70 years (± 7 years)	• the treatment did not reduce arterial wall permeability or inflammation • prolonged circulation half-life of prednisolone	[150]
PEGylated liposomes	Prednisolone	Moderate to severe active ulcerative colitis	18 patients (iv administration)	• 54 weeks after initiation of treatment only 4 patients out of 13 in remission	[155]
Liposome	Cyclosporine (lipogel or cream)	Chronic plaque psoriasis	38 patients (receiving cyclosporine lipogel or conventional cyclosporine cream or placebo	• 14 weeks after initiation of treatment, complete clearance was observed in lesion sites in 41% patients treated with cyclosporine lipogel and none for patients treated with cyclosporine cream or placebo gel	[156]
Glutatione-PEGylated liposomes	Methyl prednisolone	--	Assessment of safety, pharmacokinetics and pharmacodynamics	• slow release formulation with reduced toxicity and prolonged decrease in the lymphocyte count	[171]
PLGA	Pitavastatine	Healthy volunteers	40 patients, Phase I, iv administration	• well tolerated • no significant adverse response	[158]
Nanoemulsion (oil in water emulsion)	Tretinoin	Acnee vulgaris	10 patients with mild to moderate acnee vulgaris lesions	• clinical safety of the formulation in humans	[159]
PEGylated silica - gold nanoshells	Photothermolysis (ultrasound 10 sec to 10 W/cm²)	Acnee vulgaris	37 patients	• efficacy in inducing photothermal disruption of acne vulgaris	[172]

4. General discussion

In recent years, cellular and molecular advances have improved the comprehension of the inflammatory response, leading to the discovery of multiple targets for biological therapies against inflammatory diseases. In addition to a variety of safe and quite effective anti-inflammatory agents already available, such as aspirin and other nonsteroidal anti-inflammatory drugs, many biological agents have also been developed including antibodies and nucleic acids for cytokine inhibition or to reduce the extravasation of immune cells into the inflamed tissues[162]. In spite of promising progresses made in developing such treatments, the widespread distribution of the inflammatory signaling pathways in multiple cell types and tissues leads to important off-target side effects and to systemic toxicities. Combined with a relatively low bioavailability or/and limited half-lives, necessitating repeated and expensive high dosages responsible for severe side effects, current therapies still remain with clinical hurdles to overcome.

This has prompted the academic research to design nanocarriers in order to improve the delivery of anti-inflammatory compounds. After administration, such nanomedicines follow a kinetic process of absorption, distribution, metabolization and elimination. In addition, they distribute in a different way in the body depending if their surface is naked, decorated with PEG, or loaded with a ligand for an active targeting. In this way, numerous nanoparticles loaded with various anti-inflammatory molecules were developed and have shown real therapeutic improvements in pre-clinical models (Figure 3).

Other than being drug delivery carriers, nanoparticles have also been used as vaccine adjuvant and for modulation of the immune system. Different data suggest that the shape of the NPs can affect the interactions with innate immune system. Once injected into the body the NPs immediately encounter the innate immune system and generate specific response as foreign substances. Apart that the coating with poly (ethylene glycol) delays the protein corona formation at their surface, the physicochemical properties of NPs (size, charge, hydrophobicity and stiffness) will also determine their interaction with the innate system. For example, it was shown that the uptake of nanorods by macrophages was more efficient than the uptake of nanospheres[163]. And a comparison of the complement activation using spherical, rods and disks polystyrene NPs evidenced that rods and disks generated more important complement activation than spheres at later time points[164]. But today it remains still unclear which physical properties or chemical composition of nanoparticles can drive to immune modulation.

There is also an urgent need to develop new *in vitro* and *in vivo* pre-clinical models, better mimicking the pathophysiology of the disease in humans. For instance, the EPR effect has become during decades a general condition to allow the targeting of nanoparticles or liposomes through leaky vasculatures towards

tumor or inflamed areas, in most of the experimental pre-clinical rodent models. But in the clinical reality, the occurrence of the EPR effect is far to be systematic. Various other parameters need to be taken into consideration, like the distribution and diffusion deep into the inflamed tissue (which is bigger in humans than in mice), the extend of drug release, the blood perfusion of the inflamed area, the nature of the extracellular matrix, *etc*. Thus, concerning the inflammatory processes, are the pre-clinical models really reliable? And to what extent the observed vascular permeability in pre-clinical models is transposable to human? Answering those questions and developing clinically relevant animal models is a key to allow a better selection of disease-driven nano-formulations[165].

Different administration ways, oral, local, topical or intravenous have been tested with anti-inflammatory nanomedicines. While intravenous delivery allows a direct access to the whole body, the local delivery proved to be effective, allowing to directly concentrate the drug into the diseased tissue. If the choice of administration route depends evidently on the localization of the inflammation site, it should also customize the choice of the materials and the design of the nanomedicines (presence or not of PEG or other ligands). The route of administration such as intravenous or the direct injection into the inflamed site can influence the induction of the immune response. Thus, when NPs are administered intravenously, the protein corona formed at the surface of the NPs and the complement eventually activated can alter biodistribution and therapeutic efficacy. But when the NPs are administered locally, the immune response is mainly dependent on the tissue residential cells.

Chemical and physical properties of the NPs, including size, surface charge, and surface chemistry, are other important factors in the context of systemic inflammation. For example, it was observed that LPS-induced inflammation resulted in splenic macrophage polarization and altered leukocyte uptake of polystyrene nanoparticles depending on their size[166]. Concerning local administration, poly(lactic acid) particles need a size of at least 3 μm to guarantee the retention in inflamed joints[167].

Of note, as detailed in this review, different types of nanocarriers have been employed for the delivery of anti-inflammatory drugs, including liposomes, polymer nanoparticles, micelles or prodrugs. To compare their delivery abilities is quite hazardous because the experimental conditions are diverse. Liposomes are evidently the most advanced in terms of clinical translation and some liposomal formulations are even FDA approved. However, they generally display a lower stability in biological fluids than polymer nanoparticles or prodrugs, sometimes leading to a fast drug leakage. And their drug loading capacities are often limited. On the other hand, in case of intravenous administration, polymer micelles may disassemble due to a high critical micellar concentration which doesn’t occur with polymer nanoparticles which may be considered as frozen micelles.

But as shown in this review, the clinical translation of the nanoparticles remains still limited. This is due, in part, to the complexity related to the pharmaceutical development of nanomedicines, including their biocompatibility and safety. We also note that chronic inflammatory diseases bring together cofounding factors such as age, overweight and obesity and sometimes genetic predisposition to cite only a few. However, most of the preclinical studies to assess anti-inflammatory nanomedicines are performed on young and healthy animals, with an induced accelerated inflammatory disease and subject to normal fed. These factors should therefore be carefully considered in order to improve the translation from preclinical models to the clinic. In addition, the difference between rodent and human immune systems may represent an important obstacle for translating studies performed in mice into human clinical trials. This is the reason why there is an urgent need to develop pre-clinical experimental models with pathophysiological similarities closer to human inflammatory disease.

Bio-inspired nanodevices represent a new generation of innovative nanomedicines with the aim to mimic natural circulatory cells. They are able to increase the blood circulation time and to improve the distribution of the loaded drug towards the inflammatory cells and tissues. However, their immunogenicity, scale-up and characterization remain important hurdles before starting clinical trials.

Besides, problems related to the scaling-up, the government regulations and the overall cost-effectiveness if compared to the current available anti-inflammatory therapies are other important limitations in the success of the anti-inflammatory nanomedicines in general. The often complex architectural design of many nanomedicines described in this review, likely results in difficulties for performing reproducible sample preparations, safe and in good quantities[168]. And this is particularly important since a slight modification of the size, the shape and/or the nanoparticle surface chemistry may dramatically influence the stability, the interaction with biological media, as well as, the biodistribution and clearance of the nanocarriers. Thus, reliable and standardized methodologies to obtain reproducible nanoparticles are absolutely required[169]. There is often a gap between the academic environment where innovative nanocarriers are designed and the industrial context, where reproducible preparation and manufacturing processes supported by analytical methodologies are needed.

5. Conclusion

As shown in this review, there is an increasing interest to improve the delivery of small drug molecules or biotherapeutics (*i.e.* nucleic acids, peptides, proteins) for the resolution of inflammatory diseases. This represents a unique opportunity for pharmaceutically developable nanoscaled drug delivery systems, especially to optimize drug safety and efficacy through improved biodistribution and pharmacokinetics and to resolve the issues related to the difficulty to administer fragile biomolecules.

Acknowledgments

The authors gratefully acknowledge the financial support from the 7th EuroNanoMed-II call for proposals, project NanoHeart n°ANR-16-ENM2-0005-01.

Conflict of interest

The authors declare no competing interest.

Author Contributions

The manuscript was written with the contribution of all the authors.

Bibliography

[1] R. Chovatiya, R. Medzhitov, Stress, inflammation, and defense of homeostasis, Mol Cell, 54 (2014) 281-288.

[2] W.F.E. Hossam M. Ashour, Md. Masudur Rahman , Hatem A. Elshabrawy Insights into the Recent 2019 Novel Coronavirus (SARS-CoV-2) in Light of Past Human Coronavirus Outbreaks, Pathogens 9(2020).

[3] A.A. Meo SA, Al-Khlaiwi T, Meo IM, Halepoto DM, Iqbal M, Usmani AM, Hajjar W, Ahmed N., Novel coronavirus 2019-nCoV: prevalence, biological and clinical characteristics comparison with SARS-CoV and MERS-CoV, Eur Rev Med Pharmacol Sci, 24 (2020) 2012-2019.

[4] T.S. Xiao, Innate immunity and inflammation, Cell Mol Immunol, 14 (2017) 1-3.

[5] G.S. Hotamisligil, Endoplasmic reticulum stress and the inflammatory basis of metabolic disease, Cell, 140 (2010) 900-917.

[6] M. Antonelli, I. Kushner, It's time to redefine inflammation, FASEB J, 31 (2017) 1787-1791.

[7] D.A. Cronkite, T.M. Strutt, The Regulation of Inflammation by Innate and Adaptive Lymphocytes, J Immunol Res, 2018 (2018) 1467538.

[8] R. Medzhitov, Inflammation 2010: new adventures of an old flame, Cell, 140 (2010) 771-776.

[9] D.D. Chaplin, Overview of the immune response, J Allergy Clin Immunol, 125 (2010) S3-23.

[10] D.G. Harrison, T.J. Guzik, H.E. Lob, M.S. Madhur, P.J. Marvar, S.R. Thabet, A. Vinh, C.M. Weyand, Inflammation, immunity, and hypertension, Hypertension, 57 (2011) 132-140.

[11] R. Molinaro, C. Boada, G.M. Del Rosal, K.A. Hartman, C. Corbo, E.D. Andrews, N.E. Toledano-Furman, J.P. Cooke, E. Tasciotti, Vascular Inflammation: A Novel Access Route for Nanomedicine, Methodist Debakey Cardiovasc J, 12 (2016) 169-174.

[12] M. Durymanov, T. Kamaletdinova, S.E. Lehmann, J. Reineke, Exploiting passive nanomedicine accumulation at sites of enhanced vascular permeability for non-cancerous applications, J Control Release, 261 (2017) 10-22.

[13] E.A. Azzopardi, E.L. Ferguson, D.W. Thomas, The enhanced permeability retention effect: a new paradigm for drug targeting in infection, J Antimicrob Chemother, 68 (2013) 257-274.

[14] D. Wang, S.R. Goldring, The bone, the joints and the Balm of Gilead, Mol Pharm, 8 (2011) 991-993.

[15] F. Yuan, L.D. Quan, L. Cui, S.R. Goldring, D. Wang, Development of macromolecular prodrug for rheumatoid arthritis, Adv Drug Deliv Rev, 64 (2012) 1205-1219.

[16] P. Calvo, B. Gouritin, H. Villarroya, F. Eclancher, C. Giannavola, C. Klein, J.P. Andreux, P. Couvreur, Quantification and localization of PEGylated polycyanoacrylate nanoparticles in brain and spinal cord during experimental allergic encephalomyelitis in the rat, Eur J Neurosci, 15 (2002) 1317-1326.

[17] G. Cavaletti, A. Cassetti, A. Canta, S. Galbiati, A. Gilardini, N. Oggioni, V. Rodriguez-Menendez, A. Fasano, G.M. Liuzzi, U. Fattler, S. Ries, J. Nieland, P. Riccio, H. Haas, Cationic liposomes target sites of acute neuroinflammation in experimental autoimmune encephalomyelitis, Mol Pharm, 6 (2009) 1363-1370.

[18] I. Tabas, C.K. Glass, Anti-inflammatory therapy in chronic disease: challenges and opportunities, Science, 339 (2013) 166-172.

[19] A. Banerjee, J. Qi, R. Gogoi, J. Wong, S. Mitragotri, Role of nanoparticle size, shape and surface chemistry in oral drug delivery, J Control Release, 238 (2016) 176-185.

[20] A.B. Jindal, The effect of particle shape on cellular interaction and drug delivery applications of micro- and nanoparticles, Int J Pharm, 532 (2017) 450-465.

[21] D.H. Jo, J.H. Kim, T.G. Lee, Size, surface charge, and shape determine therapeutic effects of nanoparticles on brain and retinal diseases, Nanomedicine, 11 (2015) 1603-1611.

[22] V. Agrahari, P.A. Burnouf, T. Burnouf, Nanoformulation properties, characterization, and behavior in complex biological matrices: Challenges and opportunities for brain-targeted drug delivery applications and enhanced translational potential, Adv Drug Deliv Rev, 148 (2019) 146-180.

[23] G.A. Duncan, M.A. Bevan, Computational design of nanoparticle drug delivery systems for selective targeting, Nanoscale, 7 (2015) 15332-15340.

[24] H. Li, X. Zhang, K. Wang, H. Liu, Y. Wei, Facile preparation of biocompatible and robust fluorescent polymeric nanoparticles via PEGylation and cross-linking, ACS Appl Mater Interfaces, 7 (2015) 4241-4246.
[25] M.J. Santos-Martinez, K. Rahme, J.J. Corbalan, C. Faulkner, J.D. Holmes, L. Tajber, C. Medina, M.W. Radomski, Pegylation increases platelet biocompatibility of gold nanoparticles, J Biomed Nanotechnol, 10 (2014) 1004-1015.
[26] J. Iqbal, B.A. Abbasi, R. Ahmad, T. Mahmood, B. Ali, A.T. Khalil, S. Kanwal, S.A. Shah, M.M. Alam, H. Badshah, A. Munir, Nanomedicines for developing cancer nanotherapeutics: from benchtop to bedside and beyond, Appl Microbiol Biotechnol, 102 (2018) 9449-9470.
[27] S. Tran, P.J. DeGiovanni, B. Piel, P. Rai, Cancer nanomedicine: a review of recent success in drug delivery, Clin Transl Med, 6 (2017) 44.
[28] K.S. Kim, G. Khang, D. Lee, Application of nanomedicine in cardiovascular diseases and stroke, Curr Pharm Des, 17 (2011) 1825-1833.
[29] V.M. Martin Gimenez, D.E. Kassuha, W. Manucha, Nanomedicine applied to cardiovascular diseases: latest developments, Ther Adv Cardiovasc Dis, 11 (2017) 133-142.
[30] M.V. F. Dormont, P. Couvreur, Nanoplumbers: biomaterials to fight cardiovascular diseases, Materials Today, 21 (2018) 122-143.
[31] M. Gharagozloo, S. Majewski, M. Foldvari, Therapeutic applications of nanomedicine in autoimmune diseases: from immunosuppression to tolerance induction, Nanomedicine, 11 (2015) 1003-1018.
[32] O. Veiseh, B.C. Tang, K.A. Whitehead, D.G. Anderson, R. Langer, Managing diabetes with nanomedicine: challenges and opportunities, Nat Rev Drug Discov, 14 (2015) 45-57.
[33] M. Goldsmith, L. Abramovitz, D. Peer, Precision nanomedicine in neurodegenerative diseases, ACS Nano, 8 (2014) 1958-1965.
[34] A.V. Kabanov, H.E. Gendelman, Nanomedicine in the diagnosis and therapy of neurodegenerative disorders, Prog Polym Sci, 32 (2007) 1054-1082.
[35] R. Molinaro, C. Corbo, M. Livingston, M. Evangelopoulos, A. Parodi, C. Boada, M. Agostini, E. Tasciotti, Inflammation and Cancer: In Medio Stat Nano, Curr Med Chem, 25 (2018) 4208-4223.
[36] L. Salvioni, M.A. Rizzuto, J.A. Bertolini, L. Pandolfi, M. Colombo, D. Prosperi, Thirty Years of Cancer Nanomedicine: Success, Frustration, and Hope, Cancers (Basel), 11 (2019).
[37] D.J. Irvine, E.L. Dane, Enhancing cancer immunotherapy with nanomedicine, Nat Rev Immunol, (2020).
[38] T.G. Dacoba, A. Olivera, D. Torres, J. Crecente-Campo, M.J. Alonso, Modulating the immune system through nanotechnology, Semin Immunol, 34 (2017) 78-102.
[39] P.J. Barnes, Glucocorticoids, Chem Immunol Allergy, 100 (2014) 311-316.
[40] E. Oppong, A.C. Cato, Effects of Glucocorticoids in the Immune System, Adv Exp Med Biol, 872 (2015) 217-233.
[41] E.-M.C. Hussain Ali, Maike Windbergs, Claus-Michael Lehr, Nanomedicines for the treatment of inflammatory bowel diseases, European Journal of Nanomedicine, 5 (2013) 23-38.
[42] M. Oray, K. Abu Samra, N. Ebrahimiadib, H. Meese, C.S. Foster, Long-term side effects of glucocorticoids, Expert Opin Drug Saf, 15 (2016) 457-465.
[43] J. Youshia, A. Lamprecht, Size-dependent nanoparticulate drug delivery in inflammatory bowel diseases, Expert Opin Drug Deliv, 13 (2016) 281-294.
[44] S.J. Kshirsagar, M.R. Bhalekar, J.N. Patel, S.K. Mohapatra, N.S. Shewale, Preparation and characterization of nanocapsules for colon-targeted drug delivery system, Pharm Dev Technol, 17 (2012) 607-613.
[45] A. Kumari, A. Jain, P. Hurkat, A. Tiwari, S.K. Jain, Eudragit S100 coated microsponges for Colon targeting of prednisolone, Drug Dev Ind Pharm, 44 (2018) 902-913.
[46] B. Moulari, A. Beduneau, Y. Pellequer, A. Lamprecht, Lectin-decorated nanoparticles enhance binding to the inflamed tissue in experimental colitis, J Control Release, 188 (2014) 9-17.

[47] C.M.A. van Alem, M. Boonstra, J. Prins, T. Bezhaeva, M.F. van Essen, J.M. Ruben, A.L. Vahrmeijer, E.P. van der Veer, J.W. de Fijter, M.E. Reinders, O. Meijer, J.M. Metselaar, C. van Kooten, J.I. Rotmans, Local delivery of liposomal prednisolone leads to an anti-inflammatory profile in renal ischaemia-reperfusion injury in the rat, Nephrol Dial Transplant, 33 (2018) 44-53.
[48] P.H. Zhou, B. Qiu, R.H. Deng, H.J. Li, X.F. Xu, X.F. Shang, Chondroprotective Effects of Hyaluronic Acid-Chitosan Nanoparticles Containing Plasmid DNA Encoding Cytokine Response Modifier A in a Rat Knee Osteoarthritis Model, Cell Physiol Biochem, 47 (2018) 1207-1216.
[49] A. Verma, A. Jain, A. Tiwari, S. Saraf, P.K. Panda, G.P. Agrawal, S.K. Jain, Folate Conjugated Double Liposomes Bearing Prednisolone and Methotrexate for Targeting Rheumatoid Arthritis, Pharm Res, 36 (2019) 123.
[50] P.M. Gaafar, O.Y. Abdallah, R.M. Farid, H. Abdelkader, Preparation, characterization and evaluation of novel elastic nano-sized niosomes (ethoniosomes) for ocular delivery of prednisolone, J Liposome Res, 24 (2014) 204-215.
[51] Y. Karabey-Akyurek, A.G. Gurcay, O. Gurcan, O.F. Turkoglu, S. Yabanoglu-Ciftci, H. Eroglu, M.F. Sargon, E. Bilensoy, L. Oner, Localized delivery of methylprednisolone sodium succinate with polymeric nanoparticles in experimental injured spinal cord model, Pharm Dev Technol, 22 (2017) 972-981.
[52] U. Soiberman, S.P. Kambhampati, T. Wu, M.K. Mishra, Y. Oh, R. Sharma, J. Wang, A.E. Al Towerki, S. Yiu, W.J. Stark, R.M. Kannan, Subconjunctival injectable dendrimer-dexamethasone gel for the treatment of corneal inflammation, Biomaterials, 125 (2017) 38-53.
[53] Q. Wang, J. Jiang, W. Chen, H. Jiang, Z. Zhang, X. Sun, Targeted delivery of low-dose dexamethasone using PCL-PEG micelles for effective treatment of rheumatoid arthritis, J Control Release, 230 (2016) 64-72.
[54] A. Lee, C. De Mei, M. Fereira, R. Marotta, H.Y. Yoon, K. Kim, I.C. Kwon, P. Decuzzi, Dexamethasone-loaded Polymeric Nanoconstructs for Monitoring and Treating Inflammatory Bowel Disease, Theranostics, 7 (2017) 3653-3666.
[55] C. Dianzani, F. Foglietta, B. Ferrara, A.C. Rosa, E. Muntoni, P. Gasco, C. Della Pepa, R. Canaparo, L. Serpe, Solid lipid nanoparticles delivering anti-inflammatory drugs to treat inflammatory bowel disease: Effects in an *in vivo* model, World J Gastroenterol, 23 (2017) 4200-4210.
[56] Z. Jia, G. Zhao, X. Wei, D. Kong, Y. Sun, Y. Zhou, S.M. Lele, E.V. Fehringer, K.L. Garvin, S.R. Goldring, D. Wang, Structural optimization of HPMA copolymer-based dexamethasone prodrug for improved treatment of inflammatory arthritis, J Control Release, (2020).
[57] G.R. Greenberg, B.G. Feagan, F. Martin, L.R. Sutherland, A.B. Thomson, C.N. Williams, L.G. Nilsson, T. Persson, Oral budesonide for active Crohn's disease. Canadian Inflammatory Bowel Disease Study Group, N Engl J Med, 331 (1994) 836-841.
[58] M. Naeem, M. Choi, J. Cao, Y. Lee, M. Ikram, S. Yoon, J. Lee, H.R. Moon, M.S. Kim, Y. Jung, J.W. Yoo, Colon-targeted delivery of budesonide using dual pH- and time-dependent polymeric nanoparticles for colitis therapy, Drug Des Devel Ther, 9 (2015) 3789-3799.
[59] S. Hua, E. Marks, J.J. Schneider, S. Keely, Advances in oral nano-delivery systems for colon targeted drug delivery in inflammatory bowel disease: selective targeting to diseased versus healthy tissue, Nanomedicine, 11 (2015) 1117-1132.
[60] H. Ali, B. Weigmann, E.M. Collnot, S.A. Khan, M. Windbergs, C.M. Lehr, Budesonide Loaded PLGA Nanoparticles for Targeting the Inflamed Intestinal Mucosa--Pharmaceutical Characterization and Fluorescence Imaging, Pharm Res, 33 (2016) 1085-1092.
[61] S.Y. Vafaei, M. Esmaeili, M. Amini, F. Atyabi, S.N. Ostad, R. Dinarvand, Self assembled hyaluronic acid nanoparticles as a potential carrier for targeting the inflamed intestinal mucosa, Carbohydr Polym, 144 (2016) 371-381.
[62] S. Wongrakpanich, A. Wongrakpanich, K. Melhado, J. Rangaswami, A Comprehensive Review of Non-Steroidal Anti-Inflammatory Drug Use in The Elderly, Aging Dis, 9 (2018) 143-150.
[63] C. Sostres, C.J. Gargallo, M.T. Arroyo, A. Lanas, Adverse effects of non-steroidal anti-inflammatory drugs (NSAIDs, aspirin and coxibs) on upper gastrointestinal tract, Best Pract Res Clin Gastroenterol, 24 (2010) 121-132.

[64] R.M. Goncalves, A.C. Pereira, I.O. Pereira, M.J. Oliveira, M.A. Barbosa, Macrophage response to chitosan/poly-(gamma-glutamic acid) nanoparticles carrying an anti-inflammatory drug, J Mater Sci Mater Med, 26 (2015) 167.
[65] Q. Shang, S. Huang, A. Zhang, J. Feng, S. Yang, The binary complex of poly(PEGMA-co-MAA) hydrogel and PLGA nanoparticles as a novel oral drug delivery system for ibuprofen delivery, J Biomater Sci Polym Ed, 28 (2017) 1874-1887.
[66] P. Nirbhavane, G. Sharma, B. Singh, G.K. Khuller, V.G. Goni, A.B. Patil, O.P. Katare, Preclinical Explorative Assessment of Celecoxib-Based Biocompatible Lipidic Nanocarriers for the Management of CFA-Induced Rheumatoid Arthritis in Wistar Rats, AAPS PharmSciTech, 19 (2018) 3187-3198.
[67] W.K.E. Ip, N. Hoshi, D.S. Shouval, S. Snapper, R. Medzhitov, Anti-inflammatory effect of IL-10 mediated by metabolic reprogramming of macrophages, Science, 356 (2017) 513-519.
[68] A. Viscido, A. Capannolo, G. Latella, R. Caprilli, G. Frieri, Nanotechnology in the treatment of inflammatory bowel diseases, J Crohns Colitis, 8 (2014) 903-918.
[69] R. Toita, T. Kawano, M. Murata, J.H. Kang, Anti-obesity and anti-inflammatory effects of macrophage-targeted interleukin-10-conjugated liposomes in obese mice, Biomaterials, 110 (2016) 81-88.
[70] N. Kamaly, G. Fredman, J.J. Fojas, M. Subramanian, W.I. Choi, K. Zepeda, C. Vilos, M. Yu, S. Gadde, J. Wu, J. Milton, R. Carvalho Leitao, L. Rosa Fernandes, M. Hasan, H. Gao, V. Nguyen, J. Harris, I. Tabas, O.C. Farokhzad, Targeted Interleukin-10 Nanotherapeutics Developed with a Microfluidic Chip Enhance Resolution of Inflammation in Advanced Atherosclerosis, ACS Nano, 10 (2016) 5280-5292.
[71] D.R. Baganizi, E. Nyairo, S.A. Duncan, S.R. Singh, V.A. Dennis, Interleukin-10 Conjugation to Carboxylated PVP-Coated Silver Nanoparticles for Improved Stability and Therapeutic Efficacy, Nanomaterials (Basel), 7 (2017).
[72] M.C. Stensberg, Q. Wei, E.S. McLamore, D.M. Porterfield, A. Wei, M.S. Sepulveda, Toxicological studies on silver nanoparticles: challenges and opportunities in assessment, monitoring and imaging, Nanomedicine (Lond), 6 (2011) 879-898.
[73] L. Yildirimer, N.T. Thanh, M. Loizidou, A.M. Seifalian, Toxicology and clinical potential of nanoparticles, Nano Today, 6 (2011) 585-607.
[74] J.H. Sung, J.H. Ji, J.U. Yoon, D.S. Kim, M.Y. Song, J. Jeong, B.S. Han, J.H. Han, Y.H. Chung, J. Kim, T.S. Kim, H.K. Chang, E.J. Lee, J.H. Lee, I.J. Yu, Lung function changes in Sprague-Dawley rats after prolonged inhalation exposure to silver nanoparticles, Inhal Toxicol, 20 (2008) 567-574.
[75] K. Bilberg, M.B. Hovgaard, F. Besenbacher, E. Baatrup, *In Vivo* Toxicity of Silver Nanoparticles and Silver Ions in Zebrafish (Danio rerio), J Toxicol, 2012 (2012) 293784.
[76] R. Agarwal, T.M. Volkmer, P. Wang, L.A. Lee, Q. Wang, A.J. Garcia, Synthesis of self-assembled IL-1Ra-presenting nanoparticles for the treatment of osteoarthritis, J Biomed Mater Res A, 104 (2016) 595-599.
[77] T. Wang, Y. Tang, X. He, J. Yan, C. Wang, X. Feng, Self-Assembled Raspberry-Like Core/Satellite Nanoparticles for Anti-Inflammatory Protein Delivery, ACS Appl Mater Interfaces, 9 (2017) 6902-6907.
[78] S. Gupta, A.K. Sharma, V. Shastri, M.K. Madhu, V.K. Sharma, Prediction of anti-inflammatory proteins/peptides: an insilico approach, J Transl Med, 15 (2017) 7.
[79] R.L. Bartlett, 2nd, S. Sharma, A. Panitch, Cell-penetrating peptides released from thermosensitive nanoparticles suppress pro-inflammatory cytokine response by specifically targeting inflamed cartilage explants, Nanomedicine, 9 (2013) 419-427.
[80] S. Poh, J.B. Lin, A. Panitch, Release of anti-inflammatory peptides from thermosensitive nanoparticles with degradable cross-links suppresses pro-inflammatory cytokine production, Biomacromolecules, 16 (2015) 1191-1200.
[81] J.B. Lin, S. Poh, A. Panitch, Controlled release of anti-inflammatory peptides from reducible thermosensitive nanoparticles suppresses cartilage inflammation, Nanomedicine, 12 (2016) 2095-2100.
[82] C. He, L. Yin, Y. Song, C. Tang, C. Yin, Optimization of multifunctional chitosan-siRNA nanoparticles for oral delivery applications, targeting TNF-alpha silencing in rats, Acta Biomater, 17 (2015) 98-106.

[83] S. Yadav, S.K. Gandham, R. Panicucci, M.M. Amiji, Intranasal brain delivery of cationic nanoemulsion-encapsulated TNFalpha siRNA in prevention of experimental neuroinflammation, Nanomedicine, 12 (2016) 987-1002.
[84] T. Kanazawa, T. Kurano, H. Ibaraki, Y. Takashima, T. Suzuki, Y. Seta, Therapeutic Effects in a Transient Middle Cerebral Artery Occlusion Rat Model by Nose-To-Brain Delivery of Anti-TNF-Alpha siRNA with Cell-Penetrating Peptide-Modified Polymer Micelles, Pharmaceutics, 11 (2019).
[85] A. Bohr, N. Tsapis, I. Andreana, A. Chamarat, C. Foged, C. Delomenie, M. Noiray, N. El Brahmi, J.P. Majoral, S. Mignani, E. Fattal, Anti-Inflammatory Effect of Anti-TNF-alpha SiRNA Cationic Phosphorus Dendrimer Nanocomplexes Administered Intranasally in a Murine Acute Lung Injury Model, Biomacromolecules, 18 (2017) 2379-2388.
[86] Q. Shi, E.P. Rondon-Cavanzo, I.P. Dalla Picola, M.J. Tiera, X. Zhang, K. Dai, H.A. Benabdoune, M. Benderdour, J.C. Fernandes, *In vivo* therapeutic efficacy of TNFalpha silencing by folate-PEG-chitosan-DEAE/siRNA nanoparticles in arthritic mice, Int J Nanomedicine, 13 (2018) 387-402.
[87] A.M. Aldayel, H.L. O'Mary, S.A. Valdes, X. Li, S.G. Thakkar, B.E. Mustafa, Z. Cui, Lipid nanoparticles with minimum burst release of TNF-alpha siRNA show strong activity against rheumatoid arthritis unresponsive to methotrexate, J Control Release, 283 (2018) 280-289.
[88] M.A.A. Jansen, L.H. Klausen, K. Thanki, J. Lyngso, J. Skov Pedersen, H. Franzyk, H.M. Nielsen, W. van Eden, M. Dong, F. Broere, C. Foged, X. Zeng, Lipidoid-polymer hybrid nanoparticles loaded with TNF siRNA suppress inflammation after intra-articular administration in a murine experimental arthritis model, Eur J Pharm Biopharm, 142 (2019) 38-48.
[89] Y.C. Liu, X.B. Zou, Y.F. Chai, Y.M. Yao, Macrophage polarization in inflammatory diseases, Int J Biol Sci, 10 (2014) 520-529.
[90] S. Jain, T.H. Tran, M. Amiji, Macrophage repolarization with targeted alginate nanoparticles containing IL-10 plasmid DNA for the treatment of experimental arthritis, Biomaterials, 61 (2015) 162-177.
[91] T.H. Tran, R. Rastogi, J. Shelke, M.M. Amiji, Modulation of Macrophage Functional Polarity towards Anti-Inflammatory Phenotype with Plasmid DNA Delivery in CD44 Targeting Hyaluronic Acid Nanoparticles, Sci Rep, 5 (2015) 16632.
[92] M. Haneklaus, M. Gerlic, L.A. O'Neill, S.L. Masters, miR-223: infection, inflammation and cancer, J Intern Med, 274 (2013) 215-226.
[93] T.H. Tran, S. Krishnan, M.M. Amiji, MicroRNA-223 Induced Repolarization of Peritoneal Macrophages Using CD44 Targeting Hyaluronic Acid Nanoparticles for Anti-Inflammatory Effects, PLoS One, 11 (2016) e0152024.
[94] A.M. Carmona-Ribeiro, Preparation and characterization of biomimetic nanoparticles for drug delivery, Methods Mol Biol, 906 (2012) 283-294.
[95] C.M. Hu, R.H. Fang, K.C. Wang, B.T. Luk, S. Thamphiwatana, D. Dehaini, P. Nguyen, P. Angsantikul, C.H. Wen, A.V. Kroll, C. Carpenter, M. Ramesh, V. Qu, S.H. Patel, J. Zhu, W. Shi, F.M. Hofman, T.C. Chen, W. Gao, K. Zhang, S. Chien, L. Zhang, Nanoparticle biointerfacing by platelet membrane cloaking, Nature, 526 (2015) 118-121.
[96] H. Yan, D. Shao, Y.H. Lao, M. Li, H. Hu, K.W. Leong, Engineering Cell Membrane-Based Nanotherapeutics to Target Inflammation, Adv Sci (Weinh), 6 (2019) 1900605.
[97] K. Jin, Z. Luo, B. Zhang, Z. Pang, Biomimetic nanoparticles for inflammation targeting, Acta Pharm Sin B, 8 (2018) 23-33.
[98] V. Vijayan, S. Uthaman, I.K. Park, Cell Membrane-Camouflaged Nanoparticles: A Promising Biomimetic Strategy for Cancer Theragnostics, Polymers (Basel), 10 (2018).
[99] H. Wang, Y. Liu, R. He, D. Xu, J. Zang, N. Weeranoppanant, H. Dong, Y. Li, Cell membrane biomimetic nanoparticles for inflammation and cancer targeting in drug delivery, Biomater Sci, 8 (2020) 552-568.
[100] G.S. Firestein, I.B. McInnes, Immunopathogenesis of Rheumatoid Arthritis, Immunity, 46 (2017).
[101] M. Horckmans, L. Ring, J. Duchene, D. Santovito, M.J. Schloss, M. Drechsler, C. Weber, O. Soehnlein, S. Steffens, Neutrophils orchestrate post-myocardial infarction healing by polarizing macrophages towards a reparative phenotype, Eur Heart J, 38 (2017) 187-197.

[102] Q. Zhang, D. Dehaini, Y. Zhang, J. Zhou, X. Chen, L. Zhang, R.H. Fang, W. Gao, Neutrophil membrane-coated nanoparticles inhibit synovial inflammation and alleviate joint damage in inflammatory arthritis, Nat Nanotechnol, 13 (2018) 1182-1190.
[103] S. Thamphiwatana, P. Angsantikul, T. Escajadillo, Q. Zhang, J. Olson, B.T. Luk, S. Zhang, R.H. Fang, W. Gao, V. Nizet, L. Zhang, Macrophage-like nanoparticles concurrently absorbing endotoxins and proinflammatory cytokines for sepsis management, Proc Natl Acad Sci U S A, 114 (2017) 11488-11493.
[104] C. Boada, A. Zinger, C. Tsao, P. Zhao, J.O. Martinez, K. Hartman, T. Naoi, R. Sukhoveshin, M. Sushnitha, R. Molinaro, B. Trachtenberg, J.P. Cooke, E. Tasciotti, Rapamycin-Loaded Biomimetic Nanoparticles Reverse Vascular Inflammation, Circ Res, 126 (2020) 25-37.
[105] T. Fukuta, S. Yoshimi, T. Tanaka, K. Kogure, Leukocyte-mimetic liposomes possessing leukocyte membrane proteins pass through inflamed endothelial cell layer by regulating intercellular junctions, Int J Pharm, 563 (2019) 314-323.
[106] R. Li, Y. He, Y. Zhu, L. Jiang, S. Zhang, J. Qin, Q. Wu, W. Dai, S. Shen, Z. Pang, J. Wang, Route to Rheumatoid Arthritis by Macrophage-Derived Microvesicle-Coated Nanoparticles, Nano Lett, 19 (2019) 124-134.
[107] N. Zelcer, P. Tontonoz, Liver X receptors as integrators of metabolic and inflammatory signaling, J Clin Invest, 116 (2006) 607-614.
[108] H. He, Q. Yuan, J. Bie, R.L. Wallace, P.J. Yannie, J. Wang, M.G. Lancina, 3rd, O.Y. Zolotarskaya, W. Korzun, H. Yang, S. Ghosh, Development of mannose functionalized dendrimeric nanoparticles for targeted delivery to macrophages: use of this platform to modulate atherosclerosis, Transl Res, 193 (2018) 13-30.
[109] X.Q. Zhang, O. Even-Or, X. Xu, M. van Rosmalen, L. Lim, S. Gadde, O.C. Farokhzad, E.A. Fisher, Nanoparticles containing a liver X receptor agonist inhibit inflammation and atherosclerosis, Adv Healthc Mater, 4 (2015) 228-236.
[110] Y. Guo, W. Yuan, B. Yu, R. Kuai, W. Hu, E.E. Morin, M.T. Garcia-Barrio, J. Zhang, J.J. Moon, A. Schwendeman, Y. Eugene Chen, Synthetic High-Density Lipoprotein-Mediated Targeted Delivery of Liver X Receptors Agonist Promotes Atherosclerosis Regression, EBioMedicine, 28 (2018) 225-233.
[111] R.K. Thapa, B.K. Yoo, Evaluation of the effect of tacrolimus-loaded liquid crystalline nanoparticles on psoriasis-like skin inflammation, J Dermatolog Treat, 25 (2014) 22-25.
[112] C.G. Sen Lin, Doudou Wang, Qi Xie, Biao Wu, Jingjie Wang, Kaihui Nan*, Qinxiang Zheng*, and Wei Chen*, Overcoming the Anatomical and Physiological Barriers in Topical Eye Surface Medication Using a Peptide-Decorated Polymeric Micelle, ACS Appl. Mater. Interfaces, 11 (2019).
[113] K. Okuda, H.Y. Fu, T. Matsuzaki, R. Araki, S. Tsuchida, P.V. Thanikachalam, T. Fukuta, T. Asai, M. Yamato, S. Sanada, H. Asanuma, Y. Asano, M. Asakura, H. Hanawa, H. Hao, N. Oku, S. Takashima, M. Kitakaze, Y. Sakata, T. Minamino, Targeted Therapy for Acute Autoimmune Myocarditis with Nano-Sized Liposomal FK506 in Rats, PLoS One, 11 (2016) e0160944.
[114] A. Partoazar, S. Nasoohi, S.M. Rezayat, K. Gilani, S.E. Mehr, A. Amani, N. Rahimi, A.R. Dehpour, Nanoliposome containing cyclosporine A reduced neuroinflammation responses and improved neurological activities in cerebral ischemia/reperfusion in rat, Fundam Clin Pharmacol, 31 (2017) 185-193.
[115] S. Yadav, G. Pawar, P. Kulkarni, C. Ferris, M. Amiji, CNS Delivery and Anti-Inflammatory Effects of Intranasally Administered Cyclosporine-A in Cationic Nanoformulations, J Pharmacol Exp Ther, 370 (2019) 843-854.
[116] H. Tang, D. Xiang, F. Wang, J. Mao, X. Tan, Y. Wang, 5-ASA-loaded SiO2 nanoparticles-a novel drug delivery system targeting therapy on ulcerative colitis in mice, Mol Med Rep, 15 (2017) 1117-1122.
[117] P. Tang, Q. Sun, L. Zhao, H. Pu, H. Yang, S. Zhang, R. Gan, N. Gan, H. Li, Mesalazine/hydroxypropyl-beta-cyclodextrin/chitosan nanoparticles with sustained release and enhanced anti-inflammation activity, Carbohydr Polym, 198 (2018) 418-425.

[118] T. Yazeji, B. Moulari, A. Beduneau, V. Stein, D. Dietrich, Y. Pellequer, A. Lamprecht, Nanoparticle-based delivery enhances anti-inflammatory effect of low molecular weight heparin in experimental ulcerative colitis, Drug Deliv, 24 (2017) 811-817.
[119] P. Couvreur, B. Stella, L.H. Reddy, H. Hillaireau, C. Dubernet, D. Desmaele, S. Lepetre-Mouelhi, F. Rocco, N. Dereuddre-Bosquet, P. Clayette, V. Rosilio, V. Marsaud, J.M. Renoir, L. Cattel, Squalenoyl nanomedicines as potential therapeutics, Nano Lett, 6 (2006) 2544-2548.
[120] D. Desmaele, R. Gref, P. Couvreur, Squalenoylation: a generic platform for nanoparticular drug delivery, J Control Release, 161 (2012) 609-618.
[121] J. Feng, S. Lepetre-Mouelhi, A. Gautier, S. Mura, C. Cailleau, F. Coudore, M. Hamon, P. Couvreur, A new painkiller nanomedicine to bypass the blood-brain barrier and the use of morphine, Sci Adv, 5 (2019) eaau5148.
[122] L. Antonioli, C. Blandizzi, P. Pacher, G. Hasko, Immunity, inflammation and cancer: a leading role for adenosine, Nat Rev Cancer, 13 (2013) 842-857.
[123] G. Hasko, J. Linden, B. Cronstein, P. Pacher, Adenosine receptors: therapeutic aspects for inflammatory and immune diseases, Nat Rev Drug Discov, 7 (2008) 759-770.
[124] A. Gaudin, M. Yemisci, H. Eroglu, S. Lepetre-Mouelhi, O.F. Turkoglu, B. Donmez-Demir, S. Caban, M.F. Sargon, S. Garcia-Argote, G. Pieters, O. Loreau, B. Rousseau, O. Tagit, N. Hildebrandt, Y. Le Dantec, J. Mougin, S. Valetti, H. Chacun, V. Nicolas, D. Desmaele, K. Andrieux, Y. Capan, T. Dalkara, P. Couvreur, Squalenoyl adenosine nanoparticles provide neuroprotection after stroke and spinal cord injury, Nat Nanotechnol, 9 (2014) 1054-1062.
[125] J. Egea, I. Fabregat, Y.M. Frapart, P. Ghezzi, A. Gorlach, T. Kietzmann, K. Kubaichuk, U.G. Knaus, M.G. Lopez, G. Olaso-Gonzalez, A. Petry, R. Schulz, J. Vina, P. Winyard, K. Abbas, O.S. Ademowo, C.B. Afonso, I. Andreadou, H. Antelmann, F. Antunes, M. Aslan, M.M. Bachschmid, R.M. Barbosa, V. Belousov, C. Berndt, D. Bernlohr, E. Bertran, A. Bindoli, S.P. Bottari, P.M. Brito, G. Carrara, A.I. Casas, A. Chatzi, N. Chondrogianni, M. Conrad, M.S. Cooke, J.G. Costa, A. Cuadrado, P. My-Chan Dang, B. De Smet, B. Debelec-Butuner, I.H.K. Dias, J.D. Dunn, A.J. Edson, M. El Assar, J. El-Benna, P. Ferdinandy, A.S. Fernandes, K.E. Fladmark, U. Forstermann, R. Giniatullin, Z. Giricz, A. Gorbe, H. Griffiths, V. Hampl, A. Hanf, J. Herget, P. Hernansanz-Agustin, M. Hillion, J. Huang, S. Ilikay, P. Jansen-Durr, V. Jaquet, J.A. Joles, B. Kalyanaraman, D. Kaminskyy, M. Karbaschi, M. Kleanthous, L.O. Klotz, B. Korac, K.S. Korkmaz, R. Koziel, D. Kracun, K.H. Krause, V. Kren, T. Krieg, J. Laranjinha, A. Lazou, H. Li, A. Martinez-Ruiz, R. Matsui, G.J. McBean, S.P. Meredith, J. Messens, V. Miguel, Y. Mikhed, I. Milisav, L. Milkovic, A. Miranda-Vizuete, M. Mojovic, M. Monsalve, P.A. Mouthuy, J. Mulvey, T. Munzel, V. Muzykantov, I.T.N. Nguyen, M. Oelze, N.G. Oliveira, C.M. Palmeira, N. Papaevgeniou, A. Pavicevic, B. Pedre, F. Peyrot, M. Phylactides, G.G. Pircalabioru, A.R. Pitt, H.E. Poulsen, I. Prieto, M.P. Rigobello, N. Robledinos-Anton, L. Rodriguez-Manas, A.P. Rolo, F. Rousset, T. Ruskovska, N. Saraiva, S. Sasson, K. Schroder, K. Semen, T. Seredenina, A. Shakirzyanova, G.L. Smith, T. Soldati, B.C. Sousa, C.M. Spickett, A. Stancic, M.J. Stasia, H. Steinbrenner, V. Stepanic, S. Steven, K. Tokatlidis, E. Tuncay, B. Turan, F. Ursini, J. Vacek, O. Vajnerova, K. Valentova, F. Van Breusegem, L. Varisli, E.A. Veal, A.S. Yalcin, O. Yelisyeyeva, N. Zarkovic, M. Zatloukalova, J. Zielonka, R.M. Touyz, A. Papapetropoulos, T. Grune, S. Lamas, H. Schmidt, F. Di Lisa, A. Daiber, European contribution to the study of ROS: A summary of the findings and prospects for the future from the COST action BM1203 (EU-ROS), Redox Biol, 13 (2017) 94-162.
[126] V.M. Moia, F. Leal Portilho, T. Almeida Padua, L. Barbosa Correa, E. Ricci-Junior, E. Cruz Rosas, L. Magalhaes Rebelo Alencar, F. Savio Mendes Sinfronio, A. Sampson, S. Hussain Iram, F. Alexis, M.D. de OliveiraHenriques, R. Santos-Oliveira, Lycopene used as Anti-inflammatory Nanodrug for the Treatment of Rheumathoid Arthritis: Animal assay, Pharmacokinetics, ABC Transporter and Tissue Deposition, Colloids Surf B Biointerfaces, 188 (2020) 110814.
[127] M.O. Kadry, Liposomal glutathione as a promising candidate for immunological rheumatoid arthritis therapy, Heliyon, 5 (2019) e02162.
[128] T. Wu, X. Chen, Y. Wang, H. Xiao, Y. Peng, L. Lin, W. Xia, M. Long, J. Tao, X. Shuai, Aortic plaque-targeted andrographolide delivery with oxidation-sensitive micelle effectively treats atherosclerosis via simultaneous ROS capture and anti-inflammation, Nanomedicine, 14 (2018)

[129] R.B. Flavio Dormont, Catherine Cailleau, Franceline Reynaud, Arnaud Peramo, Amandine Gendron, Julie Mougin, Françoise Gaudin, Mariana Varna & Patrick Couvreur, Squalene-based multidrug nanoparticles for improved mitigation of uncontrolled inflammation, Science Advances, (2020).
[130] M. Varna, H.V. Xuan, E. Fort, Gold nanoparticles in cardiovascular imaging, Wiley Interdiscip Rev Nanomed Nanobiotechnol, 10 (2018).
[131] M.A. Khan, M.J. Khan, Nano-gold displayed anti-inflammatory property via NF-kB pathways by suppressing COX-2 activity, Artif Cells Nanomed Biotechnol, 46 (2018) 1149-1158.
[132] Y. Zhao, Z. He, R. Wang, P. Cai, X. Zhang, Q. Yuan, J. Zhang, F. Gao, X. Gao, Comparison of the Therapeutic Effects of Gold Nanoclusters and Gold Nanoparticles on Rheumatoid Arthritis, J Biomed Nanotechnol, 15 (2019) 2281-2290.
[133] F. Gao, Q. Yuan, P. Cai, L. Gao, L. Zhao, M. Liu, Y. Yao, Z. Chai, X. Gao, Au Clusters Treat Rheumatoid Arthritis with Uniquely Reversing Cartilage/Bone Destruction, Adv Sci (Weinh), 6 (2019) 1801671.
[134] R.P. Pannerec-Varna M, Bousquet G,Ferreira I, Leboeuf C, Boisgard R, Gapihan G,Verine J, Palpant B, Bossy E, et al., *In vivo* uptake andcellular distribution of gold nanoshells in a preclinicalmodel of xenografted human renal cancer, Gold Bull 46 (2013) 257–265.
[135] S. De Koker, J. Cui, N. Vanparijs, L. Albertazzi, J. Grooten, F. Caruso, B.G. De Geest, Engineering Polymer Hydrogel Nanoparticles for Lymph Node-Targeted Delivery, Angew Chem Int Ed Engl, 55 (2016) 1334-1339.
[136] S.N. Mueller, S. Tian, J.M. DeSimone, Rapid and Persistent Delivery of Antigen by Lymph Node Targeting PRINT Nanoparticle Vaccine Carrier To Promote Humoral Immunity, Mol Pharm, 12 (2015) 1356-1365.
[137] T.W. Chu, J. Yang, R. Zhang, M. Sima, J. Kopecek, Cell surface self-assembly of hybrid nanoconjugates via oligonucleotide hybridization induces apoptosis, ACS Nano, 8 (2014) 719-730.
[138] T.W. Chu, R. Zhang, J. Yang, M.P. Chao, P.J. Shami, J. Kopecek, A Two-Step Pretargeted Nanotherapy for CD20 Crosslinking May Achieve Superior Anti-Lymphoma Efficacy to Rituximab, Theranostics, 5 (2015) 834-846.
[139] L. Li, J. Yang, J. Wang, J. Kopecek, Amplification of CD20 Cross-Linking in Rituximab-Resistant B-Lymphoma Cells Enhances Apoptosis Induction by Drug-Free Macromolecular Therapeutics, ACS Nano, 12 (2018) 3658-3670.
[140] J. Wang, L. Li, J. Yang, P.M. Clair, M.J. Glenn, D.M. Stephens, D.C. Radford, K.M. Kosak, M.W. Deininger, P.J. Shami, J. Kopecek, Drug-free macromolecular therapeutics induce apoptosis in cells isolated from patients with B cell malignancies with enhanced apoptosis induction by pretreatment with gemcitabine, Nanomedicine, 16 (2019) 217-225.
[141] J. Wang, Y. Li, L. Li, J. Yang, J. Kopecek, Exploration and Evaluation of Therapeutic Efficacy of Drug-Free Macromolecular Therapeutics in Collagen-Induced Rheumatoid Arthritis Mouse Model, Macromol Biosci, 20 (2020) e1900445.
[142] J. Du, Y.S. Zhang, D. Hobson, P. Hydbring, Nanoparticles for immune system targeting, Drug Discov Today, 22 (2017) 1295-1301.
[143] M.S. Goldberg, Improving cancer immunotherapy through nanotechnology, Nat Rev Cancer, 19 (2019) 587-602.
[144] E. Zupancic, C. Curato, M. Paisana, C. Rodrigues, Z. Porat, A.S. Viana, C.A.M. Afonso, J. Pinto, R. Gaspar, J.N. Moreira, R. Satchi-Fainaro, S. Jung, H.F. Florindo, Rational design of nanoparticles towards targeting antigen-presenting cells and improved T cell priming, J Control Release, 258 (2017) 182-195.
[145] W. Gao, R.H. Fang, S. Thamphiwatana, B.T. Luk, J. Li, P. Angsantikul, Q. Zhang, C.M. Hu, L. Zhang, Modulating antibacterial immunity via bacterial membrane-coated nanoparticles, Nano Lett, 15 (2015) 1403-1409.
[146] A. Yeste, M.C. Takenaka, I.D. Mascanfroni, M. Nadeau, J.E. Kenison, B. Patel, A.M. Tukpah, J.A. Babon, M. DeNicola, S.C. Kent, D. Pozo, F.J. Quintana, Tolerogenic nanoparticles inhibit T cell-mediated autoimmunity through SOCS2, Sci Signal, 9 (2016) ra61.

[147] A.C. Anselmo, S. Mitragotri, Nanoparticles in the clinic, Bioeng Transl Med, 1 (2016) 10-29.
[148] A.C. Anselmo, S. Mitragotri, Nanoparticles in the clinic: An update, Bioeng Transl Med, 4 (2019) e10143.
[149] M.E. Lobatto, Z.A. Fayad, S. Silvera, E. Vucic, C. Calcagno, V. Mani, S.D. Dickson, K. Nicolay, M. Banciu, R.M. Schiffelers, J.M. Metselaar, L. van Bloois, H.S. Wu, J.T. Fallon, J.H. Rudd, V. Fuster, E.A. Fisher, G. Storm, W.J. Mulder, Multimodal clinical imaging to longitudinally assess a nanomedical anti-inflammatory treatment in experimental atherosclerosis, Mol Pharm, 7 (2010) 2020-2029.
[150] F.M. van der Valk, D.F. van Wijk, M.E. Lobatto, H.J. Verberne, G. Storm, M.C. Willems, D.A. Legemate, A.J. Nederveen, C. Calcagno, V. Mani, S. Ramachandran, M.P. Paridaans, M.J. Otten, G.M. Dallinga-Thie, Z.A. Fayad, M. Nieuwdorp, D.M. Schulte, J.M. Metselaar, W.J. Mulder, E.S. Stroes, Prednisolone-containing liposomes accumulate in human atherosclerotic macrophages upon intravenous administration, Nanomedicine, 11 (2015) 1039-1046.
[151] A Proof of Concept Study to Determine the Local Delivery and Efficacy of Nanocort - Full Text View - ClinicalTrials.gov, https://clinicaltrials.gov/ct2/show/NCT01647685.
[152] Silencing Inflammatory Activity by Injecting Nanocort in Patients at Risk for Atherosclerotic Disease - Full Text View - ClinicalTrials.gov, https://clinicaltrials.gov/ct2/show/NCT01601106.
[153] B.M. Voorzaat, J. van Schaik, K.E. van der Bogt, L. Vogt, L. Huisman, B.A. Gabreels, I.M. van der Meer, R.G. van Eps, D. Eefting, M.C. Weijmer, H.O. Groeneveld, R.C. van Nieuwenhuizen, H. Boom, C.A. Verburgh, K. van der Putten, J.I. Rotmans, Improvement of radiocephalic fistula maturation: rationale and design of the Liposomal Prednisolone to Improve Hemodialysis Fistula Maturation (LIPMAT) study - a randomized controlled trial, J Vasc Access, 18 (2017) 114-117.
[154] Website n.d. Liposome encapsulated prednisolone - AdisInsight, https://adisinsight.springer.com/drugs/800028576.
[155] n.d.h.e.n. Enceladus Pharmaceuticals BV announces positive results from a phase 2a study in patients with active ulcerative colitis with Nanocort® | Enceladus Pharmaceuticals.
[156] R. Kumar, S. Dogra, B. Amarji, B. Singh, S. Kumar, Sharma, K. Vinay, R. Mahajan, O.P. Katare, Efficacy of Novel Topical Liposomal Formulation of Cyclosporine in Mild to Moderate Stable Plaque Psoriasis: A Randomized Clinical Trial, JAMA Dermatol, 152 (2016) 807-815.
[157] n.d.h. A Evaluation of the Safety of Oncocort IV Pegylated Liposomal Dexamethasone Phosphate in Patients With Progressive Multiple Myeloma - Full Text View - ClinicalTrials.gov.
[158] K. Nakano, T. Matoba, J.I. Koga, Y. Kashihara, M. Fukae, I. Ieiri, M. Shiramoto, S. Irie, J. Kishimoto, K. Todaka, K. Egashira, Safety, Tolerability, and Pharmacokinetics of NK-104-NP, Int Heart J, 59 (2018) 1015-1025.
[159] M. Sabouri, A. Samadi, S. Ahmad Nasrollahi, E.S. Farboud, B. Mirrahimi, H. Hassanzadeh, M. Nassiri Kashani, R. Dinarvand, A. Firooz, Tretinoin Loaded Nanoemulsion for Acne Vulgaris: Fabrication, Physicochemical and Clinical Efficacy Assessments, Skin Pharmacol Physiol, 31 (2018) 316-323.
[160] S.A.P.R.o.T.I.C.S.i.A. S. Inc, (n.d.). https://www.prnewswire.com/news-releases/sebacia-announces-positive-results-of-two-independent-clinical-studies-in-acne-300026759.html.
[161] S. Hua, M.B.C. de Matos, J.M. Metselaar, G. Storm, Current Trends and Challenges in the Clinical Translation of Nanoparticulate Nanomedicines: Pathways for Translational Development and Commercialization, Front Pharmacol, 9 (2018) 790.
[162] C.A. Dinarello, Anti-inflammatory Agents: Present and Future, Cell, 140 (2010) 935-950.
[163] N. Doshi, S. Mitragotri, Macrophages recognize size and shape of their targets, PLoS One, 5 (2010) e10051.
[164] P.P. Wibroe, A.C. Anselmo, P.H. Nilsson, A. Sarode, V. Gupta, R. Urbanics, J. Szebeni, A.C. Hunter, S. Mitragotri, T.E. Mollnes, S.M. Moghimi, Bypassing adverse injection reactions to nanoparticles through shape modification and attachment to erythrocytes, Nat Nanotechnol, 12 (2017) 589-594.
[165] H.S. Leong, K.S. Butler, C.J. Brinker, M. Azzawi, S. Conlan, C. Dufes, A. Owen, S. Rannard, C. Scott, C. Chen, M.A. Dobrovolskaia, S.V. Kozlov, A. Prina-Mello, R. Schmid, P. Wick, F. Caputo, P. Boisseau, R.M. Crist, S.E. McNeil, B. Fadeel, L. Tran, S.F. Hansen, N.B. Hartmann, L.P.W. Clausen,

L.M. Skjolding, A. Baun, M. Agerstrand, Z. Gu, D.A. Lamprou, C. Hoskins, L. Huang, W. Song, H. Cao, X. Liu, K.D. Jandt, W. Jiang, B.Y.S. Kim, K.E. Wheeler, A.J. Chetwynd, I. Lynch, S.M. Moghimi, A. Nel, T. Xia, P.S. Weiss, B. Sarmento, J. das Neves, H.A. Santos, L. Santos, S. Mitragotri, S. Little, D. Peer, M.M. Amiji, M.J. Alonso, A. Petri-Fink, S. Balog, A. Lee, B. Drasler, B. Rothen-Rutishauser, S. Wilhelm, H. Acar, R.G. Harrison, C. Mao, P. Mukherjee, R. Ramesh, L.R. McNally, S. Busatto, J. Wolfram, P. Bergese, M. Ferrari, R.H. Fang, L. Zhang, J. Zheng, C. Peng, B. Du, M. Yu, D.M. Charron, G. Zheng, C. Pastore, On the issue of transparency and reproducibility in nanomedicine, Nat Nanotechnol, 14 (2019) 629-635.

[166] K.H. Chen, D.J. Lundy, E.K. Toh, C.H. Chen, C. Shih, P. Chen, H.C. Chang, J.J. Lai, P.S. Stayton, A.S. Hoffman, P.C. Hsieh, Nanoparticle distribution during systemic inflammation is size-dependent and organ-specific, Nanoscale, 7 (2015) 15863-15872.

[167] J. Pradal, P. Maudens, C. Gabay, C.A. Seemayer, O. Jordan, E. Allemann, Effect of particle size on the biodistribution of nano- and microparticles following intra-articular injection in mice, Int J Pharm, 498 (2016) 119-129.

[168] F. Dormont, M. Rouquette, C. Mahatsekake, F. Gobeaux, A. Peramo, R. Brusini, S. Calet, F. Testard, S. Lepetre-Mouelhi, D. Desmaele, M. Varna, P. Couvreur, Translation of nanomedicines from lab to industrial scale synthesis: The case of squalene-adenosine nanoparticles, J Control Release, 307 (2019) 302-314.

[169] A. Lamprecht, Nanomedicines in gastroenterology and hepatology, Nat Rev Gastroenterol Hepatol, 12 (2015) 195-204.

[170] M. Zhou, J. Hou, Z. Zhong, N. Hao, Y. Lin, C. Li, Targeted delivery of hyaluronic acid-coated solid lipid nanoparticles for rheumatoid arthritis therapy, Drug Deliv, 25 (2018) 716-722.

[171] S. Kanhai, I. Stavrakaki, W.Gladdines, P.J.Gaillard, E.S.Klaassen, G. J. Groeneveld, Glutathione-PEGylated liposomal methylprednisolone in comparison to free methylprednisolone: slow release characteristics and prolonged lymphocyte depression in a first-in-human study, British Journal of Clinical Pharmacology, 84 (2018) 1020-1028.

[172] D. Paithankar, Girish Munavalli, Arielle Kauvar, Jenifer Lloyd, Richard Blomgren, Linda Faupel, Todd Meyer, Samir Mitragotri, Ultrasonic delivery of silica–gold nanoshells for photothermolysis of sebaceous glands in humans: Nanotechnology from the bench to clinic, Journal of Controlled Release, 206 (2015) 30-36.

Chapitre 1. Squalene-based nanoparticles for the targeting of atherosclerotic lesions

Résumé détaillé

L'athérosclérose est une pathologie artérielle qui se définit par une inflammation chronique de l'intima des vaisseaux. Elle se détermine par une accumulation de lipoprotéines circulantes à faible densité (LDL) qui s'oxydent dans la paroi des artères de gros et moyens calibres, préférentiellement à des endroits soumis à un flux sanguin turbulent. Cela entraîne en réponse un processus inflammatoire avec sécrétion de médiateurs et recrutement de monocytes/macrophages[1,2]. La gestion de l'athérosclérose est un des défis majeurs de la médecine moderne. Bien que la diminution de la charge lipidique des plaques soit toujours la principale voie thérapeutique en vigueur, de nouvelles stratégies visant à directement détecter et traiter l'inflammation sont aujourd'hui activement envisagées[3, 4].

Le chapitre 1 se consacre au développement de nanoparticules à base de squalène pour le ciblage des lésions d'athérosclérose par accumulation dans les LDL endogènes. En effet, il a été précédemment montré qu'une fois conjugués au squalène, des agents thérapeutiques pouvaient interagir avec les lipoprotéines dans la circulation sanguine[5]. Cette approche novatrice exploitant indirectement les LDL endogènes s'accumulant spontanément dans les plaques d'athérosclérose, permettrait alors de transporter diverses molécules thérapeutiques ou à des fins de diagnostic. Par ailleurs, contrairement à d'autres formulations, les nanoparticules à base de squalène présentent l'avantage d'être biocompatibles et biodégradables, ne nécessitant pas de processus de synthèse et de purification compliqués.

Dans cette étude, qui se présente telle une preuve de concept, nous avons tout d'abord synthétisé et formulé des nanoparticules fluorescentes de Squalène-Rhodamine B (SQRho), par co-nanoprécipitation avec de l'acide squalénique (SQCOOH) avec un ratio optimal de 82:18 % en poids. Ces nanoparticules, stables plusieurs jours à température ambiante, présentaient une taille de l'ordre de 80 nm et un potentiel électrique de surface positif variant entre +2mV et +40mV. Nous avons ensuite montré *in vitro* par cytométrie en flux et microscopie confocale sur une lignée macrophagique, la capacité de ces nanoparticules à être internalisées et à s'accumuler dans les macrophages. En effet, les macrophages sont des cellules immunitaires présentent dans les plaques d'athérosclérose et reconnaissant naturellement les lipoprotéines oxydés, qu'ils internalisent et métabolisent par suite. Enfin, nous avons étudié la bio-distribution des nanoparticules de SQRho dans le modèle murin *ApoE*$^{-/-}$ d'athérosclérose, en les comparant à des billes de

latex fluorescentes de taille nanométrique (de l'ordre de 100 nm). D'une part, après sacrifice 24h après injection et prélèvement des aortes des souris injectées, nous les avons analysées par un système d'imagerie à fluorescence IVIS Lumina. Nous avons ainsi pu observer que les nanoparticules à base de squalène pouvaient s'accumuler de manière spécifique dans les aortes des souris *ApoE*$^{-/-}$, par comparaison aux souris témoins saines et aux souris injectées par les billes de latex fluorescentes. Les résultats suggèraient de plus une accumulation prononcée au niveau des sites de plaques d'athérosclérose. Cela fut confirmé d'autre part par des études immunohistochimiques, qui ont démontré de plus, que les nanoparticules fluorescentes de SQRho sont retrouvées dans les lésions d'athérosclérose à la fois précoces et avancées, s'accumulant dans les cellules résidentes dans les plaques (notamment macrophages et cellules musculaires lisses ayant une béta-actine activée).

Tous ces résultats ont fait l'objet d'un article scientifique :

"Brusini, R., Dormont, F., Cailleau, C., Nicolas, V., Peramo, A., Varna, M., & Couvreur, P. (2020). Squalene-based nanoparticles for the targeting of atherosclerotic lesions. *International journal of pharmaceutics*, 581, 119282."

Références :

[1]: Rafieian-Kopaei, M., Setorki, M., Doudi, M., Baradaran, A., & Nasri, H. Atherosclerosis: process, indicators, risk factors and new hopes. International journal of preventive medicine, 5(8), 927–946. (2014).
[2]: Frostegård J. Immunity, atherosclerosis and cardiovascular disease. BMC medicine, 11, 117. (2013).
[3]: R. Paoletti, A. M. Gotto Jr,D. P. Hajjar, Inflammation in atherosclerosis and implications for therapy. Circulation. 109, III-20-III-26 (2004).
[4]: Kamaly, N., Fredman, G., Fojas, J. J., Subramanian, M., Choi, W. I., Zepeda, K., Vilos, C., Yu, M., Gadde, S., Wu, J., Milton, J., Carvalho Leitao, R., Rosa Fernandes, L., Hasan, M., Gao, H., Nguyen, V., Harris, J., Tabas, I., & Farokhzad, O. C. Targeted Interleukin-10 Nanotherapeutics Developed with a Microfluidic Chip Enhance Resolution of Inflammation in Advanced Atherosclerosis. ACS nano, 10(5), 5280–5292. (2016).
[5]: Sobot, D., Mura, S., Rouquette, M., Vukosavljevic, B., Cayre, F., Buchy, E., Pieters, G., Garcia-Argote, S., Windbergs, M., Desmaële, D., & Couvreur, P. Circulating Lipoproteins: A Trojan Horse Guiding Squalenoylated Drugs to LDL-Accumulating Cancer Cells. Molecular therapy : the journal of the American Society of Gene Therapy, 25(7), 1596–1605. (2017).

Squalene-based nanoparticles for the targeting of atherosclerotic lesions

Romain Brusini[a,1], Flavio Dormont[a,1], Catherine Cailleau[a], Valerie Nicolas[b], Arnaud Peramo[a], Mariana Varna[a], Patrick Couvreur[a]*

[1] These authors contributed equally to this work.
[a] Institut Galien Paris-Sud, CNRS UMR 8612, Université Paris-Sud, Université Paris-Saclay, 92296 Châtenay-Malabry, France
[b] IPSIT, Microscopy facility, University of Paris-Sud, Université Paris-Saclay, 92296 Châtenay-Malabry, France

*Corresponding author: Patrick Couvreur

Email: patrick.couvreur@u-psud.fr

International Journal of Pharmaceutics. 2020 May 15;581:119282.
DOI: 10.1016/j.ijpharm.2020.119282.

Abstract

Native low-density lipoproteins (LDL) naturally accumulate at atherosclerotic lesions and are thought to be among the main drivers of atherosclerosis progression. Numerous nanoparticular systems making use of recombinant lipoproteins have been developed for targeting atherosclerotic plaque. These innovative formulations often require complicated purification and synthesis procedures which limit their eventual translation to the clinics. Recently, squalenoylation has appeared as a simple and efficient technique for targeting agents to endogenous lipoproteins through a bioconjugation approach. In this study, we have developed a fluorescent squalene bioconjugate to evaluate the biodistribution of squalene-based nanoparticles in an *ApoE*$^{-/-}$ model of atherosclerosis. By accumulating in LDL endogenous nanoparticles, the squalene bioconjugation could serve as an efficient targeting platform for atherosclerosis. Indeed, in this proof of concept, we show that our squalene-rhodamine (SQRho) nanoparticles, could accumulate in the aortas of atherosclerotic animals. Histological evaluation confirmed the presence of atherosclerotic lesions and the co-localization of SQRho bioconjugates at the lesion sites.

Key words: squalene-based nanoparticles, *ApoE*$^{-/-}$ mice, atherosclerotic plaque detection, plaque imaging

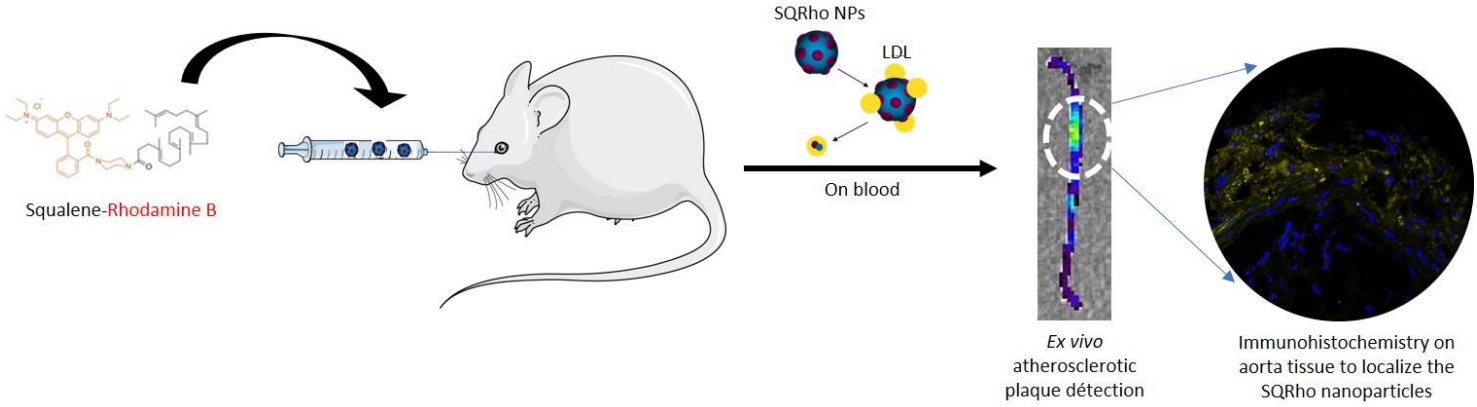

1. Introduction

Atherosclerosis is a chronic inflammatory and slowly progressing pathophysiological disease characterized by fatty deposits called atheromatous plaques appearing in the inner layers of arteries[1]. The adequate management of atherosclerosis is one of the major health challenges in modern medicine. Although lipid-lowering drugs have been applied successfully for the past 25 years, novel strategies are being developed that focused on directly detecting and treating vessel wall inflammation, a hallmark of atherosclerosis[2, 3].

In this context, therapeutic and diagnostic nanomaterials are being actively investigated for their ability to target atherosclerotic lesions and specifically deliver molecules of interest[4-6]. By taking advantage of endothelial permeability at the site of atherosclerotic lesions, several groups have used nanomedicine-based techniques for targeting atherosclerotic plaques both actively and passively[5, 7, 8]. One example is the use of hybrid iron oxide nanoparticles, which has gained interest as imaging platforms to target atherosclerotic lesions[9, 10]. Indeed, these are appealing imaging agents because of their specific features that allow the modulation of pharmacokinetics and targeting through surface moieties. However, iron oxide nanoparticles are not yet established in clinical practice for atherosclerotic plaque imaging[9].

In another way, recombinant lipoprotein-based nanoparticles have garnered attention for their innate interaction with atherosclerotic plaque[11-13]. Low-density Lipoproteins (LDL) are indeed, cholesterol-rich (40-50% w/w) cargo vehicles for the delivery of cholesterol to peripheral tissues. They consist of a lipid rich core surrounded by a monolayer of amphiphilic phospholipids and apolipoproteins (ApoB100 and ApoE). In the body, LDL naturally accumulate in atherosclerotic plaques, where they are modified by binding to proteoglycans or remnant reactive oxygen species, which enhances their recognition by macrophages via a number of unregulated receptors such as scavenger receptor A (SRA), lectin-like receptors (LOX-R) and toll-like receptors (TLR4)[14, 15]. This triggering of macrophage inflammatory pathways is a critical event in the atherosclerotic lesion development and fuels progression of the disease. Consequently, by taking advantage of this natural interaction between lipoproteins and atherosclerotic plaque several groups have described lipoprotein-like nanoparticles that aim at targeting atherosclerotic lesions. Although this represents a promising strategy, its industrial implementation and economic feasibility remain challenged by the complicated production of such LDL-like nanoparticles.

Recently, our laboratory has pioneered the exploitation of squalene, a metabolic precursor of cholesterol, as a biomimetic carrier to specifically interact with LDL[16, 17]. When conjugated to squalene, diverse therapeutic agents were shown to interact with lipoproteins in the circulation, thus demonstrating squalene to be an efficient targeting agent for these endogenous lipoprotein particles. This elegant approach exploiting LDL as indirect natural carriers towards LDL receptor expressing cells could therefore be used

to direct diverse therapeutic agents to atherosclerotic plaque, exploiting the natural accumulation of LDL at these sites.

In this study, we investigated the proof-of-concept that this nanotechnology may, indeed, target atherosclerotic plaque by using fluorescent squalene bioconjugates and evaluating their biodistribution in an *in vivo* model of atherosclerosis using *ApoE*$^{-/-}$ mice. Our data shows efficient targeting of atherosclerotic plaque and interaction with plaque resident macrophages.

2. Materials and Methods

2.1. Synthesis of Squalene-rhodamine bioconjugate

Rhodamine B was used as the fluorescent dye to evaluate the efficacy of the squalene technology to detect atherosclerotic plaques. Squalene-rhodamine (SQRho) was synthesized by direct acylation of the piperazine-rhodamine B (Sigma-Aldrich, France) after *in situ* formation of chloroformate mixed anhydride of trisnorsqualenic acid. To a solution of 30 µL (0.33 mmol) ethyl chloroformate (Sigma-Aldrich, France) in 1 mL anhydrous dichloromethane (DCM, Carlo Erba Reagents) was added 90 µL (0.6 mmol) of trimethylamine (Et3N, Carlo Erba Reagents). The mixture was cooled at 0°C and a solution of trisnorsqualenic acid (kindly provided by Holochem) containing 120 mg, (0.30 mmol) in 2 mL DCM anhydrous was added dropwise. Mixture was stirred for 30 min at 0°C and a solution of rhodamine B-piperazine (181 mg, 0.33 mmol) in DMF (1 mL) was added dropwise. After being stirred at room temperature for 16 h, dimethylformamide (DMF, Carlo Erba Reagents) was removed under vacuum. The residue was taken up in 4 mL of saturated aqueous solution NaHCO3 (sodium bicarbonate) (Sigma-Aldrich, France) and extracted with 3 × 15 mL ethyl acetate (AcOEt, Carlo Erba Reagents). The combined organic layers were washed with brine, dried over magnesium sulfate (MgSO4, Carlo Erba Reagents) and concentrated under reduced pressure. The crude was then purified by flash chromatography on silica (DCM/Methanol from 100:0 to 90:10). Fraction containing the expected product were concentrated to provide rhodamine B 4-(1,1',2-trisnorsqualenoyl)piperazine (140 mg, 56%) as a dark purple glassy solid.

1 H NMR (300 MHz, MeOD, δ in ppm): 7.76 (2H, m, H-4', H-5'), 7.70 (1H, m, H3'), 7.52 (1H, m, H-6'), 7.27 (2H, d, J = 9.5 Hz, H-1, H-8), 7.09 (2H, dd, J = 9.5 Hz, J = 2.1 Hz, H-2, H-7), 6.97 (2H, d, J = 2.4 Hz, H-4, H-5), 5.06−5.20 (5H, m, HC=C(CH3)CH2), 3.71 (8H, q, J = 7.1 Hz, H3CCH2N), 3.35−3.50 (8H, m, NCH2CH2N), 2.44 (2H, t, J= 9 Hz NOCCH2CH2), 2.21 (2H, t,J= 9Hz NOCCH2CH2), 2.13−1.93 (16H, m, =C(CH3)CH2CH2CH=), 1.68 (3H, s, HC=C(CH3)2), 1.61 (12H, s, HC=C(CH3)), 1.31 (12H, t, J = 7.1 Hz, H3CCH2N)

2.2. SQRho Nanoparticle synthesis

Squalene-rhodamine nanoparticles (SQRho NPs) were prepared by nanoprecipitation. Briefly, SQRho and squalenic acid (SQCOOH) were each dissolved in absolute ethanol, each in a different vial, at a concentration of 6 mg/mL and mixed in different ratios to obtain a final organic solution of 6 mg/mL concentration. This organic solution was added dropwise under moderate mechanical stirring to a 5% (w/v) dextrose solution (DXT 5%). The ethanol was then completely evaporated using a Rotavapor (R-215 Büchi) (90 rpm, 40°C, 42 mbar) to obtain an aqueous suspension of pure NPs (2 mg/mL). NPs size (hydrodynamic diameter) and surface charge (zeta potential) were measured using a Malvern Zetasizer Nano ZS 6.12 (173° scattering angle, 25°C, Material RI: 1.49, Dispersant Viscosity RI: 1.330, Viscosity 0.8872 cP). For the size measurements by dynamic light scattering (DLS), a good attenuator value (7−9) was obtained when suspending 50 µL of NPs in 1 mL of distilled water. The mean diameter for each preparation resulted from the average of three measurements of 60 s each. For zeta potential measurements, 70 µL of NPs was dissolved in 2 mL of KCl 1 mM before filling the measurement cell. The mean zeta potential for each preparation resulted from the average of three measurements in automatic mode, followed by the application of the Smoluchowski equation. NPs stability was assessed by measuring NPs size by DLS at different time intervals up to five days.

2.3. Cell Internalization of SQRho NPs

Flow Cytometry. A total of 50 000 Raw 264.7 (ATCC) cells/well (26 000 cells/ cm^2) were seeded in 12-well plates and cultured in DMEM (Sigma-Aldrich, France) with 10% fetal bovine serum (Sigma-Aldrich, France) for 24 h in 5% CO2 at 37°C. The cells were then incubated with 100 µM fluorescent SQRho NPs diluted in cell culture medium. At the end of the incubation period, cells were washed with 1 mL of PBS and then treated with 300 µL of 0.25% trypsin solution (Sigma-Aldrich, France) for 5 min at 37°C and 5% CO2. Trypsin solution was diluted by adding 0.7 mL of medium, and the fluorescence of the cells was recorded using a flow cytometer C6 (Accuri Cytometers Ltd.). For fluorescence detection of SQ-Rho labeled NPs, excitation was carried out using all four available channels. 10 000 cells were measured for each sample. The results were expressed as the mean fluorescence intensity (MFI) ± SEM.

Confocal Microscopy. A total of 200 000 RAW cells/well (100 000 cells/cm^2) were seeded on 12 mm glass coverslips in 6-well plates. Cells were grown for 24 hours in order to adhere to the glass slip, and then incubated with 100 µM of SQ-Rho labeled fluorescent SQAd NPs diluted in culture medium. At the end of the incubation period, cells were washed with 1 mL of PBS and fixed with 4% PFA for 15 min. Residual PFA was then neutralized by NH4Cl 50 mM for another 15 min before mounting on microscopy slides. Slides were imaged with an inverted LSM510 Zeiss confocal microscope using a PlanApochromat 63X

objective lens (NA 1.40, oil immersion) and laser set at 543 nm. Pinhole was set at 61 µm giving an optical section thickness of 0.6 µm. Numerical images were acquired with LSM 510 software version 3.2 and further image analysis was made using ImageJ software.

2.4. *In vivo* experiments

Animals. All the animal experiments comply with the ARRIVE guidelines[18, 19] and were carried out in accordance with the EU Directive 2010/63/EU and internal University Committee.

Four-week-old males, C57BL apolipoprotein E deficient (*ApoE*$^{-/-}$) mice, and age-matched male C57BL/6 mice were purchased from the from Charles River Laboratories (France). Mice were housed in a pathogen free facility with access to food and water *ad libitum* and maintained on a 12 h light/dark cycle. A group of mice received normal standard autoclaved diet for 14 months. In order to induce atherosclerotic lesions, another group received high rich diet (high cholesterol diet (HFHC) of 4.5 kcal/g, 20.0% fat, and 2% cholesterol (U8958, Verion 0250, Safe, Augy, France) for up to 12 weeks.

Nanoparticles injection and abdominal aorta imaging. The targeting efficacy of SQRho NPs was evaluated *in vivo* in a *ApoE*$^{-/-}$ knockout mouse model of atherosclerosis. After the diet period, SQRho NPs diluted at 4 mg/mL in 5% dextrose solution were intravenously injected at a dose of 15 mg/kg through the suborbital vein. Mice receiving latex nanobeads (Sigma-Aldrich, 15 mg/kg) were included as controls. Twenty-four hours after the last injection, the mice were sacrificed by intraperitoneal injection of a lethal dose of sodium pentobarbital and perfused with NaCl 0.9%. The abdominal aorta and other organs were harvested, and immediately imaged using IVIS Lumina LT Series III system (Caliper Life Science) using 560 nm (SQRho NPs) or 480 nm (Latex beads) excitation filters and 620 nm or 570 nm emission filters respectively. Images and measures of fluorescence signals were acquired and analysed with Living Imaging software (Caliper Life Sciences).

2.5. Immunofluorescence staining

Following IVIS imaging, the collected aortas were divided in small samples (from 2 to 10 mm), fixed with 4% PFA solution for 24 h and then stored at -80°C. The frozen samples were embedded in tissue-Tec O.C.T (Microm Microtech, France) and then subsequently cut in 5 µm thick histological sections.

Before staining, tissue sections were rehydrated in PBS, treated with 0.01% Triton X-100 buffer for 3 min at room temperature (RT) for membrane permeabilization, and blocked with 1% Bovine Serum Albumin (BSA) for 30 min at RT. Then, the sections were incubated overnight at 4°C with primary antibodies diluted in antibody diluent (Sigma -Aldrich, France). The following primary antibodies were used: rabbit anti-

mouse CD64 (1/200, polyclonal, GeneTex), rat anti-mouse CD68 (1/100, clone FA-11, Biolegend), rabbit anti-mouse CD36 (1/200, polyclonal, GeneTex), rat anti-mouse beta smooth muscle actin (1/200, Biolegend). After washing, IgG secondary antibodies diluted (1/2000, Sigma-Aldrich, France) in antibody diluent (Sigma -Aldrich, France) was applied for 1h30 at RT. The slides were kept in the dark during all the incubation time. Finally, slides were mounted using aqueous mounting medium with DAPI (Vector Laboratories, UK) to stain the nuclei, and then covered with a glass coverslip (VWR, France). A negative control was performed by omitting the primary antibody.

The images of immunostained aorta sections were acquired using a Leica TCS SP8 confocal microscope (Leica Microsystems) at 100X and 630X magnification. On average, we imaged between two and four different plaque areas in each arch section. The obtained images were analysed using Leica LAS-X software.

2.6. Statistics

Statistical analysis was performed with the software GraphPad Prism 7.0 (Graphpad Software Inc.). Data are presented as mean ± S.E. Comparisons between 2 groups were performed using the unpaired Student t test, considering $p<0.05$ to be statistically significant.

3. Results and Discussion

3.1. Nanoparticle synthesis and characterization

In previous studies, we have shown that squalene -based nanoparticles displayed unique LDL-targeting properties which were exploited here to accumulate these nano-vectors at sites of atherosclerotic plaque development[16, 17]. Fluorescent squalene nanoparticles were prepared using a nanoprecipitation technique after synthesis of a squalene-rhodamine (SQRho) bioconjugate. Efficient conjugation of Rhodamine to squalene was achieved after functionalization of rhodamine with piperazine, affording Rhodamine-piperazine, which could then be coupled to squalene-acetic acid in satisfying yield (56%) (Figure 1A). SQRho does not form on its own nanoparticles with satisfying stability and physico-chemical features and needs to be stabilized by co-nanoprecipitation with squalenic acid (SQCOOH). In this approach, SQCOOH and SQRho were solubilized in an ethanolic solution at different ratios, and then nanoprecipitated in a 5% dextrose solution under vigorous stirring. Upon mixture of the different solutions, instantaneous self-assembly of NPs occurred. Nanoparticle size was controlled by carefully modifying SQRho:SQCOOH ratios. Thus, SQRho NPs could be produced with a substantial hydrodynamic size range. By varying the SQRho:SQCOOH ratio from 50-90% we were able to synthesize stable nanoparticles ranging from 210 to

58 nm (Figure 1B). Zeta potential of the nanoparticles was also determined and ranged from +2.4 mV to + 40 mV (Figure 1C). This could be explained by the fact that, at physiological pH, SQCOOH bears a negative charge offsetting the positive charge of Rhodamine. With increasing SQCOOH content in the nanoparticles, the positive rhodamine charge was reduced, leading to a lower absolute zeta potential and a poorer colloidal stability. A ratio of SQRho:SQCOOH 82:18 wt% was found to be the best compromise to obtain stable formulations of the desired mean hydrodynamic diameter and size distribution (thereafter named SQRho NPs).

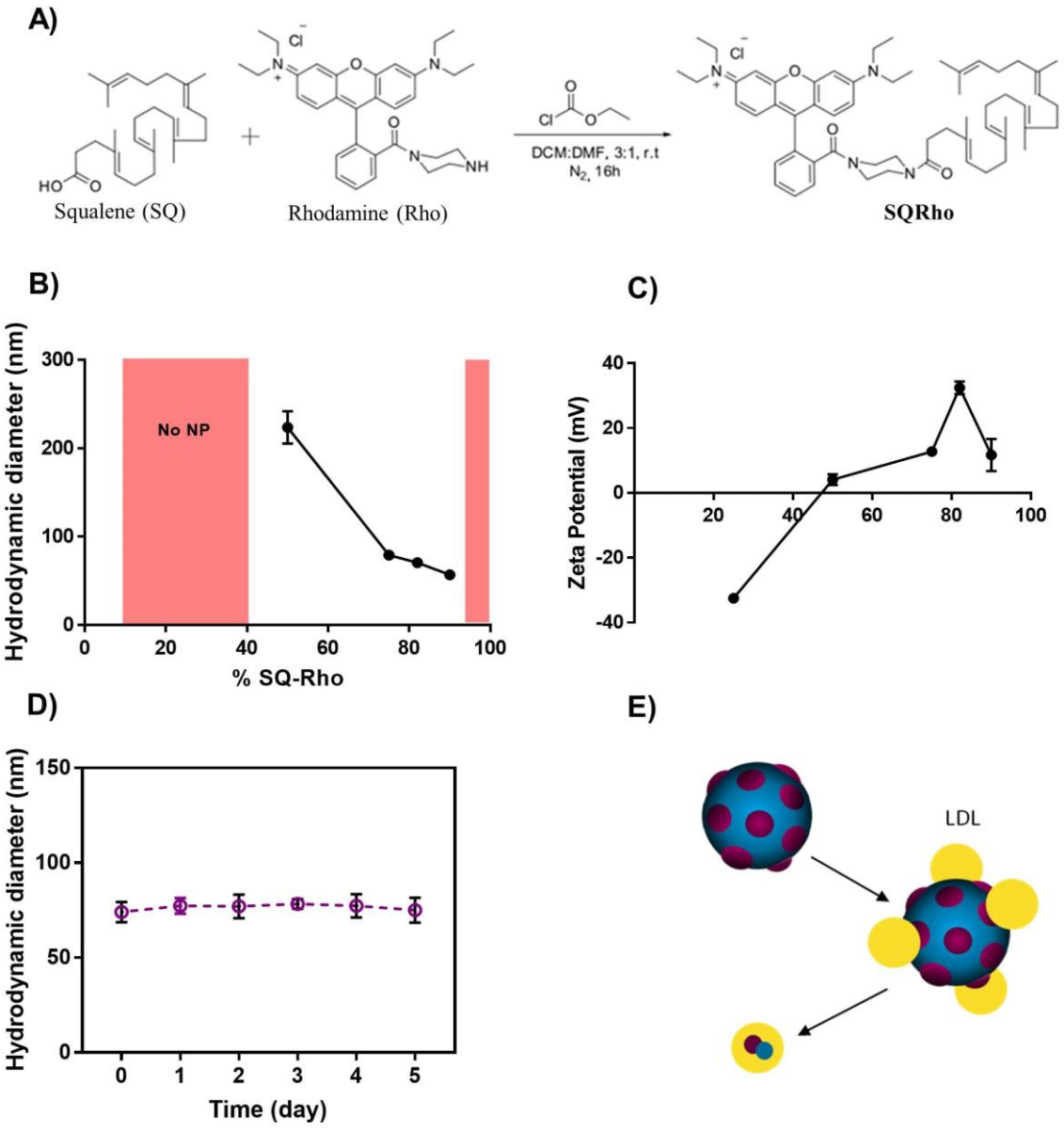

Figure 1: Nanoparticle synthesis and characterization

(**A**) Scheme of rhodamine-piperazine coupling with squalenic acid. (**B**) Hydrodynamic size of SQRho:SQCOOH NPs (diameter, nanometers) measured by dynamic light scattering (DLS). Analysis of the light intensity fluctuation correlation function was done by intensity size distribution (**C**) Measurement of surface ζ-potential of SQRho:SQCOOH NPs. (**D**) Stability study of SQRho: SQCOOH (82:18 wt%) in PBS over 5 days. (**E**) Supposed LDL interaction of squalene-bioconjugate based nanoparticles with endogenous LDL.

SQ-Rho nanoparticles stability was evaluated in PBS over 5 days by DLS (Figure 1D). Therefore, and as we have done previously, stable multi-bioconjugate nanoparticles were obtained and could allow to study squalene biodistribution.

3.2. *In vitro* cellular uptake

We then set out to investigate if SQRho NPs could take advantage of certain biological properties of LDL such as accumulation in plaque resident macrophages. Squalene is a precursor of cholesterol which strongly interacts with the LDL receptor expressed on plaque resident macrophages, enabling clathrin mediated endocytosis[20]. To investigate the ability of SQRho nanoparticles to efficiently target and accumulate in plaque macrophages, SQRho NPs were incubated with murine macrophage cells (RAW 264.7) in FBS rich medium and cell internalization was monitored by fluorescence microscopy and flow cytometry. SQRho NPS were found to gradually accumulate inside of cells over time (Figure 2A). This was confirmed by confocal imaging which showed pockets of fluorescence inside of RAW 264.7 cells where endosomes accumulated the fluorescent endocytosed material (Figure 2B-C). When cells were incubated with SQRho at 4°C instead of 37°C, cell fluorescence intensity dramatically decreased, pointing to endocytosis as the major pathway for cell internalization of SQRho NPs.

Macrophages naturally have a very active LDL metabolism[15]. Native LDL are recognized by the LDL receptor expressed at the surface of macrophages, and then endocytosed before trafficking into lysosomes, where cholesteryl ester is hydrolyzed into free cholesterol by acidic lipase. Here, we showed that SQRho bioconjugates accumulated inside the macrophages. Although other nanoparticle types are scavenged by macrophages, the structural similarity of squalene with cholesterol and its ability to specifically interact with endogenous LDL (Figure 1E) makes it an interesting candidate to target plaque resident macrophages.

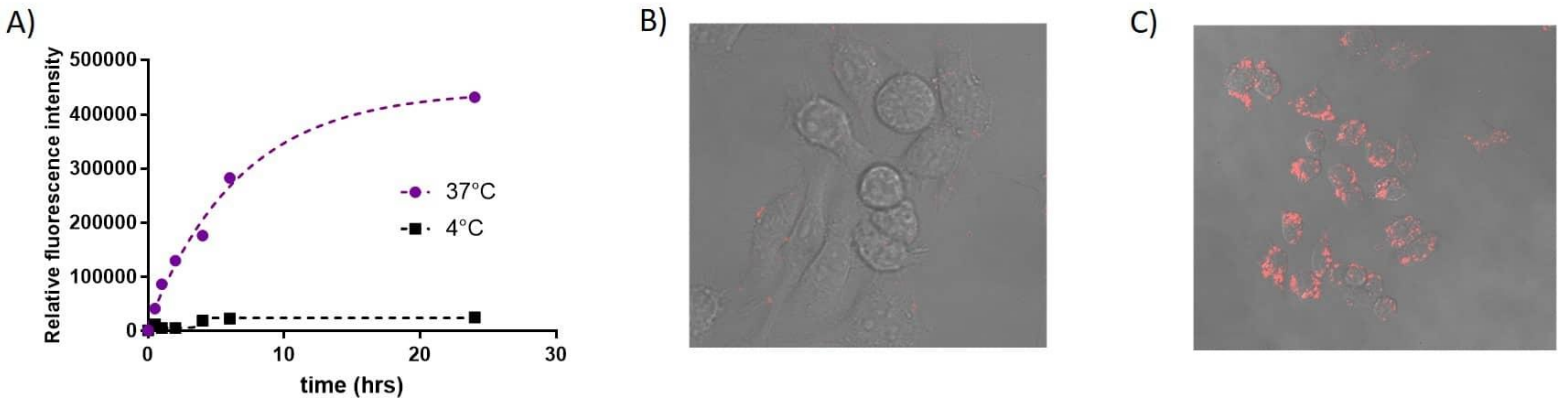

Figure 2: *In vitro* cellular uptake

(**A**) Flow cytometry of RAW 264.7 microphages incubated with 100 µM of SQRho at different time intervals at 37°C and 4°C. (**B**) Phase contrast confocal microscopy image of RAW 264.7 macrophages incubated with 100 µM of SQRho for 30 min. Scale bar= 10 µm. (**C**) Phase contrast confocal microscopy image of RAW 264.7 macrophages incubated with 100 µM of SQRho for 4 hrs. Scale bar= 10 µm.

3.3. *In vivo* plaque targeting

To assess whether SQRho nanoparticles accumulated in atherosclerotic lesions and were taken up by plaque macrophages *in vivo*, we conducted a biodistribution study on a mouse model of atherosclerosis. *ApoE*$^{-/-}$ mice are a common model for human atherosclerosis, which features apparition of fatty streaks in atherosclerosis-prone regions and chronic inflammation of the lesions with monocyte infiltration[21, 22]. Either wild type mice or mice injected with fluorescent latex nanobeads were used as controls to evaluate the specific ability of SQ NPs to target the atherosclerotic lesions.

In an initial experiment, the detection limit of our imaging system was evaluated by imaging directly SQRho or latex nanobeads at different dilutions in a Dextrose 5% solution (Figure 3A). The maximum concentration corresponds to 4mg/mL, which is the concentration of the mice injected dose. It was observed that the limit of detection corresponded to a concentration of SQRho near 4 µg/ml, which was acceptable for further *in vivo* experiments.

To assess whether SQ based nanoparticles accumulated in atherosclerotic lesions, we injected wild type C57BL/6J mice (n=3) or *ApoE*$^{-/-}$ mice on a high cholesterol diet (n=3) with SQRho nanoparticles and the biodistribution of the nanoparticles at atherosclerosis prone areas (namely the aorta) was investigated. The hypothesis was that if SQRho could accumulate in atherosclerotic plaque, an increase of fluorescence in the aortas of *ApoE*$^{-/-}$ mice would be observable. Twenty-four hours post-injection, the mice were euthanized, their aortas excised and directly imaged on an IVIS Lumina imaging system. The ex vivo imaging showed that, in comparison with the control wild-type mice, a sharp increase in the aorta radiant efficiency could be detected after intravenous injection of SQRho NPs in the *ApoE*$^{-/-}$ mice (Figure 3B-C). These data indicated pronounced accumulation of SQRho bioconjugates at the sites of the atherosclerotic

plaque lesion. To investigate whether this accumulation was SQ-nanoparticle dependent, we performed a second set of control experiments where a C57BL/6J mouse and an *ApoE*$^{-/-}$ mouse on a high cholesterol diet were injected with commercial 100 nm fluorescent polystyrene nanobeads. Twenty-four hours post-injection, the mice were euthanized, their aortas excised and directly imaged on an IVIS Lumina imaging system. This time, no preferential accumulation in the atherosclerotic mice could be observed.

It has been shown that the vasa vasorum present in advanced atherosclerotic lesions can allow passive accumulation mechanisms similar to the enhanced permeation and retention (EPR) effect observed in tumor tissue[23, 24]. Our experiments showed that the accumulation of non-targeted latex nanobeads through this passive mechanism was minimal. Conversely, likely via lipoproteins that actively accumulate in atherosclerotic lesions, SQRho NPs were observed to significantly accumulate in the aorta of atherosclerotic mice. This is in accordance with recent literature making use of lipoprotein-like nanoparticles to achieve similar targeting effects[13, 14]. The advantage of the squalene platform being that it circumvents the complicated synthesis processes making use of recombinant LDL or HDL proteins but rather relied on a simple bioconjugation step to achieve plaque-targeting properties.

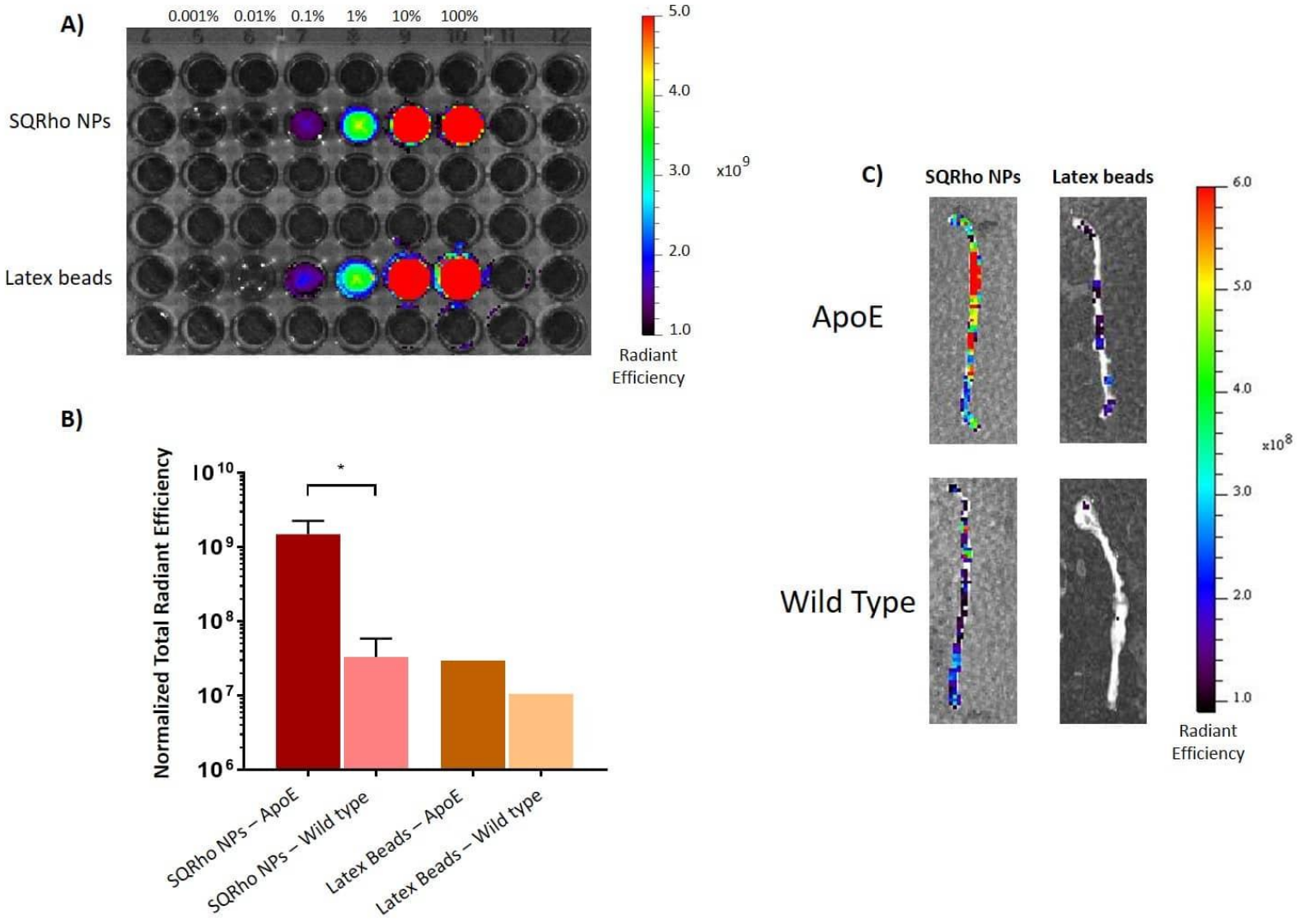

Figure 3: *In vivo* plaque targeting

(**A**) Detection limit experiment. SQRho NPs (top row) and Fluorescent latex beads (bottom row) were dispersed at a concentration of 4 mg/mL in 5% Dextrose at different dilution factors (%). The plate was imaged by epi-fluorescence in the IVIS Lumina system with excitation filter set at 560 nm for SQRho NPs and at 480nm for latex beads and emission filter set at 620 nm or 570 nm respectively. Color scale: Min = $1.00e^9$ / Max = $5.00e^9$. (**B**) Normalized total radiant efficiency in the aortas of interest. n=3 mice for SQRho NPs treatment, n=1 mouse for latex beads treatment. Data are mean ± SD. *P<0.05 (Student's t-test). Wild type mice are C57Bl/6J mice. (**C**) Biodistribution of SQRho NPs (left images) or fluorescent latex beads (right images) in the aortas of *ApoE*$^{-/-}$ mice or wild type C57Bl/6J animals, 24 hrs post-injection. Images were taken in epifluorescence in the IVIS Lumina system with excitation filter set at 560 nm for SQRho NPs and at 480nm for latex beads and emission filter set at 620 nm or 570nm; respectively. Color scale: Min = $9.00e^7$ / Max = $6.00e^8$

3.4. Immuno-histochemistry

To confirm the presence of SQRho inside atherosclerotic plaque, we conducted an immuno-histochemistry experiment on harvested aortas. Atherosclerotic lesions can typically be classified in terms of early lesions (type I-III), characterized by adaptive thickening of the intima, macrophage foam cell accumulation and advanced lesions (type IV-VI) which are characterized by various degrees of disarrangement of the intimal

structure[25]. After washing with PBS, aortas were frozen, cut in histological sections, and stained with DAPI, macrophage markers anti-CD36, anti-CD68- or anti-beta smooth muscle actin antibody.

Figure 4 shows a V type lesion, with characteristic core of extracellular lipids, fibrous thickening and obstructed vessel lumen. Macrophage labelling using both CD64 and CD36 showed extensive presence of macrophages that had migrated in the vessel intima, a hallmark of the atherosclerotic lesion environment. Interestingly, SQRho NPs strongly colocalized with these plaque macrophages which confirmed the previous *ex vivo* experiment. In advanced plaques, smooth muscle cells differentiated and acquired a phagocytic phenotype. This was evidenced through the beta-actin marking, showing that SQRho accumulated in these differentiated muscle cells characteristic of advanced atherosclerotic plaque. In Figure 5, early type II-III lesions with macrophage migration in the intima and small lipid pools could be observed. Again, SQRho NPs appeared to accumulate in the small plaques, as well as, in the plaque resident macrophages as can be seen on the CD68, CD36 and CD64 overlay images. On the contrary, latex nanobeads did not provide accumulation in these early plaques, as can be seen in Figure 6.

Overall, these experiments confirmed that *ApoE*$^{-/-}$ model developed both advanced and early type atherosclerotic lesions. In both cases, SQRho NPs were found to have accumulated in the fatty lesions, being uptaken by plaque resident phagocytic cells (both beta-actin activated smooth muscle cells and macrophages).

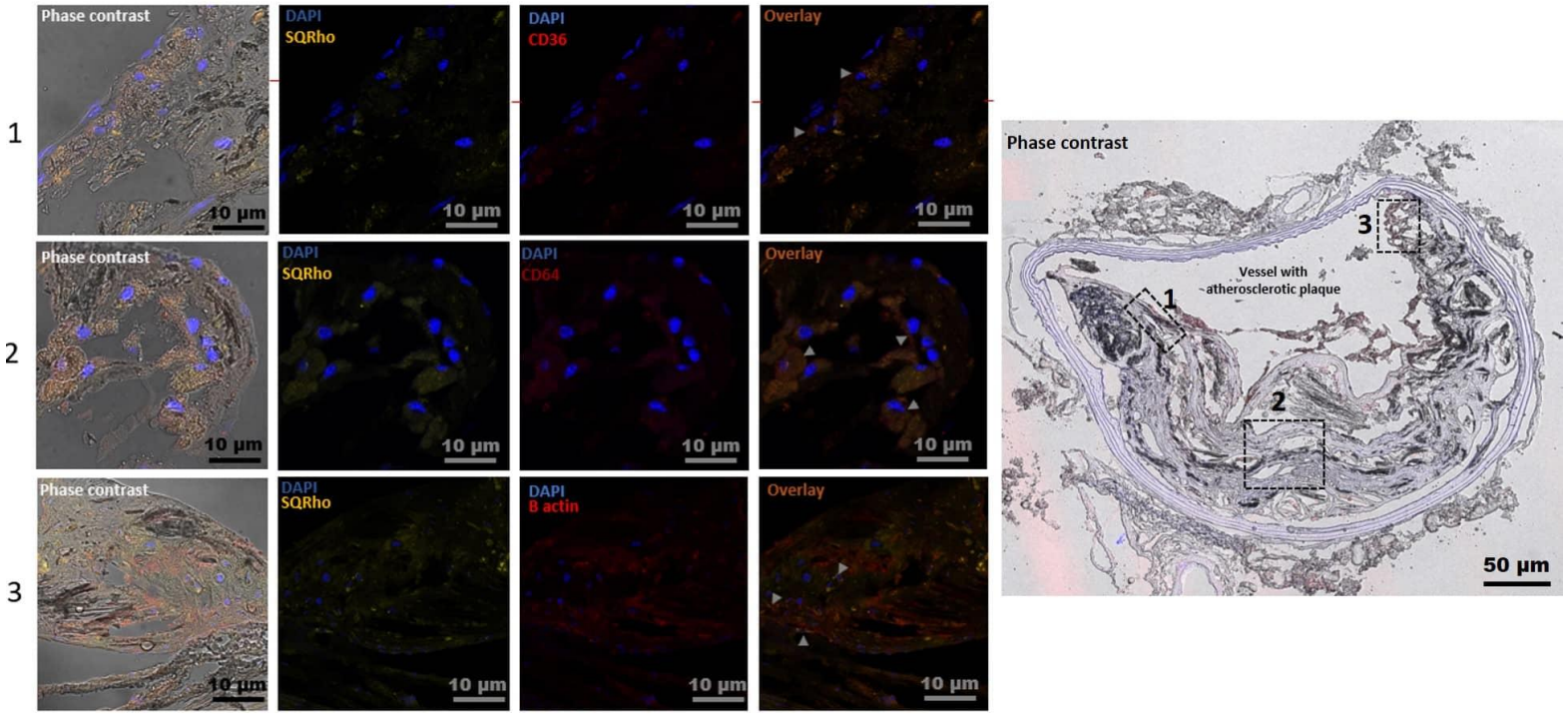

Figure 4: Immuno-histochemistry of advanced atherosclerotic lesions treated with SQRho NPs.

Assessment of SQRho NPs localization (in yellow) in intraplaque macrophages after their immunostaining with CD64 and CD36 (in red) (1 & 2). Assessment of SQRho NPs localization (in yellow) on proliferative smooth muscle cells positive for beta-actin (in red) (3).

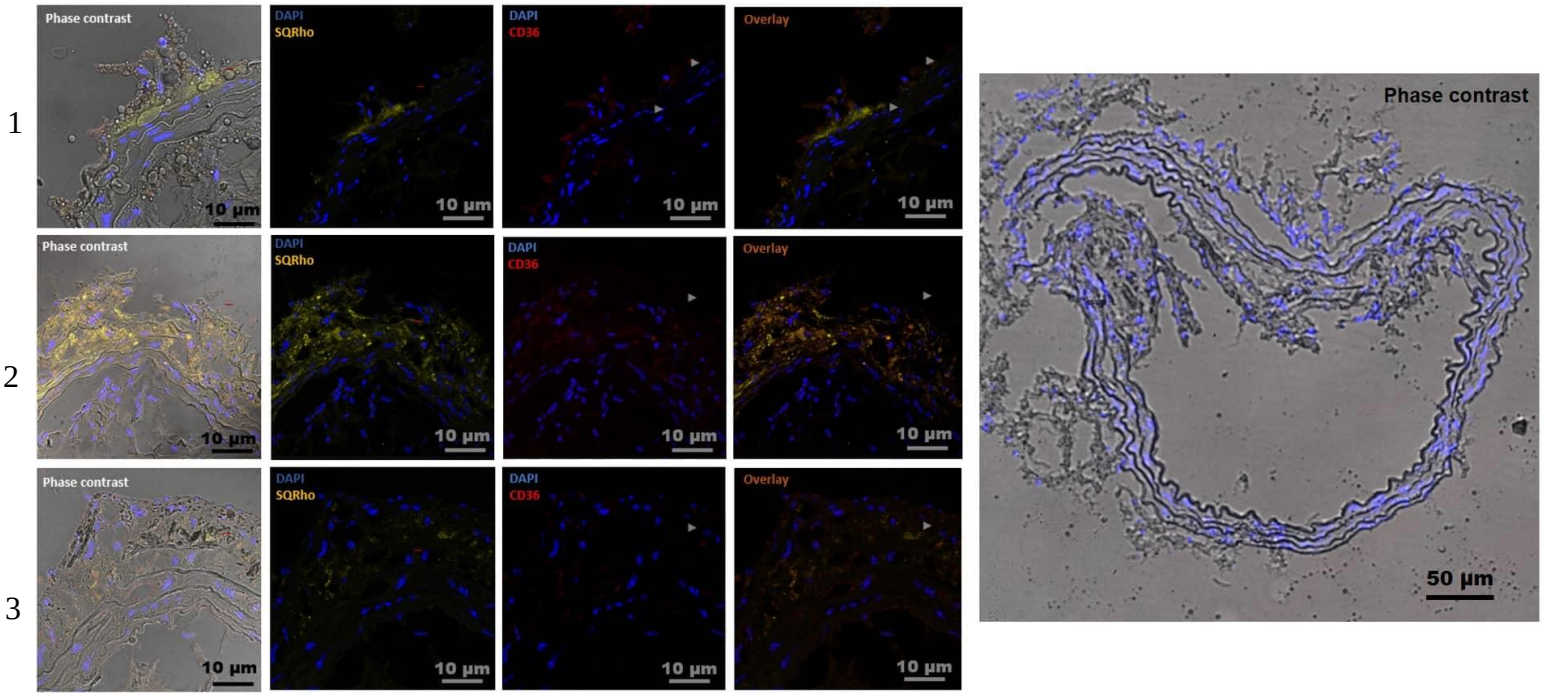

Figure 5: Immuno-histochemistry on early atherosclerotic lesions.

Assessment of SQRho NPs localization (in yellow) on intraplaque macrophages after their immunostaining with CD64 and CD36 (in red) (1 & 2). Assessment of SQRho NPs localization (in yellow) on proliferative smooth muscle cells positive for beta-actin (in red) (3).

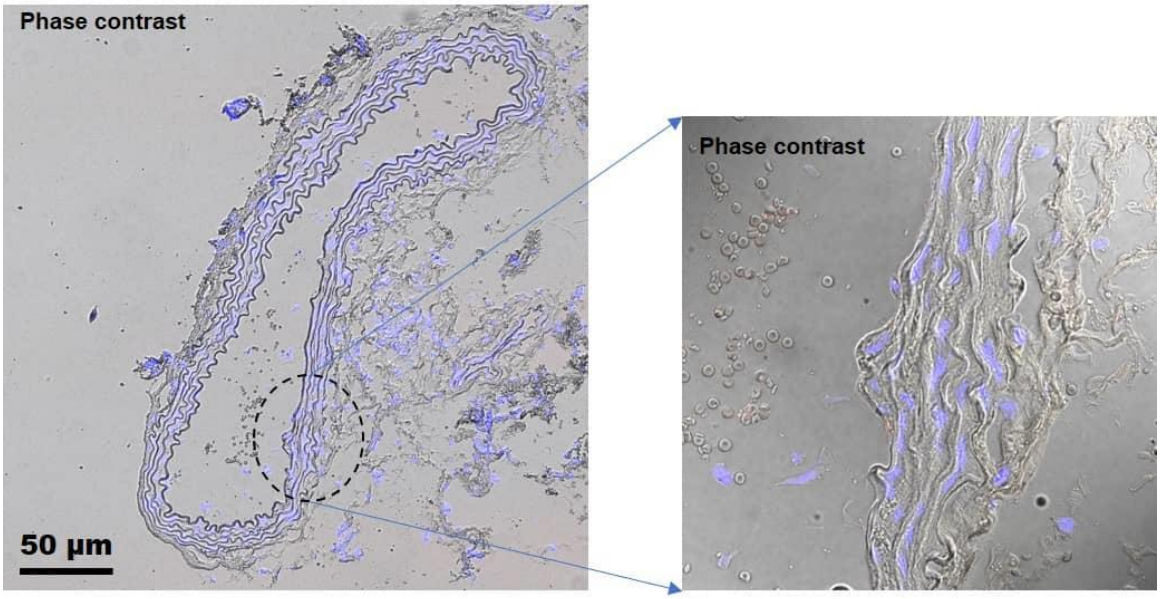

Figure 6: Latex nanobeads accumulation in early plaques.

Assessment of fluorescent latex nanobeads (in orange/red) localization in early plaques. A lack of accumulation of latex nanobeads is noted

4. Conclusions

This study provides the proof-of-concept that SQ-based nanoparticles were able to target atherosclerotic plaque. Indeed, our results highlighted a significant accumulation of SQRho NPs in both early and advanced atherosclerotic plaque, in *ApoE*$^{-/-}$ mice. Histological study confirmed the presence of fluorescent SQRho in the plaque and interaction with plaque resident macrophages. Further efforts will be necessary to more precisely identify the mechanism of accumulation of squalene nanoparticles in atherosclerotic plaque. This study opens now interesting perspectives for exploring different squalene-based theranostic possibilities, such as the use of Squalene-Gadolinium bioconjugates for non-invasive plaque imaging by MRI and/or the local delivery of a variety of siRNA-based, anti-inflammatory or antiproliferative therapeutic agents.

Declaration of interest

The authors declare no conflict of interest.

Acknowledgements

*Funding***:** The authors gratefully acknowledge the financial support from the 7th EuroNanoMed-II call for proposals, project NanoHeart n°ANR-16-ENM2-0005-01. This work was further supported by la Fondation pour la Recherche Médicale (FRM) grant number ECO20160736101.

Besides, the authors are grateful to Severine Domenichini (UMS IPSIT, Université Paris-Saclay, Châtenay-Malabry, France) for assistance with confocal microscopy experiments.

Author contributions

Romain Brusini: the conception and design of the study, acquisition of data & data analysis and interpretation of data, drafting the article

Flavio Dormont: the conception and design of the study, acquisition of data & data analysis and interpretation of data, drafting the article

Catherine Cailleau: design of the study, acquisition of data & data analysis

Valerie Nicolas: acquisition of data & data analysis

Arnaud Peramo: acquisition of data & data analysis

Mariana Varna: the conception and design of the study, acquisition of data & data analysis and interpretation of data, drafting the article**,** supervision, funding *acquisition*

Patrick Couvreur: drafting the article, supervision, funding acquisition, final approval of the version to be submitted.

References

1. Rafieian-Kopaei M, Setorki M, Doudi M, Baradaran A, Nasri H. Atherosclerosis: process, indicators, risk factors and new hopes. Int J Prev Med. 2014 5(8):927-46.
2. Kamaly N, Fredman G, Fojas JJ, Subramanian M, Choi WI, Zepeda K, Vilos C, Yu M, Gadde S, Wu J, et al. Targeted Interleukin-10 Nanotherapeutics Developed with a Microfluidic Chip Enhance Resolution of Inflammation in Advanced Atherosclerosis. ACS Nano 2016, 10:5280-5292.
3. Paoletti R, Gotto AM, Jr., Hajjar DP. Inflammation in atherosclerosis and implications for therapy. Circulation 2004, 109:III20-26.
4. Fredman G, Kamaly N, Spolitu S, Milton J, Ghorpade D, Chiasson R, Kuriakose G, Perretti M, Farokzhad O, Tabas I. Targeted nanoparticles containing the proresolving peptide Ac2-26 protect against advanced atherosclerosis in hypercholesterolemic mice. Sci Transl Med 2015, 7:275ra220.
5. Lobatto ME, Calcagno C, Millon A, Senders ML, Fay F, Robson PM, Ramachandran S, Binderup T, Paridaans MP, Sensarn S, et al. Atherosclerotic plaque targeting mechanism of long-circulating nanoparticles established by multimodal imaging. ACS Nano 2015, 9:1837-1847.
6. Winter PM, Morawski AM, Caruthers SD, Fuhrhop RW, Zhang H, Williams TA, Allen JS, Lacy EK, Robertson JD, Lanza GM, et al. Molecular imaging of angiogenesis in early-stage atherosclerosis with alpha(v)beta3-integrin-targeted nanoparticles. Circulation 2003, 108:2270-2274.
7. Juenet M, Varna M, Aid-Launais R, Chauvierre C, Letourneur D. Nanomedicine for the molecular diagnosis of cardiovascular pathologies. Biochem Biophys Res Commun 2015, 468:476-484.
8. Nakhlband A, Eskandani M, Omidi Y, Saeedi N, Ghaffari S, Barar J, Garjani A. Combating atherosclerosis with targeted nanomedicines: recent advances and future prospective. Bioimpacts 2018, 8:59-75.
9. Heidt T, Nahrendorf M. Multimodal iron oxide nanoparticles for hybrid biomedical imaging. NMR Biomed. 2013 26(7):756-65.
10. Dengfeng Cheng, Xiao Li, Chunfu Zhang, Hui Tan, Cong Wang, Lifang Pang, Hongcheng Shi. Detection of Vulnerable Atherosclerosis Plaques with a Dual-Modal Single-Photon-Emission Computed Tomography/Magnetic Resonance Imaging Probe Targeting Apoptotic Macrophages. ACS Appl Mater Interfaces 2015 7(4),2847-2855
11. Frias JC, Williams KJ, Fisher EA, Fayad ZA. Recombinant HDL-like nanoparticles: a specific contrast agent for MRI of atherosclerotic plaques. J Am Chem Soc 2004, 126:16316-16317.
12. Lobatto ME, Fuster V, Fayad ZA, Mulder WJ. Perspectives and opportunities for nanomedicine in the management of atherosclerosis. Nat Rev Drug Discov 2011, 10:835-852.
13. Sanchez-Gaytan BL, Fay F, Lobatto ME, Tang J, Ouimet M, Kim Y, van der Staay SE, van Rijs SM, Priem B, Zhang L, et al. HDL-mimetic PLGA nanoparticle to target atherosclerosis plaque macrophages. Bioconjug Chem 2015, 26:443-451.
14. Getz GS, Reardon CA. Atherogenic lipids and macrophage subsets. Curr Opin Lipidol 2015, 26:357-361.
15. Linton MRF, Yancey PG, Davies SS, Jerome WG, Linton EF, Song WL, Doran AC, Vickers KC. The Role of Lipids and Lipoproteins in Atherosclerosis. 2000.
16. Sobot D, Mura S, Rouquette M, Vukosavljevic B, Cayre F, Buchy E, Pieters G, Garcia-Argote S, Windbergs M, Desmaele D, et al. Circulating Lipoproteins: A Trojan Horse Guiding Squalenoylated Drugs to LDL-Accumulating Cancer Cells. Mol Ther 2017, 25:1596-1605.
17. Sobot D, Mura S, Yesylevskyy SO, Dalbin L, Cayre F, Bort G, Mougin J, Desmaele D, Lepetre-Mouelhi S, Pieters G, et al. Conjugation of squalene to gemcitabine as unique approach exploiting

endogenous lipoproteins for drug delivery. Nat Commun 2017, 8:15678.
18. Kilkenny C, Browne W, Cuthill IC, Emerson M, Altman DG. Animal research: reporting i*n vivo* experiments: the ARRIVE guidelines. Br J Pharmacol 2010, 160:1577-1579.
19. Kilkenny C, Browne W, Cuthill IC, Emerson M, Altman DG. Animal research: reporting *in vivo* experiments--the ARRIVE guidelines. J Cereb Blood Flow Metab 2011, 31:991-993.
20. Kzhyshkowska J, Neyen C, Gordon S. Role of macrophage scavenger receptors in atherosclerosis. Immunobiology 2012, 217:492-502.
21. Plump AS, Smith JD, Hayek T, Aalto-Setala K, Walsh A, Verstuyft JG, Rubin EM, Breslow JL. Severe hypercholesterolemia and atherosclerosis in apolipoprotein E-deficient mice created by homologous recombination in ES cells. Cell 1992, 71:343-353.
22. Von Scheidt M, Zhao Y, Kurt Z, Pan C, Zeng L, Yang X, Schunkert H, Lusis AJ. Applications and Limitations of Mouse Models for Understanding Human Atherosclerosis. Cell Metab 2017, 25:248-261.
23. Golombek SK, May JN, Theek B, Appold L, Drude N, Kiessling F, Lammers T. Tumor targeting via EPR: Strategies to enhance patient responses. Adv Drug Deliv Rev 2018, 130:17-38.
24. Greish K. Enhanced permeability and retention (EPR) effect for anticancer nanomedicine drug targeting. Methods Mol Biol 2010, 624:25-37.
25. Stary HC, Chandler AB, Dinsmore RE, Fuster V, Glagov S, Insull W, Jr., Rosenfeld ME, Schwartz CJ, Wagner WD, Wissler RW. A definition of advanced types of atherosclerotic lesions and a histological classification of atherosclerosis. A report from the Committee on Vascular Lesions of the Council on Arteriosclerosis, American Heart Association. Circulation 1995, 92:1355-1374.

Chapitre 2. Squalene-Adenosine Nanoparticles protect hearts from ischemia/reperfusion injuries in mice

Résumé détaillé

L'infarctus du myocarde est une des causes principales de mortalité dans le monde. C'est une lésion cardiaque majeure émergeant d'une ischémie myocardique prononcée et durable, c'est-à-dire l'arrêt du flux sanguin artériel vers le cœur entraînant un manque d'oxygène dans le tissu cardiaque. Ceci arrive généralement suite à la rupture ou l'érosion d'une plaque lipidique d'athérosclérose formée dans l'artère coronaire[1, 2]. Paradoxalement, le rétablissement du flux sanguin et la réoxygénation sont les seuls moyens d'empêcher la mort tissulaire, mais cela entraîne aussi une exacerbation des lésions du myocarde combiné à une forte réponse inflammatoire (on parle alors de lésions de reperfusion). Les lésions d'ischémie/reperfusion myocardique (ou cardiaque) se réfèrent alors aux effets délétères qui se produisent à la fois pendant l'ischémie et la restauration ultérieure du flux sanguin[2].

La mise en place de nouvelles stratégies pharmacologiques de cardio-protection pour préserver la fonction cardiaque et limiter les effets néfastes des lésions d'ischémie-reperfusion apparaissent indispensables. L'adénosine, un nucléoside endogène essentiellement produit par dégradation de l'adénosine triphosphate (ATP), et présentant de nombreuses fonctions biologiques remarquables parmi lesquels des effets anti-apoptotiques et anti-inflammatoires, est une des options thérapeutiques attrayantes. Toutefois, du fait d'une métabolisation très rapide, de fortes doses sont nécessaires afin d'observer ces résultats, engendrant des effets secondaires et une toxicité sévère, ce qui limite son utilisation en clinique[3, 4].

Pour pallier ces limitations, une solution innovante consiste en l'encapsulation de l'adénosine au sein de nanoparticules. Notamment, le couplage chimique de l'adénosine et du squalène par le phénomène de « squalénisation » a prouvé que cela permet de concevoir un bio-conjugué capable de former de manière spontanée en milieu aqueux des nanoparticules biodégradables et bio-compatibles stables de l'ordre d'une centaine de nanomètres. Ces nanoparticules ont en outre fait preuve d'efficacité dans un modèle murin de lésions d'ischémie/reperfusion du cerveau[5]. Le chapitre 2 se consacre ainsi à l'étude des nanoparticules de squalène-adénosine (SQAd) et à leur capacité de cardioprotection dans un modèle murin de lésions d'ischémie/reperfusion cardiaque.

Dans le chapitre ci-après ont été exposés les résultats de cette étude obtenus jusqu'à ce jour. Des analyses complémentaires sont en cours de réalisation, et l'ensemble des résultats feront l'objet d'un article scientifique.

Dans un premier temps, nous avons présenté et caractérisé les nanoparticules de squalène-adénosine obtenues. Il s'agit de nanoparticules stables dans le temps (au moins pendant 14 jours) à température ambiante et à 4°C, avec une taille de l'ordre d'une centaine de nanomètres et avec un potentiel électrique de surface négatif de l'ordre de -20 mv.

Dans un second temps, nous avons évalué les capacités d'internalisation, la cytotoxicité et le potentiel pharmacologique des nanoparticules de SQAd sur la lignée cellulaire HL-1 de cardiomyocytes. Nous avons notamment prouvé par microscopie confocale que ces nanoparticules s'accumulent progressivement dans les cardiomyocytes. Nous avons aussi montré qu'elles ne présentent pratiquement aucune cytotoxicité cardiaque au moins jusqu'à 24h de traitement, que ce soit à faibles ou fortes doses, comme le témoignent les résultats des tests MTT. Ces résultats furent confirmés par cytométrie en flux, et nous avons même pu observer un effet cardioprotecteur des nanoparticules dans des modèles *in vitro* d'ischémie et d'ischémie/reperfusion conçus le plus proche possible des conditions réelles.

Dans un troisième temps, nous avons analysé le potentiel pharmacologique cardioprotecteur des nanoparticules de SQAd dans un modèle murin de lésions d'ischémie/reperfusion cardiaque. Au travers de mesures macroscopiques de tailles d'infarctus, d'analyse en cytométrie en flux de tissus cardiaques, et d'examens histopathologiques et immuno-histochimiques sur coupes de cœurs, nous avons pu observer une tendance des nanoparticules de SQAd à réduire la taille de l'infarctus et à protéger le cœur de la mort cellulaire. Des études complémentaires sont toujours en cours d'analyse au sein de notre laboratoire afin de préciser l'origine de cet effet pharmacologique en se concentrant notamment sur le niveau de macrophages pro-inflammatoires (M1) et anti-inflammatoires (M2).

Références :

[1]: Boateng, S., & Sanborn, T. Acute myocardial infarction. Disease-a-month : DM, 59(3), 83–96. (2013).
[2]: Kalogeris T. et al. Ischemia/Reperfusion (review), Comprehensive physiology. (2017).
[3]: Sommerschild HT, Kirkebøen KA. Adenosine and cardioprotection during ischaemia and reperfusion--an overview. Acta Anaesthesiol Scand.44(9):1038-55. (2000).
[4]: Layland, J., Carrick, D., Lee, M., Oldroyd, K., & Berry, C. Adenosine: physiology, pharmacology, and clinical applications. JACC. Cardiovascular interventions, 7(6), 581–591. (2014).
[5]: Gaudin, A., Yemisci, M., Eroglu, H., Lepetre-Mouelhi, S., Turkoglu, O. F., Dönmez-Demir, B., Caban, S., Sargon, M. F., Garcia-Argote, S., Pieters, G., Loreau, O., Rousseau, B., Tagit, O., Hildebrandt, N., Le Dantec, Y., … Couvreur, P. Squalenoyl adenosine nanoparticles provide neuroprotection after stroke and spinal cord injury. Nature nanotechnology, 9(12), 1054–1062. (2014).

Squalene-Adenosine Nanoparticles protect hearts from ischemia/reperfusion injuries in mice

Abstract

Myocardial ischemia/reperfusion injury represents the harmful pathological events occurring after a myocardial ischemia episode and its subsequent reperfusion. It is responsible for up to 50% of the myocardial infarct size. Although a large amount of research studies was led in the past few years, effective treatments against the deleterious effects of myocardial ischemia/reperfusion injury are lacking. Thanks to its remarkable biological functions such as anti-apoptotic and anti-inflammatory effects, the nucleoside adenosine appears as one of the possible therapeutic approach. However, its clinical use is very limited due to rapid metabolization and severe toxic side effects, induced by the necessary important dosage. To overcome these limitations, we have considered the conjugation of adenosine to squalene, a natural and biocompatible lipid allowing the formation of nanoparticles. In this study, the pharmacological efficacy of squalene-adenosine nanoparticles has been evaluated in a mouse model of myocardial ischemia/reperfusion injury. The cardioprotective effects have been tested *in vitro.* By exploiting the Enhanced Permeability and Retention effect observed during myocardial ischemia/reperfusion, it was observed that the adenosine-squalene nanoparticles could accumulate in the infarcted cardiac tissue allowing to display a promising cardioprotective effect.

1. Introduction

Cardiovascular diseases are a major health challenge of the XXIth century due to various contemporary risk factors such as obesity, hypertension, hyperlipidemia, diabetes and atherosclerotic plaque progress[1]. Acute myocardial infarction, the leading cause of death worldwide, causes chronic heart failure and myocardial ischemia, thereby inducing absence of nutrients and oxygen that leads to harmful metabolic and biochemical changes. Reperfusion strategies are the only currently available therapeutic strategies although it also promotes serious cardiomyocyte dysfunction. Myocardial ischemia-reperfusion (I/R) injury thus refers to the deleterious effects that occurs both during ischemia and during the subsequent restoration of the blood flow[2,3]. Besides, I/R injury induces a strong inflammatory response that contributes to the pathology and expand the final infarct size[4].

Given the worldwide prevalence of this devastating disease, developing pharmacological cardioprotective strategies to preserve cardiac function and limit the deleterious effects of I/R injury remains an important medical challenge. Nevertheless, only few clinical therapeutic options are currently available, despite significant amount of research and encouraging preclinical results. One therapeutic approach is based on the delivery of adenosine, an endogenous purine nucleoside, mainly produced by the degradation of adenosine triphosphate and displaying numerous tissue-specific biological functions[5]. Adenosine has shown various cardioprotective effects during I/R, either on preclinical studies[6, 7] or in clinical trials[8-10]. However, because of its very short plasma half-life (t1/2 of 10 sec), high doses are needed, resulting in important side effects and severe toxicity, therefore limiting its use in clinics[11].

There is, therefore, an urgent need to develop innovative pharmaceutical strategies to improve adenosine delivery into the heart and to fully exploit its therapeutic potential. Nanomedicines appear to be an interesting option, allowing to prevent adenosine from degradation, to promote a drug sustained release and to decrease adenosine dosage[12, 13]. However, many of the previously tested nanodevices require substantial design or complex functionalization to achieve cardiac targeting of adenosine, and showed some disadvantages such as immunogenic toxicity, poor biodegradability, low entrapment of adenosine or important burst release[12, 13]. For example, Galagudza *et al.* developed adenosine-loaded silica nanoparticles for cardiac I/R treatment, that accumulate also in the liver and remain in the liver 30 days after injection, whereas silica nanoparticles raise the question of particle toxicity with regard to long-term trials[12]. These issues thus restrained the pharmaceutical development and pharmacological activity of adenosine nanoformulations.

To overcome these issues, we propose here to chemically link adenosine to squalene, a natural and biocompatible lipid, precursor of the cholesterol's biosynthesis (*i.e.* the so-called "squalenoylation" approach"[14]). The squalene-adenosine conjugate display the unique ability to easily self-assemble in water as non-toxic spherical nanoparticles (NPs) that protects the drug from degradation with high drug loading and prolonged blood circulation[14, 15]. The squalene-adenosine (SQAd) NPs already demonstrated an impressive neuroprotective efficacy in both a murine model of brain ischaemia–reperfusion and in a rat model of spinal cord injury[16]. In this study, we investigated the pharmacological efficacy of these nanoparticles in I/R injury both in an immortalized cardiac muscle cell line *in vitro* and in a mouse myocardial ischemia/reperfusion pre-clinical model *in vivo*. Cell capture experiments were conducted using fluorescently labelled nanoparticles

2. Materials and Methods

2.1. Materials

Squalenyl acetic acid and SQAd bioconjugate were provided by Holochem (France). Adenosine, D-(+)-Glucose (dextrose, DXT), Dulbecco's phosphate buffered saline (PBS), Dulbecco's Modified Eagle's Medium (DMEM) classical composition with high glucose and basic formulation without glucose, L-glutamine, phenol red, sodium pyruvate and sodium bicarbonate, Claycomb's Medium, trypsin, penicillin-streptomycin solution, glutamine, norepinephrine, HEPES, 3-(4,5-dimethylthiazol-2-yl)-2,5-diphenyltetrazolium bromide (MTT), Trypan Blue, Evans Blue, 2,3,5-triphenyltetrazolium chloride (TTC), and Bovine Serum Albumin (BSA) were all purchased from Sigma-Aldrich (France). Fetal Bovine Serum (FBS) was purchased from Life Technologies (France). Absolute ethanol came from VWR Chemicals (France), while dimethyl sulfoxide was from Carlo Erba Reagents (France). Ultra-pure water was purified using a MilliQ system from Millipore Corporation (France). CholEsteryl 4,4-Difluoro-5-(4-Methoxyphenyl)-4-Bora-3a,4a-Diaza-s-Indacene-3-Undecanoate (CholEsteryl BODIPY™ 542/563 C11) was purchased from ThermoFisher Scientific (France). ROTI® Histofix 4% was obtained from Carl Roth (France). HL-1 cells originated from ATCC (USA). Antibodies were purchased from different manufacturers, among others Biolegend (Germany), Sigma-Aldrich, and Genetex (France). Collagenase I was taken from Alfa Aesar (USA). C57Bl/6J mice and Sprague-Dawley rats were obtained from Janvier Labs (France). All anaesthesia and analgesia materials were kindly provided by our animal house Animex (Châtenay-Malabry, France). ELISA MAX™ Deluxe set Mouse TNF-α and ELISA MAX™ Deluxe set Mouse IL-10 were purchased from Biolegend (Germany). Fluorescein isothiocyanate (FITC) conjugated Annexin V Apoptosis Detection Kit I was purchased from BD Bioscience (France), while the Mouse cTnT/TNNT2(Troponin T Type 2, Cardiac) ELISA Kit was from Elabscience (France).

The TUNEL Assay Kit - BrdU-Red was obtained from Abcam (England). All other chemicals were of analytical grade and obtained from standard commercial sources.

2.2. Preparation and characterization of Squalene-Adenosine Nanoparticles

SQAd was synthesized as previously described and the nanoparticles (SQAd NPs) were prepared using the nanoprecipitation technique [16]. Briefly, SQAd bioconjugate was dissolved in absolute ethanol at a concentration of 6 mg/mL and 333 µL of the solution was added dropwise into a 5% (w/v) dextrose (DXT) solution under strong mechanical stirring. Ethanol was then completely removed by evaporation using a Rotavapor (80-90 rpm, 40 °C, 43 mbar) to obtain a 2 mg/mL aqueous suspension of pure nanoparticles. Fluorescent SQAd NPs were prepared using the same methodology, with the only difference that 0.1% (wt/wt) of CholEsteryl BODIPY 542/563 C11 was dissolved in the ethanolic phase before addition to the dextrose solution.

SQAd NPs size (hydrodynamic diameter), polydispersity index and surface charge (zeta potential) were assessed by Dynamic Light Scattering (DLS) after preparation, and up to 14 days for stability studies, using a Malvern Zetasizer Nano ZS (173° scattering angle, 25 °C, Material RI: 1.49, Dispersant Viscosity RI: 1.330, Viscosity 0.8872 cP). For each preparation, the mean diameter resulted from the average of three measurements of 60 s each and the mean zeta potential resulted from the average of three measurements in automatic mode, followed by the application of the Smoluchowski equation.

NPs morphology was evaluated by Cryogenic Transmission Electron Microscopy (cryo-TEM), as follows. Drops of NPs suspensions at 2 mg/mL concentration were deposited on electron microscopy grids covered with a holey carbon film (Quantifoil R2/2) previously treated with a plasma glow discharge. Observations were conducted at low temperature (−180°C) on a JEOL 2010 FEG microscope operated at 200 kV. Images were recorded with a Gatan camera.

2.3. Cell culture

HL-1 cells, an immortalized cardiac muscle cell line derived from mouse atrial cardiomyocyte tumor lineage, were obtained from ATCC (USA) and cultured in Claycomb's medium supplemented with 10% (v/v) FBS, 2 mM of L-Glutamine, 0.1 mM of Norepinephrin, and 1% (v/v) of penicillin-streptomycin solution. Routinely, cells were plated on 75cm² cell culture flask at a cell confluence of 40-50% and maintained in a humidified incubator at 37°C in normoxia (air with 5% CO_2). Cells were then cultured until reaching a confluence of 70-80%, passaged twice a week and used for experiments between passages 4 and 12.

2.4. Ischemia/Reperfusion model *in vitro*

HL-1 cells went through different times of ischemic conditions, followed or not by reperfusion in normoxic conditions. For this purpose, cells were plated into 6, 12 or 96-well plates at a density of 200.000, 100.000 or 8.000 cells per well respectively, and left to adhere overnight before any further procedure. Cells were then incubated in a very restraint DMEM medium (without glucose, L-glutamine, phenol red, sodium pyruvate, sodium bicarbonate), deprived of serum and subjected to hypoxia (1% O2, 5% CO_2, 37°C in a humidified atmosphere) in a controlled hypoxic incubator for 2h to 24h. Following ischemia, in some set of experiments, cells were washed with PBS and placed in complete medium with FBS in normoxic conditions for different reperfusion times. Evaluation of cellular uptake, cell viability or apoptosis/necrosis levels were performed using cells subjected to nanoparticles or controls treatment either in ischemia only or in ischemia and reperfusion conditions.

2.5. *In vitro* Cellular uptake of fluorescent SQAd NPs

Fluorescent SQAd NPs labelled using CholEsteryl BODIPY 542/563 C11 (SQAd-BP NPs) were used to investigate the cell internalization of the nanoparticles. First, in 6-well plates, a total of 100 000 HL1 cells/well were seeded on 12 mm glass coverslips and left to adhere and grow on the glass slips in normoxia conditions for 24h. Then, cells were incubated with SQAd-BP NPs diluted in complete culture medium for 30 min to 24h. Following the incubation step, cells were washed with PBS and fixed with 4% paraformaldehyde (PFA) for 15 min. A 50 mM NH_4Cl solution in dH_2O was then added in each well for 15 min, in order to neutralize residual PFA. Finally, coverslips were mounted on microscopy slides and imaged in confocal microscopy with an inverted LSM510 Zeiss confocal microscope using a PlanApochromat 63X objective lens (NA 1.40, oil immersion) and a laser at 543 nm. Numerical images were acquired and analysed with LSM 510 software version 3.2.

2.6. Cell viability

Cell viability was assessed by performing 3-(4,5-dimethylthiazol-2-yl)-2,5-diphenyltetrazolium bromide (MTT) colorimetric assay following manufacturer's recommendations. Briefly, HL1 cells were seeded in 96-well plates at 8 000 cells per well and incubated in normoxic conditions for 24h. Cells were then washed with PBS and subjected to different treatments, with concentration of nanoparticles ranging from 1 µM to 200 µM. Subsequently, cells were washed with PBS, and incubated for 2h with medium containing 0.5 mg/mL of MTT. Finally, medium was removed and formazan crystals were solubilized by addition of 200µL per well of dimethyl sulfoxide (DMSO). After 10-15 min of moderate shaking on an orbital shaker, absorbance was measured at 570 nm to determine cell viability using a Perkin Elmer microplate reader. Each treatment was assessed with 6 replicates, experiments were performed in triplicate.

2.7. *In vitro* cardioprotective effects of SQAd NPs

Cell apoptosis and necrosis were analysed by flow cytometry using an Annexin V-FITC Apoptosis detection kit (BD Bioscience). The staining procedure was adapted from the manufacturer's recommendations. Briefly, cells were seeded in 6-well plates at 200 000 cells/well and left to adhere in normoxia conditions for 24h. Then, cells were incubated for diverse ischemia and reperfusion time points with different treatments. After various incubation times, cells were washed with cold PBS after removal of the medium and harvested using very short time and low quantity of trypsin solution to avoid damages on cells membranes and extracellular matrix[17, 18] (200µL, 1 min at 37°C before inactivation with complete medium containing FBS) and mechanical detachment was performed by soft cell scraping. Subsequently, after centrifugation at 200 g for 5min to remove all residual trypsin, cells were resuspended in 400 µL of 1X Annexin V buffer solution and split into four 1.5 mL Eppendorf tubes. In three of these tubes, a staining reagent was applied for 20 min at room temperature in the dark : (1) 5 µL of Annexin V, (2) 5 µL of 7-amino-actinomycine (7-AAD), and (3) 5 µL of Annexin V + 5 µL of 7-AAD. Finally, 400 µL of cold 1X Annexin V buffer solution was used to dilute the markers, then the Eppendorf tubes were placed on ice, and cell fluorescence was recorded on a flow cytometer BD Accuri™ C6 (Accuri Cytometers Ltd.). Excitation was carried out using all four available channels. 10 000 cells were measured for each sample. The results were expressed as the mean fluorescence intensity ± SEM and analysed with the BD Accuri™ C6 Software.

2.8. Animal care

6 to 8-week-old male C57BL/6J mice were purchased from Janvier Labs (France) for ischemia and reperfusion studies. 225-249g Sprague-Dawley rats were purchased from Janvier Labs for pharmacokinetics and biodistribution studies. Animals were housed in groups of five for mouse and groups of 3 for rats, and allowed seven days to acclimatize in a standard controlled environment (22° ± 1°C, 60% relative humidity, 12-hour light/dark cycles) with food and water available *ad libitum*. All experimental protocols were approved by the Animal Care Committee of the University Paris-Saclay, in accordance with principles of laboratory animal care and European legislation 2010/63/EU. All efforts were made following the 3R strategies (Reduction, Replacement and Refinement) in order to reduce animal numbers and minimize their suffering, as defined in the specific agreement.

2.9. Mouse myocardial ischemia/reperfusion model

All surgical procedures of the mouse myocardial Ischemia and Reperfusion (IR) model were performed based on previously described protocol[19]. Briefly, mice were mildly anaesthetized by intraperitoneal injection of a Ketamine/Xylazine mix solution (100 mg/kg of Ketamine and 10 mg/kg of xylazine) for first

sedation and analgesia, followed by full anaesthesia with 3% isoflurane and 0.2 L/min oxygen in adapted mouse nose mask. Mice remained under this anaesthesia until there was a clear loss of paw and tail reflexes. Then, mice were endotracheally intubated and placed on a homeothermic heating pad under mechanical ventilation with a rodent respirator (Harvard Asparatus) with 1% isoflurane anaesthesia for the rest of the surgery. Mice were shaved, scrubbed with betadine and 70% ethanol and positioned into a right lateral decubitus position under a dissecting microscope. Left thoracotomy was then performed in the third intercostal space. The thoracic cage was maintained open thanks to chest retractors, the pericardium was gently separated, and Left Anterior Descending (LAD) ligation was performed using a 7-0 silk suture ligated around a piece of PE-10 tubing, 1-2 mm below the left auricle. A second ligation was placed without tying it up for future staining experiments. Complete occlusion of the vessel was confirmed by the whitening of ventricle under the ligation. After 30 min of ischemia, the tubing was removed, first ligation was cut to allow reperfusion of the heart. Directly after reperfusion, intravenous injection of the treatment was performed into the left jugular vein. Subsequently, pneumothorax was evacuated manually, mice were sutured and subcutaneously injected with buprenorphine (0.1 mg/kg body weight) analgesia. Gaz anaesthesia was stopped, intubation was removed after the mice begin to breathe on their own, and finally allowed to recover in an oxygenated and heated chamber for few hours, before returning in normal housing conditions for different periods of reperfusion.

2.10. Area at Risk (AAR) and infarct Area (IA) evaluation

24 h, 72 h or 168 h after reperfusion, mice were sacrificed to obtain blood samples and hearts for measuring the infarct size. Briefly, mice were intraperitoneally injected with high dose of pentobarbital (>100 mg/kg). The right femoral vein was exposed, and the maximum amount of blood was collected (generally between 500-800 µL) using heparin-coated syringes. Blood samples were directly put on ice, plasma was separated by centrifugation (2000g, 10 min at 4°C) and finally stored at -80°C. After blood was collected, 20 mL of PBS was injected intracardially in the apex of the left ventricle to wash out residual blood. Subsequently, the LAD artery was re-occluded with the suture left *in* situ, and 5 mL of 0.5% Evans Blue solution was injected in the same spot to delimitate the ischemic Area at Risk (AAR). Hearts were then excised, put into a saturated KCl solution to stop the heart at the diastolic phase; auricles were removed, and hearts were sliced into 1-mm thick perpendicular cross sections. Heart sections were then incubated with a 1% 2,3,5-triphenyltetrazolium chloride (TTC) solution at 37°C for 15 min to determine the Infarct Area (IA). After TTC staining, both sides of each section were imaged thanks to a Zeiss microscope and IA (negative for TTC and Blue Evans staining and appearing pale white), AAR (appearing pink/pale red, without Blue Evans staining) and total left ventricular area (LV) were assessed using Zeiss Zen software in a blind manner. The percentage of area at risk was measured as the ration (AAR/LV) x100, and the infarct size

was calculated as (IA/AAR) x100. Imaged were analysed in a blind manner to avoid bias. Sections were kept in 4% paraformaldehyde solution for 24h, and finally either dry frozen at -80°C or put into FBS/DMSO solution (90:10 %v/v) and frozen at -80°C.

2.11. Histological and immuno-histochemical analyses

Heart sections were either embedded in paraffin and cut in serial 5 µm-thick cross sections, using a microtome, or directly cut in serial 5 µm-thick frozen cross sections, using a cryostat microtome. Firstly, Haematoxylin and Eosine (H&E) staining was performed on paraffin sections and analysed by microscopy. Diseased areas with scar tissues - areas with abnormal modifications such as infiltration of inflammatory cells, apoptotic/necrotic cells, fibrosis - were delimited and compared between treatment groups.

Immunohistochemical analyses are currently in progress and won't be presented here. They were performed both on paraffin and frozen sections for investigation of the expression of inflammatory biomarkers. For this purpose, sections are subjected to diverse antibodies, such, anti-CD31, anti-CD64, anti-iNoS antibodies. Antibodies were used at dilutions following manufacturer's recommendations. Alexa 687-linked secondary antibodies were used for fluorescence detection. Digital imaging of stained sections was performed on 6-10 fields in the scar tissue by confocal microscopy, using 40X objective and manually counted using ImageJ software.

2.12. Evaluation of apoptosis in tissue sections

Apoptosis was evaluated on paraffin sections by DNA fragmentation detection by Terminal deoxynucleotidyl transferase dUTP nick-end labeling (TUNEL) staining, using an *in situ* BrdU-Red DNA fragmentation assay kit, according to the manufacturer's recommendations.

Briefly, paraffin sections were deparaffinized and rehydrated through successive incubations in toluene, and then in ethanolic solutions less and less concentrated. After immersing sections in PBS, Proteinase K solution was added for 15 min at room temperature to retrieve antigens. Then, cells were labelled using the manufacturer DNA labelling solution for 60 min at 37°C. After washing the section slides in PBS, the manufacturer antibody solution comprising anti-BrdU-Red antibody was added for 30 min in the dark at room temperature. A DNA counterstaining was finally performed using the manufacturer 7-AAD/RNase A staining buffer for 30 min in the dark at room temperature. After last incubations in ddH2O washing solution, coverslips were added, and sections were analysed by fluorescence confocal microscopy with 40X objective (Ex/Em = 488/576 nm (BrU-Red) and Ex/Em = 488/655 nm (7-AAD)). TUNEL-positive nuclei and total nuclei were indicated by red and blue fluorescence, respectively. The number of TUNEL-positive nuclei was counted by examining 6 areas around the ischemic zone on the sections.

2.13. Flow cytometry on tissue sections

The frozen section of each heart which was frozen in FBS/DMSO was used for cardiac macrophages evaluation by flow cytometry. Briefly, sections were thawed, minced finely with scalpel and mechanically crushed with tissue grinder, and placed into a lysis solution composed of 150 U/mL of collagenase I (Alfa Aesar) in DMEM complete medium for 30 min at 37°C with gentle vortexing every 10 min. After addition of PBS supplemented with 2% FBS and 0.2% Bovine serum albumin (BSA) to deactivate enzymes, cells were filtered through 40 µM cell strainer and centrifuged at 500 g for 10 min. Cells were then washed, resuspended in PBS/FBS/BSA and counted. 10^6 cells in suspension were subsequently taken, centrifuged again at 500 g for 10 min and suspended in 100 µL of Cell Staining buffer (Biolegend). Cells were finally stained with immunophenotyping antibodies for 30min at 4°C in the dark, diluted in 300 µL of cold Cell Staining buffer and directly analysed by flow cytometry (BD Accuri™ C6, Accuri Cytometers Ltd). The antibodies used for this study were mouse anti-F4/80-FITC, anti-CD206-FITC antibodies combined with anti-CD64-PE antibodies. 5-6 samples per treatment were analysed.

2.14. Statistical analyses

Data are expressed as mean ± S.D. Calculations were performed using the GraphPad Prism 7.0 software (GraphPad Software, Inc.). Statistical differences between two groups were evaluated using the unpaired Student t test, considering $p<0.05$ as statistically significant.

3. Results and Discussion

3.1. Squalene-Adenosine nanoparticles stability and characterization

Prodrug squalene-adenosine was synthetized by covalently linking adenosine to the lipid moiety with high drug loading (37%) in order to protect the fragile drug from quick metabolization as previously described[16]. Formation of SQAd nanoparticles allowed a monodisperse aqueous suspension suitable for intravenous injection in animals[20] which was confirmed by cryo-transmission electron microscopy (Figure 1a-c). Nanoparticles stability was evaluated by dynamic light scattering (DLS) in water supplemented with 5% dextrose at 4°C and room temperature (RT). NPs appeared stable over time until 14 days with a mean hydrodynamic diameter of 92.8 ± 1.03 nm at 4°C and 94.1 ± 1.72 nm at RT, a polydispersity index of 0.094 ± 0.017 at 4°C and 0.109 ± 0.015 at RT, and a negative surface zeta potential of -15.7 ± 2.7 mV at 4°C and -17.8 ± 2.6 mV at RT (Figure 1d-e).

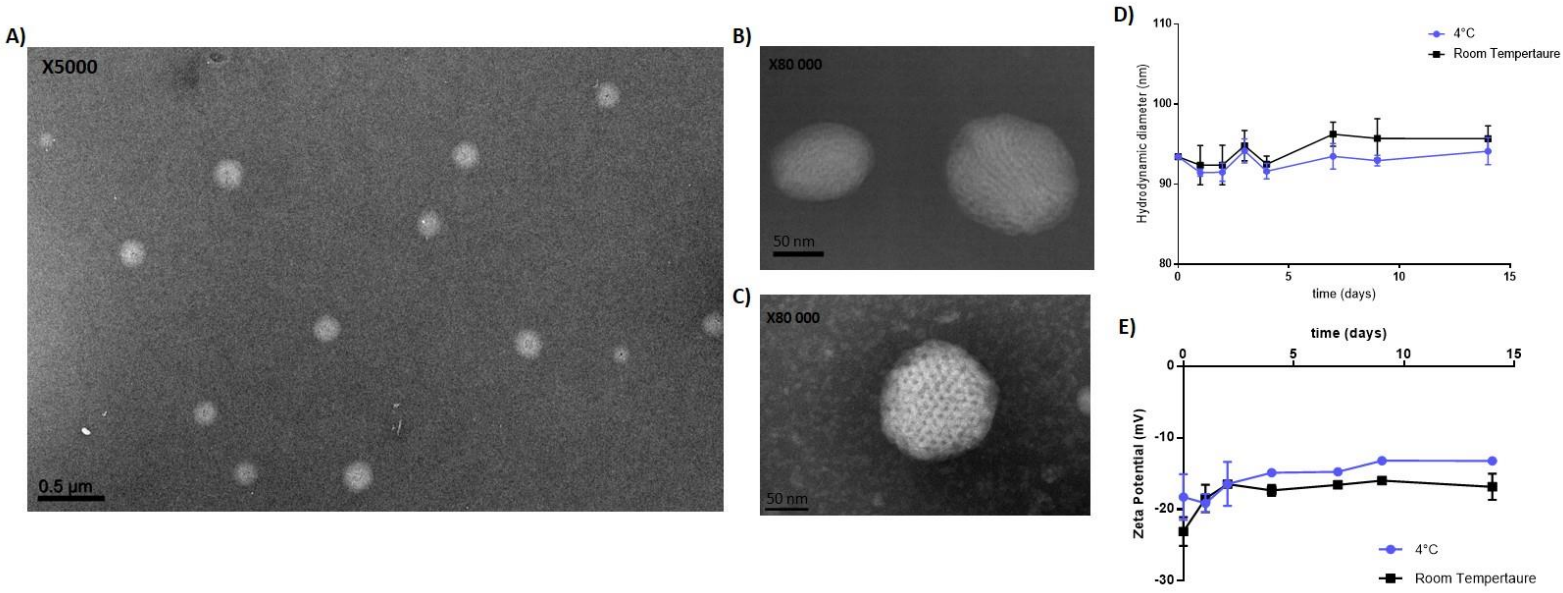

Figure 1. Characterization and stability assessment of SQAd NPs

(**A-C**) Cryo-TEM images of SQAd NPs obtained by nanoprecipitation of an ethanolic solution in 5% dextrose solution, at x5000 magnification (**A**, scale bar = 0,5 µm) and x80000 magnification (**B and C**, scale bar = 50 nm). DLS monitoring of size (**D**) and zeta potential (**E**) of SQAd NPs stability over 14 days in water supplemented with 5% dextrose. In black = stability at room temperature, in blue = stability at 4°C. N=4 replicates per condition

These results were consistent with those found in the study of Dormont *et al.*[21], characterizing SQAd NPs and their pharmaceutical development from laboratory to industrial scale. The nanoprecipitation procedure is very accessible without requiring any excipients and allowing freeze-drying with preservation of nanoparticles diameter, zeta potential and supramolecular structure[22]. This represents a significant benefit for the scaling-up and clinical translation, in comparison to the more complex nanomedicines currently in development for cardiac diseases treatment, as discussed in the introduction[23].

3.2. Pharmacological efficiency on cardiomyocyte cell line

HL-1 cardiomyocyte cell line, derived from mouse atrial cardiomyocyte tumour cells, has been extensively explored as an *in vitro* model of cardiac ischemia-reperfusion injury with similar drug responses to I/R as primary cardiomyocytes[24 - 26]. Thus, HL-1 has been chosen as the cell model for the evaluation of the cell viability, cell death, and cell internalization of SQAd NPs in normoxia, ischemia and ischemia and reperfusion conditions.

3.2.1. SQAd NPs internalization by cardiac cells

To investigate the cellular uptake of SQAd NPs, fluorescent SQAd-BP NPs were incubated with HL-1 cells in complete medium and internalization was monitored by confocal microscopy.

A gradual increase of the fluorescence localized in the cytoplasm, of HL-1 cells was observed over time, from 2h to 24h (Figure 2a, c, e). Of note, no fluorescence was visible when the cells were incubated with the fluorescent probe alone (Figure 2b, d, e). This suggested that SQAd NPs progressively accumulate in a specific manner into HL-1 cardiac cells over time.

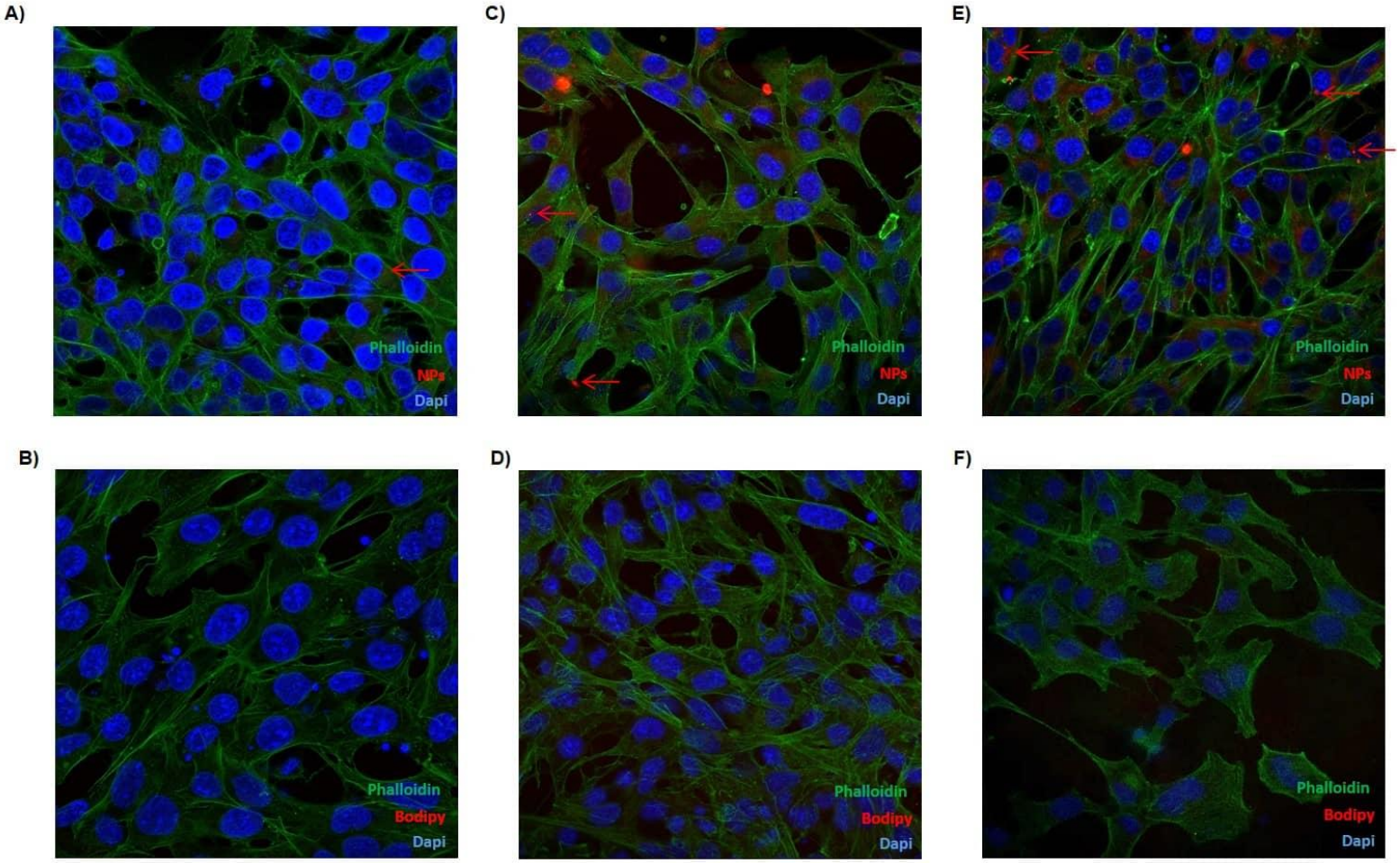

Figure 2. SQAd NPs are captured by HL-1 cardiac cells.

All images represent confocal images of HL-1 cardiac cells exposed to either SQAd-Bodipy (SQAd-BP) NPs or free Bodipy during 2h (**A-B**), 6h (**C-D**), or 24h (**E-F)** in normoxic cell culture conditions. Phalloidin is stained in green to delimit cells, cell nucleus are stained in blue, and SQAd-Bp NPs (**A-C-E**) or free Bodipy (**B-D-F**) are red. Accumulation of some SQAd-BP NPs are spotted by red arrows.

3.2.2. SQAd NPs cytotoxicity

Since adenosine and adenosine derivatives can modulate adenosinergic signalling, these molecules could trigger an efficient defensive mechanism against cardiac ischemia/reperfusion injury[27, 28]. However, the use of adenosine was also reported to be associated with unwanted cardiotoxic adverse responses. Particularly, cardiovascular pathological changes and apoptosis could occur, resulting from potent vasodilatory and positive inotropic effects[29, 30]. This is the reason why cardiac cytotoxicity of NPs has been assessed by MTT assay at different incubation time in normoxic conditions (Figure 3a-c).

It was noted that the presence of dextrose in the formulations slightly decreased cell viability by around 5-10% which should, however, not impact the cardiomyocyte viability of this excipient *in vivo*, since the quantity of dextrose will be strongly diluted after i.v. injection.

Comparatively to the controls, SQAd NPs did not disturb the cellular viability after 2h, 6h and 24h of treatment, neither at low nor at high concentration. Even at 150 µg/mL, no cytotoxicity was noted. Free adenosine and squalenylacetic acid nanoparticles (SQCOOH NPs) were tested as controls and did neither show any cytotoxicity at the equivalent maximum concentration of SQAd NPs (Figure 3a-c). These results showed that SQAd NPs were not cardiotoxic *in vitro* and could further be assessed as a cardioprotective agent.

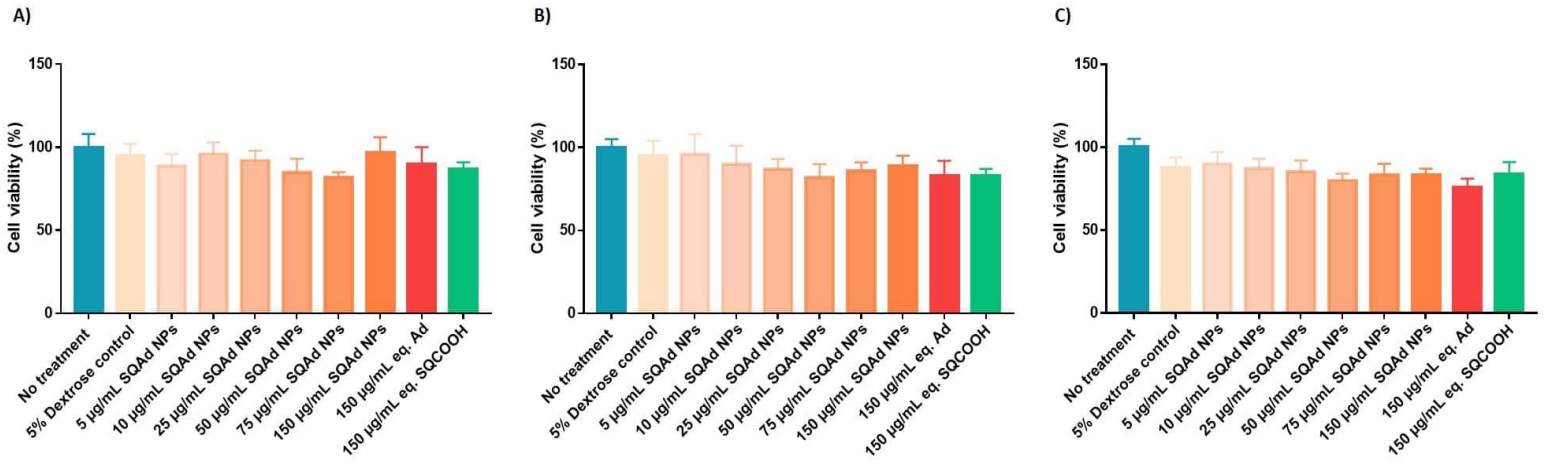

Figure 3. Cytotoxicity of SQAd NPs and their controls

The cell viability was evaluated by MTT colorimetry assay on HL-1 cells after 2h (**A**), 6h (**B**) or 24h (**C**) incubation in normoxia with or without treatment. Control without treatment was considered as 100% cell viability. SQAd NPs were tested with increasing concentrations from 5 µg/mL to 150 µg/mL. Free adenosine and SQCOOH NPs controls were tested at the equivalent maximum dose. N=6 replicates by condition.

3.2.3. *In vitro* cardioprotective effects of SQAd NPs

Adenosine has been shown to be capable of modulating the proliferation and survival of many cardiac cells within the heart. Acting on different receptor subtypes, this molecule may trigger several and sometimes opposite pharmacological activities. Particularly, it has been proved that adenosine promotes cell death in cardiomyocytes [31, 32], although it may also provide strong cytoprotective functions in the heart during ischemia[33, 34]. Therefore, cytoprotective activity of SQAd NPs was assessed by flow cytometry in normoxia, as well as, in an *in vitro* model of strict ischemia or ischemia/reperfusion on HL-1 cells.

First, in normoxic conditions, SQAd NPs decreased the number of apoptotic and necrotic cells, this effect being more pronounced at the highest SQAd NPs concentration (i.e. 15% of apoptotic/necrotic cells without treatment *versus* 9% at 5 µg/mL and 6-6.5% at 150 µg/mL SQAd NPs; Figure 4a). This confirmed the absence of cytotoxicity resulting from this treatment which even appeared to protect cells from death, suggesting that the cardioprotective effect of adenosine remained still active in the form of nanoparticles. On the contrary, free adenosine did not induce any modification in the percentage of cell death, demonstrating its quick metabolization in the presence of serum in the medium.

In strict ischemic conditions, percentage of apoptotic and necrotic cells was increased for control untreated cells (i.e. 40% after 6h of ischemia). When SQAd NPs treatment was applied, a significant reduction of cell death was noticed but it was more pronounced at low dose of nanoparticles (attenuation of ischemia-induced cell death almost by half), compared to high dose (attenuation of around 8% of ischemia-induced cell death) (Figure 4b). This difference was explained by the observation that at a concentration of 150 µg/mL, SQAd NPs started to aggregate in the restraint minimum DMEM medium without serum, which also reduced the effect of the treatment. Indeed, in the absence of serum proteins, a protein corona couldn't form at the NPs surface, allowing their colloidal stabilization [35, 36]. The use of free adenosine at equivalent doses also showed a significant strong reduction in cell death, recovering the same percentage of cell death than in normoxia, with a 25-30% decrease at low and high concentrations (Figure 4b). Noteworthy, in the absence of serum the rapid metabolization of adenosine do not occur which explains that the protective activity of adenosine was kept intact.

Finally, we assessed the pharmacological activity of SQAd NPs in ischemia/reperfusion conditions. Practically, the HL-1 cells were treated after 6h of ischemia, during 30 min of reperfusion, in complete medium with serum (Figure 4c). Although reperfusion usually induces new damages on cardiomyocytes after ischemia[3], we observed that 30 min of reperfusion without treatment did not generate any damages by itself on HL-1 cells, highlighting the limits of the *in vitro* model.

At 30 min reperfusion, apoptosis and necrosis were, however, high enough compared to those in normoxic conditions, which allowed to evaluate the pharmacological activity of SQAd NPs treatment. And it was discovered that the addition of 5 µg/mL of SQAd NPs at reperfusion promoted a considerable decrease in cell death by around a quarter (Figure 4c). Further experiments are still ongoing in order to confirm these results *in vitro,* compare these results with free adenosine control and test other doses of NPs.

Overall, in a model of ischemia/reperfusion injury on HL-1 cardiac cells, SQAd NPs appeared to be a potent and non-cytotoxic drug that exerted cardio-protection against both ischemia-induced cell death and ischemia/reperfusion-induced cell death. Despite the *in vitro* model was designed to be as close as possible from living models, it still displayed some limitations. Indeed, this "2D one layer" *in vitro* model, didn't take into account the interactions with other myocardial cells, in particular fibroblasts and endothelial cells. Hence, we further assessed the pharmacological efficacy on a murine model of ischemia and reperfusion.

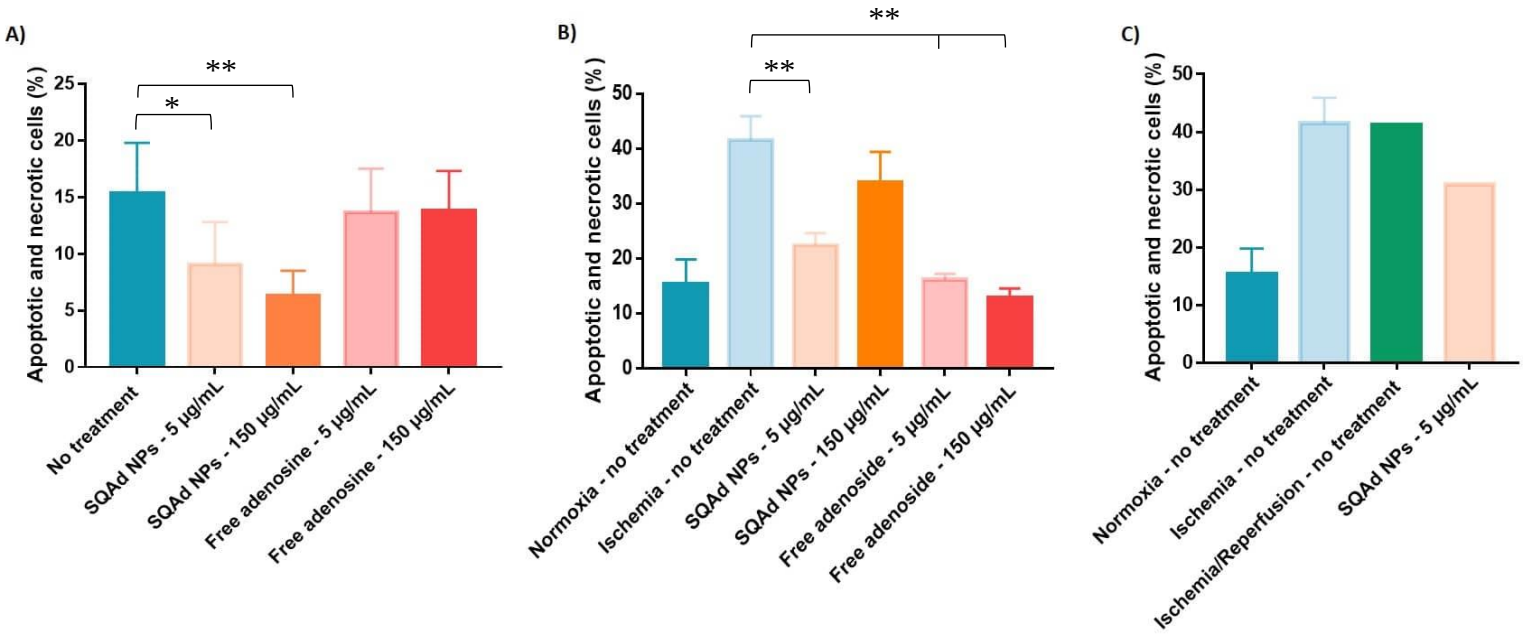

Figure 4. *In vitro* cardioprotective effects of SQAd NPs and free adenosine on HL-1 cells.

The percentage of apoptotic and necrotic HL-1 cells is determined after 6h of normoxia (**A**), after 6h of ischemia (**B**), and after 6h of ischemia followed by 30 min of reperfusion (**C**). Treatments were performed just before ischemia and at reperfusion for the ischemia/reperfusion model. Experiments are performed by flow cytometry after AnnexinV and 7-AAD co-staining. Nanoparticles are tested as protective treatment at low (5 µg/mL) and high (150 µg/mL) doses. Free adenosine control is tested at the same equivalent doses. N=1-5 replicates by conditions. Data are the mean ± SD. *P < 0.05, **P < 0.01, and ***P < 0.001 significance is evaluated using GraphPad Prism 7.0 Software, with student t test analysis between groups.

3.3. Murine myocardial ischemia/reperfusion injury model and infarct size measurements

Due to the complication in reproducing *in vitro* conditions that would reflect the pathophysiology of coronary heart diseases, animal models of myocardial I/R injury are mandatory, especially for investigating cardioprotective treatments. Left anterior descending (LAD) coronary artery ligation is the "gold standard" for a murine model to simulate the I/R events associated with myocardial infarction[37-39]. Here, we performed LAD artery ligation for 30 min followed by 3 or 7 days of reperfusion. Treatment was administered in the jugular vein directly after reperfusion. Our model operative mortality rate was inferior to 13% during the surgery, and inferior to 3% during the following reperfusion period.

At the end of treatment time, animals were sacrificed, and hearts were excised and cut in 1 mm thick slices. Before excision, Evans Blue and triphenyltetrazolium chloride staining were performed to delimit the infarct area (IA, pale white) and the area at risk of infarction (AAR, pink/pale red) from the healthy area (blue). Then, slices were freshly macroscopically imaged as presented in figure 5a-c.
When treatment was applied for 3 days, the AAR and IA sizes were smaller in the SQAd NPs treated group (27.4% ± 10%) than in the free adenosine treated group (41.4 ± 6.5%) and the dextrose 5% treated control group (40% ± 6% %). Same trends were observed with 7 days of treatment (figure 5d,e). However, these findings showed no significance.

These findings suggested that the encapsulation of adenosine into squalene-based nanoparticles protected the drug from quick metabolization, allowing a tissue protective effect against myocardial I/R which was not observed after administration of the drug free.

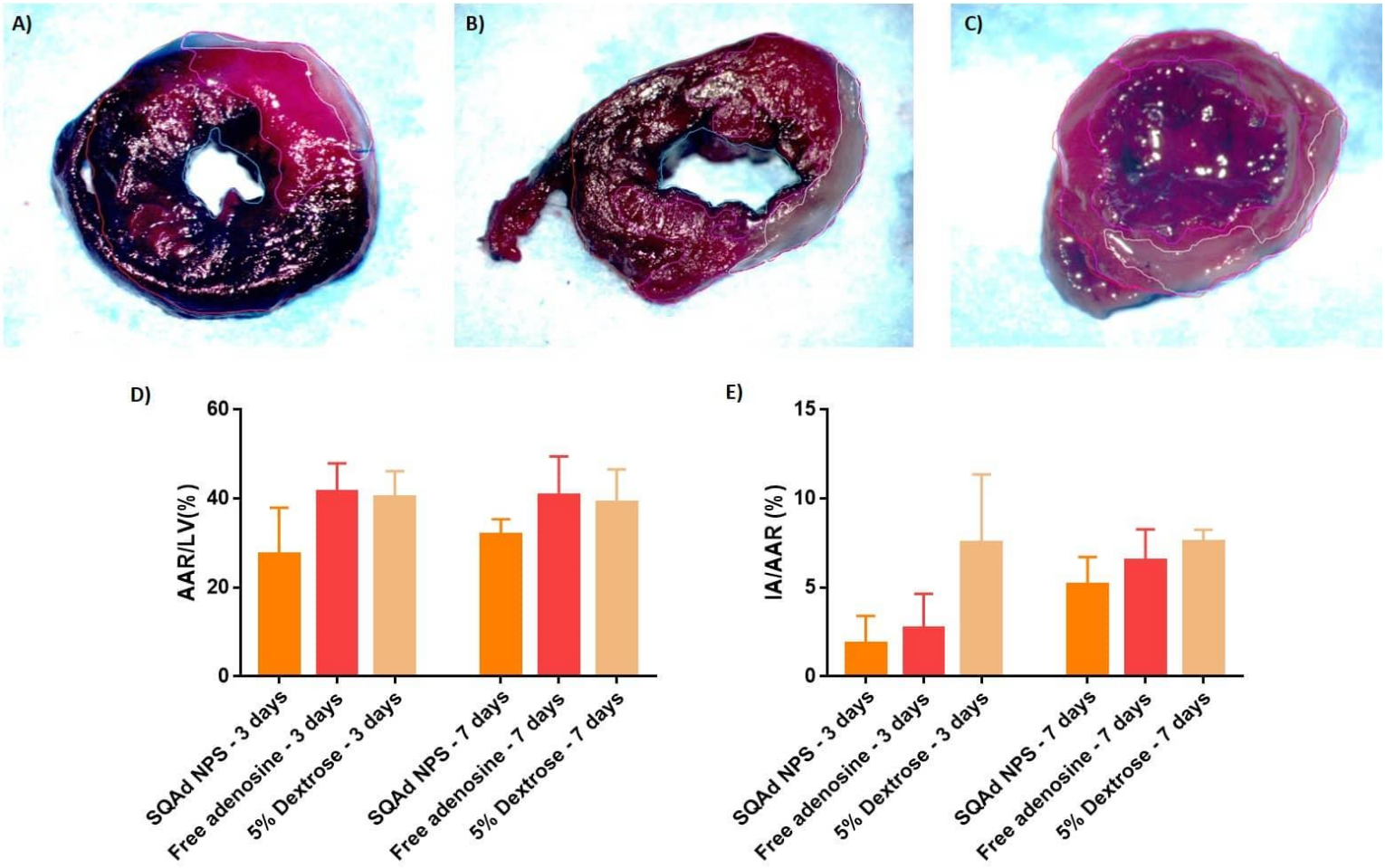

Figure 5. Efficacy of NPs treatment on the Area at risk (AAR) and Infarct area (IA) sizes in a mice model of I/R.

(A-C): Representative stereomicrographic images of typical heart sections double-stained with Evans Blue and TTC, from mouse subjected to 7 days treatment with SQAd NPs (A), Free adenosine (B) or 5% Dextrose solution (C). Left ventricle (LV) area is delimited in red, AAR in pink, and IA in white. (D) Graphical representation of the percentage of AAR/LV between treatment groups. (E) Graphical representation of the percentage of IA/AAR between treatment groups. Results are expressed as means ± SD of 8-13 animals per condition. Significance was evaluated using GraphPad Prism 7.0 Software, with student t test analysis between groups ($p<0,05$) but showed no significance.

3.4. Histopathological examination of heart sections

After stereo-microscopical analysis of heart sections, sections were embedded in paraffin and more finely cut to 5µm sections. 5µm heart sections were stained with haematoxylin and Eosin for histopathological examinations. As expected, myocardial ischemia/reperfusion induced various injury to the myocardial tissue structure[3]. These abnormal modifications included infiltration of inflammatory cells, dead cells, oedema and fibrosis(figure 6a,b). The arbitrarily-named ”diseased areas” – area exhibiting these injuries – were delimited and their sizes were measured and compared between treatment groups(figure 6c). Consistently with the previous results, diseased area expressed as percentage of left ventricle were significantly bigger in the 5% dextrose control group and the free adenosine group compared to the SQAd NPs group, either at days 3 or 7 post-treatment. More precisely, SQAd NPs treated mice displayed a mean

diseased area of 12.46 % ± 9.97 % and 11.75 % ± 5.38 %, respectively at 3 and 7 days post-treatment, *versus* 20.83 % ± 17.08 % and 20.35 % ± 9.66 % for free adenosine treated mice and 24.96 % ± 7.89 % and 21.46 % ± 11.85 % for 5% dextrose treated mice at 3 and 7 days post treatment (Figure 6c).

These data confirmed the cardioprotective effect of SQAd NPs against myocardial ischemia/reperfusion injury. It should, however, be taken into consideration that there was an important variability between mice in each treatment group, as shown by the important standard deviation values which didn't allow to reach significance.

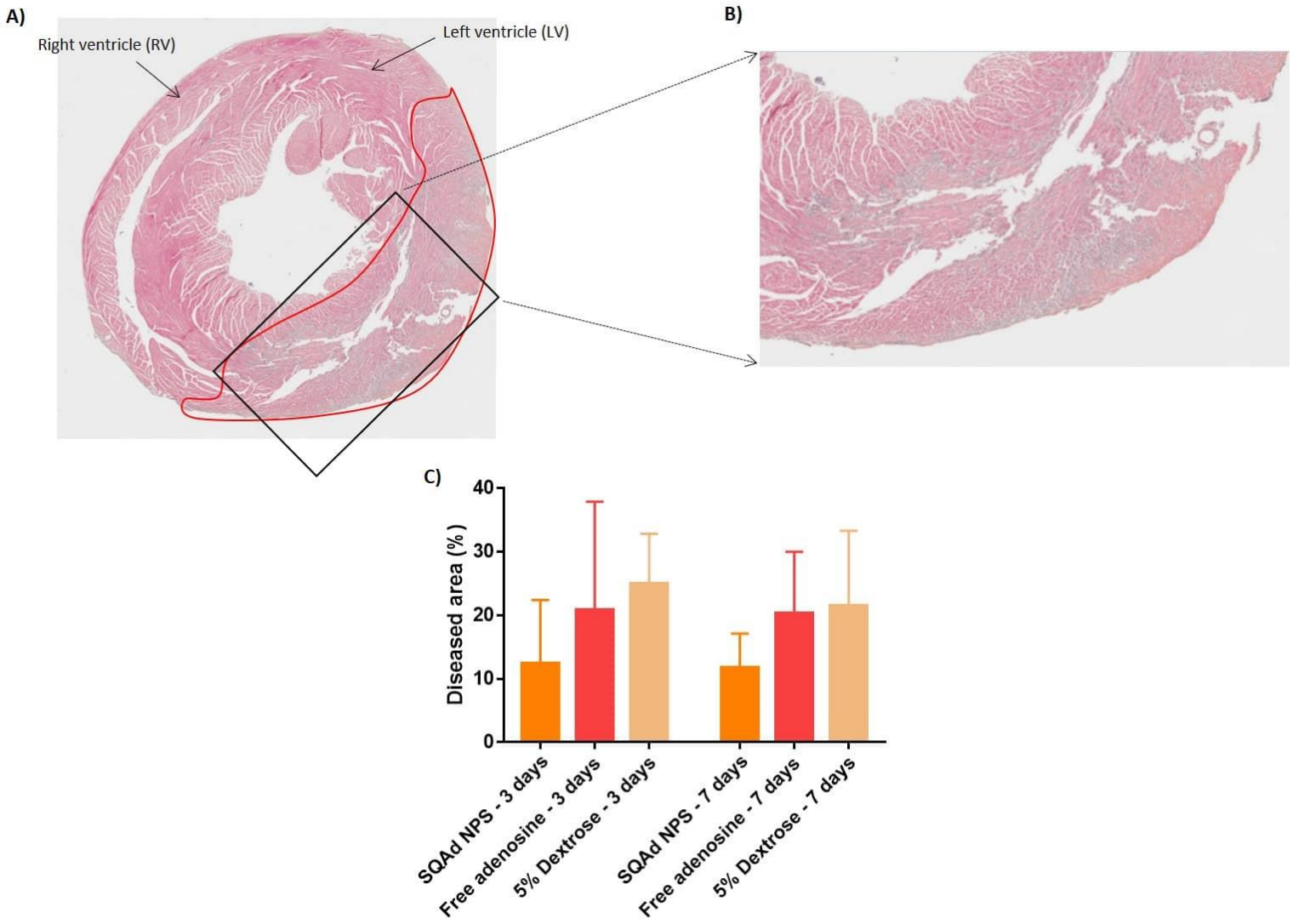

Figure 6. Histopathological examination of heart sections.

(**A**): Representative microscopical image of a histological heart section stained with haematoxylin and eosin. The red-delimited zone represents the diseased area, presenting abnormal modifications such as infiltration of inflammatory cells, apoptotic/necrotic cells, scar tissue and fibrosis. (**B**): Zooming on the diseased area of the histological sections. (**C**): Graphical comparison of the percentage of diseased area between treatment groups. Results are expressed as means ± SD of 4-8 animals per condition. Significance was evaluated using GraphPad Prism 7.0 Software, with student t test analysis between groups but showed not significant differences between groups due to the strong variability.

3.5. Immuno-histochemical evaluation of heart sections

Due to the anti-apoptotic effects of adenosine, we first hypothesized that SQAd NPs could play a role on Myocardial apoptosis. Myocardial apoptosis was investigated and measured by TUNEL assay on paraffined heart sections (figure 7). It was observed that SQAd NPs treatment significantly decreased the number of TUNEL-positive nuclei – thus the number of apoptotic cells – either after 3 or 7 days of treatment, compared to the dextrose 5% control solution. Indeed, the number of apoptotic cells was 2-2.5 times lower than in the dextrose treatment group. Free adenosine treatment also induced a decrease in the number of apoptotic cells. At day 3, the diminution of apoptotic cells was even similar to that obtained with SQAd NPs, but not at 7 days post treatment when the number of apoptotic cells was only 1.3 times lower than in the control group. Interestingly, the treatment with SQAd NPs remained efficient for a longer period of time, at least until 7 days.

This tends to indicate that the encapsulation of adenosine into squalene-based nanoparticles hindered myocardial apoptosis following ischemia/reperfusion injury in a rather prolonged manner, a possible consequence of the protection of adenosine.

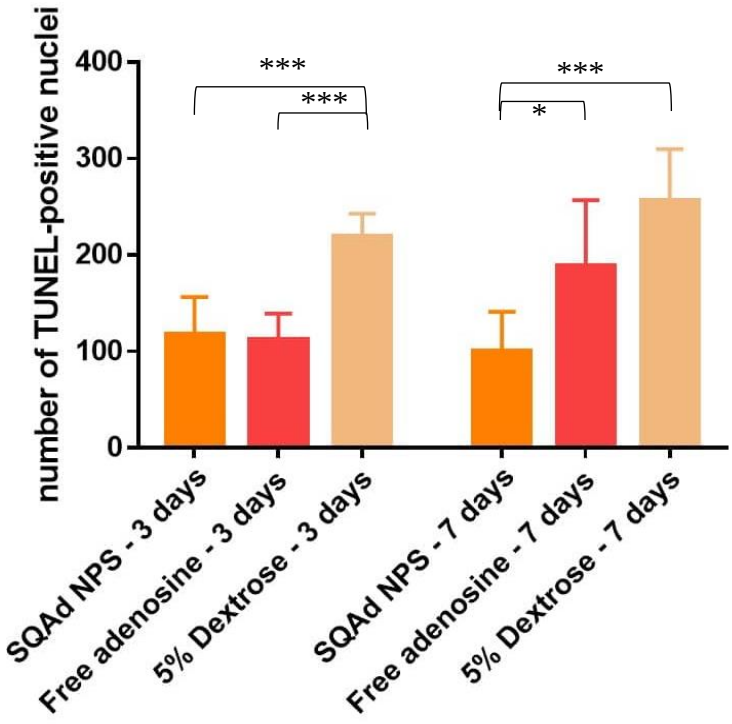

Figure 7. Immuno-histochemical evaluation of cell apoptosis on heart sections.

Graphical comparison of the number of TUNEL-positive nuclei between the 6 treatment groups. Results are expressed as means ± SD of 6-8 animals per condition. *P < 0.05, **P < 0.01, and ***P < 0.001 significance are evaluated using GraphPad Prism 7.0 Software, with student t test analysis between groups.

Besides apoptosis, histological staining to evaluate the impact of SQAd NPs treatment on inflammation remains of great interest. Indeed, inflammation plays a crucial role during myocardial ischemia/reperfusion; there is an important recruitment of white blood cells in heart tissue, associated with overproduction of cytokines, chemokines and other pro-inflammatory modulators in addition to activation of the complement system[3, 40]. These studies are currently in progress particularly for the staining of activated macrophages, which exhibit both a pro- and anti-inflammatory phenotype, essential for removing injured tissue and facilitating repair.

3.6. Influence of SQAd NPs treatment on heart macrophages levels

Macrophages are key mediators of the inflammatory response initiated following myocardial ischemia/reperfusion injury. Notably, the heart resident macrophages and monocyte-derived infiltrating macrophages possess a specific role in the regulation of cardiac function. Especially, tissue resident cells facilitate coronary development and tissue homeostasis, while monocyte-derived infiltrating cells have a predominant role in tissue injury and destruction[41]. Besides, sustained activation of pro-inflammatory macrophages induces remodelling of cardiac tissue, ultimately leading to deterioration of cardiac function and heart failure[41, 42]. Thus, thanks to the anti-inflammatory activity of adenosine[28], it was hypothesized that SQAd NPs treatment could influence heart macrophages levels. This is the reason why activated macrophages M1 and M2 were observed by antibody staining in a flow cytometry examination of heart slices (figure 8).

First, to support the choice of our antibodies, we tested mouse igG1, igG2a and igG2b isotype controls, which shows a low mean fluorescence intensity. Then, we tested F4/80 as a marker of the whole activated macrophages pool and CD64/CD206 as markers of M1 and M2 macrophages, respectively. However, the variability of the obtained results between animals couldn’t lead to a solid conclusion, even if there was a tendency that with SQAd NPs treatment, the mean fluorescence intensity of all types of macrophages was raising from 3 to 7 days post-treatment, which was not observed with free adenosine or dextrose control group.

These results seemed to indicate that SQAd NPs treatment could play a role in delaying the inflammatory response. By doing so, it could delay the damages on the cardiac tissue due to reperfusion, since the strong inflammatory response is one of the main consequences of reperfusion.

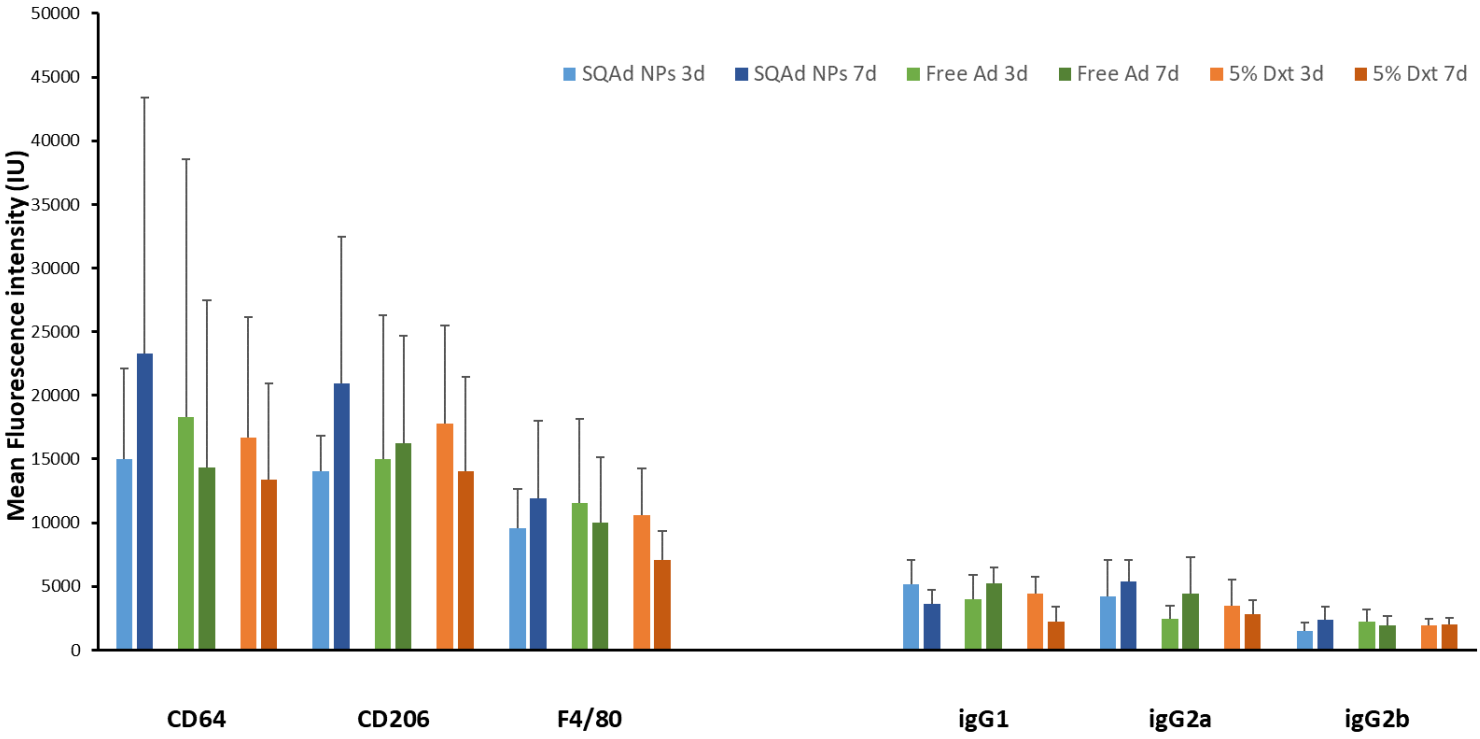

Figure 8. Evaluation of heart macrophages levels by flow cytometry.

Comparison of the mean fluorescence intensity of 3 macrophages antibodies and their respective igGs isotype control between the treatment groups. F4/80 is used as a marker of the whole activated macrophages pool and CD64/CD206 are used as a marker of M1 and M2 macrophages, respectively. Results are expressed as the mean of mean fluorescence intensity ± SD of 6-8 animals per condition. No significant differences were observed.

4. Conclusions

The study we presented here aimed to find a new therapeutic strategy to protect heart after myocardial ischemia/reperfusion injury by using squalene-adenosine nanoparticles as a new nanomedicine. Notably, we report evidence that SQAd NPs could exert a promising cardioprotective effect in mouse model of myocardial ischemia-reperfusion injury. Encapsulation of adenosine into squalene-based nanoparticles allowed to overcome some limitations of the conventional adenosine treatment. Particularly, our encouraging *in vitro* and *in vivo* data proved that SQAd nanoparticles are non-cytotoxic and could reduce the infarct size and protect heart tissue from cell death. Although some of the first results obtained on the level of inflammatory biomarkers were not significant or not conclusive, additional efforts are ongoing to further precise and refine the main mechanisms under these effects. Overall, these SQAd nanoparticles represent an interesting innovative approach that may provide a protective effect against myocardial ischemia/reperfusion injury in mouse.

Declaration of interest

The authors declare no conflict of interest.

Acknowledgements

We wish to gratefully thank Denis Calise (INSERM/UPS/ENVT US006 CREFRE, Toulouse, France) for his help with the development and application of the murine model of myocardial ischemia/reperfusion injury. We also want to thank Valérie Domergue and Severine Domenichini (UMS IPSIT, Université Paris-Saclay, Châtenay-Malabry, France) for their assistance with confocal microscopy experiments.

The authors gratefully acknowledge the financial support from the 7th EuroNanoMed-II call for proposals, project NanoHeart n°ANR-16-ENM2-0005-01.

References

[1]: World Health Organization website: https://www.who.int/news-room/fact-sheets/detail/cardiovascular-diseases-(cvds)

[2]: Li, X., Liu, M., Sun, R., Zeng, Y., Chen, S., & Zhang, P. (2016). Protective approaches against myocardial ischemia reperfusion injury. Experimental and therapeutic medicine, 12(6), 3823−3829.

[3]: Kalogeris, T., Baines, C. P., Krenz, M., & Korthuis, R. J. (2016). Ischemia/Reperfusion. Comprehensive Physiology, 7(1), 113−170.

[4]: Toldo, S., Mauro, A. G., Cutter, Z., & Abbate, A. (2018). Inflammasome, pyroptosis, and cytokines in myocardial ischemia-reperfusion injury. American journal of physiology. Heart and circulatory physiology, 315(6), H1553–H1568.

[5]: Sommerschild HT, Kirkebøen KA. (2000). Adenosine and cardioprotection during ischaemia and reperfusion--an overview. Acta Anaesthesiol Scand.44(9):1038-55.

[6]: Forman MB, Stone GW, Jackson EK. (2006). Role of adenosine as adjunctive therapy in acute myocardial infarction. Cardiovasc Drug Rev.24(2):116-47.

[7]: Peart, J., Matherne, G. P., Cerniway, R. J., & Headrick, J. P. (2001). Cardioprotection with adenosine metabolism inhibitors in ischemic-reperfused mouse heart. Cardiovascular research, 52(1), 120−129.

[8]: Forman, M. B., & Jackson, E. K. (2007). Importance of tissue perfusion in ST segment elevation myocardial infarction patients undergoing reperfusion strategies: role of adenosine. Clinical cardiology, 30(11), 583−585.

[9]: Mahaffey, K. W., Puma, J. A., Barbagelata, N. A., DiCarli, M. F., Leesar, M. A., Browne, K. F., Eisenberg, P. R., Bolli, R., Casas, A. C., Molina-Viamonte, V., Orlandi, C., Blevins, R., Gibbons, R. J., Califf, R. M., & Granger, C. B. (1999). Adenosine as an adjunct to thrombolytic therapy for acute myocardial infarction: results of a multicenter, randomized, placebo-controlled trial: the Acute Myocardial Infarction STudy of ADenosine (AMISTAD) trial. Journal of the American College of Cardiology, 34(6), 1711−1720.

[10]: Ross, A. M., Gibbons, R. J., Stone, G. W., Kloner, R. A., Alexander, R. W., & AMISTAD-II Investigators (2005). A randomized, double-blinded, placebo-controlled multicenter trial of adenosine as an adjunct to reperfusion in the treatment of acute myocardial infarction (AMISTAD-II). Journal of the American College of Cardiology, 45(11), 1775−1780.

[11]: Layland, J., Carrick, D., Lee, M., Oldroyd, K., & Berry, C. (2014). Adenosine: physiology, pharmacology, and clinical applications. JACC. Cardiovascular interventions, 7(6), 581−591.

[12]: Galagudza, M., Korolev, D., Postnov, V., Naumisheva, E., Grigorova, Y., Uskov, I., & Shlyakhto, E. (2012). Passive targeting of ischemic-reperfused myocardium with adenosine-loaded silica nanoparticles. International journal of nanomedicine, 7, 1671−1678.

[13]: Takahama, H., Minamino, T., Asanuma, H., Fujita, M., Asai, T., Wakeno, M., Sasaki, H., Kikuchi, H., Hashimoto, K., Oku, N., Asakura, M., Kim, J., Takashima, S., Komamura, K., Sugimachi, M., Mochizuki, N., & Kitakaze, M. (2009). Prolonged targeting of ischemic/reperfused myocardium by liposomal adenosine augments cardioprotection in rats. Journal of the American College of Cardiology, 53(8), 709−717.

[14]: Couvreur, P., Stella, B., Reddy, L. H., Hillaireau, H., Dubernet, C., Desmaële, D., Lepêtre-Mouelhi, S., Rocco, F., Dereuddre-Bosquet, N., Clayette, P., Rosilio, V., Marsaud, V., Renoir, J. M., & Cattel, L. (2006). Squalenoyl nanomedicines as potential therapeutics. Nano letters, 6(11), 2544−2548.

[15]: Reddy, L. H., Dubernet, C., Mouelhi, S. L., Marque, P. E., Desmaele, D., & Couvreur, P. (2007). A new nanomedicine of gemcitabine displays enhanced anticancer activity in sensitive and resistant leukemia types. Journal of controlled release : official journal of the Controlled Release Society, 124(1-2), 20−27.

[16]: Gaudin, A., Yemisci, M., Eroglu, H., Lepetre-Mouelhi, S., Turkoglu, O. F., Dönmez-Demir, B., Caban, S., Sargon, M. F., Garcia-Argote, S., Pieters, G., Loreau, O., Rousseau, B., Tagit, O., Hildebrandt, N., Le Dantec, Y., …, Couvreur, P. (2014). Squalenoyl adenosine nanoparticles provide neuroprotection after stroke and spinal cord injury. Nature nanotechnology, 9(12), 1054−1062.

[17]: Piercy, K. T., Donnell, R. L., Kirkpatrick, S. S., Mundy, B. L., Stevens, S. L., Freeman, M. B., & Goldman, M. H. (2001). Effect of harvesting and sorting on beta-1 integrin in canine microvascular cells. The Journal of surgical research, 100(2), 211−216.

[18]: Huang, H. L., Hsing, H. W., Lai, T. C., Chen, Y. W., Lee, T. R., Chan, H. T., Lyu, P. C., Wu, C. L., Lu, Y. C., Lin, S. T., Lin, C. W., Lai, C. H., Chang, H. T., Chou, H. C., & Chan, H. L. (2010). Trypsin-induced proteome alteration during cell subculture in mammalian cells. Journal of biomedical science, 17(1), 36.

[19]: Xu Z., McElhanon K.E., Beck E.X., Weisleder N. (2018) A Murine Model of Myocardial Ischemia–Reperfusion Injury. In: Tharakan B. (eds) Traumatic and Ischemic Injury. Methods in Molecular Biology, vol 1717. Humana Press, New York, NY

[20]: Desmaële, D., Gref, R., & Couvreur, P. (2012). Squalenoylation: a generic platform for nanoparticular drug delivery. Journal of controlled release : official journal of the Controlled Release Society, 161(2), 609−618.

[21]: Dormont, F., Rouquette, M., Mahatsekake, C., Gobeaux, F., Peramo, A., Brusini, R., Calet, S., Testard, F., Lepetre-Mouelhi, S., Desmaële, D., Varna, M., & Couvreur, P. (2019). Translation of nanomedicines from lab to industrial scale synthesis: The case of squalene-adenosine nanoparticles. Journal of controlled release : official journal of the Controlled Release Society, 307, 302−314.

[22]: Rouquette, M., Ser-Le Roux, K., Polrot, M., Bourgaux, C., Michel, J. P., Testard, F., Gobeaux, F., & Lepetre-Mouelhi, S. (2019). Towards a clinical application of freeze-dried squalene-based nanomedicines. Journal of drug targeting, 27(5-6), 699−708.

[23]: Hua, S., de Matos, M., Metselaar, J. M., & Storm, G. (2018). Current Trends and Challenges in the Clinical Translation of Nanoparticulate Nanomedicines: Pathways for Translational Development and Commercialization. Frontiers in pharmacology, 9, 790.

[24]: Claycomb, W. C., Lanson, N. A., Jr, Stallworth, B. S., Egeland, D. B., Delcarpio, J. B., Bahinski, A., & Izzo, N. J., Jr (1998). HL-1 cells: a cardiac muscle cell line that contracts and retains phenotypic characteristics of the adult cardiomyocyte. Proceedings of the National Academy of Sciences of the United States of America, 95(6), 2979−2984.

[25]: Chen T, Vunjak-Novakovic G. *In vitro* Models of Ischemia-Reperfusion Injury. Regen Eng Transl Med. 2018;4(3):142–153.
[26]: Teixeira, G., Abrial, M., Portier, K., Chiari, P., Couture-Lepetit, E., Tourneur, Y., Ovize, M., & Gharib, A. (2013). Synergistic protective effect of cyclosporin A and rotenone against hypoxia-reoxygenation in cardiomyocytes. Journal of molecular and cellular cardiology, 56, 55−62.
[27]: Li, X., Liu, M., Sun, R., Zeng, Y., Chen, S., & Zhang, P. (2016). Protective approaches against myocardial ischemia reperfusion injury. Experimental and therapeutic medicine, 12(6), 3823−3829.
[28]: Antonioli, L., Blandizzi, C., Pacher, P., & Haskó, G. (2013). Immunity, inflammation and cancer: a leading role for adenosine. Nature reviews. Cancer, 13(12), 842−857.
[29]: Schmidt, J., & Ferk, P. (2017). Safety issues of compounds acting on adenosinergic signalling. The Journal of pharmacy and pharmacology, 69(7), 790−806.
[30]: Schrier, S. M., van Tilburg, E. W., van der Meulen, H., Ijzerman, A. P., Mulder, G. J., & Nagelkerke, J. F. (2001). Extracellular adenosine-induced apoptosis in mouse neuroblastoma cells: studies on involvement of adenosine receptors and adenosine uptake. Biochemical pharmacology, 61(4), 417−425.
[31]: Shneyvays, V., Jacobson, K. A., Li, A. H., Nawrath, H., Zinman, T., Isaac, A., & Shainberg, A. (2000). Induction of apoptosis in rat cardiocytes by A3 adenosine receptor activation and its suppression by isoproterenol. Experimental cell research, 257(1), 111−126.
[32]: Jacobson, K. A., Hoffmann, C., Cattabeni, F., & Abbracchio, M. P. (1999). Adenosine-induced cell death: evidence for receptor-mediated signalling. Apoptosis : an international journal on programmed cell death, 4(3), 197−211.
[33]: Shen Y. et al. (2018) Activation of adenosine A2b receptor attenuates high glucose-induced apoptosis in H9C2 cells via PI3K/Akt signaling. *In Vitro* Cell Dev Biol Anim. 54(5):384-391
[34]: Bès, S., Ponsard, B., El Asri, M., Tissier, C., Vandroux, D., Rochette, L., & Athias, P. (2002). Assessment of the cytoprotective role of adenosine in an in vitro cellular model of myocardial ischemia. European journal of pharmacology, 452(2), 145−154.
[35]: Ahsan, S. M., Rao, C. M., & Ahmad, M. (2018). Nanoparticle-Protein Interaction: The Significance and Role of Protein Corona. Advances in experimental medicine and biology, 1048, 175−198.
[36]: Pareek, V., Bhargava, A., Bhanot, V., Gupta, R., Jain, N., & Panwar, J. (2018). Formation and Characterization of Protein Corona Around Nanoparticles: A Review. Journal of nanoscience and nanotechnology, 18(10), 6653−6670.
[37]: Xu, Z., Alloush, J., Beck, E., & Weisleder, N. (2014). A murine model of myocardial ischemia-reperfusion injury through ligation of the left anterior descending artery. Journal of visualized experiments : JoVE, (86), 51329.
[38]: Virag J.A.I., Lust R.M. (2011). Coronary artery ligation and intramyocardial injection in a murine model of infarction. J Vis Exp.
[39]: Xu, Z., McElhanon, K. E., Beck, E. X., & Weisleder, N. (2018). A Murine Model of Myocardial Ischemia-Reperfusion Injury. Methods in molecular biology (Clifton, N.J.), 1717, 145−153.
[40]: Ioannou, A., Dalle Lucca, J., & Tsokos, G. C. (2011). Immunopathogenesis of ischemia/reperfusion-associated tissue damage. Clinical immunology (Orlando, Fla.), 141(1), 3−14.
[41]: O'Rourke, S. A., Dunne, A., & Monaghan, M. G. (2019). The Role of Macrophages in the Infarcted Myocardium: Orchestrators of ECM Remodeling. Frontiers in cardiovascular medicine, 6, 101.
[42]: Chen, B., Brickshawana, A., & Frangogiannis, N. G. (2019). The Functional Heterogeneity of Resident Cardiac Macrophages in Myocardial InjuryCCR2+ Cells Promote Inflammation, Whereas CCR2- Cells Protect. Circulation research, 124(2), 183−185.

Chapitre 3. Squalene-based multidrug nanoparticles for improved mitigation of uncontrolled inflammation

Résumé détaillé

Le sepsis est un syndrome complexe caractérisé par une inflammation systémique incontrôlée causée par une infection grave qui peut commencer localement. Cela touche principalement des patients au système immunitaire affaibli et se présente sous la forme de fièvre ou hypothermie, respiration et rythme cardiaque accélérés, ainsi que d'une augmentation ou diminution du nombre de globules blancs du sang. Tout cela s'accompagne d'une sur-production de médiateurs inflammatoires et de la dysfonction de certains organes[1, 2]. Par ailleurs, un nombre grandissant d'études récentes tendent à prouver que cet état d'inflammation aiguë incontrôlée serait provoqué par la conjonction de deux facteurs : des signaux pro-inflammatoires, combinés à un épisode de stress oxydant. Ces deux facteurs contribuent à s'alimenter mutuellement, établissant ainsi un cercle vicieux propageant la réponse inflammatoire[3, 4].

A l'heure actuelle, très peu de traitements s'avèrent efficaces pour traiter ces inflammations sévères et ceux qui existent ont des effets secondaires indésirables. Le traitement du sepsis s'oriente principalement autour de l'administration d'antibiotiques pour aider à lutter contre l'infection primaire, de l'utilisation de vasopresseurs pour préserver le volume et tonus intravasculaire, ainsi que d'une thérapie au « cas par cas » nécessaire au maintien des fonctions vitales[1, 5]. Aucun traitement moléculaire n'a jusque-là prouvé d'efficacité. De plus, bien que des progrès considérables ont été réalisés dans la compréhension de la physiopathologie, et que de multiples essais cliniques furent tentés, aucune nouvelle thérapie n'a vu le jour ces dernières années. Notamment, il n'existe aucun traitement efficace ciblant le couplage entre inflammation et stress oxydant de manière spécifique.

Au sein de notre équipe, afin d'apporter une atténuation renforcée de l'inflammation systémique incontrôlée qui a lieu au cours du sepsis, nous avons entrepris le développement de nanoparticules bimodales à base de squalène. Ces nanoparticules combinent en effet un principe actif anti-inflammatoire et immunomodulateur, l'adénosine, et un anti-oxydant naturel, l'alpha-tocophérol (vitamine E). Dans cette étude portée par Flavio Dormont, un ancien étudiant en Thèse dans notre équipe, nous avons d'abord préparé et caractérisé des nanoparticules de squalène-adénosine/tocophérol (SQAd/VitE) contenant 50% en masse de tocophérol. Cela correspond à la formulation ayant fourni la plus forte charge totale en principe actif avec une stabilité colloïdale adéquate selon les résultats obtenus par F. Dormont. Le diamètre hydrodynamique moyen des nanoparticules était de l'ordre de 70nm avec un potentiel électrique de surface

négatif de l'ordre de -14.3 mV. Des études de bio-distribution *in vivo* ont ensuite été menées et ont montré une accumulation des nanoparticules aux sites d'inflammation aiguë et de dysfonction de l'endothélium dans des modèles murins. A la fois localement dans un modèle d'inflammation de la patte, mais aussi dans un modèle d'inflammation systémique au LPS. Cela a permis de constater que l'on obtient une amélioration de la biodisponibilité des principes actifs une fois formulés sous forme de nanoparticules. Cela suggère par conséquent que l'encapsulation dans des nanoparticules à base de squalène peut potentiellement limiter leurs effets secondaires.

In vitro, ces nanoparticules sont captées par les cellules, et se sont montrées efficaces pour limiter la production intracellulaire d'espèces réactives de l'oxygène de manière dose dépendante dans un modèle de stress oxydant par incubation avec du H2O2. Cela a aussi amélioré significativement la survie cellulaire. Ces effets n'ont pas été aussi prononcés avec des nanoparticules uniquement composées de SQAd ou de SQVitE, ainsi qu'avec les principes actifs seuls. Par ailleurs, dans un modèle d'inflammation sur une lignée macrophagique stimulée au LPS, le traitement par nanoparticules de SQAd/VitE a engendré une inhibition conséquente de la réponse pro-inflammatoire et une diminution significative de la production d'espèces réactive de l'azote. De manière générale, les résultats *in vitro* ont donc prouvé que les nanoparticules de SQAd/VitE peuvent réduire la production d'espèces réactives de l'oxygène et de l'azote et produire des effets anti-inflammatoires de manière concentration-dépendante *via* l'effet combiné de l'adénosine et du tocophérol. Ces résultats ont ensuite été confirmés *in vivo* dans un modèle murin d'endotoxémie. En effet, l'injection à une dose totale de 30 mg/kg de nanoparticules de SQAd/VitE a montré de multiples effets. Premièrement, il a pu être observé une diminution significative en cytokines pro-inflammatoires circulantes (TNF-α) et celles présentes dans les organes (MCP-1 et IL-6), associée à une augmentation en médiateurs anti-inflammatoires (IL-10) de façon dose-dépendante. Deuxièmement, ces nanoparticules ont affiché un effet anti-oxydant en entraînant une réduction de la peroxydation des lipides dans les poumons de manière plus importante comparé aux groupes témoins. Troisièmement, contrairement à un traitement avec les principes actifs libres qui induit une diminution conséquente de la pression sanguine dû à l'adénosine, la formulation nanoparticulaire n'a montré aucun effet négatif significatif sur la pression sanguine. Cela a donc confirmé que l'encapsulation sous forme de nanoparticules à base de squalène aide à protéger les animaux des effets secondaires induits par une thérapie avec de l'adénosine. Enfin, dans un modèle murin d'injection de LPS à dose léthale, il a été constaté une amélioration des scores cliniques et une meilleure protection de la dégradation des organes avec l'utilisation des nanoparticules de SQAd/VitE comparé aux groupes témoins.

Cette étude a ainsi démontré que les nanoparticules multi-médicaments de SQAd/VitE permettent d'améliorer significativement l'activité pharmacologique des deux médicaments dans des modèles d'inflammation aigüe, tout en réduisant les effets secondaires. Ces nanoparticules permettant notamment

une bio-distribution ciblée et spécifique d'agents thérapeutiques en exploitant les perturbations de la barrière endothéliale au niveau des sites d'inflammation, réduisant de fait les effets secondaires néfastes des principes actifs non-encapsulés. Ainsi, les nanoparticules de SQAd/VitE représentent un nouvel outil thérapeutique pour lutter contre le phénomène d'inflammation incontrôlée en se basant sur l'approche originale de traiter le couplage entre l'inflammation et le stress oxydant.

Tous les résultats présentés dans ce chapitre ont fait l'objet d'un article scientifique :

« Dormont, F., Brusini, R., Cailleau, C., Reynaud, F., Peramo, A., Gendron, A., Mougin, J., Gaudin, F., Varna, M., & Couvreur, P. (2020). Squalene-based multidrug nanoparticles for improved mitigation of uncontrolled inflammation in rodents. *Science advances,* 6(23), eaaz5466. »

Pour ma part, j'ai notamment participé à la préparation et à la caractérisation des nanoparticules utilisées au cours de cette étude. J'ai aussi pris part aux mesures de fluorescence au Lumina dans le cadre des études de bio-distribution des nanoparticules de SQAd/VitE. Enfin, j'ai contribué au développement du modèle murin d'injection de LPS à dose léthale et à l'observation de l'évolution des scores cliniques.

Références :

[1]: Cecconi, M., Evans, L., Levy, M., & Rhodes, A. Sepsis and septic shock. Lancet (London, England), 392(10141), 75–87. (2018).

[2]: site internet de l'institut Pasteur : https://www.pasteur.fr/fr/centre-medical/fiches-maladies/sepsis-septicemie#:~:text=Le%20sepsis %20est%20la%20cons%C3%A9quence,le%20syst%C3%A8me%20immunitaire%20est%20affaibli.

[3]: Biswas S. K. Does the Interdependence between Oxidative Stress and Inflammation Explain the Antioxidant Paradox?. Oxidative medicine and cellular longevity, 2016, 5698931. (2016).

[4]: J. Lugrin, N. Rosenblatt-Velin, R. Parapanov,L. Liaudet, The role of oxidative stress during inflammatory processes. Biological chemistry. 395, 203-230 (2014)

[5]: Rello, J., Valenzuela-Sánchez, F., Ruiz-Rodriguez, M., & Moyano, S. Sepsis: A Review of Advances in Management. Advances in therapy, 34(11), 2393–2411. (2017).

Squalene-based multidrug nanoparticles for improved mitigation of uncontrolled inflammation in rodents

Flavio Dormont[1], Romain Brusini[1], Catherine Cailleau[1], Franceline Reynaud[1,2], Arnaud Peramo[1], Amandine Gendron[1], Julie Mougin[1], Françoise Gaudin[3,4], Mariana Varna[1] and Patrick Couvreur[1,*]

[1]Institut Galien Paris-Sud, CNRS UMR 8612, Université Paris-Sud, Université Paris-Saclay, 92296 Châtenay-Malabry, France.

[2]School of Pharmacy, Federal University of Rio de Janeiro, 21944-59 Rio de Janeiro, Brazil.

[3]Plateforme d'Histologie Immunopathologie de Clamart (PHIC) Université Paris-Saclay, Inserm, CNRS, Institut Paris Saclay d'Innovation thérapeutique, 92296 Châtenay-Malabry, France.

[4]Université Paris-Saclay, Inserm, Inflammation, Microbiome and Immunosurveillance, 92140 Clamart, France.

*Corresponding author: Patrick Couvreur
Email: patrick.couvreur@universite-paris-saclay.fr

Science Advances 05 Jun 2020:Vol. 6, no. 23, eaaz5466
DOI: 10.1126/sciadv.aaz5466

Abstract

Uncontrolled inflammatory processes are at the root of numerous pathologies. Most recently, studies on confirmed COVID-19 cases have suggested that mortality might be due to virally induced hyperinflammation. Uncontrolled pro-inflammatory states are often driven by continuous positive feedback loops between pro-inflammatory signalling and oxidative stress, which cannot be resolved in a targeted manner. Here, we report on the development of multidrug nanoparticles for the mitigation of uncontrolled inflammation. The nanoparticles are made by conjugating squalene, a natural lipid, to adenosine, an endogenous immunomodulator, and then encapsulating α-tocopherol, as antioxidant. This resulted in high drug loading, biocompatible, multidrug nanoparticles. By exploiting the endothelial dysfunction at sites of acute inflammation, these multidrug nanoparticles delivered the therapeutic agents in a targeted manner, conferring survival advantage to treated animals in models of endotoxemia. Selectively delivering adenosine and antioxidants together could serve as a novel therapeutic approach for safe treatment of acute paradoxical inflammation.

Significance Statement

Growing evidence has indicated that uncontrolled inflammation is often driven by continuous positive feedback loops between pro-inflammatory signalling and oxidative stress. There are currently no effective ways to counter this crosstalk in a targeted manner. Herein, we demonstrate the therapeutic potential of squalene prodrug-based nanoparticles for inflammation control through a powerful two-drug neutralization process: adenosine as a potent inflammation mediator and tocopherol for efficient protection against oxidative stress. The multidrug nanoparticles are able to target the site of acute inflammation because of the vascular permeability that appears there. This therapeutic option may provide a first-in class adenosine and antioxidant-based treatment that may ultimately improve the clinical outcome of patients suffering from uncontrolled inflammatory disorders.

1. Introduction

Uncontrolled inflammation is a key health challenge and is associated with numerous diseases (***1***–***3***). Recently, coronavirus disease 2019 (COVID-19) infections have been recognized as leading to a hyperinflammatory state characterized by a fulminant cytokine storm (hypercytokinemia) before acute respiratory distress syndrome and death (***4***). A growing understanding of the pathophysiology accompanying acute inflammation can help devise novel therapeutics for inflammatory diseases (***5***). Of particular relevance is that severe inflammation is associated with significant alterations to redox balance (***6***), inducing oxidative stress to tissues and cells. Evidence accumulated over the past two decades has pointed to significant connections between inflammation and oxidative stress, both processes contributing to fuel one another, thereby establishing a vicious cycle able to perpetuate and propagate the inflammatory response (***7***, ***8***).

Inhibiting pathological inflammatory responses and the crosstalk between oxidative stress and inflammation presents various challenges (***9***). For instance, while potent anti-inflammatory agents—such as corticosteroids—already exist, these have fallen short in acute inflammatory conditions such as sepsis, because of their negative effects on tissue repair and the reported adrenocortical insufficiency common in patients with sepsis (***10***). Adenosine (Ad), an endogenous purine, and Ad receptor agonists have shown promise by promoting the resolution of inflammation (***11***, ***12***), but their systemic administration is associated with rapid clearance (***13***) and unacceptable medical side effects related to untargeted activation of their cognate receptors (***14***, ***15***). Another challenge consists in the fact that, during the evolution of systemic inflammatory insults, the initial response performed by the innate immune system is transferred from the plasma to tissues and cells where it results in disturbed signaling, cell dysfunction, and eventually organ failure. Therefore, efficient therapies against such processes need to be targeted to the inflammation sites. Similarly, antioxidant supplementation has been attempted (***16***–***18***) to scavenge reactive species during acute inflammation but remains limited by poor pharmacodynamics and tissue penetration (***19***). Recently, multidrug treatments of low-dose hydrocortisone with antioxidants have emerged as a promising approach for the mitigation of uncontrolled inflammation (***20***), simultaneously inhibiting pro-inflammatory cascades and scavenging reactive oxygen species (ROS). However, so far, most of the antioxidants used in this context perform their action predominantly in the plasma. While this is useful during the initial hyperinflammatory stages of the body response, it is ineffective at inhibiting the pathological redox cycles happening inside cells and tissues (***19***)—as plasma antioxidant levels poorly correlate with intracellular antioxidant levels (***21***).

To improve on these issues, and taking into account the potential of Ad and multidrug therapies for the resolution of inflammation, we propose here a novel prodrug-based nanoparticle (NP) formulation, ena-

bling the targeted delivery of Ad and tocopherol (VitE) to the sites of acute inflammation. Recently, conjugation of therapeutic molecules to squalene (SQ), an endogenous lipid, has been shown to enhance blood circulation time (***22***), provide interesting targeting properties (***23***) and lower toxicity (***24***). Here, we show that the bioconjugation of Ad to SQ and further nanoformulation with VitE led to the formation of stable multidrug NPs allowing (i) efficient encapsulation of both drugs, (ii) reduced side effects, and (iii) promising anti-inflammatory and protective effects in models of endotoxemia and lethal systemic shock. Furthermore, we also report evidence that these SQ-based NPs could target inflamed tissues in multiple murine models of inflammation for selective Ad receptor activation and antioxidant action. These functionalities together enabled a therapeutic intervention with significant potential for the antioxidant management of acute inflammatory diseases and improved the use of Ad as a pro-resolving pharmaceutical agent.

2. Materials and Methods

2.1. Preparation of SQ-based NPs

SQAd was synthesized as previously described (25), and the resulting NPs were prepared using the nanoprecipitation technique. Briefly, SQAd was dissolved in absolute ethanol (6 mg/ml) and added dropwise under strong stirring to a 5% (w/v) dextrose solution. Ethanol was then completely evaporated using a Rotavapor (90 rpm, 40°C, 42 mbar) to obtain an aqueous suspension of pure SQAd NPs (2 mg/ml). Multidrug SQAd/VitE NPs (50:50 wt %) were obtained by dissolving SQAd (3 mg/ml) and VitE (3 mg/ml) (α-tocopherol, Sigma-Aldrich) in absolute ethanol and adding the solution dropwise under strong stirring to a 5% dextrose solution with subsequent ethanol evaporation to obtain an aqueous suspension of SQAd/VitE NPs (2 mg/ml). Fluorescent NPs were obtained by the same procedure, except 1% (w/w) of fluorescent probe (SQRho) or DiD perchlorate (Thermo Fisher Scientific) was added to the ethanolic phase. All NP sizes (hydrodynamic diameter) and surface charges (zeta potential) were measured using a Malvern Zetasizer Nano ZS 6.12 (173° scattering angle, 25°C). For the size measurements by DLS, a good attenuator value (7–9) was obtained when suspending 20 µl of NPs in 1 ml of distilled water. The mean diameter for each preparation resulted from the average of three measurements of 60 s each. For zeta potential measurements, 70 µl of NPs was dissolved in 2 ml of 1 mM KCl before filling the measurement cell. The mean zeta potential for each preparation resulted from the average of three independent measurements in automatic mode, followed by application of the Smoluchowski equation. Morphology was observed by cryo-TEM. For this, drops of the NP suspensions (2 mg/ml) were deposited on electron microscopy grids covered with a holey carbon film (Quantifoil R2/2) previously treated with a plasma glow discharge. Observations were conducted at low temperature (−180°C) on a JEOL 2010 field emission gun microscope operated at 200 kV. Images were recorded with a Gatan camera.

2.2. Encapsulation efficiency experiment

SQAd/VitE NPs with different VitE content were formulated in 5% dextrose solution and subsequently washed with water twice using an ultrafiltration device (molecular weight cutoff, 100,000). NPs were dissolved in ethanol and measured by HPLC to determine VitE content. HPLC Waters Alliance 1695 (Waters, Milford, MA), equipped with a Waters DAD 2996 photodiode array detector, Hewlett-Packard computer with a Waters Empower 3 software, and a Waters autosampler with a 50-μl loop, was used, with simultaneous spectra detection wavelengths from 200 to 600 nm recorded for all peaks. A Waters XSelect LC-18 column (2.1 mm by 150 mm, 3.5 μm) was used with a nongradient mobile phase of acetonitrile and methanol (50:50, v/v) at a constant flow rate of 1 ml/min. The VitE peak was measured at a wavelength of 216 nm and quantitatively determined by comparing with a standard curve.

2.3. *In vitro* release of Ad from NPs in serum

Foetal bovine serum (3 ml) was prepared with 172 μl of EHNA (erythro-9-(2-hydroxy-3-nonyl)adenine) [Ad deaminase inhibitor (1 mg/ml), NaCl 0.9%; Sigma-Aldrich] and 4.8 μl of dipyridamole [Ad uptake inhibitor (30 mg/ml), dimethyl sulfoxide; Sigma-Aldrich]. SQAd/VitE NPs (180 μl; 2 mg/ml) were incubated at different time intervals with 180 μl of the foetal bovine serum solution in various Eppendorf vials, each for one time point. At the predetermined time intervals (i.e., 5 min, 30 min, 2 hours, 15 hours, 24 hours, and 48 hours), aliquots (100 μl) were collected and added into 500 μl of MeOH to denature and precipitate the enzymes and proteins of the serum, which were removed after centrifugation (16,000g for 10 min). To quantify the remaining SQAd bioconjugate and the released Ad, the remaining supernatants (150 μl) were evaporated to dryness at 40°C under nitrogen flow and then solubilized in 100 μl of MeOH. Quantification was performed using a reversed-phase HPLC on a Halo C18 column (4.6 mm by 250 mm, 5 μm; Interchim), a 1525 Binary LC Pump (Waters), a 2707 Autosampler (Waters), and a 2998 PDA detector (Waters). The HPLC was carried out using a gradient elution with the mobile phase composed of 80% 10 mM potassium phosphate in Milli-Q water (pH 4.0) 20% MeOH (phase A) and MeOH (phase B). Elution was carried out at a flow rate of 0.8 ml/min. The system was held at 100% of A for 8 min, followed by 1-min linear gradient from 100% A to 100% B, kept at 100% B for 12 min, and brought back to initial condition by a 1-min linear gradient from 100% B to 100% A. The sample run was maintained for 7 min with 100% A to equilibrate the column pressure. Temperature was set at 30°C, and ultraviolet detection was monitored at 260 nm for Ad and 272 nm for SQAd. The detection limit of the HPLC technique was 2 μg/ml for Ad and 10 μg/ml for SQAd. This method exhibited linearity (R^2 = 0.9988) over the assayed concentration ranges (2 to 200 μg/ml).

2.4. Intracellular ROS detection assay

H9c2 cells (50,000 cells per well) were seeded in a 12-well plate and cultured for 24 hours at 37°C. The cells were treated for 2 hours with SQAd/VitE NPs or controls diluted in culture medium at a concentration of 10 µg/ml for standard tests or according to the described dose for dose-response experiments. Cells were washed with PBS and incubated with medium containing hydrogen peroxide (H_2O_2; final concentration, 0.5 mM; Sigma-Aldrich). After 30 min, H_2O_2-containing medium was removed, and the cells were washed with PBS. Intracellular ROS production was detected using Abcam Cellular ROS Assay Kit (Deep Red) per manufacturer's instructions. Briefly, the ROS detection probe was diluted in PBS, and cells were incubated with this staining solution for 30 min. Staining solution was removed, and cells were washed with PBS and treated with 300 µl of 0.25% trypsin solution for 5 min at 37°C. The trypsin solution was inhibited by adding 0.7 ml of medium, and cell fluorescence was recorded using an Accuri flow cytometer C6 (Accuri Cytometers Ltd.). Necrotic cell death was assessed by propidium iodide staining at 10 µg/ml.

2.5. Nitric oxide assay

Nitrite (NO_2^-) release was assessed with freshly prepared Griess reagent. Briefly, in 96-well plates (20,000 cells per well), RAW 264.7 cells were treated for 2 hours with SQAd/VitE NPs or controls diluted in culture medium at a concentration of 10 µg/ml. LPS (Sigma-Aldrich O111:B4) was added at a final concentration of 1 µg/ml for 24 hours for macrophage stimulation. For co-treatment experiments, SQAd/VitE NP treatment was also performed concurrently to LPS stimulation. After LPS stimulation, the Griess reagent was added in equal volume to culture supernatants. The absorbance at 550 nm was measured on a PerkinElmer absorbance reader after 10 min of incubation in the dark at room temperature. The NO_2^- concentrations were determined using standard curves prepared from sodium nitrite ($NaNO_2$) at various concentrations.

2.6. *In vitro* evaluation of pro-inflammatory cytokine production

LPS stimulation and drug treatments were performed in the same way than with nitric oxide assays. After LPS stimulation for 24 hours, cell supernatants were retrieved and centrifuged for 5 min at 1000g to remove cell debris. Inflammatory cytokine production was evaluated using a BioLegend ELISA mouse TNF-α cytokine detection kit per manufacturer's instructions (BioLegend, USA). Supernatants were diluted 20× with Assay Diluent before detection experiment.

2.7. Animal care

Male C57BL/6J and female BALB/c mice were purchased from Janvier Labs (France) for systemic inflammation and NP tracking studies, respectively. Animals were housed in a standard controlled environment

(22° ± 1°C, 60% relative humidity, 12-hour light/dark cycles) with food and water available ad libitum. Experiments were approved by the Animal Care Committee of the University Paris-Sud, in accordance with the principles of laboratory animal care and European legislation 2010/63/EU. All efforts were made to reduce animal numbers and minimize their suffering, as defined in the specific agreement (registration no. APAFIS#16257).

2.8. NP tracking studies

For the paw inflammation study, experiments were performed on 18-week-old female BALB/c mice. Paw inflammation was caused by intraplantar injection in the right paw of 100 ng of LPS (Sigma-Aldrich O111:B4) dissolved at 5 mg/ml in physiological saline (NaCl, 0.9%). Animals received a control injection of 20 µl of saline in the left paw. *In vivo* imaging studies were performed after 2 hours, following intravenous injection of fluorescent SQAd/VitE or PLGA NPs (100 µl, 2 mg/ml, containing 1% DiD) or control fluorescent DiD solution (100 µl, 20 µg/ml in 5% dextrose solution). The biodistribution of the NPs was recorded at 0.5, 2, 4, and 24 hours with the IVIS Lumina LT Series III system (Caliper Life Sciences) using 640-nm excitation and 695-nm emission filters. During imaging, mice were kept on the imaging stage under anaesthesia with 2% isoflurane gas in oxygen flow (1 liter/min) and were imaged in ventral position. Images and measures of fluorescence signals were acquired and analysed with Living Imaging software (Caliper Life Sciences).

For the systemic inflammation study, experiments were performed on 12-week-old male C57BL/6J mice. Systemic inflammation was caused by intraperitoneal injection of LPS (Sigma-Aldrich O111:B4) at a dose of 7.5 mg/kg. Noninflamed control animals did not receive the LPS injection. After 2 hours, animals received intravenous injection of fluorescent SQAd/VitE NPs (100 µl, 2 mg/ml, containing 1% SQRho) or control fluorescent rhodamine B solution (100 µl, 20 µg/ml in 5% dextrose solution). After 24 hours, animals were deeply anesthetized with an intraperitoneal sodium pentobarbital injection before euthanasia by intracardial perfusion of 40 ml of saline (8 ml/min), until the fluid exiting the right atrium was entirely clear. The liver, heart, lungs, kidneys, and spleen were excised and immediately imaged with the IVIS imager using 560-nm excitation and 620-nm emission filters. Images and measures of fluorescence signals were acquired and analysed with Living Imaging software (Caliper Life Sciences).

2.9. *In vivo* efficacy

The therapeutic efficacy of SQAd/VitE NPs was evaluated *in vivo* in a mouse endotoxemia model with 8- to 12-week-old male C57BL/6J mice. To evaluate the efficacy through cytokine production, endotoxemia was induced by intraperitoneal injection of a dose of LPS (7.5 mg/kg; Sigma O111:B4) diluted at 1.875 mg/ml in buffered saline. Mice injected with LPS alone were used as controls. Thirty minutes after LPS

injection, SQAd/VitE NPs [SQAd (15 mg/kg), i.e., Ad (equivalent 5.5 mg/kg) and VitE (15 mg/kg)], SQAd NPs [SQAd (15 mg/kg) and Ad (equivalent 5.5 mg/kg)], or free Ad/VitE [Ad (5.5 mg/kg) and VitE (15 mg/kg) with 1% Pluronic F-123 vehicle for VitE solubilization] were intravenously injected via the suborbital vein. Following the injections, blood samples (~100 μl) were collected at predetermined time points via submandibular puncture before terminal cardiac puncture and organ collection. Plasma was obtained by centrifuging blood samples at 2000 rcf (relative centrifugal force) for 10 min and stored at −78°C before further analysis. In the plasma, cytokines, including IL-10 and TNF-α, were quantified by BioLegend ELISA mouse kit per manufacturer's instructions. Organ homogenates were obtained with a Heidolph Instruments (Germany) RZR-2021 organ homogenizer in PBS at a concentration of 500 mg/ml. Pro-inflammatory cytokines in organ homogenates were quantified using a cytometric bead array per manufacturer's instruction (BD Biosciences). For MDA content in the lungs, 10 mg of lung tissues was homogenized on ice in 300 μl of MDA lysis buffer containing 3 μl of BHT (butylated hydroxytoluene) antioxidant solution as per manufacturer's instruction (Biovision, Lipid Peroxidation MDA Fluorometric Assay Kit). To evaluate efficacy through survival in the lethal LPS model, mice were sensitized to the lethal effects of LPS with D-galactosamine hydrochloride (Roth, Germany) via intraperitoneal injection of an 8-mg dose concurrently to LPS injection at 2 μg/kg. After 30 min, NPs or free drugs as controls were injected intravenously. Signs of disease severity were evaluated at predetermined time points using a previously described disease scoring system (53). For histological evaluation, organs were fixed for 24 hours in 4% paraformaldehyde and then embedded in paraffin. Sections (5 μm) were deparaffinized and stained with H&E (VWR, France). Slides were scanned with a digital slide scanner NanoZoomer 2.0-RS (Hamamatsu, Japan), which allowed an overall view of the samples. Images were digitally captured from the scan slides using the NDP.view2 software (Hamamatsu).

2.10. Blood pressure measurements

For blood pressure measurements, a Kent Scientific (Torrington, USA) Coda tail-cuff VPR blood pressure measurement system was used. C57BL/6J mice were acclimated to the procedure for 2 days before measurements to avoid undue stress and experimental artifact. For all measurements, an experimental session of 10 acclimation cycles and 10 measurement cycles was used. Only measurement cycles that passed Coda software acceptance criteria were retained. For animals that received free drug Ad/VitE or SQAd/VitE (30 mg/kg or equivalent), the blood pressure measurement was started immediately after intravenous injection.

2.11. Statistics

Statistics were computed with GraphPad Prism 6. Differences in group means were calculated by one-way analysis of variance (ANOVA) followed by Holm-Sidak's multiple comparison test or Kruskal-Wallis test

(nonparametric) followed by Dunn's multiple comparison test when samples failed equality of variance or normality statistical tests (Shapiro-Wilk). A value of $P < 0.05$ was considered significant. For studies requiring grouped analyses, a two-way ANOVA followed by Tukey's multiple comparison test was performed.

3. Results and Discussion

3.1 Preparation and characterization SQAd/VitE NPs

The preparation of squalene-Ad (SQAd)/VitE NPs first required conjugation of Ad to squalenic acid as previously described (25). This conjugation step was performed with moderate yield (45%) and afforded SQAd, which could then be used as a prodrug-based nanocarrier for VitE (Fig. 1A). The second step in the preparation of multidrug SQ-based NPs consisted in encapsulating VitE in SQAd NPs, which was performed by a nanoprecipitation technique. Following nanoprecipitation and solvent removal, the VitE content of the NPs was evaluated. For SQAd/VitE nanoformulations containing 50 weight % (wt %) VitE or less, most of the VitE present in the precursor organic solution was found to be incorporated in the NPs (Fig. 1B). For the rest of this study, we used the SQAd/VitE NP formulation, which afforded the highest total drug loading with proper colloidal stability, i.e., SQAd/VitE (50:50) wt %. The total drug loading of the multidrug NPs was therefore 68.6 wt %: 50 wt % VitE and 18.6 wt % Ad. When measured by dynamic light scattering (DLS), the multidrug SQAd/VitE NPs displayed a uniform size distribution with a mean hydrodynamic diameter of 71.2 ± 3 nm and a polydispersity index inferior to 0.2 (Fig. 1C). Surface zeta potential was measured to be −14.29 ± 1.01 (SEM) mV, similar to SQAd NP only (−15.45 ± 1.52 mV), ensuring proper colloidal stability (Fig. 1D). The obtained multidrug NPs were also observed by cryogenic transmission electron microscopy (cryo-TEM) imaging, revealing uniform NPs (Fig. 1E). Following their formulation, SQAd/VitE NPs were suspended in 50% serum and showed satisfactory colloidal stability over 5 days (Fig. 1F). To evaluate drug release, we measured the amount of free Ad and VitE released from the formulation over time by high-performance liquid chromatography (HPLC).

The incubation of SQAd/VitE NPs in serum resulted in a slow, progressive decrease in detected SQAd bioconjugate, which correlated with a release of free Ad (Fig 1G). After 48 hours of incubation, about 6% of the initial Ad was found to have been released from SQAd/VitE NPs, while no VitE release could be detected (see Supplementary Discussion).

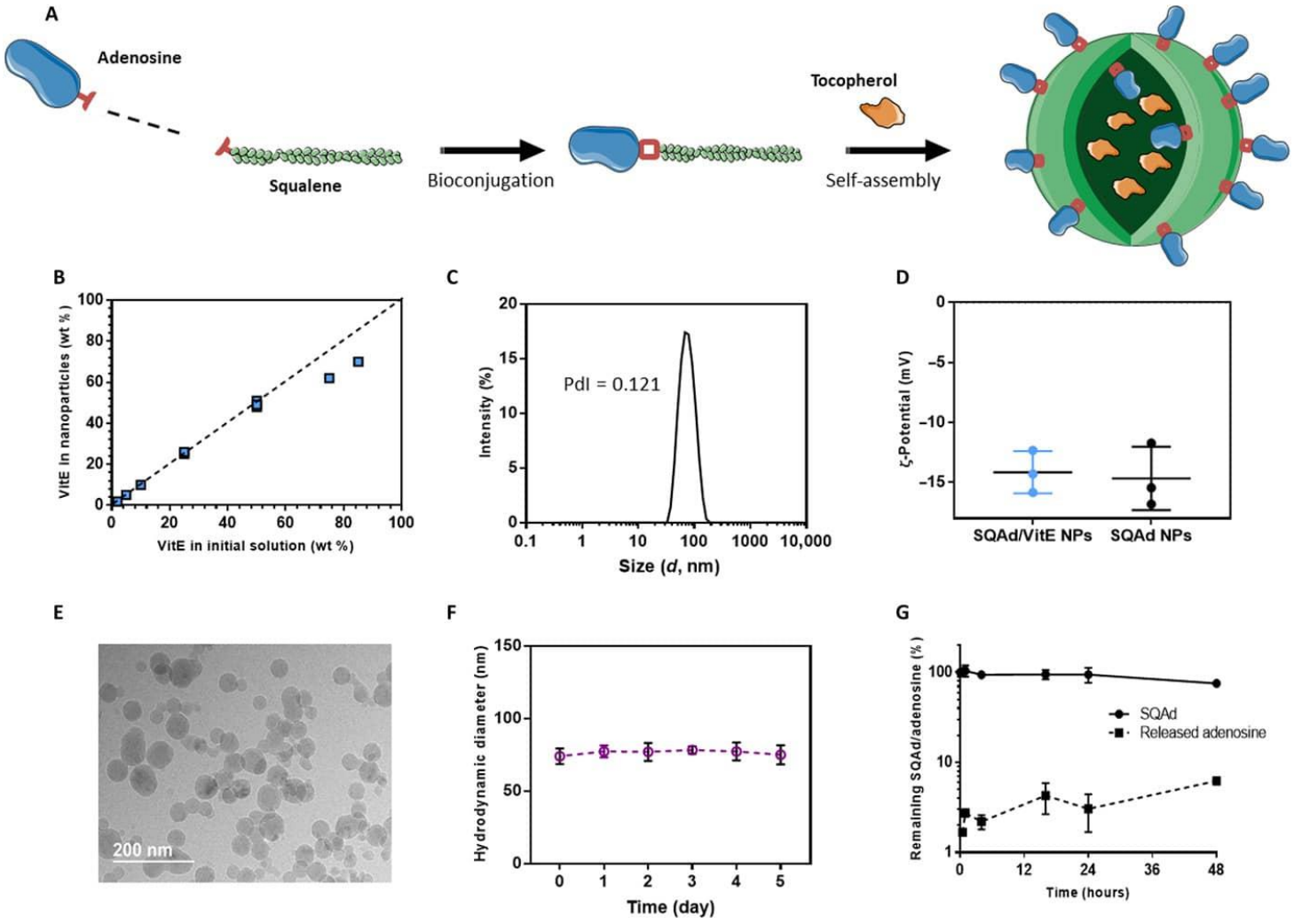

Figure 1: Formulation and characterization of multidrug SQAd/VitE NPs.

(**A**) Schematic representation of SQAd bioconjugation and VitE encapsulation to afford SQAd/VitE NPs. (**B**) VitE encapsulation efficiency in SQAd/VitE NPs as measured by high-performance liquid chromatography (HPLC). wt %, weight %. (**C**) Hydrodynamic size of SQAd/VitE NPs (diameter, nanometers) measured by DLS. Pdi, polydispersity index. (**D**) Measurement of surface ζ-potential of SQAd/VitE and SQAd NPs. (**E**) cryo-TEM images of SQAd/VitE NPs (scale bar, 200 nm). (**F**) Stability of SQAd/VitE NPs in 50% fetal bovine serum (FBS) over 5 days as measured by DLS. (**G**) Release of Ad from SQAd/VitE NPs in 50% FBS.

SQ is an endogenous precursor of cholesterol, which forms stable colloidal phases in water (26). VitE is insoluble in water and usually colocalizes with cholesterol in low-density lipoproteins (LDLs) *in vivo* (27). Accordingly, our results showed that VitE was efficiently encapsulated in SQAd NPs to form stable multidrug NPs. Overall, the preparation of SQAd/VitE NPs is very straightforward because it simply requires an ethanolic solution of SQAd and VitE to be added in water medium before ethanol evaporation. The total synthesis also did not require any excipients, which makes the scaling-up affordable as shown

previously with the ability of SQAd bioconjugates to be produced as an industrial sample (24). Noteworthy, this may represent an asset over the current trend of developing ever more sophisticated nanomedicines, whose physicochemical complexity represents an important factor to slow the speed and even the feasibility of nanomedicine translation into the clinic.

3.2. NP tracking studies

To investigate whether SQ NPs could improve the bioavailability of the encapsulated therapeutic agents and direct them to the inflammation foci, we evaluated the *in vivo* biodistribution of SQAd/VitE NPs in two different models, one of local acute inflammation and one of systemic inflammation. First, the *in vivo* circulation of SQAd/VitE NPs was followed after intravenous injection of fluorescent DiD (1,1-dioctadecyl-3,3,3,3-tetramethylindodicarbocyanine, 4-chlorobenzenesulfonate salt)–labeled SQAd/VitE NPs in a murine lipopolysaccharide (LPS)–induced paw inflammation model. Animals received 100 ng of LPS in their right paw and a control saline injection in the left paw. The fluorescence in tissues was monitored noninvasively up to 24 hours, from the abdomen side using an *In Vivo* Imaging System (IVIS) Lumina. The real-time *in vivo* imaging showed that, in comparison with the control healthy left paw, a strong increase in the radiant efficiency of the inflamed right paw could be detected after intravenous injection of fluorescent SQAd/VitE NPs (Fig. 2, A to E). In a control experiment, when the mice received a free DiD solution, no significant accumulation of fluorescence was observed in the inflamed paw (Fig. 2B) (see Supplementary Discussion). The relative fluorescence signals detected in the right (inflamed) paw versus left (noninflamed) paw of the studied animals can be found in fig. S4. In another control experiment, comparing the observed accumulation of SQ NPs with that of PLGA [poly(lactic-co-glycolic) acid] NPs, it was observed that the accumulation of SQAd/VitE NPs occurred faster, providing higher accumulation into the inflamed paw in comparison to PLGA NPs (fig. S3). A detailed discussion about this observation is provided in Supplementary Discussion.

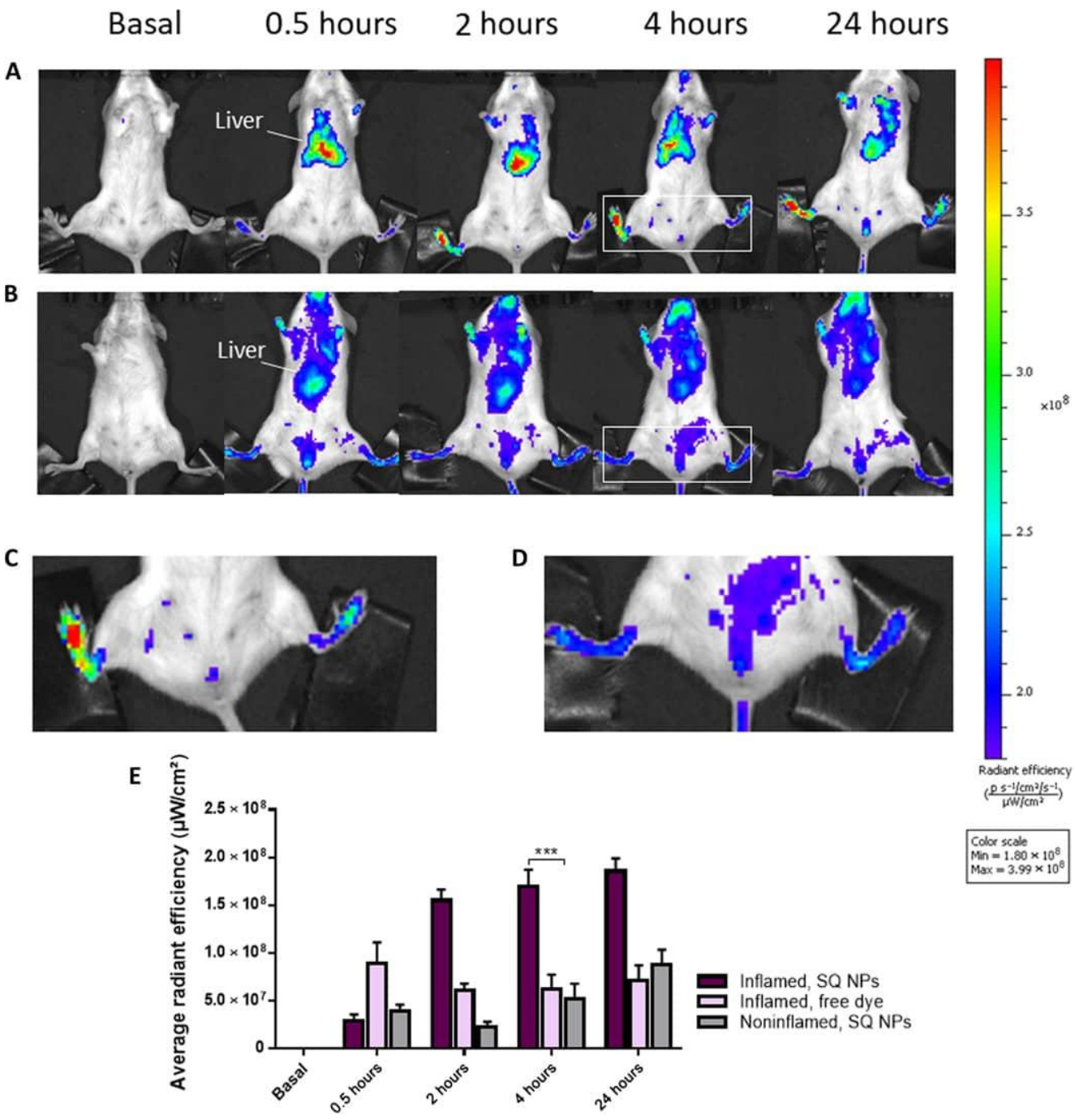

Figure 2: IVIS Lumina scan of mice after intravenous administration of fluorescent SQAd/VitE NPs or control fluorescent dye solution (ventral view).

(**A**) Tracking of fluorescent SQAd/VitE NPs in mice with inflamed right hind paw and noninflamed left hind paw. (**B**) Tracking of the free dye in mice with inflamed right hind paw. (**C**) Zoomed-in view of group A at 4 hours. (**D**) Zoomed-in view of group B at 4 hours. (**E**) Analysis of the measured total radiant efficiency in the region of interest. n = 3 mice per group. Data are mean ± SD. *P < 0.05, **P < 0.01, and ***P < 0.001 [two-way analysis of variance (ANOVA) followed by Tukey's multiple comparison test]

In a second study, we evaluated the ability of SQAd/VitE NPs to accumulate in organs in a model of LPS-induced sepsis. Loss of endothelial integrity is one of the hallmarks of sepsis, and LPS injection has been shown to induce capillary leakage in a β1-integrin–dependent mechanism (28). Here, rhodamine B covalently linked to SQ (SQRho; figs. S1 and S2) was used as a fluorescent marker for SQAd/VitE NPs. Animals received LPS intraperitoneally and, after 2 hours, an intravenous injection of fluorescent SQAd/VitE NPs. After 24 hours, the mice were deeply anesthetized and intracardially perfused with 40 ml of phosphate-buffered saline (PBS) to remove blood. The fluorescence signal in the different organs was measured using an IVIS Lumina. Mice that did not receive an LPS challenge were used as noninflamed controls. The fluorescent imaging showed that, in comparison with healthy mice, LPS-inflamed animals had a significant increase in the levels of total radiant efficiency in the lungs, liver, and kidneys (Fig. 3). In a control experiment, when LPS-treated mice were intravenously injected with a free rhodamine probe solution, no significant accumulation occurred in the studied organs except the kidney, most probably because of the renal clearance of rhodamine.

During inflammation, neutrophils interact with the vascular endothelium leading to barrier dysfunction and increased permeability. This constitutes a unique opportunity for nanomedicines to accumulate at the sites of organ injury and selectively deliver therapeutic agents through enhanced permeation and retention effects (29). In the present *in vivo* studies, SQAd/VitE NPs were found to accumulate at the sites of acute inflammation and endothelial dysfunction in models of both local and systemic inflammation. When injected *in vivo*, free Ad is readily catabolized into inosine and hypoxanthine, resulting in an extremely short blood half-life of 10 s (13). This requires Ad to be administered continuously and in high doses to achieve a pharmacological response, resulting in side effects related to the unchecked activation of the ubiquitous Ad receptors. The targeted accumulation achieved by SQAd/VitE NPs could therefore potentially limit the side effects induced by Ad treatment and enhance the bioavailability of both drugs at the sites of inflammation for improved therapeutic action.

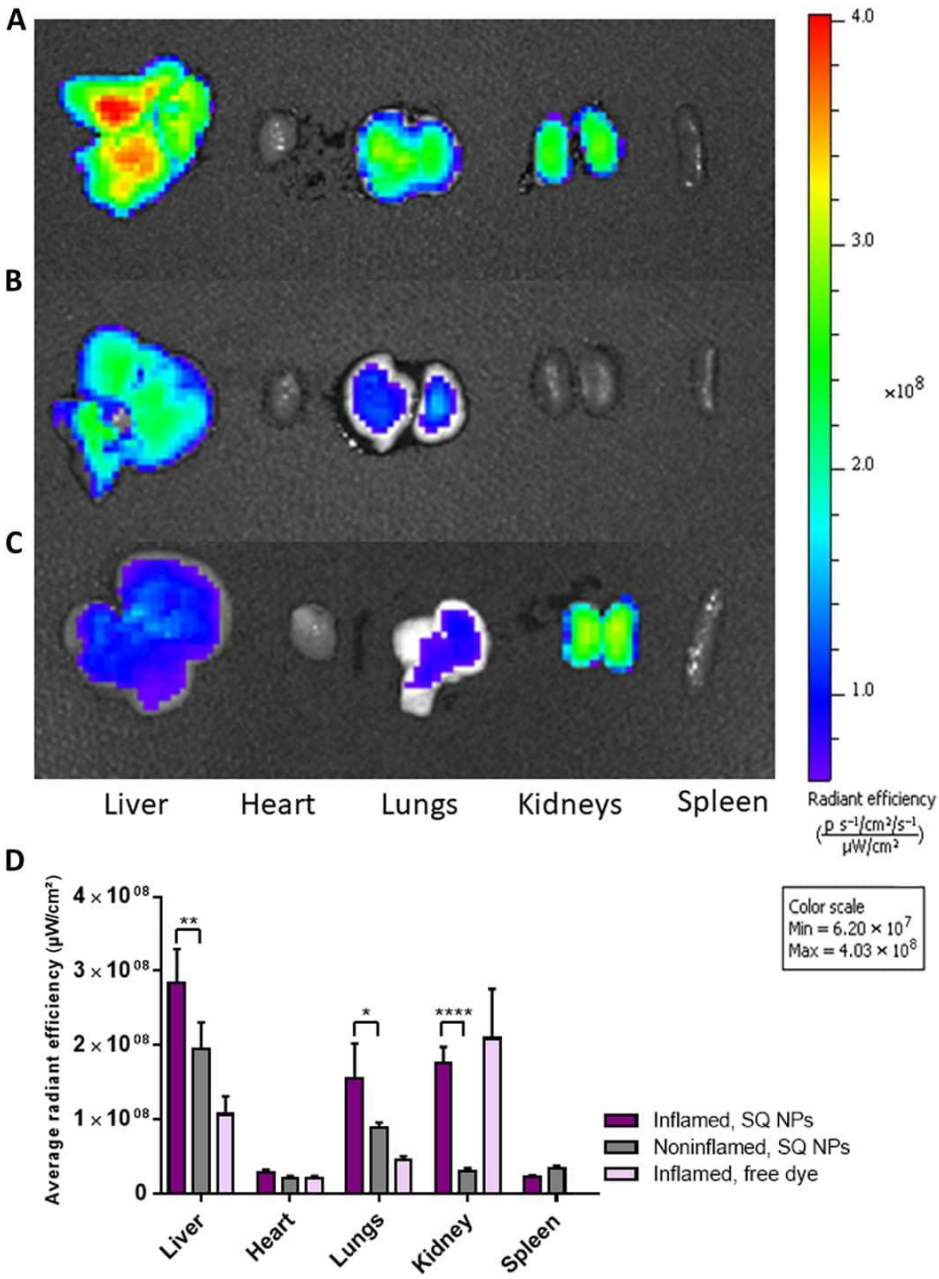

Figure 3: Ex vivo IVIS Lumina scan of mice organs after intravenous administration of fluorescent SQAd/VitE NPs in a septic shock model.

Organs displayed from left to right: liver, heart, lungs, kidneys, and spleen. (**A**) Tracking of fluorescent SQAd/VitE NPs labeled in mice that received a LPS challenge. (**B**) Tracking of fluorescent SQAd/VitE NPs in noninflamed mice (did not receive LPS challenge). (**C**) Tracking of free dye in mice that received a LPS challenge. (**D**) Analysis of the measured total radiant efficiency in the different organs. n = 3 mice per group. Data are mean ± SD. *P < 0.05, **P < 0.01, and ****P < 0.0001 (two-way ANOVA followed by Tukey's multiple comparison test).

3.3. *In vitro* evaluation

To investigate whether SQAd/VitE NPs could effectively enact protection against oxidative stress, we first developed an *in vitro* model of oxidative insult. In inflamed tissue, immune cells produce ROS such as hydrogen peroxide (H2O2) that can cross the cellular membrane and produce intracellular oxidative stress

(30) to tissue cells. When H9c2 murine cardiac cells were incubated with H2O2 for 30 min, a strong increase in intracellular ROS was detected by flow cytometry using a ROS-sensitive fluorescent probe. Treatment with SQAd/VitE NPs was efficient at limiting intracellular ROS production in a dose-dependent manner (Fig. 4, A and B). While SQAd NP and SQ NP controls did not provide this protection, free drug Ad/VitE in the medium did induce some protection against the oxidative insult, most probably because of the antioxidant action of VitE. This effect was less pronounced than with SQAd/VitE NPs. The reduction in intracellular ROS correlated positively with improved cell survival to the oxidative insult as measured by propidium iodide straining. In SQAd/VitE NP–treated samples, only 20% of cells were found to be necrotic, while nontreated cell populations contained 80% of necrotic cells (Fig. 4, C and D). SQAd/VitE NPs were found to be readily taken up by cells (fig. S5), likely through LDL receptor–mediated mechanisms as shown previously with SQAd-only NPs (31). Thus, after accumulating at the sites of inflammation, SQAd/VitE NPs are most likely able to enter cells, where they can deliver their therapeutic cargo intracellularly. As it has been suggested (19, 32), and as demonstrated here, the intracellular delivery of the antioxidant VitE improved its capacity to diminish oxidative stress. This cellular uptake also likely allows SQAd/VitE NPs to generate the active Ad in a localized manner after hydrolysis of SQAd (33). It was previously observed that after LDL receptor–dependent internalization, the SQAd NPs located in endo-lysosomal compartments where they acted as intracellular reservoirs for the encapsulated Ad. Once the hydrolysis of the amide bond released Ad, equilibrative nucleoside transporters (ENTs) discharged the drug Ad outside of the cell where it interacted with Ad receptors (32).

We next evaluated the ability of SQAd/VitE NPs to efficiently inhibit pro-inflammatory signalling. For this, RAW 264.7 macrophages were used in an *in vitro* LPS-induced inflammation model. RAW macrophages respond to LPS stimulation by releasing pro-inflammatory cytokines (34). Accordingly, when RAW macrophages were stimulated with LPS (1 μg/ml), a significant increase in tumor necrosis factor–α (TNF-α) cytokine was measured in the supernatant. This pro-inflammatory response was inhibited by treatment with SQAd/VitE NPs at a concentration of 10 μg/ml for 2 hours. Here, SQAd and SQAd/VitE NPs had similar effects on the release of inflammatory cytokines, indicating that Ad could be the main effector of the observed anti-inflammatory effect (Fig. 4E). When SQAd/VitE treatment was performed simultaneously to the LPS challenge, no significant inhibition of pro-inflammatory signalling was observed, contrary to free drug Ad/VitE. This substantiated the idea that SQAd is not active as an anti-inflammatory agent but needs to be activated in situ to perform anti-inflammatory activity (33).

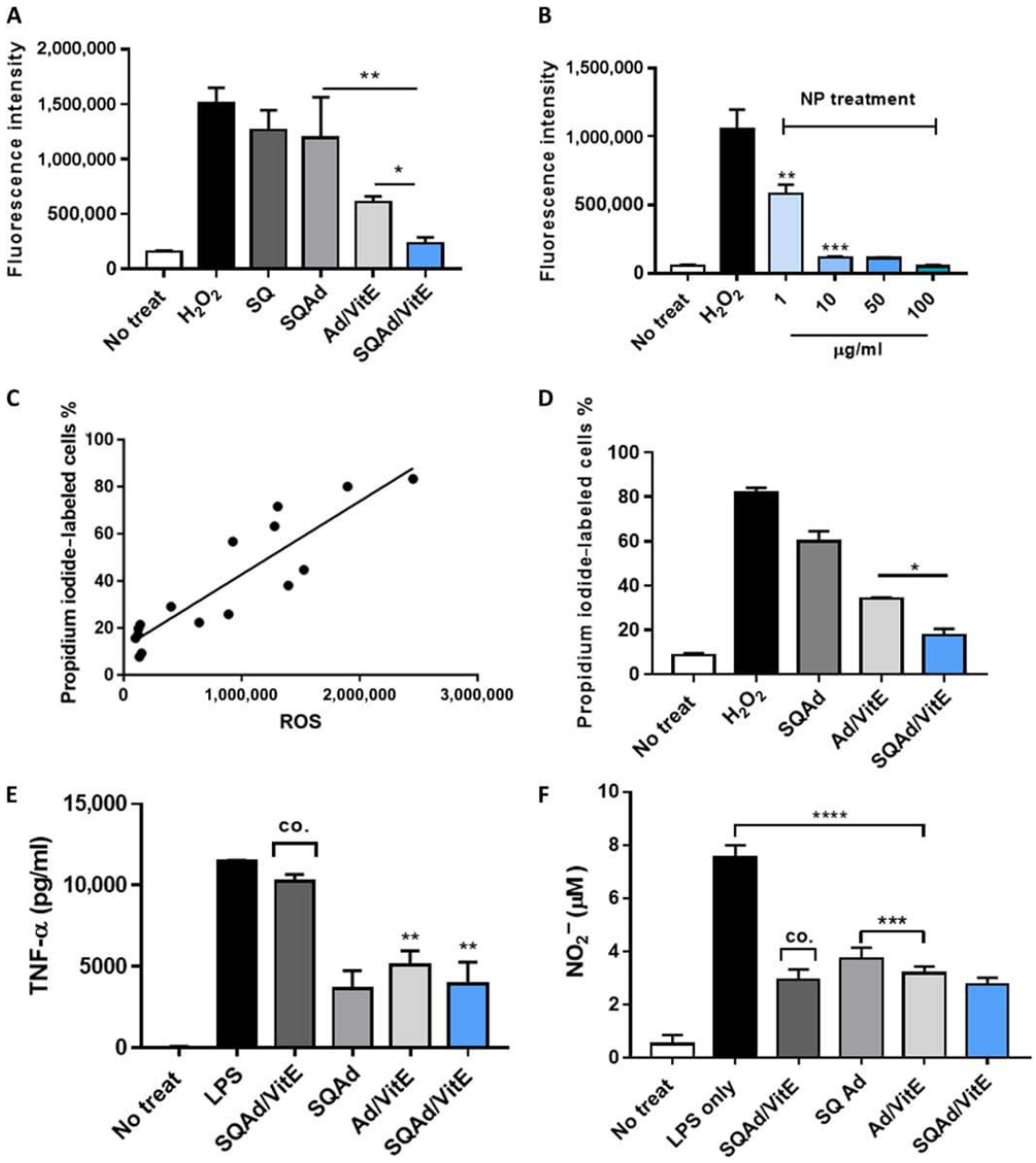

Figure 4: *In vitro* antioxidant and anti-inflammatory properties of SQAd/VitE NPs.

(**A**) Fluorescent detection of ROS in H9c2 cells showing that SQAd/VitE NPs efficiently scavenge intracellular ROS compared to free-drug or single-drug controls. (**B**) Dose dependence of the ROS protective effect of SQAd/VitE NPs on H9c2 cells. (**C**) Correlation of necrotic cell death with the amount of detected intracellular ROS. (**D**) Evaluation of necrotic cell death by propidium iodide staining. (**E**) Quantification of pro-inflammatory cytokine TNF-α production in LPS-stimulated RAW 264.7 cells treated with SQAd/VitE NPs or controls. co. SQAd/VitE NP treatment concurrently to LPS challenge. (**F**) Evaluation of nitrite content in cell medium following LPS stimulation of RAW 264.7 macrophages with or without SQAd/VitE NP treatment and controls. Data are the mean ± SD. n = 3 independent experiments. *P < 0.05, **P < 0.01, ***P < 0.001, and ****P < 0.0001 (one-way ANOVA followed by Holm-Sidak's multiple comparison test).

LPS stimulation of macrophages also causes overproduction of nitric oxide by inducible nitric oxide synthase (iNOS) (35), which results in further pro-inflammatory signalling and oxidative stress by reactive nitrogen species (NOx) (36). Thus, RAW 264.7 macrophages were stimulated with LPS, and nitrite accumulation was monitored by Griess reagent to evaluate the consequence of SQAd/VitE NP treatment

on NOx formation. Stimulation by LPS (1 μg/ml) resulted in 7.5 μM nitrite content in the supernatant, but NOx production was significantly inhibited after incubation of SQAd/VitE NPs at 10 μg/ml (Fig. 4F). Free drugs Ad/VitE controls also showed efficient inhibition of nitrite accumulation, which likely resulted from free Ad, acting on its cognate receptors A2A and A2B, inhibiting iNOS expression (37, 38). Here, there was no difference in the SQAd/VitE groups between pre-treated cells or cells simultaneously treated with NPs at the time of LPS challenge (see also Supplementary Discussion). Noteworthy, nitrite production was significantly lower in SQAd/VitE NP–treated cells compared to cells that only received SQAd. This showed that increasing drug loading through the use of prodrug-based nanocarriers might be advantageous for inflammation therapy.

Overall, these results showed that multidrug SQAd/VitE NPs could effectively scavenge ROS in a concentration-dependent manner and established effective pro-resolving action through the combined effects of SQAd and VitE *in vitro*. By using a prodrug-based nanoformulation, SQAd/VitE NPs did not trigger Ad signalling until Ad release, which could limit deleterious side effects associated with Ad therapy.

3.4. *In vivo* efficacy of SQAd/VitE NPs in endotoxemia model

We then proceeded to evaluate the *in vivo* ability of SQAd/VitE NPs to promote the resolution of inflammation in mice by examining their effect on the acute inflammatory response to endotoxin. In the blood, recognition of LPS by circulating macrophages activates the redox-controlled nuclear factor κB (NF-κB) by Toll-like receptor 4 (TLR4)–mediated mechanisms. This event potentiates downstream inflammation cascades, resulting in the pathological "cytokine storm." In our experiments, LPS was injected in mice intraperitoneally, after which blood and organs were collected at various time points to measure the levels of pro-inflammatory and anti-inflammatory cytokines by enzyme-linked immunosorbent assay (ELISA). In the blood, pro-inflammatory cytokine levels reached a maximum 1 hour after the LPS challenge, while anti-inflammatory cytokines followed with a peak 2 hours after LPS injection (fig. S6). In the treatment group where SQAd/VitE NPs were injected at a dose of 30 mg/kg [corresponding to Ad (5.5 mg/kg) and VitE (15 mg/kg)], a significant decrease in TNF-α together with an increase in anti-inflammatory interleukin-10 (IL-10) could be observed, comparatively to control groups that received either no treatment, free drugs Ad/VitE, SQAd NPs, or SQVitE NPs only at equivalent doses (Fig. 5, A and B). This effect took place in a dose-dependent manner (fig. S7). Free drug Ad and VitE have limited

bioavailability due to extremely fast metabolization and poor cell localization, respectively. These initial *in vivo* results pointed to an improved pharmacological profile of these compounds, thanks to their formulation as NPs and protection from early degradation. Next, we evaluated in organ homogenates the levels of two key pro-inflammatory cytokines MCP-1 (monocyte chemoattractant protein-1) and IL-6, responsible, respectively, for recruiting immune cells to the sites of inflammation and mediating the acute-phase response (39). In the lungs and kidneys, 4 hours after the initial LPS challenge, treatment with SQAd/VitE NPs at 30 mg/kg significantly reduced the amount of MCP-1 and IL-6 compared to nontreated or free drug–treated controls (Fig. 5C). In the liver, results failed to reach significance, but a tendency for mitigated acute inflammation could be observed.

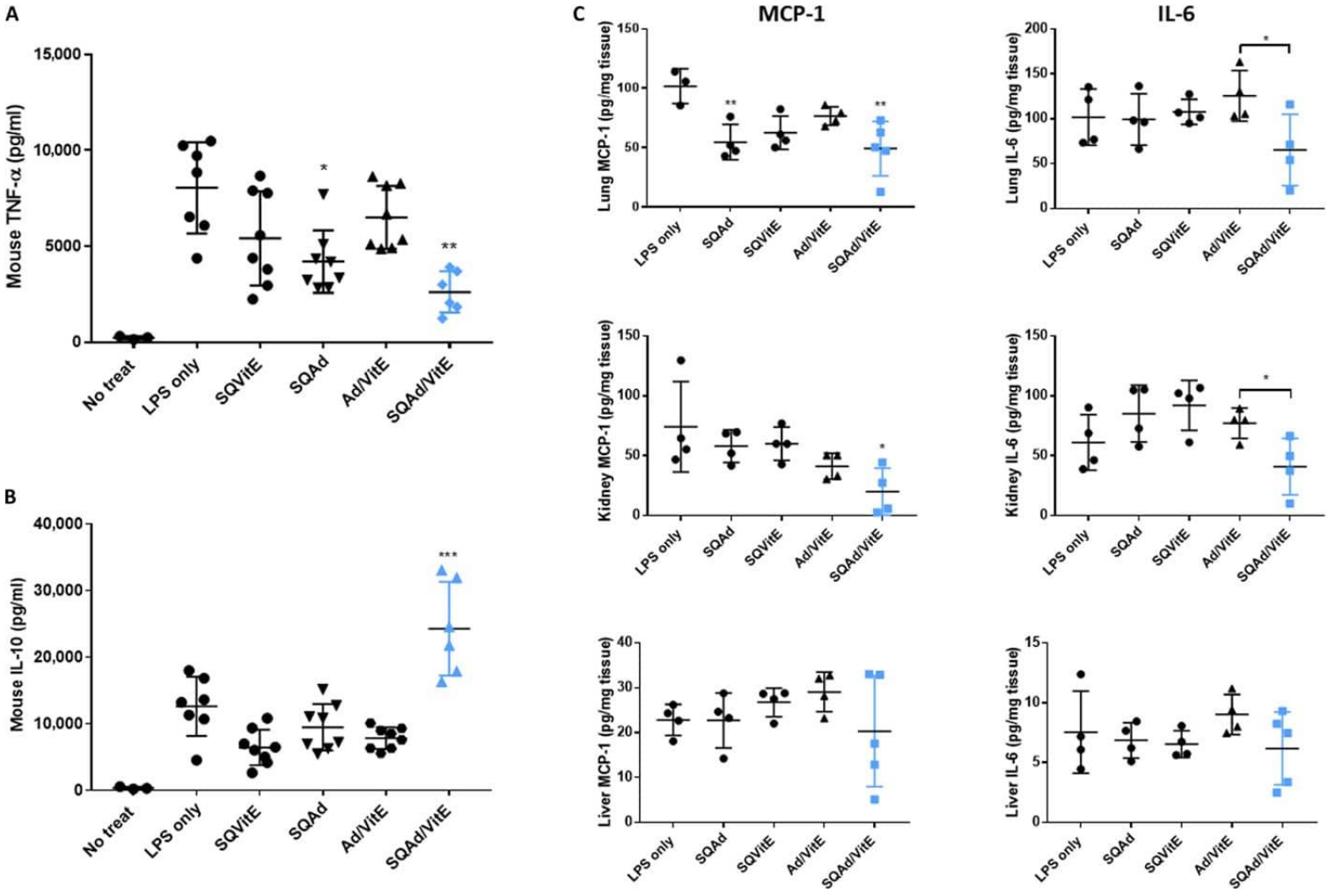

Figure 5: *In vivo* influence of SQAd/VitE NPs on inflammatory cytokines.

(**A**) Mouse TNF-α in plasma 1 hour after LPS challenge as measured by ELISA. (**B**) Mouse IL-10 in plasma 1 hour after LPS challenge as measured by ELISA. (**C**) Pro-inflammatory cytokines including MCP-1 and IL-6 from the lungs, liver, and kidneys, 4 hours after LPS challenge as measured by cytometric bead array. Nontreated controls did not reach detection threshold and were not shown. n = 4 to 8 mice per group. Data are mean ± SD. ns, not significant; *P < 0.05, **P < 0.01, and ***P < 0.001 significance to LPS only control unless specified (one-way ANOVA followed by Holm-Sidak's multiple comparison test).

We next evaluated the antioxidant effects of SQAd/VitE NPs *in vivo* by measuring the amount of lipid peroxidation products in the lungs following the LPS challenge. During acute systemic inflammation, the immune cells recruited by the extensive pulmonary capillary bed induce high levels of oxidative stress in the lungs, resulting in substantial lipid peroxidation (40). LPS challenge resulted in an increase in lipid peroxidation products as measured by reaction of malondialdehyde (MDA) with thiobarbituric acid reactive substance (TBARS test) (5.5 nmol of MDA/mg protein versus 2.75 nmol of MDA/mg protein). Basal MDA levels in mice typically range around 2 nmol of MDA/mg protein (41−43). Although it could not be abrogated, the increase in MDA was most strongly mitigated in the SQAd/VitE NP treatment group, where MDA levels reached only 4.04 nmol of MDA/mg protein (Fig. 6A).

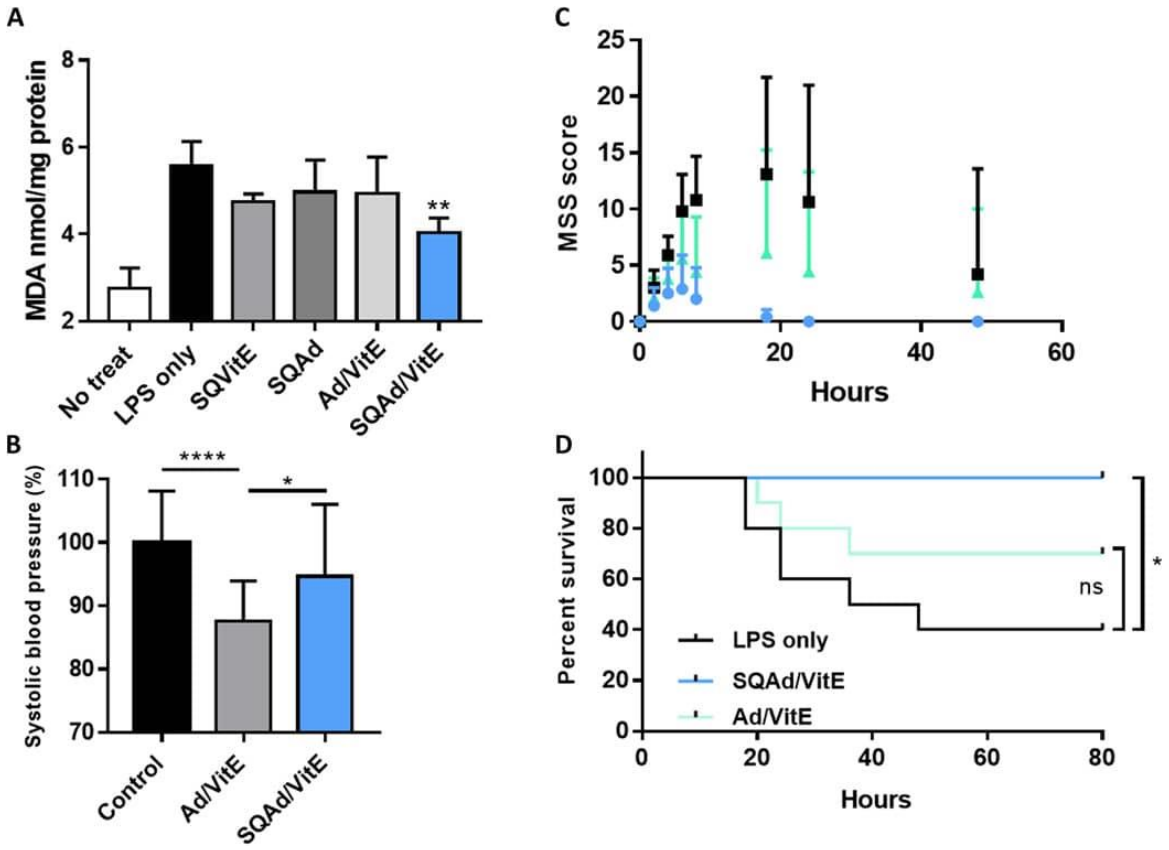

Figure 6: *In vivo* therapeutic efficacy of SQAd/VitE NPs in endotoxemia models.

(**A**) Level of lipid peroxidation in the lungs as measured by TBARS quantification of MDA. n = 3 mice per group. (**B**) Systolic blood pressure determination as % of control in healthy animals following SQAd/VitE or Ad/VitE treatment. n = 3 animals per group, five measurements per animal. (**C**) MSS (murine sepsis score) clinical score of animals undergoing LPS endotoxemic shock. n = 10 mice per group. (**D**) Survival followed after lethal LPS injection for 80 hours. n = 10 mice per group. Data are the mean ± SD. *P < 0.05, **P < 0.01, and ***P < 0.001 significant difference to LPS only control unless specified (one-way ANOVA followed by Holm-Sidak's multiple comparison test). For survival evaluation, a log-rank (Mantel-Cox) test was used, giving a P = 0.0130.

Together, these *in vivo* studies demonstrated an efficient and targeted resolution of inflammation by multidrug SQAd/VitE NPs. While single-drug NPs did display some efficacy at inhibiting plasma TNF-α, they did not reach the therapeutic efficacy of SQAd/VitE NPs. Contrary to what was observed in *in vitro* studies, *in vivo* free drug Ad/VitE controls consistently failed to induce a significant therapeutic response. This could be explained by the quick metabolization of Ad after a bolus injection (44) and poor bioavailability of VitE. Our prodrug-based NPs thus increased the efficacy of both drugs by simultaneously delivering them to the sites of inflammation.

3.5. Side effects on healthy animals and efficacy in lethal LPS model

To further validate the *in vivo* capability of SQAd/VitE NPs, we then investigated the hemodynamic effects of SQAd/VitE NPs comparatively to free drugs Ad/VitE. The effects of a single injection of SQAd/VitE NPs on blood pressure were measured noninvasively on healthy mice. While the NP-encapsulated drugs had no significant effect on blood pressure compared to nontreated controls, free drugs Ad/VitE induced a measurable decrease in blood pressure due to Ad, in accordance with published literature (Fig. 6B) (45). These results confirmed that the SQAd/VitE NP formulation helped to protect animals from the deleterious side effects induced by Ad therapy.

We therefore proceeded to evaluate the efficacy of SQAd/VitE NPs in a model of lethal LPS challenge (46). Mice in the treatment groups received either SQAd/VitE NPs at a dose of 30 mg/kg or free drugs Ad/VitE at an equivalent dose. In the group treated with SQAd/VitE NPs, all mice survived the lethal LPS challenge, whereas free drug Ad/VitE failed to significantly improve the survival rate, compared to the untreated control animals (Fig. 6D). Improvements in the clinical scores of the animals paralleled the improvements in survival rates for all groups (Fig. 6C). Last, the consequence of the treatment with SQAd/VitE NPs was histologically investigated regarding signs of inflammation. In the previous LPS lethality model, organs from either SQAd/VitE NP–treated mice or LPS only–treated controls were harvested at the 24-hour point and analysed for histological signs of tissue stress following haematoxylin and eosin (H&E) staining. Inflammatory changes including mononuclear cell infiltration, endothelial disruption, and haemorrhage were noticeably reduced in animals that received SQAd/VitE NP treatment. In the liver, nontreated animals displayed severe injuries, which were not observed in SQAd/VitE NP–treated animals (figs. S8 and S9); these included haemorrhagic sinusal occlusion, advanced hepatocellular stress, and disseminated steatosis. In the lungs, although both animal groups showed signs of inflammatory stress, the nontreated animals displayed more advanced loss of structure, alveolar thickening, and haemorrhage (fig. S9).

As is the case with many animal models, lethal endotoxemia sepsis models, although widely used to study anti-inflammatory therapies (47−49), have inherent drawbacks. The main limitation of this model is the speed at which it induces a severe inflammatory insult. Numerous studies have investigated therapeutic compounds in the context of sepsis by pre-treating animals before LPS injection (50, 51). Other studies investigated treatment at the time of LPS injection (52). In clinical practice, patients with sepsis usually receive treatment after the onset of the pro-inflammatory insult but before the insult reaches "peak severity". In this endotoxemia model, we found that pro-inflammatory cytokines such as TNF-α reached a maximum about 1 hour after LPS injection (see fig. S6). As a result, we decided to inject our treatments at the 30-min time point, halfway between the onset and the peak of the inflammatory response, which is probably the best time point to fit with the clinical conditions.

4. Conclusion

We presented here the first example of targeted delivery of Ad, and of multidrug anti-inflammatory/antioxidant NPs, for the mitigation of inflammation. Bioconjugation of Ad to SQ allowed to obtain a prodrug-based nanocarrier, which, after nanoformulation with VitE, yielded stable multidrug NPs, improving the bioavailability of both drugs with significant pharmaceutical activity in models of acute inflammatory injury. With the ability to specifically target and deliver Ad at tissue foci of acute inflammation and the capacity to react with intracellular reactive species at the target site, SQAd/VitE NPs represent a promising therapeutic intervention overcoming limitations of both conventional Ad and antioxidant therapy. Our extensive *in vivo* data support this hypothesis that opens the way to explore the plethora of available specific Ad receptor agonists and antioxidants. Additional efforts will also allow to further characterize SQ-based NP biodistribution. Overall, these SQ-based multidrug NPs represent a unique approach for inhibiting the pathological cross-talk between oxidative stress and inflammation, delivering therapeutic agents at the loci of inflammation, and thus afford a new tool in the fight against the complex and multifactorial phenomenon of uncontrolled inflammation.

Acknowledgments

We wish to thank P. Van Tassel for helpful corrections to the manuscript and F. Gobeaux of UMR 3685 for help with cryo-TEM imaging.

Funding

The authors gratefully acknowledge the financial support from the 7th EuroNanoMed-II call for proposals, project NanoHeart no. ANR-16-ENM2-0005-01. This work was further supported by la Fondation pour la Recherche Médicale (FRM) grant no. ECO20160736101.

Author contributions

F.D., M.V., P.C., designed the research. F.D., R.B., C.C., F.R., A.P., A.G., F.G., M.V. conducted experiments. F.D., F.R., F.G., M.V., P.C. analysed the data. F.D. wrote the paper, and all authors reviewed the manuscript. Competing interests: The authors declare that they have no competing interests.

Data and materials availability

All data needed to evaluate the conclusions in the paper are present in the paper and/or the Supplementary Materials. Additional data related to this paper may be requested from the authors.

References

1. H. Gomez, C. Ince, D. De Backer, P. Pickkers, et al., A unified theory of sepsis-induced acute kidney injury: inflammation, microcirculatory dysfunction, bioenergetics and the tubular cell adaptation to injury. Shock (Augusta, Ga.). 41, 3 (2014)
2. F. Dormont, M. Varna,P. Couvreur, Nanoplumbers: biomaterials to fight cardiovascular diseases. Materials Today. 21, 122-143 (2018)
3. R. B. Goodman, J. Pugin, J. S. Lee,M. A. Matthay, Cytokine-mediated inflammation in acute lung injury. Cytokine & growth factor reviews. 14, 523-535 (2003)
4. T. Van Der Poll, F. L. Van De Veerdonk, B. P. Scicluna,M. G. Netea, The immunopathology of sepsis and potential therapeutic targets. Nature Reviews Immunology. 17, 407 (2017)
5. C. A. Prauchner, Oxidative stress in sepsis: pathophysiological implications justifying antioxidant cotherapy. Burns. 43, 471-485 (2017)
6. S. K. Biswas, Does the interdependence between oxidative stress and inflammation explain the antioxidant paradox? Oxidative medicine and cellular longevity. 2016, (2016)
7. J. Lugrin, N. Rosenblatt-Velin, R. Parapanov,L. Liaudet, The role of oxidative stress during inflammatory processes. Biological chemistry. 395, 203-230 (2014)
8. A. Dandekar, R. Mendez,K. Zhang (2015) Cross talk between ER stress, oxidative stress, and inflammation in health and disease. Stress Responses, (Springer), 205-214.
9. B. Gibbison, J. A. López-López, J. P. Higgins, T. Miller, et al., Corticosteroids in septic shock: a systematic review and network meta-analysis. Critical Care. 21, 78 (2017)
10. B. N. Cronstein,G. Haskó, Regulation of inflammation by adenosine. Frontiers in immunology. 4, 85

(2013)
11. G. Hasko, C. Szabó, Z. H. Németh, V. Kvetan, et al., Adenosine receptor agonists differentially regulate IL-10, TNF-alpha, and nitric oxide production in RAW 264.7 macrophages and in endotoxemic mice. The Journal of Immunology. 157, 4634-4640 (1996)
12. U. Söderbäck, A. Sollevi,B. Fredholm, The disappearance of adenosine from blood and platelet suspension in relation to the platelet cyclic AMP content. Acta physiologica scandinavica. 129, 189- 194 (1987)
13. L. Belardinelli, J. Linden,R. M. Berne, The cardiac effects of adenosine. Progress in cardiovascular diseases. 32, 73-97 (1989)
14. H. Mangge, K. Becker, D. Fuchs,J. M. Gostner, Antioxidants, inflammation and cardiovascular disease. World journal of cardiology. 6, 462 (2014)
15. H. F. Goode, H. C. Cowley, B. E. Walker, P. D. Howdle, et al., Decreased antioxidant status and increased lipid peroxidation in patients with septic shock and secondary organ dysfunction. Critical care medicine. 23, 646-651 (1995)
16. M. M. Berger,R. L. Chioléro, Antioxidant supplementation in sepsis and systemic inflammatory response syndrome. Critical care medicine. 35, S584-S590 (2007)
17. E. Borrelli, P. Roux-Lombard, G. E. Grau, E. Girardin, et al., Plasma concentrations of cytokines, their soluble receptors, and antioxidant vitamins can predict the development of multiple organ failure in patients at risk. Critical care medicine. 24, 392-397 (1996)
18. M. É. Andrades, A. Morina, S. Spasić,I. Spasojević, Bench-to-bedside review: sepsis-from the redox point of view. Critical Care. 15, 230 (2011)
19. P. E. Marik, V. Khangoora, R. Rivera, M. H. Hooper, et al., Hydrocortisone, vitamin C, and thiamine for the treatment of severe sepsis and septic shock: a retrospective before-after study. Chest. 151, 1229-1238 (2017)
20. N. Lane, A unifying view of ageing and disease: the double-agent theory. Journal of Theoretical Biology. 225, 531-540 (2003)
21. F. Dormont, M. Rouquette, C. Mahatsekake, F. Gobeaux, et al., Translation of nanomedicines from lab to industrial scale synthesis: The case of squalene-adenosine nanoparticles. Journal of Controlled Release. (2019)
22. B. Shrum, R. V. Anantha, S. X. Xu, M. Donnelly, et al., A robust scoring system to evaluate sepsis severity in an animal model. BMC research notes. 7, 233 (2014)
23. D. Desmaële, R. Gref,P. Couvreur, Squalenoylation: a generic platform for nanoparticular drug delivery. Journal of controlled release. 161, 609-618 (2012)
24. H. Esterbauer, M. Dieber-Rotheneder, G. Striegl,G. Waeg, Role of vitamin E in preventing the oxidation of low-density lipoprotein. The American journal of clinical nutrition. 53, 314S-321S (1991)
25. L. Hakanpaa, E. A. Kiss, G. Jacquemet, I. Miinalainen, et al., Targeting β1-integrin inhibits vascular leakage in endotoxemia. Proceedings of the National Academy of Sciences. 115, E6467-E6476 (2018)
26. E. A. Azzopardi, E. L. Ferguson,D. W. Thomas, The enhanced permeability retention effect: a new paradigm for drug targeting in infection. Journal of Antimicrobial Chemotherapy. 68, 257-274 (2012)
27. B. Halliwell,J. M. Gutteridge (2015) Free radicals in biology and medicine (Oxford University Press, USA).
28. A. Gaudin, O. Tagit, D. Sobot, S. Lepetre-Mouelhi, et al., Transport mechanisms of squalenoyladenosine nanoparticles across the blood–brain barrier. Chemistry of Materials. 27, 3636-3647 (2015)

29. H. F. Galley, Bench-to-bedside review: targeting antioxidants to mitochondria in sepsis. Critical care. 14, 230 (2010)
30. M. Rouquette, S. Lepetre-Mouelhi, O. Dufrançais, X. Yang, et al., Squalene-adenosine nanoparticles: ligands of adenosine receptors or adenosine prodrug? Journal of Pharmacology and Experimental Therapeutics. 369, 144-151 (2019)
31. D. J. Wadleigh, S. T. Reddy, E. Kopp, S. Ghosh, et al., Transcriptional activation of the cyclooxygenase2 gene in endotoxin-treated RAW 264.7 macrophages. Journal of Biological Chemistry. 275, 6259-6266 (2000)
32. A. T. Jacobs,L. J. Ignarro, Lipopolysaccharide-induced expression of interferon-β mediates the timing of inducible nitric-oxide synthase induction in RAW 264.7 macrophages. Journal of Biological Chemistry. 276, 47950-47957 (2001)
33. R. Korhonen, A. Lahti, H. Kankaanranta,E. Moilanen, Nitric oxide production and signaling in inflammation. Current Drug Targets-Inflammation & Allergy. 4, 471-479 (2005)
34. K. Hensley, K. A. Robinson, S. P. Gabbita, S. Salsman, et al., Reactive oxygen species, cell signaling, and cell injury. Free Radical Biology and Medicine. 28, 1456-1462 (2000)
35. C. Brodie, P. M. Blumberg,K. A. Jacobson, Activation of the A2A adenosine receptor inhibits nitric oxide production in glial cells. FEBS letters. 429, 139-142 (1998)
36. D. Yang, Y. Zhang, H. G. Nguyen, M. Koupenova, et al., The A 2B adenosine receptor protects against inflammation and excessive vascular adhesion. The Journal of clinical investigation. 116, 1913-1923 (2006)
37. M. A. Dobrovolskaia,S. N. Vogel, Toll receptors, CD14, and macrophage activation and deactivation by LPS. Microbes and Infection. 4, 903-914 (2002)
38. S. L. Deshmane, S. Kremlev, S. Amini,B. E. Sawaya, Monocyte chemoattractant protein-1 (MCP-1): an overview. Journal of interferon & cytokine research. 29, 313-326 (2009)
39. P. Damas, D. Ledoux, M. Nys, Y. Vrindts, et al., Cytokine serum level during severe sepsis in human IL-6 as a marker of severity. Annals of surgery. 215, 356 (1992)
40. C.-W. Chow, M. T. Herrera Abreu, T. Suzuki,G. P. Downey, Oxidative stress and acute lung injury. American journal of respiratory cell and molecular biology. 29, 427-431 (2003)
41. K. Sato, M. B. Kadiiska, A. J. Ghio, J. Corbett, et al., *In vivo* lipid-derived free radical formation by NADPH oxidase in acute lung injury induced by lipopolysaccharide: a model for ARDS. The FASEB Journal. 16, 1713-1720 (2002)
42. E. Snoeck, K. Ver Donck, P. Jacqmin, H. Van Belle, et al., Physiological red blood cell kinetic model to explain the apparent discrepancy between adenosine breakdown inhibition and nucleoside transporter occupancy of draflazine. Journal of Pharmacology and Experimental Therapeutics. 286, 142-149 (1998)
43. U. Flögel, S. Burghoff, P. L. Van Lent, S. Temme, et al., Selective activation of adenosine A2A receptors on immune cells by a CD73-dependent prodrug suppresses joint inflammation in experimental rheumatoid arthritis. Science translational medicine. 4, 146ra108-146ra108 (2012)
44. B. E. Barton,J. V. Jackson, Protective role of interleukin 6 in the lipopolysaccharide-galactosamine septic shock model. Infection and immunity. 61, 1496-1499 (1993)

Supplementary Data

Supplementary Discussion

Drug Release from SQAd/VitE NPs

Given these experiments and previous studies from our laboratory, our current understanding of drug release from SQAd/VitE NPs can be summarized in the following way: 1) SQAd/VitE NPs are compact and stable nanoparticles which do not release hydrophobic compounds, like Vit E, readily. 2) The use of an amide bond for the bioconjugation of adenosine to squalene ensures a slow release of adenosine following the hydrolysis of the amide linker. It was found that after 48 hours, 6.1% of the initial adenosine was released in serum. 3) These *in vitro* results on stability and drug release are likely not predictive of what occurs *in vivo* where dynamic phenomena can lead to interaction with organs and endogenic lipid carriers that lead to new complex partition phenomena (23).

Renal Filtration

In the kidney, convective and diffusive forces at the glomerulus capillaries compel the filtration of blood solutes from the capillary lumen to the Bowman's capsule through a highly fenestrated endothelium. These fenestrations, 60-80 nm in size, are covered by a thick glycocalyx layer and exert quantitative and qualitative control on what is filtered out of the blood. Typically, proteins with hydrodynamic diameters smaller than 5 to 6 nm are freely filtered by the glomerulus, while larger solutes are retained in the circulation. As a result, most nanoparticles- and the SQ NPs studied here- are too large to be filtered by the kidneys without prior biodegradation (notable exceptions being quantum dots up to 5.5 nm in size or carbon nanotubes).

Specificity of accumulation

The question of the specific accumulation merits an important distinction to be made concerning the mechanism of nanoparticle targeting at inflamed sites. Generally speaking, NP accumulation at the inflamed sites results from two consecutive phenomena, first extravasation of the nanoparticles from the blood circulation to the tissue, followed by the retention at the inflamed site. While most macromolecules and particulates can extravasate through permeable endothelium, retention at inflammation sites requires to some extent specific interaction with host cells in the target tissue. This is different than what happens inside of tumors where the impaired lymphatic system ensures passive accumulation. In inflamed tissue, lymphatic capillaries expand and actively participate in the removal of cellular debris (54).

Therefore, the accumulation at inflammation sites, while initiated by an unselective endothelial permeability phenomenon, is driven by specific inflammatory and tissue cell interaction. Improved uptake of a material by cells at the inflammation site would therefore result in improved retention and accumulation.

Comparison with PLGA nanoparticles

Recently, it was shown that squalene-based bioconjugates are taken up by LDLs in the bloodstream ensuring high blood residence time in a method assimilated to a "trojan-horse" technique (23). During inflammation, immune cells that switch to an inflammatory phenotype increase their LDL uptake via LDL receptors in an effort to keep up with their higher metabolic demands. It was our understanding that this increased LDL receptor expression would result in preferential accumulation of SQAd/VitE NPs in inflamed tissue through the mechanisms mentioned above. Interestingly, when accumulation profiles of PLGA NPs was compared to that of fluorescently labelled SQAd/VitE NPs (Supp Fig. S3.), significant differences were observed. Namely, accumulation resulting from SQ NPs targeting happened faster and to a higher extend than with PLGA NPs, which could be linked to the higher retention of squalene-based nanoparticles at the site of inflammation.

Effect of SQAd/VitE NPs on NO production of RAW 264.7 macrophages

When RAW 264.7 macrophages detect pathogen associated molecular patterns such as LPS, a rapid cellular response leads to the activation of the iNOS enzyme which produces high quantities of nitric oxide. NO is relatively non-reactive and reacts mostly with transition metals or reactive radicals such as hydroperoxide or superoxide. As such, it is unlikely that the observed effect was caused by the direct reaction of VitE with NO. Rather, it has been shown that iNOS activity can be inhibited by blocking either NFkappaB or NADPH oxidase activity (55, 56)). Both these pathways are redox regulated and have been shown to be inhibited by tocopherol (57-59).

Supplementary Methods

SQAd carrier NMR

SQAd was obtained as a colorless oil.; **1H NMR (300 MHz, CDCl3)**

δ: 9,39 (broad s, 1H, NHCO), 8.41 (s, 1H, H8), 8.21 (s, 1H, H2), 5.98 (d, 1H, J = 5.4 Hz, H1'), 5.32 (t, 1H, J = 6.3 Hz, HC=C(CH3)), 5.05–4.93 (m, 5H, HC=C(CH3)), 4.61 (t, 1H, J = 4.9 Hz, H2'), 4.18 (m, 1H, H3'), 3.98 (m, 1H, H4'), 3.69 (dd, 1H, J = 11.9 Hz, J = 3.7 Hz, H5'), 3.57 (dd, J = 11.9 Hz, J = 3.3 Hz, 1H, H5'), 2.98 (t, 2H, J = 7.8 Hz, O2CCH2CH2), 2.45 (t, 2H, J = 7.8 Hz, O2CCH2CH2), 2.11–1.93 (m, 20H, =C(CH3)CH2CH2), 1.62 (s, 3H, C=C(CH3)), 1.60 (s, 3H, C=C(CH3)), 1.54 (s, 15H, C=C(CH3)).

Fluorescent PLGA Nanoparticle Synthesis

Commercial PLGA polymer (LR 706S, Evonik Health, poly(L-lactic-co-glycolic) acid, 70:30, 80kDa) was solubilized in acetonitrile at a concentration of 6 mg/mL with 1 % w/w DiD. The organic solution was nanoprecipitated in an aqueous solution containing 1% Pluronic (F-123). Acetonitrile was removed under reduced pressure and the resulting colloidal suspension was analysed by DLS for size distribution and zeta potential (Supp. Fig. S2).

Synthesis of SQRho

SQRho was synthesized by direct acylation of the piperazine-rhodamine B after in situ formation of chloroformate mixed anhydride of trisnorsqualenic acid.

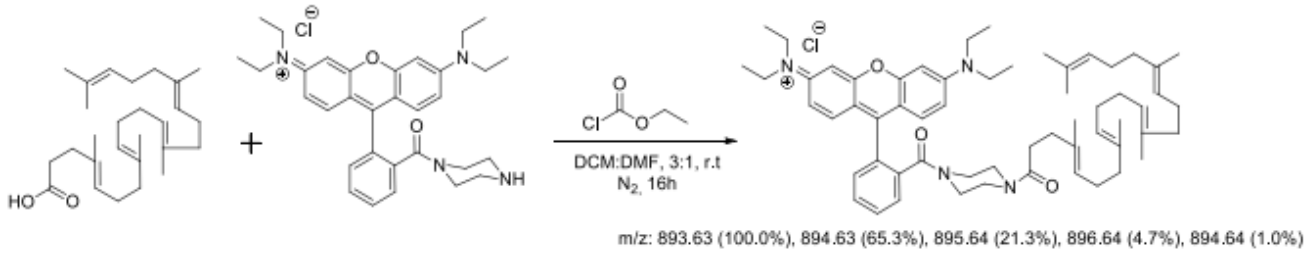

Supp. Fig. S1. Synthesis scheme for SQRho

To a solution of ethyl chloroformate (30 µL, 0.33 mmol) in anhydrous DCM (1 mL) was added Et3N (90 µL, 0.6 mmol). The mixture was cooled at 0 °C and a solution of trisnorsqualenic acid (120 mg, 0.30 mmol) in anhydrous DCM (2 mL) was added dropwise. Mixture was stirred for 30 min at 0 °C and a solution of rhodamine B piperazine (181 mg, 0.33 mmol) in DMF (1 mL) was added dropwise. After being stirred at room temperature for 16h, DMF was removed under vacuum. The residue was taken up in sat. NaHCO3 aqueous solution (4 mL) and extracted with AcOEt (3 × 15 mL). The combined organic layers were washed

with brine, dried over MgSO4 and concentrated under reduced pressure. The crude was then purified by flash chromatography on silica (CH2Cl2/Methanol from 100:0 to 90:10). Fraction containing the expected product were concentrated to provide rhodamine B 4-(1,1',2-trisnorsqualenoyl)piperazine (140 mg, 56%) as a dark purple glassy solid.

1 H NMR (300 MHz, MeOD, δ in ppm): 7.76 (2H, m, H-4', H-5'), 7.70 (1H, m, H3'), 7.52 (1H, m, H6'), 7.27 (2H, d, J = 9.5 Hz, H-1, H-8), 7.09 (2H, dd, J = 9.5 Hz, J = 2.1 Hz, H-2, H-7), 6.97 (2H, d, J = 2.4 Hz, H-4, H-5), 5.06−5.20 (5H, m, HC=C(CH3)CH2), 3.71 (8H, q, J = 7.1 Hz, H3CCH2N), 3.35−3.50 (8H, m, NCH2CH2N), 2.44 (2H, t, J= 9 Hz NOCCH2CH2), 2.21 (2H, t,J= 9Hz NOCCH2CH2), 2.13−1.93 (16H, m, =C(CH3)CH2CH2CH=), 1.68 (3H, s, HC=C(CH3)2), 1.61 (12H, s, HC=C(CH3)), 1.31 (12H, t, J = 7.1 Hz, H3CCH2N) .

Formulation of fluorescent SQAd/VitE NPs

Fluorescent SQAd/VitE NPs were prepared by the nanoprecipitation method (see Materials and Methods) after adding 1% of fluorescent probe (either DiD or SQRho) to the organic phase.

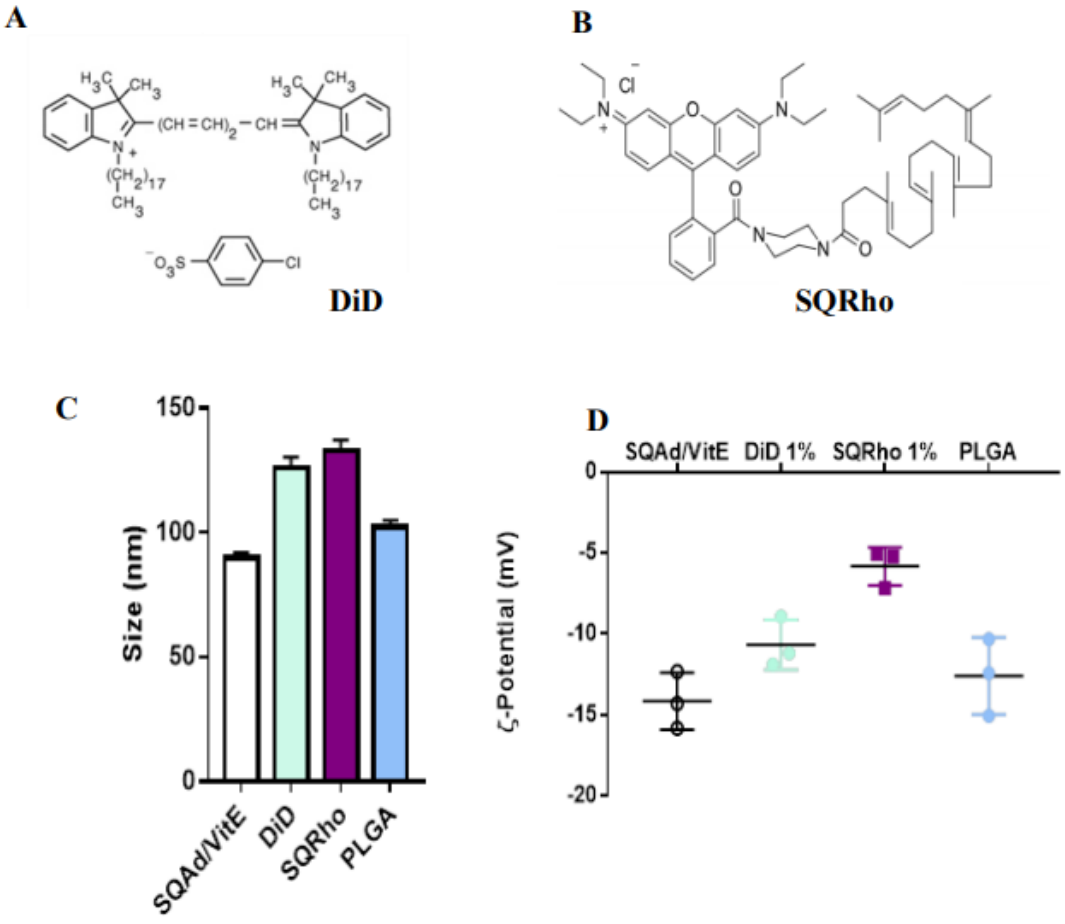

Supp. Fig. S2. Characterization of fluorescent NPs.

(**A**) Structure of 1,1′-dioctadecyl-3,3,3′,3′- tetramethylindodicarbocyanine perchlorate (DiD). (**B**) Structure of SQRho. (**C**) Hydrodynamic size of fluorescently labelled NPs (diameter, nanometers) measured by dynamic light scattering (DLS). (**D**) Measurement of surface ζ-potential of fluorescently labelled SQAd/VitE and PLGA NPs.

Comparison with PLGA NPs

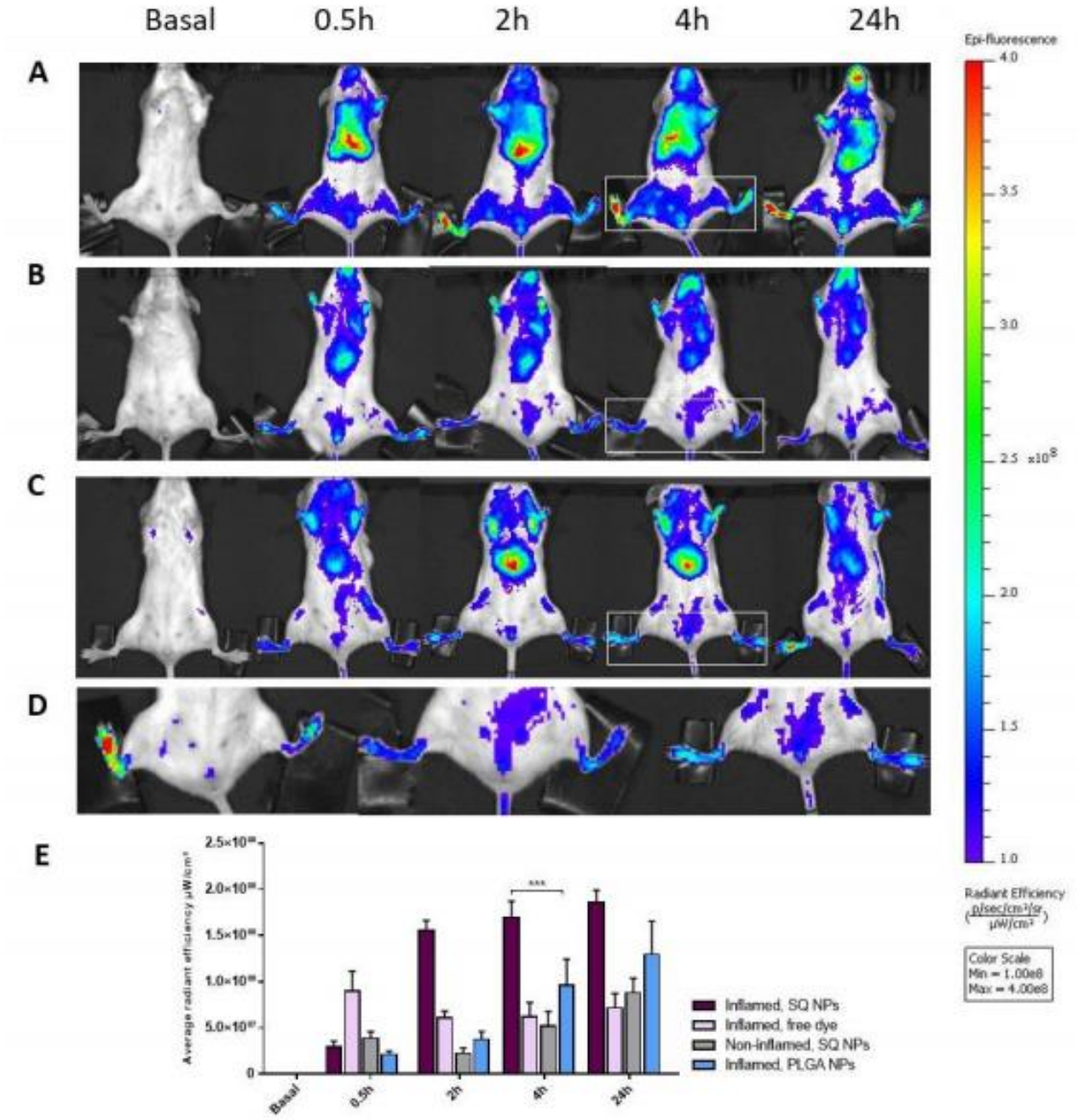

Supp. Fig. S3: IVIS Lumina scan of mice after intravenous administration of fluorescent SQAd/VitE NPs, fluorescent PLGA NPs or control fluorescent dye solution (ventral view).

(**A**) Biodistribution of fluorescent SQAd/VitE NPs in mice with inflamed right hind paw and non-inflamed left hind paw. (**B**) Biodistribution of the free dye in mice with inflamed right hind paw. (**C**) Biodistribution of fluorescent PLGA NPs in mice with inflamed right hind paw and non-inflamed left hind paw Zoom of group A at 4 hours. (**D**) Zoom of groups A, B and C at 4 hours. (**E**) Analysis of the measured radiant efficiency in the region of interest. n=3 mice per group. Data are mean ± SD. *P<0.05, **P<0.01, ***P<0.001 (Two-way ANOVA followed by Holm-Sidak's multiple comparison test).

Relative fluorescence in inflamed vs non inflamed paw.

The ratios of detected fluorescence in the right (inflamed) paw over left (non-inflamed) paw were calculated.

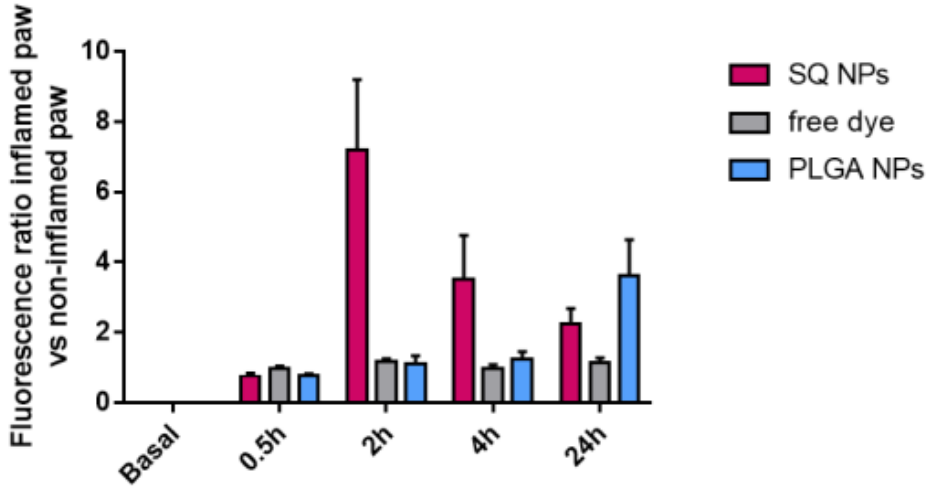

Supp Fig. S4: Ratio of detected fluorescence in the inflamed paw vs non-inflamed paw following injection of DiD labelled SQAd/VitE NPs or DiD labeled PLGA NPs or free DiD.

Cellular uptake of fluorescent SQAd/VitE NPs

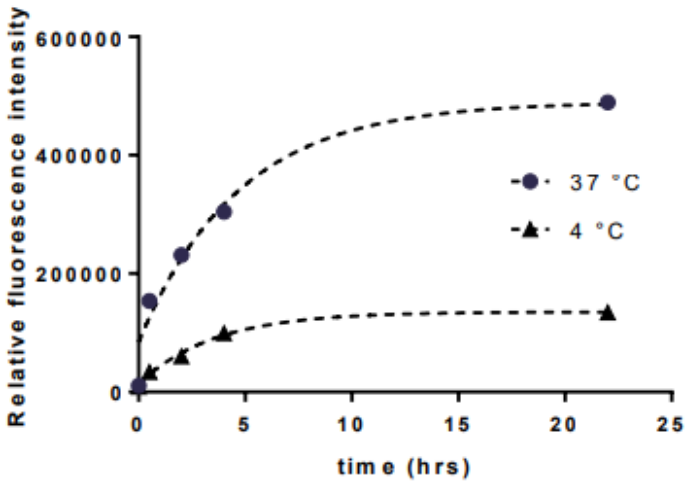

Supp. Fig. S5: H9c2 cells/well (26 000 cells/ cm2) were seeded in 12-well plates and cultured for 24 h at 37°C. The cells were then incubated at 37 °C or 4°C with fluorescent SQRho tagged SQAd/VitE NPs diluted in cell culture medium for different durations. At the end of the incubation period, cells were washed with 1 mL of PBS and then treated with 300 µL of 0.25% trypsin solution for 5 min at 37 °C and 5% CO2. Trypsin solution was diluted by adding 0.7 mL of medium, and the fluorescence of the cells was recorded using a flow cytometer C6 (Accuri Cytometers Ltd.). For fluorescence detection of SQ-Rho labelled NPs, excitation was carried out using a 488 nm

argon laser and emission fluorescence was measured at 515 nm. 10 000 cells were measured for each sample. The results were expressed as the mean relative fluorescence intensity (MFI) ± SEM.

Pro and anti-inflammatory cytokine kinetics after LPS challenge

The levels of different cytokines were assessed in the plasma by ELISA after initial LPS challenge (7.5 mg/kg).

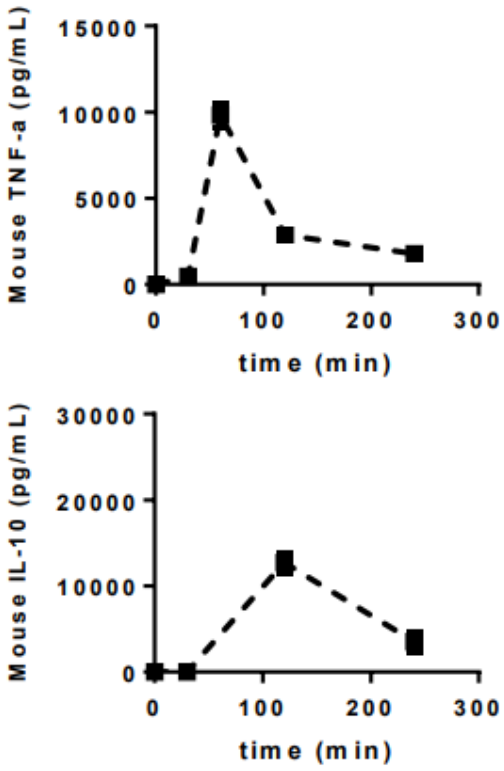

Supp. Fig. S6: TNF-α and IL-10 levels in plasma of untreated 8-wk-old male C57BL6 mice after LPS challenge. Endotoxemia was induced by intraperitoneal injection of a 7.5 mg/kg dose of LPS (Sigma O111:B4) diluted at 1.875 mg/mL in buffered saline. Following LPS injections, blood samples (~50 µL) were collected at predetermined time points via submandibular puncture. Plasma was obtained by centrifuging blood samples at 2000 rcf for 10 min and stored at –78°C before further analysis. Cytokines levels were quantified by Biolegend ELISA mouse kit per manufacturer instructions.

Dose dependency of SQAd/VitE NPs effect on cytokines *in vivo*.

Animals received SQAd/VitE NPs treatment (15 mg/kg or 30 mg/kg) after initial LPS challenge

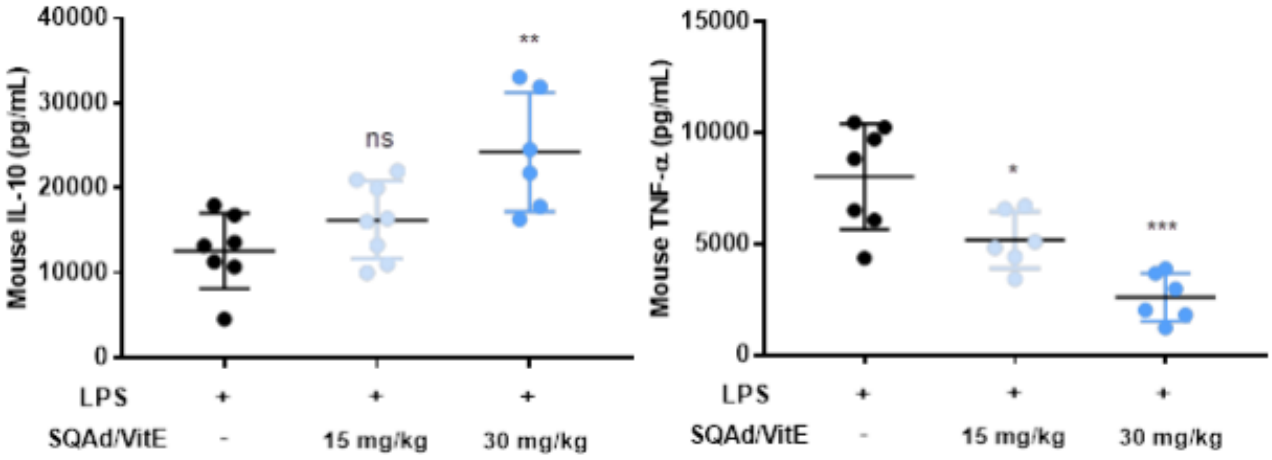

Supp. Fig. S7: Plasma TNF-α and IL-10 levels in 8-wk-old male C57BL6 mice after LPS challenge and SQAd/VitE NPs treatments at 15 mg/kg or 30 mg/kg. Endotoxemia was induced by intraperitoneal injection of a 7.5 mg/kg dose of LPS (Sigma O111:B4) diluted at 1.875 mg/mL in buffered saline. Following LPS injections, blood samples (~50 µL) were collected at 1h after NPs injection via submandibular puncture. Data are mean ± SD. ns: non-significant, *P<0.05, **P<0.01,***P<0.001 (One-way ANOVA followed by Holm-Sidak's multiple comparison test).

Anti-inflammatory efficacy of SQAd/VitE NPs.

After lethal LPS challenge, Liver of treated vs non treated animals were compared for signs of disease severity.

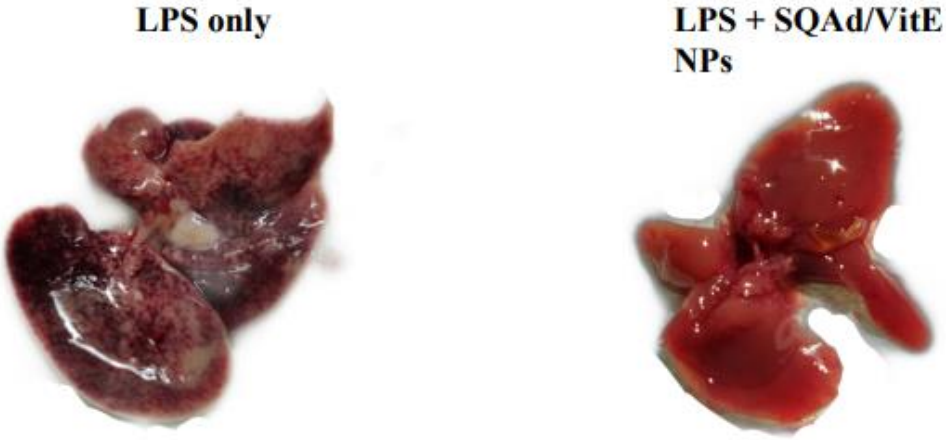

Supp. Fig. S8: Liver of non-treated vs treated animal in lethal LPS challenge model harvested at the 24 hours time point. C57BL/6J mice (n=10 animals/group) were sensitized to the lethal effects of LPS by i.p. injection of 8 mg of D-galactosamine hydrochloride. A single i.p. dose of LPS at 2 µg/kg caused 60% mortality within 48 hours. Mice in the treatment groups received SQAd/VitE NPs i.v. at a dose of 30 mg/kg and the liver was visually compared to LPS

only treated animals.

Representative histological images of organ tissue after lethal LPS challenge

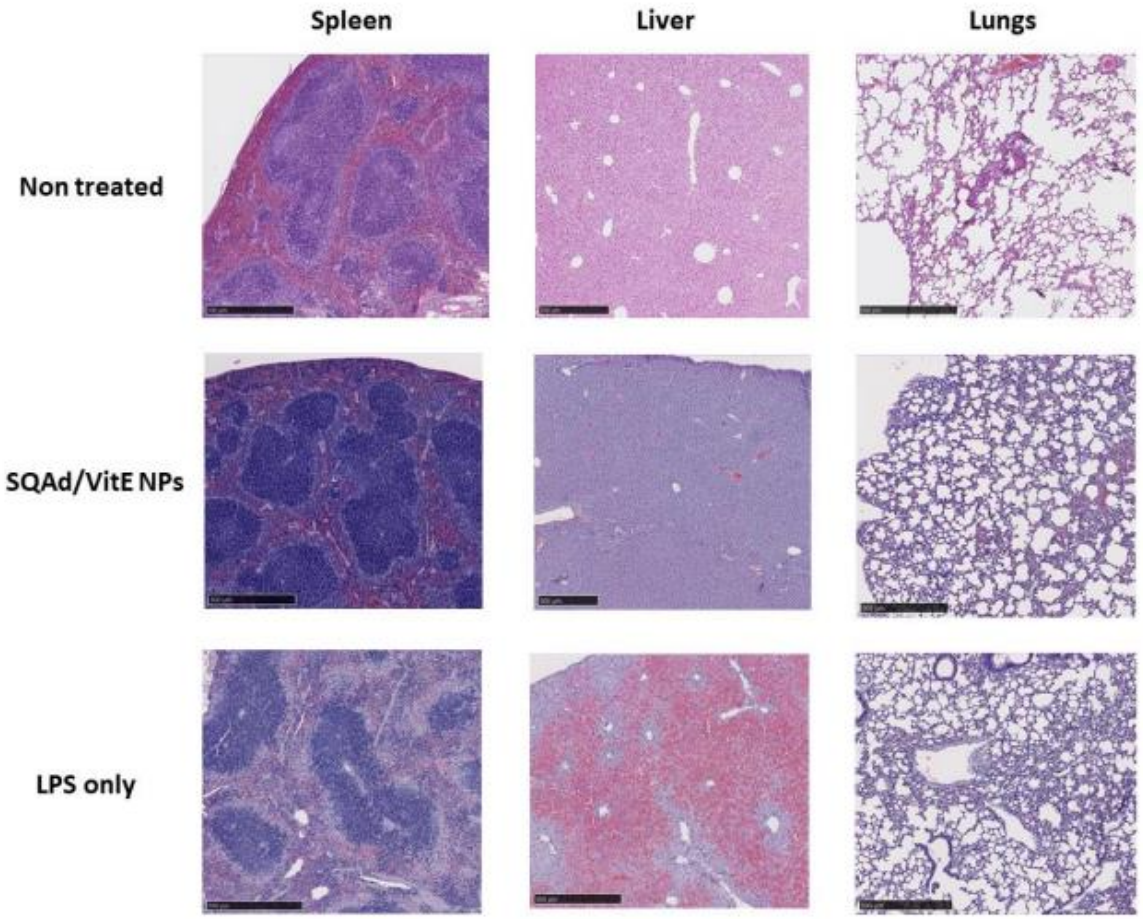

Supp. Fig. S9: At the 24 h time point, an animal was chosen at random from the NP treated and LPS only groups for histological comparison as well as non-treated healthy control. Liver: LPS only group shows widespread haemorrhage and steatosis, non-treated and SQAd/VitE NP groups show no histological changes. Spleen: Healthy and NP treated groups show a well-organized white pulp with easily discernible peri-arteriolar sheath, germinal centre, mantle zone and marginal zone. The spleen of non-treated controls shows a disorganized white pulp with loss in boundaries definition and barely distinct follicular structure. Lungs: Non treated group: no histological changes. NP treated group: thickening of the alveolar septa. Non treated group: Disruption of alveolar structure, thickening of alveolar septa. All scale bars are 500 µm.

Discussion générale et Conclusions

Ce projet de Thèse s'inscrit dans le cadre du projet Eurononamed II – NanoHeart avec pour but d'évaluer des nanomédicaments à base de squalène dans des maladies cardiovasculaires et inflammatoires. Nous avons tout d'abord commencé par tester les nanoparticules à base de squalène comme outils de diagnostic dans un modèle d'athérosclérose, maladie inflammatoire chronique qui caractérise les artères de gros et moyen calibre. Puis nous avons évalué ces mêmes nanoparticules comme traitement potentiel dans un modèle de lésions d'ischémie/reperfusion cardiaque, qui se produit principalement suite à la rupture ou l'érosion d'une plaque lipidique d'athérosclérose formée dans l'artère coronaire. Le processus inflammatoire accompagne en outre chaque étape de cette maladie. Enfin, nous avons évalué ces nanoparticules de squalène dans un modèle de sepsis, syndrome inflammatoire généralisé et incontrôlé amenant à la dysfonction des organes et pouvant aussi être lié à l'ischémie/reperfusion. En effet, si la sévérité des lésions d'ischémie/reperfusion ou si le volume du tissu cardiaque ischémié est trop large, un sepsis ainsi que de multiples défaillances des organes peuvent s'ensuivre[1, 2]. A l'inverse, de récentes études tendent à montrer que les patients ayant contracté un choc septique sont plus prompts à développer des problèmes cardiovasculaires et des attaques cardiaques[3, 4]. L'inflammation fut ainsi la ligne directrice de toute cette étude d'évaluation de nanoparticules à base de squalène.

L'ensemble de ces travaux de Thèse, fondamentalement pluridisciplinaire, est le résultat de collaborations enrichissantes ayant permis d'obtenir des conclusions intéressantes :

- La preuve de concept que les **nanoparticules à base squalène sont capables de cibler et s'accumuler dans les plaques d'athérosclérose**. Les résultats ont en particulier montré que les nanoparticules fluorescentes de squalène-rhodamine B s'accumulent à la fois dans les plaques d'athérosclérose précoces et avancées dans le modèle murin *ApoE*$^{-/-}$. Les nanoparticules sembleraient notamment interagir avec les macrophages résidents.

- **L'effet cardioprotecteur des nanoparticules de squalène-adénosine dans un modèle murin de lésion d'ischémie/reperfusion cardiaque**. Les résultats, bien que mitigés, ont notamment démontré que l'encapsulation de l'adénosine dans des nanoparticules de squalène ne présente pas de cytotoxicité ni *in vitr*o ni *in vivo*, et qu'elles tendent à réduire la taille de la zone d'infarctus et à diminuer la mort cellulaire dans le tissu cardiaque.

- **Le développement de nanoparticules de squalène-adénosine-vitamine E pour atténuer l'inflammation aigüe chez la souris**. Les résultats ont illustré la possibilité d'utiliser le squalène pour encapsuler plusieurs principes actifs au sein d'une même nanoparticule, améliorant la biodisponibilité de chacun. C'est ici le premier exemple de nanoparticules de squalène « multi-médicamenteuse », à la fois anti-inflammatoire et antioxydante, pour lutter contre l'inflammation, et présentant une activité

pharmacologique significative dans des modèles murins d'épisodes inflammatoires aigües.

Ces conclusions constituent une modeste mais intéressante contribution à l'évaluation des nanoparticules à base de squalène pour le diagnostic et le traitement de maladies cardiovasculaires et inflammatoires. Toutefois, les multiples expériences ayant mené à ces résultats de Thèse présentent des limites sur plusieurs aspects. Par ailleurs, bien qu'ouvrant la porte à de nombreuses perspectives intéressantes, des efforts supplémentaires seront nécessaires pour mieux appréhender les mécanismes de fonctionnement des différentes nanoparticules de squalène. Tout cela va être discuté dans la suite de ce manuscrit.

Dans un premier temps, nous discuterons de l'utilisation du squalène-rhodamine pour l'imagerie des plaques d'athérosclérose et des freins à leur utilisation en clinique. Nous évoquerons aussi les perspectives et solutions que nous pourrions apporter pour contourner ces limitations. Dans un deuxième temps, nous aborderons les modèles pré-cliniques d'ischémie/reperfusion cardiaque, à la fois *in vitro* et *in vivo*. Nous justifierons les choix que nous avons faits tout en soulevant les limites des modèles utilisés. Dans un troisième temps, nous évoquerons l'utilisation de l'adénosine pour traiter les lésions d'ischémie/reperfusion cardiaque et nous discuterons des avantages et inconvénients de la « squalénisation » pour une application thérapeutique potentielle dans ce domaine.

1. Nanoparticules à base de squalène pour l'imagerie de l'athérosclérose

Imager le développement des plaques d'athérosclérose constitue l'un des défis majeurs de ces dernières décennies. Cela représente un moyen de mieux comprendre le processus systémique et diffus de l'athérosclérose, depuis l'initiation jusqu'à la déstabilisation des plaques. Mais aussi, cela représente un moyen d'améliorer le diagnostic et ainsi de pouvoir intervenir préventivement pour une meilleure gestion thérapeutique de la maladie. De nouvelles techniques d'imagerie telles que l'imagerie ultrason intravasculaire des artères carotides sont déjà appliquées en clinique[5, 6]. D'autres techniques telles que l'imagerie par résonance magnétique (IRM) ou la tomographie par émissions de positrons (TEP) représentent aussi un fort potentiel clinique.

En même temps que l'avancée des techniques d'imagerie, le développement de nouveaux agents de contraste et autres composés chimiques d'imagerie a gagné un intérêt grandissant. Le but est d'améliorer la sensibilité, tout en améliorant l'identification et la quantification de molécules ou structures spécifiques[7]. En particulier, des études approfondies ont été menées ces dernières années sur l'utilisation de nanoparticules comme outils d'imagerie performants et innovants[7-10].

Intérêt de l'utilisation de nanoparticules de squalène pour l'imagerie de l'athérosclérose et défis futurs

Tout est parti du constat que lors de la formation et du développement d'une plaque d'athérosclérose, il y a une accumulation de lipoprotéines, notamment de LDL, dans l'intima des vaisseaux, qui s'oxydent et finissent par être captées par les cellules résidentes dans les plaques (notamment les macrophages)[11]. Or, dans notre laboratoire, Dunja Sobot, une ancienne étudiante en thèse, a démontré que des nanoparticules de squalène-Gemcitabine, et plus généralement les nanoparticules à base de squalène, interagissent de manière spontanée avec les lipoprotéines plasmatiques circulantes riches en cholestérol[12]. Cela nous a ainsi conduit à penser qu'une fois injectées dans le sang, les nanoparticules squalénées devraient interagir spontanément avec les lipoprotéines riches en cholestérol, qui vont alors conduire les nanoparticules dans les vaisseaux jusqu'aux plaques d'athérosclérose (voir figure 1). Or chez le rongeur, le manque de transfert de cholesteryl-ester des HDL aux LDL et VLDL a pour conséquence un système lipoprotéique différent de l'Homme, avec une très petite population de LDL et une plus large population en HDL qui acquiert de ce fait le rôle de transporteur de cholestérol[13].

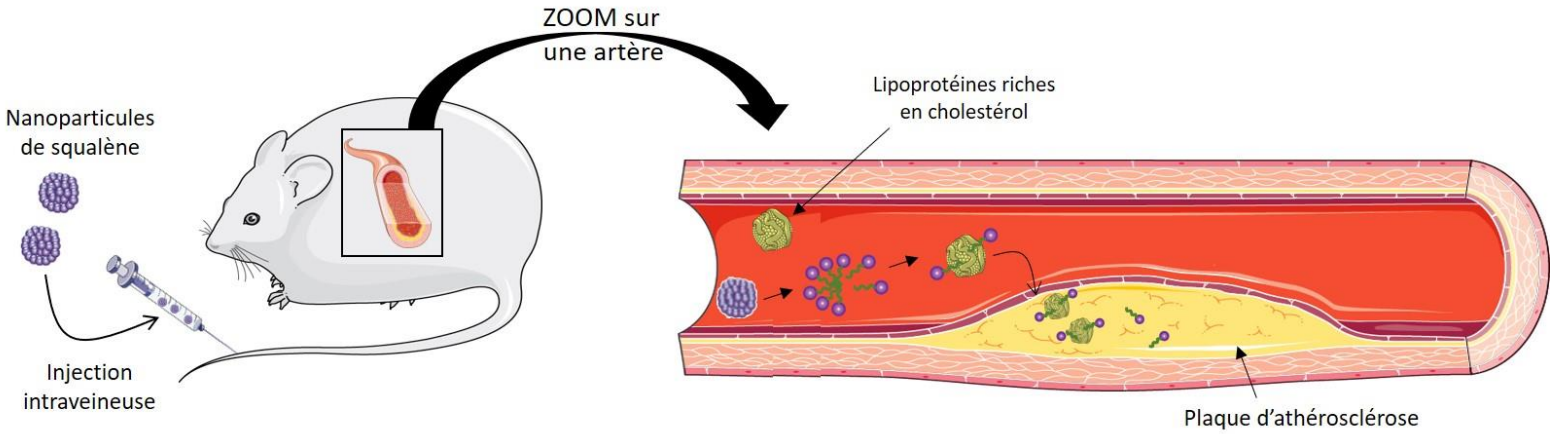

Figure 1 : Les lipoprotéines riches en cholestérol, des transporteurs endogènes de bio-conjugués squalénés ?

Schématisation de notre hypothèse. Une fois injecté dans le sang, les nanoparticules de squalène se débobinent, et les bio-conjugués se lient au LDL (chez l'Homme) ou HDL (chez le rongeur). Ceux-ci circulent alors dans le sang et finissent pour certains par s'accumuler dans les paques d'athérosclérose, accumulant ainsi le squalène couplé au principe actif.

L'emploi du squalène présente plusieurs avantages. Tout d'abord, il s'agit d'un lipide biocompatible et biodégradable, précurseur du cholestérol. C'est en cela que les bio-conjugués de squalène interagissent bien avec les LDL. Par ailleurs, ces bio-conjugués qui forment spontanément en milieu aqueux des nanoparticules, présentent un pouvoir de charge élevé permettant un relargage contrôlé du principe actif. Ces caractéristiques en faisaient un bon candidat pour l'imagerie des plaques d'athérosclérose.

De ce fait, comme présenté dans le chapitre 1, nous avons développé des nanoparticules fluorescentes de

squalène-rhodamine B pour prouver l'utilité du squalène pour l'imagerie des plaques d'athérosclérose. Et les résultats obtenus tendent à corroborer notre hypothèse de travail. L'accumulation des nanoparticules dans les plaques semble bien être dû à une interaction entre le squalène et les LDL, et non à un autre effet car des billes fluorescentes de latex utilisée comme nanoparticules témoins ne s'accumulaient pas dans les plaques. De plus, de façon intéressante, des études ont montré qu'on assiste à une forte activation de la synthèse des récepteurs aux LDLs dans les cellules immunitaires (dont les macrophages) lors d'épisodes inflammatoires associés à des troubles métaboliques comme durant l'athérosclérose[14, 15]. Cela conforte donc l'hypothèse de départ.

Toutefois, nos résultats ne permettent pas de conclure avec précision sur la manière avec laquelle les nanoparticules de squalène s'accumulent dans les plaques. Si les nanoparticules demeurent longtemps dans la circulation, elles pourraient par exemple aussi être captées par des cellules du système immunitaire, phénomène qu'exploitent certains groupes de recherche pour adresser certaines nanoparticules au niveau des sites inflammatoires[16].
Nous n'avons, en effet, pas confirmé l'interaction des nanoparticules de squalène-rhodamine B avec les lipoprotéines même si l'on peut supposer qu'elles se comportent de la même manière que les nanoparticules de squalène-Gemcitabine[12]. D'autre part, cette étude est une preuve de concept, et nous n'avons pas étudié en détail les mécanismes cellulaires responsables de l'accumulation des nanoparticules dans les plaques. Nous n'avons regardé que l'accumulation 24h après injection et non à d'autre temps. De plus, nous avons constaté que les nanoparticules sont retrouvées dans les macrophages et les cellules musculaires lisses. Mais des études complémentaires seraient certainement nécessaires pour expliquer comment elles s'accumulent dans ces cellules.

Nanoparticules de squalène-rhodamine, des nanoparticules inadaptées pour l'Homme

Pour ce projet, nous avons décidé de coupler le squalène à la rhodamine B pour plusieurs raisons. La rhodamine B est un colorant organique fluorescent rouge de la classe des xanthènes, largement répandu comme teinture dans l'industrie textile mais aussi comme traceur fluorescent dans l'eau. Il est aussi abondamment utilisé dans des applications de biotechnologie (microscopie à fluorescence, cytométrie en flux, …)[17-19]. Il fut donc assez aisé d'observer la fluorescence de la rhodamine dans notre laboratoire. D'autre part, la synthèse du squalène-rhodamine est relativement simple et rapide tel que présentée en détail dans le chapitre 1.

Cependant, son utilisation en clinique reste inenvisageable. En se basant sur les données actuelles, la Rhodamine B est considérée comme potentiellement toxique pour l'Homme. En plus de causer des irritations de la peau, des yeux et des dommages au niveau de l'appareil respiratoire, des études ont prouvé

que ce colorant était génotoxique, neurotoxique et carcinogène vis-à-vis de l'Homme et des animaux[19-21]. Il a notamment était suggéré que la Rhodamine B est capable de se lier à des séquences d'ADN, entraînant des dommages irréparables[21]. Pour ces raisons, des souris contrôles n'ont pas pu être injectées avec la même dose de Rhodamine B libre que celle encapsulée dans les NPs. Cela a représenté un frein majeur à notre étude. Mais le squalène garde tout son intérêt car il pourrait être couplé avec d'autres agents d'imagerie plus adaptés[22, 23].

Vers des nanoparticules de squalène plus sophistiquées ?

Bien que la Rhodamine B ne soit pas compatible avec une application clinique, la technique de squalénisation offre d'intéressantes perspectives en tant que plateforme d'imagerie ou de théranostique pour l'athérosclérose ainsi que pour d'autres maladies inflammatoires. En effet, nous avons montré que les nanoparticules de squalène-adénosine-vitE (SQAd-VitE) s'accumulaient au niveau des sites inflammatoires (voir Chapitre 3). Le couplage du squalène à un agent de contraste et à une molécule anti-inflammatoire devrait donc permettre de suivre l'effet d'un traitement anti-inflammatoire sur le développement d'une plaque d'athérosclérose ou tout autre trouble inflammatoire localisé comme la polyarthrite rhumatoïde.

De nombreuses avancées technologiques ont fourni une large gamme d'outils de diagnostic pour caractériser les plaques d'athérosclérose à haut-risque, avancées ou déjà rompues. Cela permet principalement de mesurer la sévérité de la maladie, les conséquences anatomiques et hémodynamiques, en donnant des détails sur la composition de la plaque et l'activité métabolique. Parmi ces méthodes, l'on retrouve, par exemple, l'angiographie par rayon X, par tomodensitométrie, l'échographie intravasculaire, la tomographie d'émission monophotonique, l'imagerie moléculaire, ainsi que l'imagerie par résonance magnétique[24]. Toutefois, nous manquons encore de techniques d'imagerie pour visualiser précocement le développement d'une plaque.

Les nanoparticules de squalène pourraient ainsi offrir de nouvelles perspectives d'imagerie plus précoces des plaques en clinique si couplé avec les technologies d'imagerie actuelle. Des nanoparticules de squalène-gadolinium avec une forte charge utile en ion Gd(3+) ont d'ailleurs déjà été développées dans notre équipe[22]. Cette nano-plateforme présente des caractéristiques intéressantes telles que l'absence d'agents tensioactifs et de solvants toxiques pour leur préparation. La synthèse de ces nanoparticules de squalène-gadolinium reste cependant assez lourde et complexe[22].
Par ailleurs, des nanoparticules de squalène-adénosine contenant des USPIO comme agent de contraste supra-paramagnétique furent récemment testées comme outils de théranostique pour les accidents vasculaires cérébraux et pourraient également présenter des perspectives intéressantes pour le suivi et le traitement de l'athrosclérose[23](figure 2).

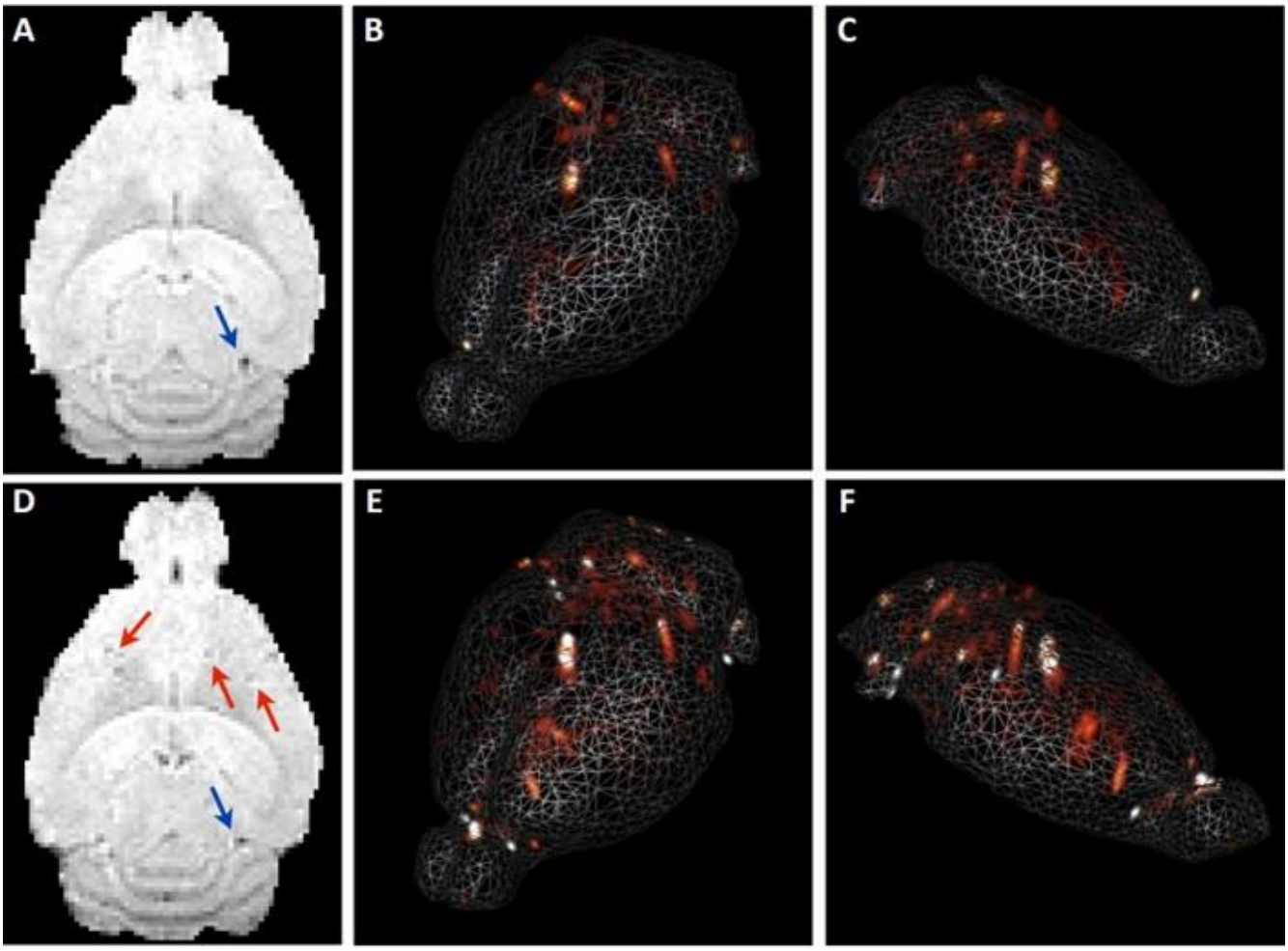

Figure 2 : Exemple d'imagerie *in vivo* des nanoparticules de SQAd-USPIO.

Images obtenues par Alice Gaudin. Une séquence FLASH T_2* fut acquise juste avant (**A-B-C**) et juste après (**D-E-F**) l'injection intraveineuse de nanoparticules de SQAd-USPIO chez la souris. Avant administration, les vaisseaux majeurs du cerveau pouvaient être observés en hyposignal (**A,** flèches bleues), dû au fer endogène circulant dans le flux sanguin. Suite à l'injection de nanoparticules, le nombre d'hyposignaux était plus important (**A**, flèches rouges), confirmant la circulation des nanoparticules dans le système vasculaire cérébral. Des visualisations 3D reconstruits à partir d'angiogramme en utilisant BrainVISA/Anatomist ont permis de détecter clairement le plus grand nombre de vaisseaux cérébraux après injection (**E-F**) comparé à avant injection (**B-C**)

2. Les modèles pré-cliniques d'ischémie/reperfusion, des modèles complexes présentant des limitations ?

Du fait de l'incidence mondiale de l'ischémie/reperfusion cardiaque, de nombreux modèles pré-cliniques ont été développés afin de mimer au mieux les conditions cliniques pour tester de nouveaux traitements. La variété de modèles pré-cliniques disponibles s'étend des modèles cellulaires de cardiomyocyte, aux modèles *ex* vivo de cœurs isolés, jusqu'aux divers modèles animaux comprenant une occlusion permanente ou transitoire de l'artère coronaire, une ablation de l'artère, en passant par diverses cardiomyopathies[25]. Tous ces modèles permettent de mimer les différents stades de l'ischémie cardiaque qui surviennent chez

les patients. Cela permet également de mieux comprendre comment le cœur répond et s'adapte à l'ischémie et aussi de mieux appréhender les mécanismes. Tous ces modèles possèdent leurs propres avantages et inconvénients. Nous nous focaliserons ici sur le modèle cellulaire HL-1 et le modèle murin, qui furent utilisés au cours de notre étude.

Modèles in vitro d'ischémie/reperfusion cardiaque et difficultés de simuler la complexité du vivant

Les modèles *in vitro* sur lignée cellulaire de cardiomyocytes permettent l'étude de l'effet direct des traitements sur les cardiomyocytes. Cela nous a permis d'identifier préalablement une éventuelle cytotoxicité de nos nanoparticules mais aussi de mettre en évidence leur effet protecteur. Il existe dans la littérature de très nombreux modèles d'ischémie/reperfusion, avec différentes façons de contrôler les facteurs externes stimulant la pathologie (temps, température, pourcentage en O_2, …)[26]. L'ischémie est généralement réalisée par culture des cellules en milieu appauvri, sans substrats métaboliques, et avec parfois même des inhibiteurs de glycolyse[27, 28]. Les cellules sont par ailleurs cultivées en conditions d'hypoxie, soit en chambre hypoxique avec de faibles concentrations en O_2 (entre 0 et 10%), soit par inhibition métabolique pour décroitre la consommation en oxygène[28, 30]. La reperfusion est quant à elle généralement simulée en remplaçant le milieu restreint d'ischémie pour éliminer les déchets métaboliques par du milieu complet avec sérum et nutriments [26, 31].

Au cours de la Thèse, nous avons justement développé un modèle *in vitro* d'ischémie/reperfusion sur la lignée cellulaire HL-1 avec du milieu sans nutriments, une incubation à différents temps dans une chambre hypoxique avec 1% en dioxygène et avec une reperfusion par remplacement du milieu d'ischémie par du milieu complet. Comme nous l'avons vu précédemment, grâce à ces conditions, nous avons pu mimer au mieux le processus d'ischémie, avec une période de 6h pour laquelle un grand nombre de cellules entraient en apoptose/nécrose (Cf. chapitre 2, figure 3). Toutefois, la reperfusion n'a pas permis de simuler réellement les lésions de reperfusion physiologique. En effet, à l'inverse de ce que l'on attendait, la reperfusion n'a pas induit de dommages supplémentaires. Eventuellement, certaines cellules sont mortes à cause de la reperfusion mais pendant que d'autres qui étaient en état de « stase » métabolique, ou bien venant d'entrer en apoptose de manière réversible, ont repris leur métabolisme de base avec la reprise de condition de culture adéquate. Nous avons testé différents temps de reperfusion, et avons observé qu'avec une reperfusion de plus de 30min, le nombre de cellules en apoptose/nécrose diminuait. Une reperfusion trop longue a donc semblé « sauver » une partie des cellules. Et le nombre de cellules en apoptose/nécrose est devenu trop proche de celui observé en normoxie sans traitement (viabilité cellulaire de base). Il était donc difficile dans ces conditions d'évaluer un effet des traitements, car au mieux les traitements permettaient de récupérer le même nombre de cellules en apoptose/nécrose qu'en normoxie sans traitement (figure 4).

Par ailleurs, dans ce modèle, il n'y a pas de flux et d'échange entre les différents types cellulaires comme cela se produit au niveau du tissu cardiaque complet. Ici, le modèle *in vitro* utilisé ne permet donc pas de retranscrire la complexité du vivant, mais il reste néanmoins intéressant au titre de pre-screening d'un traitement avant son utilisation *in vivo*.

Dans de futures études, il pourrait être suggéré de réaliser des modèles *in vitro* en 3 dimensions, comme par exemple des sphéroïdes, en incorporant plusieurs lignées cellulaires pour mieux mimer la complexité cardiaque. Nous pourrions aussi envisager des cultures cellulaires sur des puces (« on-chip ») permettant de simuler avec précision des conditions d'écoulement tels que le flux sanguin.

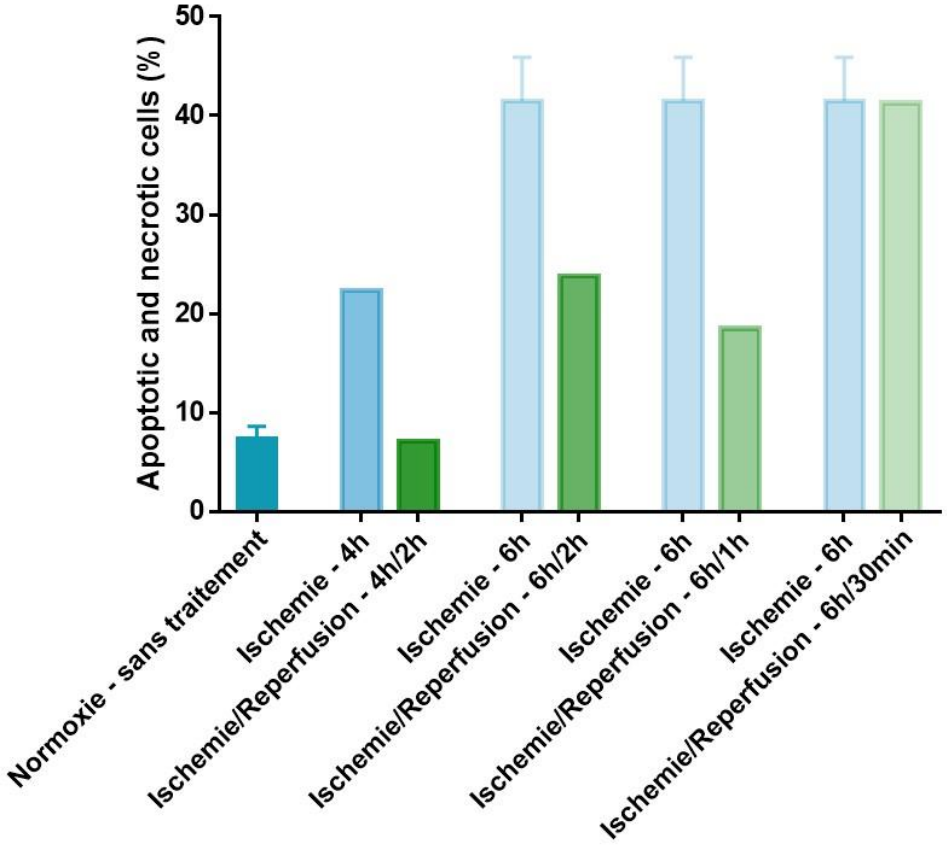

Figure 3 : Effets de différents temps d'ischémie et de reperfusion sur la viabilité cellulaire

Evaluation du pourcentage de cellules HL-1 en apoptose/nécrose après différents temps d'ischémie et de reperfusion. Aucun traitement n'a été ajouté ici. Evaluation par cytométrie en flux après co-marquage Annexine V et 7-AAD.

Les modèles murins de lésions d'ischémie/reperfusion cardiaque, des chirurgies complexes

En complémentarité des modèles *in vitro*, des modèles *in vivo* sont nécessaires pour étudier les effets à moyen et long terme de l'ischémie/reperfusion cardiaque et d'un traitement potentiel. Dans le projet européen Nanoheart dont nous faisons partie, plusieurs animaux modèles furent envisagés, à savoir souris, rat et cochons. Pour notre part, nous avons réalisé toutes nos études sur souris de laboratoire.

Nous avons adapté la méthode chirurgicale classique, qui consiste en la ligation de l'artère coronaire antérieure descendante par ouverture thoracique avec l'animal placé sous respirateur[32]. Cette méthode est la plus contrôlée et la plus viable d'un point de vue éthique et de reproductibilité. D'autres méthodes ont été publiées, notamment sans ventilation (chirurgie « pop-up »[33]) mais celles-ci ne sont pas largement reconnus par la communauté et présentent des biais éthiques considérables. Toutefois, l'approche méthodologique que nous avons choisie reste une chirurgie lourde avec plusieurs points critiques (gestion de l'anesthésie, intubation, ligation de la coronaire, …), induisant de la mortalité pendant et jusqu'à plusieurs jours après l'opération. La température de l'animal pendant la chirurgie est aussi un point important à prendre en compte car l'hypothermie peut engendrer à elle seule une cardioprotection[34].

La chirurgie présente également une limitation en termes de reproductibilité. En effet, la position de la ligation joue un rôle capital sur la taille de la zone ischémiée qui en découle (figure 4). De plus, les souris possèdent un cœur bien individualisé mais avec une microcirculation propre à chacune et qui peut aussi influencer la taille de la zone ischémiée. Tout cela a contribué à la forte variabilité des résultats obtenus entre les souris d'un même groupe de traitement comme présenté dans le chapitre 2. De ce fait, bien que nous puissions observer des tendances, des efforts supplémentaires sont nécessaires pour augmenter le nombre de souris opérées afin de minimiser les écarts-types et d'augmenter la significativité de l'étude.

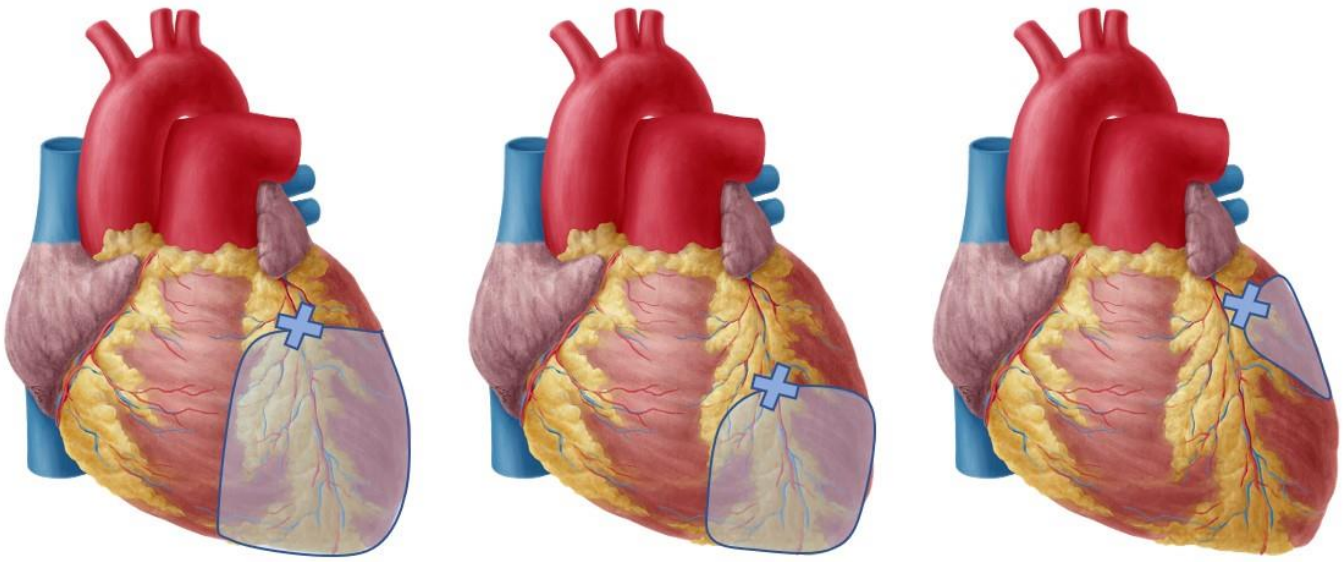

Figure 4 : modèle *in vivo* de lésions d'ischémie/reperfusion : importance de la position de la ligation de l'artère coronaire antérieure descendante
La croix bleue correspond à la position de la ligation. La zone bleue légèrement transparente est la zone à risque résultante. Suivant la position de la ligation, et la branche d'artère obstruée, la zone à risque sera nettement différente, influençant la reproductibilité des résultats.

Un intervalle d'ischémie de 30min a été adopté, ce qui est suffisant pour induire des changements irréversibles au niveau tissulaire et cellulaire, tout en n'induisant pas des dommages trop conséquents et une inflammation trop importante[35, 36]. Par ailleurs, nous avons pu constater que le taux de survie des souris post-chirurgie était fortement corrélé à la qualité et à la rapidité du geste chirurgical, d'où notre choix d'une ischémie de 30min. Ceci est d'ailleurs cohérent avec l'étude de Michael *et al*. qui a prouvé que chez la souris, la qualité de la chirurgie impactait directement les marqueurs analysés par la suite[37]. Justement, concernant les marqueurs évalués après reperfusion, nous avons décidé d'évaluer la taille de l'infarctus, les biomarqueurs plasmatiques ainsi que les marqueurs de l'inflammation. Ceci est en accord avec ceux évoqués dans l'étude de Lindsey *et al.*[35]. Nous n'avons toutefois pas pu faire d'échocardiographie pour évaluer l'activité cardiaque par faute de matériel. De telles analyses complémentaires seraient certainement nécessaires pour compléter l'étude *in vivo*.

Par ailleurs, il est important de préciser que nous avons parfois été confrontés à des problèmes de qualité des échantillons de coupes tissulaires et des coupes histologiques, ce qui a était préjudiciable pour certaines analyses post-chirurgie. Ce fut notamment le cas pour les analyses macroscopiques de zones à risque et de zones d'ischémie. La qualité des colorations et l'épaisseur de certaines coupes, rendaient en effet l'analyse irréalisable et celles-ci ont dû être retirées des résultats (figure 5).

Figure 5 : Illustration des limites rencontrées dans l'analyse macroscopique des coupes tissulaires post-chirurgie

Images macroscopiques prises avec un stéréomicroscope de coupes de cœur (1mm d'épaisseur) présentant un double-marquage Bleu Evans et TTC. Les images ont été choisies pour illustrer les différents problèmes rencontrés au cours de l'analyse macroscopique des zones à risque et des zones infarciées. (**A**) : Exemple de coupe de cœur dont la coloration au Bleu Evans était trop forte et empêche de voir le marquage TTC. (**B**) : Exemple de cœur où la coloration au Bleu Evans n'est pas suffisante pour délimiter les différentes zones sur le cœur. (**C**) : Exemple de coupe de cœur dont la coupe a posé problème et manquant de ce fait d'une partie du ventricule gauche.

3. L'adénosine pour les lésions d'ischémie/reperfusion cardiaque

L'adénosine est un nucléoside endogène formé par la dégradation enzymatique de l'adénosine triphosphate (ATP), principale source d'énergie chez l'Homme. Il agit en activant un de ses 4 récepteurs membranaires, A1, A2a, A2b, A3, ce qui déclenche différentes voies métaboliques. Toutes peuvent jouer potentiellement un rôle sur les lésions d'ischémie/reperfusion cardiaque[38, 39], ce qui en fait un candidat thérapeutique intéressant.

Adénosine vs. autres thérapies possibles pour traiter les lésions d'ischémie/reperfusion cardiaque

De nos jours, le traitement des lésions d'ischémie/reperfusion cardiaque est principalement de soutien. Aucune thérapie ciblée n'a été validée jusqu'ici. Compte tenu de la prévalence mondiale des maladies cardiovasculaires, le développement de nouvelles stratégies est ainsi nécessaire. De nombreuses approches thérapeutiques sont envisageables (figure 6). D'une part, il est possible d'adopter des approches protectives non-pharmacologiques tels que le pré-conditionnement ou le post-conditionnement ischémique, l'hypothermie thérapeutique ou encore le conditionnement par ischémie non léthale d'un autre organe[40-42]. D'autres part, divers agents pharmacologiques pourraient aussi être utilisés pour protéger le cœur. Parmi ces agents, l'on peut citer des inhibiteurs des transporteurs antiports sodium-hydrogène (Na+/H+)[43], l'activation de la voie de signalisation cGMP/PKG[44], l'inhibition de l'ouverture des pores mPTP durant la reperfusion[45, 46], ainsi que l'activation de la voie PI3K-AKT par activation des récepteurs aux protéines G[40, 47]. Et parmi ces derniers, on trouve notamment l'adénosine et d'autres agonistes de ses récepteurs.

L'adénosine peut donc interagir avec 4 récepteurs et a de multiples voies d'action. En plus de posséder de effets anti-inflammatoires et anti-apoptotiques[48, 49], des effets de cardio-protection ont été démontrés, parmi lesquels une réduction de la libération de cytokines et la formation d'espèces réactives de l'oxygène, des effets sur les leucocytes, ou encore un fort effet vasodilatateur[40, 49, 50]. Par ailleurs, il a été prouvé dans différents modèles animaux que l'activation des récepteurs A1 et A3 de l'adénosine avant ischémie avait un effet cardioprotecteur[51]. L'administration d'agonistes du récepteur A2a pendant la reperfusion réduirait également la taille de l'infarctus du myocarde[52]. Plus récemment, il a aussi été montré que le récepteur A2b pouvait aussi jouer un rôle important pour moduler les lésions reperfusion[38, 53]. Ainsi, l'adénosine possède probablement un des plus gros potentiels pour le traitement des lésions d'ischémie/reperfusion cardiaque.

Cependant, l'utilisation de l'adénosine en clinique est fortement restreinte car son administration systémique peut induire de graves effets secondaires tels que la suppression de la fonction cardiaque, des

hypotensions, ou des effets sédatifs. Ceci est principalement dû au fait que l'adénosine est très rapidement métabolisée (temps de demi-vie plasmatique de l'ordre de 10 sec) ce qui nécessite l'administration de très fortes doses induisant les effets secondaires décrits ci-dessus[54, 55].

En prenant en compte tous ces critères, l'encapsulation de l'adénosine dans des nanoparticules de squalène nous est apparu comme judicieux, permettant de profiter de ses nombreux effets thérapeutiques tout en protégeant da molécule de la métabolisation rapide.

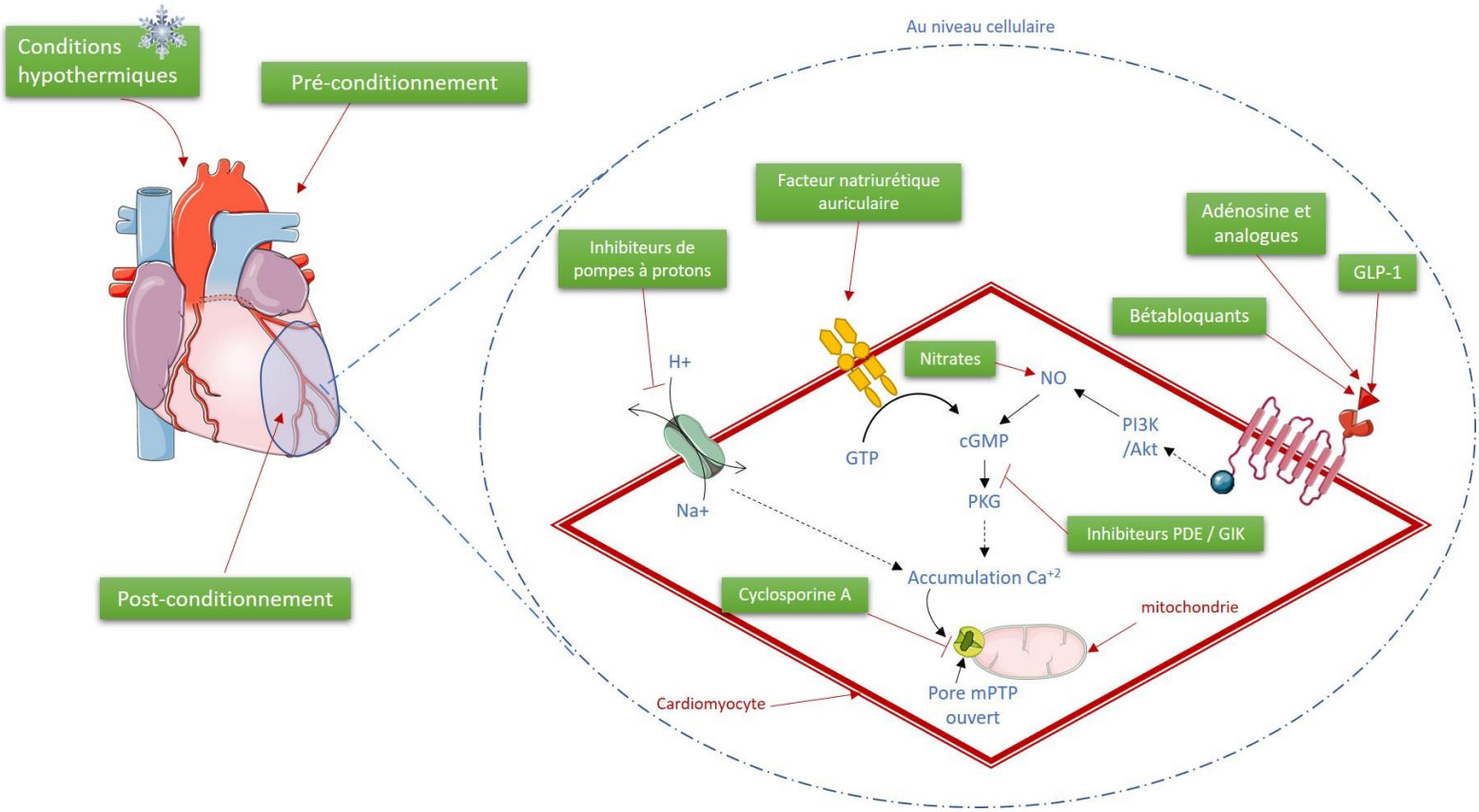

Figure 6 : Principales stratégies thérapeutiques pour traiter les lésions d'ischémie/reperfusion cardiaque

Figure inspirée de l'article de Li X *et al.*[40]. En encadré vert sont les différentes stratégies thérapeutiques envisageables. 3 protéines membranaires sont représentées sur le cardiomyocyte : en vert un canal échangeur H+/Na+, en jaune la guanylate cyclase, et en rouge un récepteur aux protéines G activant la voie du PI3K/AKT.
Abréviations : cGMP = guanosine monophosphate cyclique, GIK = glucose-insuline-potassium, GLP-1 = glucagon-like peptide 1, GTP = guanosine triphosphate, NO = oxide nitrique, PDE = Phosphodiestérase, PKG = protéine kinase G

Limites à l'utilisation de l'adénosine dans les modèles pré-cliniques

Afin d'évaluer l'efficacité des nanoparticules de squalène-adénosine dans les modèles de lésions d'ischémie/reperfusion cardiaque, il est nécessaire de pouvoir comparer leurs effets avec ceux de l'adénosine sous forme libre comme traitement témoin. Toutefois, en plus des problèmes évoqués précédemment concernant les modèles pré-cliniques, nous avons pu constater au cours de cette Thèse qu'il était aussi difficile d'étudier l'effet l'adénosine seule à la fois *in vitro* et *in vivo*.

Tout d'abord, examiner les effets de l'adénosine sur un modèle cellulaire n'est pas aisé. Le milieu appauvri d'ischémie ne présente aucun nutriment et ne possède pas les enzymes susceptibles de métaboliser l'adénosine. Par ailleurs, il n'y a pas de de flux sanguins ni d'érythrocytes ou autres cellules éliminant très rapidement l'adénosine comme cela se produit *in vivo*[55]. C'est pourquoi, l'effet d'un traitement avec de l'adénosine libre en condition ischémique est aussi bénéfique sinon plus qu'un traitement avec des nanoparticules de SQAd mais cela ne représente guère la réalité chez l'animal entier (chapitre 2 figure 4b). Dans d'autres expériences, nous avons tenté d'optimiser le milieu d'ischémie par addition de petites quantités de sérum de veau fœtal ou d'adénosine désaminase, une hydrolase dégradant l'adénosine en inosine. Toutefois, l'ajout de sérum réduit considérablement l'ischémie, et la désaminase n'a par ailleurs démontré aucun effet inhibiteur au cours du traitement témoin par l'adénosine libre (Figure 7). La raison probable est que l'inosine possède aussi un effet cardioprotecteur sur les cardiomyocytes[56, 57].
A l'avenir, il serait nécessaire d'envisager de nouveaux modèles plus complexes, par l'ajout d'inhibiteurs de l'adénosine, ou l'addition de phosphorylases de nucléosides, ainsi que par la réalisation de modèle en 3 dimensions ou sur puces

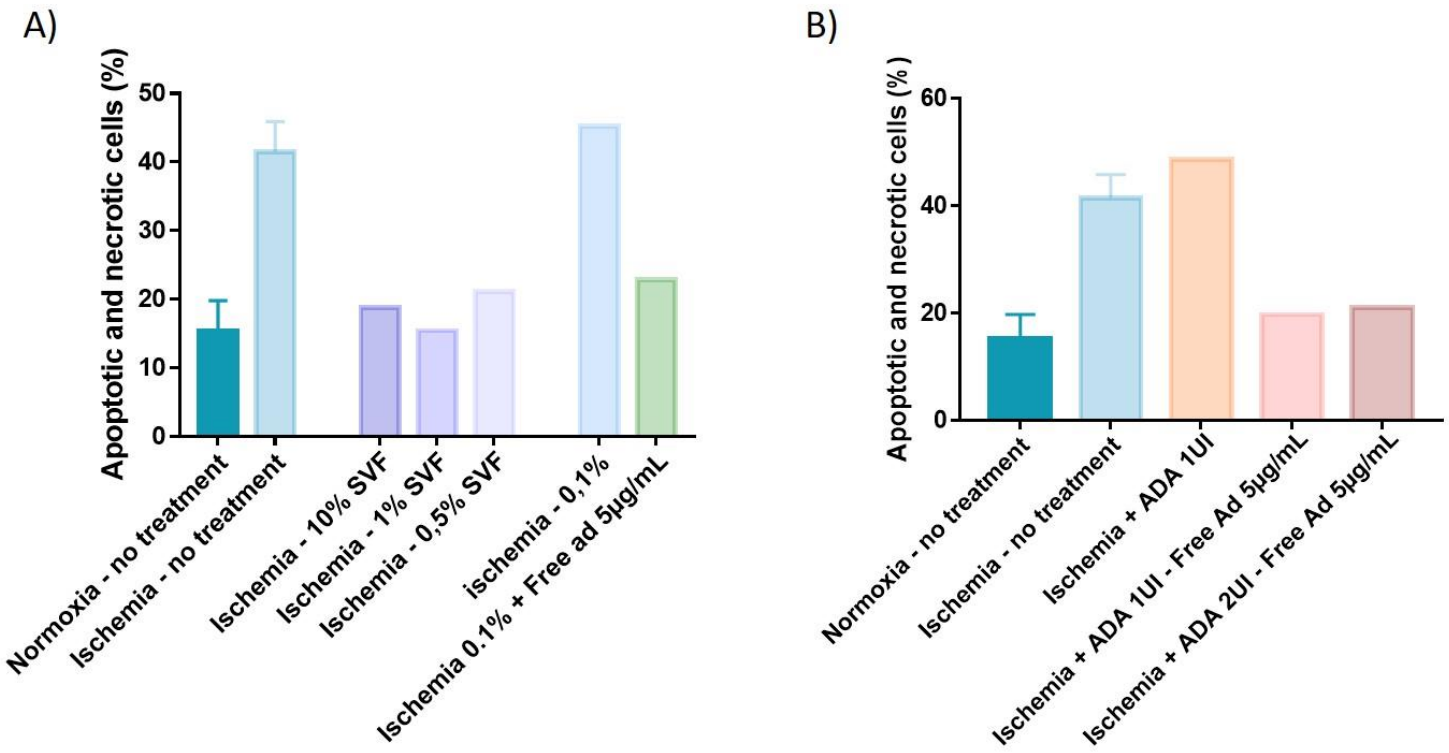

Figure 7 : Tentatives d'amélioration du modèle *in vitro* d'ischémie/reperfusion

Evaluation par cytométrie en flux du pourcentage de cellules HL-1 apoptotiques après 6h d'ischémie avec addition de sérum de veau fœtal SVF (**A**), ou d'adénosine désaminase ADA (**B**) à différentes concentrations. Le SVF et l'ADA ont été directement ajouté dans le milieu d'ischémie avant incubation des cellules. (**A**) : des concentrations de 10%, 1%, 0.5% et 0.1% de SVF ont été testées. Seul 0.1% de SVF n'induit pas une perte des effets de l'ischémie, mais cette concentration ne suffit pas à inhiber l'effet de l'adénosine libre. (**B**) : L'ajout d'ADA à 1 ou 2 unités internationale (UI) ne perturbe pas les effets d'ischémie, mais ne permet pas non plus d'inhiber efficacement les effets de l'adénosine libre.

.

Espoirs pour une application clinique des nanoparticules de squalène-adénosine ?

Les nanoparticules à base de squalène offrent des perspectives intéressantes en vue d'une future application en clinique. Il a été démontré que le squalène en lui-même n'est pas toxique pour l'Homme et qu'il n'induit pas de réaction immunitaire à son égard, facilitant son introduction éventuelle dans un essai clinique[58, 59]. Une méthode de lyophilisation des nanoparticules à base de squalène a permis de préserver leur stabilité colloïdale, tout en conservant leur absence de toxicité[60]. Des start-ups ont été créées (Medsqual en 2007 et Squal Pharma en 2019) dans le but de développer à des fins cliniques des nanomédicaments à base de squalène pour diverses pathologies telles que les cancers, la dermatologie et la gestion de la douleur[61]. Ainsi à terme, les nanoparticules de squalène-adénosine pourraient être employées dans diverses pathologies inflammatoires.

Toutefois, dans le cadre des maladies évoquées au cours de cette étude, plusieurs limitations viennent freiner leur passage en clinique. Premièrement, le profil en lipoprotéines chez l'Homme est différent de celui de la souris. Deuxièmement, les résultats observés pour le traitement des lésions d'ischémie/reperfusion cardiaque sont trop incertains, pas assez significatifs, et pas assez avancés pour espérer un futur essai clinique. Par contre, les nanoparticules multi-médicaments de squalène-adénosine associées à la vitamine E pourraient se révéler utiles dans le traitement d'inflammations paradoxales non maîtrisées., Cependant, des études supplémentaires sont encore nécessaires pour caractériser la bio-distribution des nanoparticules et comparer leur effet aux autres traitements déjà sur le marché.

.

Références

[1] : Kalogeris, T., Baines, C. P., Krenz, M., & Korthuis, R. J. (2016). Ischemia/Reperfusion. Comprehensive Physiology, 7(1), 113−170.

[2] : Adembri C., De Gaudio A.R., Novelli G.P. (2000) Ischaemia-Reperfusion in Sepsis. In: Baue A.E., Berlot G., Gullo A., Vincent JL. (eds) Sepsis and Organ Dysfunction. Springer, Milano.

[3] : Ou, S. M., Chu, H., Chao, P. W., Lee, Y. J., Kuo, S. C., Chen, T. J., Tseng, C. M., Shih, C. J., & Chen, Y. T. (2016). Long-Term Mortality and Major Adverse Cardiovascular Events in Sepsis Survivors. A Nationwide Population-based Study. American journal of respiratory and critical care medicine, 194(2), 209–217.

[4] : Mankowski, R. T., Yende, S., & Angus, D. C. (2019). Long-term impact of sepsis on cardiovascular health. Intensive care medicine, 45(1), 78–81.

[5] : Owen, D. R., Lindsay, A. C., Choudhury, R. P., & Fayad, Z. A. (2011). Imaging of atherosclerosis. Annual review of medicine, 62, 25−40.

[6] : Tarkin, J. M., Dweck, M. R., Evans, N. R., Takx, R. A., Brown, A. J., Tawakol, A., Fayad, Z. A., & Rudd, J. H. (2016). Imaging Atherosclerosis. Circulation research, 118(4), 750−769.

[7] : Sheng, Y., Liao, L. D., Thakor, N. V., & Tan, M. C. (2014). Nanoparticles for molecular imaging. Journal of biomedical nanotechnology, 10(10), 2641−2676.

[8] : Lobatto, M. E., Calcagno, C., Millon, A., Senders, M. L., Fay, F., Robson, P. M., Ramachandran, S., Binderup, T., Paridaans, M. P., Sensarn, S., Rogalla, S., Gordon, R. E., Cardoso, L., Storm, G., Metselaar, J. M., Contag, C. H., Stroes, E. S., Fayad, Z. A., & Mulder, W. J. (2015). Atherosclerotic plaque targeting mechanism of long-circulating nanoparticles established by multimodal imaging. ACS nano, 9(2), 1837−1847.

[9] : Bejarano, J., Navarro-Marquez, M., Morales-Zavala, F., Morales, J. O., Garcia-Carvajal, I., Araya-Fuentes, E., Flores, Y., Verdejo, H. E., Castro, P. F., Lavandero, S., & Kogan, M. J. (2018). Nanoparticles for diagnosis and therapy of atherosclerosis and myocardial infarction: evolution toward prospective theranostic approaches. Theranostics, 8(17), 4710−4732.

[10] : Herranz, F., Salinas, B., Groult, H., Pellico, J., Lechuga-Vieco, A. V., Bhavesh, R., & Ruiz-Cabello, J. (2014). Superparamagnetic Nanoparticles for Atherosclerosis Imaging. Nanomaterials (Basel, Switzerland), 4(2), 408−438.

[11] : Libby, P., Buring, J. E., Badimon, L., Hansson, G. K., Deanfield, J., Bittencourt, M. S., Tokgözoğlu, L., & Lewis, E. F. (2019). Atherosclerosis. Nature reviews. Disease primers, 5(1), 56.

[12] : Sobot, D., Mura, S., Yesylevskyy, S. O., Dalbin, L., Cayre, F., Bort, G., Mougin, J., Desmaële, D., Lepetre-Mouelhi, S., Pieters, G., Andreiuk, B., Klymchenko, A. S., Paul, J. L., Ramseyer, C., & Couvreur, P. (2017). Conjugation of squalene to gemcitabine as unique approach exploiting endogenous lipoproteins for drug delivery. Nature communications, 8, 15678.

[13] : Oschry, Y. & Eisenberg, S. Rat plasma lipoproteins: re-evaluation of a lipoprotein system in an animal devoid of cholesteryl ester transfer activity. J. Lipid Res. 23, 1099–1106 (1982).

[14] : M. F. Linton, P. G. Yancey, S. S. Davies, W. G. Jerome, et al. (2019) The role of lipids and lipoproteins in atherosclerosis. Endotext [Internet], (MDText. com, Inc.).

[15] : Ross R. (1999). Atherosclerosis--an inflammatory disease. The New England journal of medicine, 340(2), 115−126.

[16] : Chu, D., Gao, J., & Wang, Z. (2015). Neutrophil-Mediated Delivery of Therapeutic Nanoparticles across Blood Vessel Barrier for Treatment of Inflammation and Infection. ACS nano, 9(12), 11800−11811.

[17] : Richardson, S. D., Willson, C. S., & Rusch, K. A. (2004). Use of Rhodamine water tracer in the marshland upwelling system. Ground water, 42(5), 678−688.

[18] : Pubchem Website: Rhodamine B (Compound)
https://pubchem.ncbi.nlm.nih.gov/compound/Rhodamine-B#section=GHS-Classification

[19] : Jain, R., Mathur, M., Sikarwar, S., & Mittal, A. (2007). Removal of the hazardous dye rhodamine B through photocatalytic and adsorption treatments. Journal of environmental management, 85(4), 956−964.

[20] : Islam, Md. M., Chakraborty, M., Pandya, P., Masuma, A. A., Gupta, N., Mukhopadhyay, S. (2013) Binding of DNA with rhodamine B: spectroscopic and molecular modeling studies. Dyes Pigm. 2013, 99, 412–422.

[21] : IARC, 1987. Overall Evaluations of Carcinogenicity: An Updating of IARC Monographs, vol. 1–42

[22] : Othman, M., Desmaële, D., Couvreur, P., Vander Elst, L., Laurent, S., Muller, R. N., Bourgaux, C., Morvan, E., Pouget, T., Lepêtre-Mouelhi, S., Durand, P., & Gref, R. (2011). Synthesis and physicochemical characterization of new squalenoyl amphiphilic gadolinium complexes as nanoparticle contrast agents. Organic & biomolecular chemistry, 9(11), 4367−4386.

[23] : Arias, J. L., Reddy, L. H., Othman, M., Gillet, B., Desmaële, D., Zouhiri, F., Dosio, F., Gref, R., & Couvreur, P. (2011). Squalene based nanocomposites: a new platform for the design of multifunctional pharmaceutical theragnostics. ACS nano, 5(2), 1513−1521.

[24] : Tarkin, J. M., Dweck, M. R., Evans, N. R., Takx, R. A., Brown, A. J., Tawakol, A., Fayad, Z. A., & Rudd, J. H. (2016). Imaging Atherosclerosis. Circulation research, 118(4), 750−769.

[25] : Lindsey, M. L., Bolli, R., Canty, J. M., Jr, Du, X. J., Frangogiannis, N. G., Frantz, S., Gourdie, R. G., Holmes, J. W., Jones, S. P., Kloner, R. A., Lefer, D. J., Liao, R., Murphy, E., Ping, P., Przyklenk, K., Recchia, F. A., Schwartz Longacre, L., Ripplinger, C. M., Van Eyk, J. E., & Heusch, G. (2018). Guidelines for experimental models of myocardial ischemia and infarction. American journal of physiology. Heart and circulatory physiology, 314(4), H812−H838.

[26] : Chen, T., & Vunjak-Novakovic, G. (2018). In vitro Models of Ischemia-Reperfusion Injury. Regenerative engineering and translational medicine, 4(3), 142−153.

[27] : Diaz, R. J., Harvey, K., Boloorchi, A., Hossain, T., Hinek, A., Backx, P. H., & Wilson, G. J. (2014). Enhanced cell volume regulation: a key mechanism in local and remote ischemic preconditioning. American journal of physiology. Cell physiology, 306(12), C1191−C1199.

[28] : Diaz, R. J., & Wilson, G. J. (2006). Studying ischemic preconditioning in isolated cardiomyocyte models. Cardiovascular research, 70(2), 286−296.

[29] : Si, J., Wang, N., Wang, H., Xie, J., Yang, J., Yi, H., Shi, Z., Ma, J., Wang, W., Yang, L., Yu, S., & Li, J. (2014). HIF-1α signaling activation by post-ischemia treatment with astragaloside IV attenuates myocardial ischemia-reperfusion injury. PloS one, 9(9), e107832.

[30] : Strijdom, H., Genade, S., & Lochner, A. (2004). Nitric Oxide synthase (NOS) does not contribute to simulated ischaemic preconditioning in an isolated rat cardiomyocyte model. Cardiovascular drugs and therapy, 18(2), 99−112.

[31] : Chang, G., Zhang, D., Liu, J., Zhang, P., Ye, L., Lu, K., Duan, Q., Zheng, A., & Qin, S. (2014). Exenatide protects against hypoxia/reoxygenation-induced apoptosis by improving mitochondrial function in H9c2 cells. Experimental biology and medicine (Maywood, N.J.), 239(4), 414−422.

[32] : Xu Z., McElhanon K.E., Beck E.X., Weisleder N. (2018) A Murine Model of Myocardial Ischemia–Reperfusion Injury. In: Tharakan B. (eds) Traumatic and Ischemic Injury. Methods in Molecular Biology, vol 1717. Humana Press, New York, NY

[33] : Gao, E., Lei, Y. H., Shang, X., Huang, Z. M., Zuo, L., Boucher, M., Fan, Q., Chuprun, J. K., Ma, X. L., & Koch, W. J. (2010). A novel and efficient model of coronary artery ligation and myocardial infarction in the mouse. Circulation research, 107(12), 1445−1453.

[34] : Kohlhauer, M., Pell, V. R., Burger, N., Spiroski, A. M., Gruszczyk, A., Mulvey, J. F., Mottahedin, A., Costa, A., Frezza, C., Ghaleh, B., Murphy, M. P., Tissier, R., & Krieg, T. (2019). Protection against cardiac ischemia-reperfusion injury by hypothermia and by inhibition of succinate accumulation and oxidation is additive. Basic research in cardiology, 114(3), 18.

[35] : Lindsey, M. L., Bolli, R., Canty, J. M., Jr, Du, X. J., Frangogiannis, N. G., Frantz, S., Gourdie, R. G., Holmes, J. W., Jones, S. P., Kloner, R. A., Lefer, D. J., Liao, R., Murphy, E., Ping, P., Przyklenk, K., Recchia, F. A., Schwartz Longacre, L., Ripplinger, C. M., Van Eyk, J. E., & Heusch, G. (2018). Guidelines for experimental models of myocardial ischemia and infarction. American journal of physiology. Heart and circulatory physiology, 314(4), H812−H838.

[36] : Jennings, R. B., Murry, C. E., Steenbergen, C., Jr, & Reimer, K. A. (1990). Development of cell injury in sustained acute ischemia. Circulation, 82(3 Suppl), II2−II12.

[37] : Michael LH, Ballantyne CM, Zachariah JP, Gould KE, Pocius JS, Taffet GE, Hartley CJ, Pham TT, Daniel SL, Funk E, Entman ML. (1999). Myocardial infarction and remodeling in mice: effect of reperfusion. Am J Physiol Heart Circ Physiol 277: H660–H668,

[38] : Headrick, J. P., & Lasley, R. D. (2009). Adenosine receptors and reperfusion injury of the heart. Handbook of experimental pharmacology, (193), 189−214.

[39] : Peart, J. N., & Headrick, J. P. (2007). Adenosinergic cardioprotection: multiple receptors, multiple pathways. Pharmacology & therapeutics, 114(2), 208−221.

[40] : Li X., Liu M., Sun R., Zeng Y., Chen S. and Zhang P. (2016). Protective approaches against myocardial ischemia reperfusion injury (Review). Exp Ther Med 12: 3823-3829.

[41] : Buja L. M. (2005). Myocardial ischemia and reperfusion injury. Cardiovascular pathology : the official journal of the Society for Cardiovascular Pathology, 14(4), 170−175.

[42] : Heusch G. (2013). Cardioprotection: chances and challenges of its translation to the clinic. Lancet (London, England), 381(9861), 166−175.

[43] : Rupprecht, H. J., vom Dahl, J., Terres, W., Seyfarth, K. M., Richardt, G., Schultheibeta, H. P., Buerke, M., Sheehan, F. H., & Drexler, H. (2000). Cardioprotective effects of the Na(+)/H(+) exchange inhibitor cariporide in patients with acute anterior myocardial infarction undergoing direct PTCA. Circulation, 101(25), 2902−2908.

[44] : Yang, X. M., Philipp, S., Downey, J. M., & Cohen, M. V. (2006). Atrial natriuretic peptide administered just prior to reperfusion limits infarction in rabbit hearts. Basic research in cardiology, 101(4), 311−318.

[45] : Piot, C., Croisille, P., Staat, P., Thibault, H., Rioufol, G., Mewton, N., Elbelghiti, R., Cung, T. T., Bonnefoy, E., Angoulvant, D., Macia, C., Raczka, F., Sportouch, C., Gahide, G., Finet, G., André-Fouët, X., Revel, D., …, Ovize, M. (2008). Effect of cyclosporine on reperfusion injury in acute myocardial infarction. The New England journal of medicine, 359(5), 473−481.

[46] : Ghaffari, S., Kazemi, B., Toluey, M., & Sepehrvand, N. (2013). The effect of prethrombolytic cyclosporine-A injection on clinical outcome of acute anterior ST-elevation myocardial infarction. Cardiovascular therapeutics, 31(4), e34−e39.

[47] : Ibanez, B., Cimmino, G., Prat-González, S., Vilahur, G., Hutter, R., García, M. J., Fuster, V., Sanz, J., Badimon, L., & Badimon, J. J. (2011). The cardioprotection granted by metoprolol is restricted to its administration prior to coronary reperfusion. International journal of cardiology, 147(3), 428−432.

[48] : Mantovani, A., Biswas, S. K., Galdiero, M. R., Sica, A. & Locati, M. (2013). Macrophage plasticity and polarization in tissue repair and remodelling. J. Pathol. 229, 176–185.

[49] : Antonioli, L., Blandizzi, C., Pacher, P., & Haskó, G. (2013). Immunity, inflammation and cancer: a leading role for adenosine. Nature reviews. Cancer, 13(12), 842−857.

[50] : Riksen, N. P., Rongen, G. A., Yellon, D., & Smits, P. (2008). Human in vivo research on the vascular effects of adenosine. European journal of pharmacology, 585(2-3), 220−227.

[51] : Hill, R. J., Oleynek, J. J., Magee, W., Knight, D. R., & Tracey, W. R. (1998). Relative importance of adenosine A1 and A3 receptors in mediating physiological or pharmacological protection from ischemic myocardial injury in the rabbit heart. Journal of molecular and cellular cardiology, 30(3), 579−585.

[52] : Guerrero A. (2018). A2A Adenosine Receptor Agonists and their Potential Therapeutic Applications. An Update. Current medicinal chemistry, 25(30), 3597−3612.

[53] : Busse, H., Bitzinger, D., Höcherl, K., Seyfried, T., Gruber, M., Graf, B. M., & Zausig, Y. A. (2016). Adenosine A2A and A2B Receptor Substantially Attenuate Ischemia/Reperfusion Injury in Septic rat Hearts. Cardiovascular drugs and therapy, 30(6), 551−558.

[54] : Guieu, R., Deharo, J. C., Maille, B., Crotti, L., Torresani, E., Brignole, M., & Parati, G. (2020). Adenosine and the Cardiovascular System: The Good and the Bad. Journal of clinical medicine, 9(5), 1366.

[55] : Kazemzadeh-Narbat, M., Annabi, N., Tamayol, A., Oklu, R., Ghanem, A., & Khademhosseini, A. (2015). Adenosine-associated delivery systems. Journal of drug targeting, 23(7-8), 580−596.

[56] : Szabó, G., Stumpf, N., Radovits, T., Sonnenberg, K., Gerö, D., Hagl, S., Szabó, C., & Bährle, S. (2006). Effects of inosine on reperfusion injury after heart transplantation. European journal of cardio-thoracic surgery : official journal of the European Association for Cardio-thoracic Surgery, 30(1), 96−102.

[57] : Shafy, A., Molinié, V., Cortes-Morichetti, M., Hupertan, V., Lila, N., & Chachques, J. C. (2012). Comparison of the effects of adenosine, inosine, and their combination as an adjunct to reperfusion in the treatment of acute myocardial infarction. ISRN cardiology, 2012, 326809.

[58] : Schultze, V., D'Agosto, V., Wack, A., Novicki, D., Zorn, J., & Hennig, R. (2008). Safety of MF59 adjuvant. Vaccine, 26(26), 3209−3222.

[59] : O'Hagan, D. T., Ott, G. S., De Gregorio, E., & Seubert, A. (2012). The mechanism of action of MF59 - an innately attractive adjuvant formulation. Vaccine, 30(29), 4341−4348.

[60] : Rouquette, M., Ser-Le Roux, K., Polrot, M., Bourgaux, C., Michel, J. P., Testard, F., Gobeaux, F., & Lepetre-Mouelhi, S. (2019). Towards a clinical application of freeze-dried squalene-based nanomedicines. Journal of drug targeting, 27(5-6), 699−708.

[61] : Squal Pharma Website : https://squalpharma.com/about-squal-pharma/

ÉCOLE DOCTORALE
Innovation thérapeutique
du fondamental à l'appliqué
(ITFA)

Titre : Applications des nanoparticules à base de Squalène dans les maladies cardiovasculaires et inflammatoires : Exemples pour l'ischémie/reperfusion cardiaque, l'athérosclérose et le sepsis

Mots clés : Nanoparticules de Squalène, inflammation, ischémie/reperfusion cardiaque, athérosclérose, sepsis

Résumé : Ces dernières années, le développement de nouveaux nanomédicaments suscite un intérêt grandissant du fait de leurs propriétés physicochimiques et biologiques remarquables. Les nanoparticules possèdent une grande flexibilité en termes de matériaux, taille, forme et caractéristiques de surface, offrant ainsi la possibilité de dépasser les limitations des traitements conventionnels. En effet, les thérapies actuelles demeurent parfois limitées et peuvent présenter une faible spécificité et des problèmes de bio-distribution entraînant des effets secondaires. C'est notamment le cas pour le traitement de l'inflammation, réaction majeure de défense immunitaire de l'organisme qui participe au développement et à la pathophysiologie de nombreuses maladies complexes, telles que l'athérosclérose, les lésions d'ischémie/reperfusion du myocarde ou le sepsis.

Au sein de notre laboratoire, nous avons développé des nanomédicaments à base de squalène, une biomolécule naturelle précurseur du cholestérol. Le couplage chimique entre un dérivé du squalène et un principe actif comme l'adénosine permet de former spontanément en milieu aqueux des nanoparticules qui ont déjà fourni des résultats encourageants dans un modèle pré-clinique d'ischémie cérébrale.
Ce projet de thèse a ainsi pour but d'évaluer ces nanoparticules à base de squalène dans des modèles pré-cliniques de pathologies inflammatoires (i) pour le ciblage des lésions d'athérosclérose, (ii) pour protéger des lésions d'ischémie/reperfusion cardiaque, et (iii) pour traiter le processus inflammatoire dans le cadre du sepsis.

Title: Applications of Squalene-based nanoparticles in cardiovascular and inflammatory diseases: Examples for cardiac ischemia/reperfusion, atherosclerosis, and sepsis

Keywords: Squalene-based nanoparticles, inflammation, cardiac ischemia/reperfusion, atherosclerosis, sepsis

Abstract: During the last years, the development of new nanomedicines has generated a growing interest due to their exciting physicochemical and biological properties. Nanoparticles possess an extensive modularity in terms of materials, size, shape and surface characteristics, offering the possibility to overcome limitations of conventional treatments. Current therapies remain sometimes limited due to low specificity and non-optimal bioavailability which induce side effects. This is especially the case for the treatment of inflammation, indispensable immune reaction of body's defence which drives, however the genesis of complex diseases, such as atherosclerosis, myocardial ischemia/reperfusion injury or sepsis.

In our laboratory, we have used squalene, a natural biomolecule precursor of the cholesterol's biosynthesis, to prepare various squalene-based nanomedicines. Chemical linkage between a squalene derivative and an active principle, like adenosine, can form nanoparticles in water, which has already provided promising results in a brain ischemia model.
This thesis aims at evaluating squalene-based nanoparticles in various pre-clinical models of inflammatory diseases (i) for targeting atherosclerotic lesions, (ii) protecting from myocardial ischemia/reperfusion injury, and (iii) for the treatment of the inflammatory process in sepsis.

Université Paris-Saclay
Espace Technologique / Immeuble Discovery
Route de l'Orme aux Merisiers RD 128 / 91190 Saint-Aubin, France